https://theses.gla.ac.uk/

Theses Digitisation:

https://www.gla.ac.uk/myglasgow/research/enlighten/theses/digitisation/

This is a digitised version of the original print thesis.

Copyright and moral rights for this work are retained by the author

A copy can be downloaded for personal non-commercial research or study, without prior permission or charge

This work cannot be reproduced or quoted extensively from without first obtaining permission in writing from the author

The content must not be changed in any way or sold commercially in any format or medium without the formal permission of the author

When referring to this work, full bibliographic details including the author, title, awarding institution and date of the thesis must be given

Enlighten: Theses
https://theses.gla.ac.uk/
research-enlighten@glasgow.ac.uk

RADIONUCLIDE MOVEMENT AND GEOCHEMISTRY IN INTERTIDAL SEDIMENTS IN SOUTH WEST SCOTLAND

YOUSEF ALI BEN-SHABAN BSc MSc

Scottish Universities Research and Reactor Centre

presented as a thesis for the degree of

Doctor of Philosphy

in the University of Glasgow

November 1989

ProQuest Number: 11007365

All rights reserved

INFORMATION TO ALL USERS
The quality of this reproduction is dependent upon the quality of the copy submitted.

In the unlikely event that the author did not send a complete manuscript
and there are missing pages, these will be noted. Also, if material had to be removed,
a note will indicate the deletion.

ProQuest 11007365

Published by ProQuest LLC (2018). Copyright of the Dissertation is held by the Author.

All rights reserved.
This work is protected against unauthorized copying under Title 17, United States Code
Microform Edition © ProQuest LLC.

ProQuest LLC.
789 East Eisenhower Parkway
P.O. Box 1346
Ann Arbor, MI 48106 – 1346

LIST OF CONTENTS

LIST OF TABLES

LIST OF FIGURES

ACKNOWLEDGEMENTS

I have received invaluable help and advice from many people during this research. Particular thanks are due to my supervisor Dr A B MacKenzie, for all his expert advice, patience, constant guidance and encouragement. I am indebted to Dr R D Scott for the advice and encouragement. I would like to express my sincere gratitude to Professor M S Baxter for his guidance and helpful suggestions.

I would also like to thank the following people for their constant help and support:-

Dr G T Cook for his valuable help and advice my fellow research students: Mr Ihsanullah, Dr P McDonald and Mr P Clark in whose company much of the experimental work was carried out. Mr R Stewart and Mr M Sherriff for their cooperation during my stay at the Centre. Miss G M Thomson for typing of manuscript; my parents - I am especially grateful for their encouragement and moral support during the whole period of my study. My wife and children (Akram, Eman and Ali) for their continuous patience and reliable help.

Finally I wish to acknowledge financial support from the Marine Biology Research Centre, Tajura.

ABSTRACT

This thesis describes a study of the distribution and behaviour of natural and manmade radionuclides in the intertidal environment of south west Scotland. This work is particularly concerned with transport processes affecting radionuclides and with the application of radionuclides as tracers of natural environmental processes. Results are presented for study sites at Ardmore Bay in the Clyde Sea Area and Skyreburn Bay, Wigtown Martyr's Stake and Netherclifton in the Solway Firth with the radionuclides investigated being ^{134}Cs, ^{137}Cs, ^{210}Pb, ^{238}Pu, $^{239,240}Pu$ ^{241}Am, ^{238}U, ^{232}Th and ^{230}Th.

The study confirms and extends an existing model for particle associated Sellafield waste radionuclide transport to the intertidal areas of the Solway Firth and the work, moreover, establishes that the same supply mechanism operates in the floodplain, or merse, areas of the Solway Firth.

Inventories of the order of 10^5, 10^4 and 10^4 Bq m^{-2} are derived for ^{137}Cs, ^{241}Am and $^{239,240}Pu$ respectively in the merse sediments, indicating inventories for these nuclides of the order of 7, 1 and 1 TBq in the total area of the merse deposits of the Solway Firth.

A description is provided of a study of uranium movement through the Solway floodplain silts in the vicinity of a uranium mineralization vein and it is established that uranium migration for distances of up to 55m can be observed with continuous removal from solution during transport by uptake by iron/manganese oxides and organic materials. The removal process is characterised by a 10m halving distance.

The radionuclide data are considered in the context of tracer studies of various environmental processes including large scale sediment movement in the Irish Sea, local sediment movement in particular bays and, at individual sites, mixing and accumulating processes.

AIMS OF THE PROJECT

The theme of this research project was centred around the investigation of the distribution and geochemical behaviour of natural and manmade radionuclidesin the intertidal sediments of south west Scotland; characterisation of radionuclide transport mechanisms and assessment of the potential of radionuclides for investigation of sedimentary processes in the intertidal region. The following topics were of main importance in the work.

1 Testing an existing model for transport of Sellafield waste radionuclides to the intertidal sediments of the Solway Firth.

2 Establishing a model for transport of Sellafield waste radionuclides to the merse (floodplain) sediments of the Solway Firth.

3 Assessing the inventories and behaviour of manmade radionuclides in the merse sediment of the Solway Firth.

4 Investigation of the potential of natural and manmade radionuclides for characterisation of sedimentary processes in the intertidal environment of south west Scotland and, where appropriate, application of radionuclides in the study of such processes.

1. INTRODUCTION

1.1 RADIOACTIVITY AND RADIOANALYTICAL METHODS

1.1.1 Radioactive Decay

Radioactivity may be defined as a process in which nuclides undergo spontaneous nuclear changes and nuclides which undergo such changes are known as radionuclides. Only certain combinations of protons and neutrons form stable nuclei and these lie in a relatively well defined band in the chart of the nuclides (Seelman - Eggebert et al, 1981). At the beginning of the periodic table, stable nuclides have nuclei composed of roughly equal numbers of protons and neutrons, but with increasing atomic number, a preponderance of neutrons is necessary for stability. If there are more protons or more neutrons present in a nucleus relative to the optimum combination, the nucleus will attempt to correct the imbalance by the emission of radiation.

A variety of radioactive decay modes are observed and the characteristics of some of the more important processes are described below.

Alpha decay involves the emission of an alpha particle consisting of two protons and two neutrons (ie. a He nucleus of mass 4 a.m.u. and charge +2) and is observed for heavy, proton-rich nuclides. Alpha particles are emitted in one or more groups of mono-energetic particles, the decay energy generally being in the range 4 to 10MeV. Different alpha emitting nuclides therefore give different characteristic energies of alpha particles so that particle energies can be used to identify the species undergoing decay.

Beta decay occurs when the nucleus has excess neutrons and in this process a neutron is converted into a proton to give increased stability. In this case a negatively charged electron known as a beta particle and an anti-neutrino are emitted simultaneously from the nucleus. The anti-neutrino is a particle with zero mass and zero electrical charge, but which has both energy and momentum. The beta particle and anti-neutrino share the available decay energy in varying amounts and in consequence, a continuous spectrum of beta particle energies is obtained for any beta emitting radionuclide. Thus beta decay is not characterized by a unique value for the energy of the beta particle and this leads to complexity in the analysis of beta emitters. On the other hand, nuclei which have an excess of protons relative to neutrons can spontaneously undergo a decay process in which a proton is converted to a neutron within the nucleus by the weak interaction process and a positively charged electron called a positron and a neutrino are emitted. Again, the positron and neutrino share the available decay energy.

Each time an alpha particle is emitted, the mass number of the nucleus decreases by four units and the atomic number decreases by two units, while after a beta decay, the mass number is unchanged, but the atomic number is increased by one unit.

An alternative mechanism to positron decay is the capture of one of the K or L-orbital electrons by a proton within the nucleus, accompanied by the emission of a neutrino, and this process is known as Electron Capture. The capture of the atomic orbital electron from the K-shell leaves a vacancy in this shell which is filled by an electron dropping down from the

L-shell, and X-ray emission always follows this process.

Following the radioactive decay of a nucleus by one of the processes described above, the daughter nucleus may be left with excess energy ie. an excited state. These excited nuclei generally undergo immediate de-excitation and this excitation energy is emitted from the nucleus in the form of photons of electromagnetic energy called gamma radiation. Gamma radiation consists of mono-energetic photons of electromagnetic radiation and the photon energies are characteristic of the species undergoing decay. Thus gamma photons are characteristic of the decay process and this fact can be utilised in gamma spectroscopy.

De-excitation can occur by a transition from an excited state to the ground state or from one excited state to a lower energy excited state and different de-excitation routes can be followed by different nuclei of the same radionuclide. The fraction of the total number of decays proceeding by way of a given gamma emission is called the Intensity for that energy. Excited nuclei with finite life-times are sometimes formed and these are known as Metastable States or Isomers. Decay of metastable states follows first order kinetics and such de-excitations are called isomeric transitions.

In addition to the types of radioactive decay discussed above some heavy nuclei can undergo decay by spontaneous fission, in which the nucleus divides into fragments of comparable size. This phenomenon occurs only in the heavy element region of the periodic table and is dominantly observed for elements with Z-values greater than 90. Two or three neutrons are liberated as the result of this process in addition to the main

fragments and fission leaves the product nucleus in an excited state, which may be de-excited by emission of gamma radiation.

Further complexity can be introduced in radioactive decay in cases where a nuclide can undergo decay by two or more competitive processes in branching decay (eg. ^{212}Bi undergoes 35% alpha decay and 65% beta decay) or where the daughter product is radioactive giving successive decay (eg. the natural decay series).

The overall process in radioactive decay can therefore be complex and the characteristics of decay of individual nuclei are presented in decay schemes as comprehensively summarized by Lederer and Shirley (1978) and Browne and Firestone (1986). The decay characteristics of ^{134}Cs, ^{137}Cs, ^{210}Pb, ^{210}Po, ^{238}Pu, ^{239}Pu, ^{240}Pu, ^{241}Am, ^{234}U, ^{235}U, ^{238}U and ^{230}Th which were the main nuclides of interest in the present work are summarized in Table 1.1.

1.1.2 Equations of Radioactive Decay and Growth

Radioactive decay is a statistical process in which the number of nuclei of a particular type undergoing decay in unit time (the decay rate) is proportional to the number of nuclei of the nuclide. Thus for a large number, N, of nuclei of a singly decaying nuclide:

$$-\frac{dN}{dt} = \lambda N$$

where λ is a proportionality constant called the decay constant and has a unique value for any given radionuclide. $-dN/dt$ is in this simple case, equal to the activity, A, but generally, $A = \lambda N$. If the number of nuclei of the radionuclide present at time, t, equal

Nuclide Isotope	Half Life	Decay Mode	Energy(MeV)	Intensity %
^{134}Cs	2.062Y	ß	0.890	28
		ß	0.658	70
		ß	0.662	71
		γ	0.605	98
		γ	0.796	88
		γ	0.475	15
		γ	0.563	8
		γ	0.569	14
		γ	0.802	9
^{137}Cs	30.174Y	ß	0.514	94
		ß	1.176	6
		γ	0.662	84.8
^{210}Pb	22.26 Y	α	0.015	81
^{210}Po	138.4d	α	5.304	99
^{222}Rn	3.8235d	α	5.490	99
^{226}Ra	1599Y	α	4.784	94
		α	4.601	6
^{228}Th	1.913Y	α	5.421	73
		α	5.339	27
^{230}Th	8.0×10^{4}Y	α	4.687	76
		α	4.621	23
^{232}Th	1.41×10^{10}Y	α	4.016	77
			3.957	23
^{234}U	2.446×10^{5}Y	α	4.774	72
		α	4.723	28
^{235}U	7.038×10^{8} Y	α	4.397	57
		α	4.367	18
^{232}U	71.7Y	α	5.321	69
		α	5.264	31
^{238}U	4.468×10^{9}Y	α	4.196	77
		α	4.149	23
^{236}Pu	2.851Y	α	5.768	69
		α	5.721	31
^{238}Pu	87.71Y	α	5.498	71
		α	5.454	29
^{239}Pu	2.413×10^{4}Y	α	5.155	73
		α	5.143	15
^{240}Pu	6.57×10^{3}Y	α	5.159	75
		α	5.115	24
^{241}Pu	14.355Y	ß	0.020	99
^{241}Am	432.0Y	α	5.486	86
		α	5.443	13

Table 1.1: Decay characteristics of radionuclides of interest in this study (Lederer and Shirley, 1978)

to zero is N_o, then the number left after elapsed time, t, is given by:

$$N_t = N_o e^{-\lambda t} \qquad (1.1)$$

where,

N_t = the number of atoms of the radionuclide which have not decayed after time, t, from which it follows that:

$$A_t = A_o e^{-\lambda t}$$

The time required for the decay of exactly one half of the original number of nuclei present in a radioactive sample is called the half life or, $t_{½}$.

$$\text{Thus } ½N_o = N_o e^{-\lambda t_{½}} \qquad (1.2)$$

or

$$\ln 2 = \lambda t_{½} \qquad (1.3)$$

therefore,

$$t_{½} = \frac{\ln 2}{\lambda} = \frac{0.693}{\lambda}$$

The nuclide obtained as the result of a radioactive decay event is called the daughter nuclide, whereas the original radionuclide is known as the parent. In some cases, the daughter is itself radioactive and decays to form another nuclide, called the grand -daughter and the grand-daughter may in turn also be unstable. Such a series of radioactive decays is known as serial decay and a particularly important example

of this occurs in the decay series of the naturally occurring radionuclides, ^{238}U, ^{232}Th and ^{235}U as shown in Figure 1.1. In serial decay several different types of situation can develop depending upon the relative half lives of the parent - daughter pair as discussed below.

Considering the general parent - daughter relationship in which a parent nuclide, A, decays to produce nuclide B, then:

$$\text{Rate of production of B} = \frac{dA}{dt} = \lambda_A N_A$$

$$\text{Rate of decay of B} = \lambda_B N_B$$

$\therefore$ Overall rate of change of N_B is:

$$\frac{dN_B}{dt} = \lambda_A N_A - \lambda_B N_B$$

From equation (1.1) we can write $N_A = (N_A)_o e^{-\lambda_A t}$ and use this to eliminate N_A from equation (1.2). This gives

$$\frac{dN_B}{dt} = \lambda_A (N_A)_o e^{-\lambda_A t} - \lambda_B N_B$$

If we transpose $\lambda_B N_B$ and multiply by the integrating factor $e^{\lambda_B t} dt$, we have

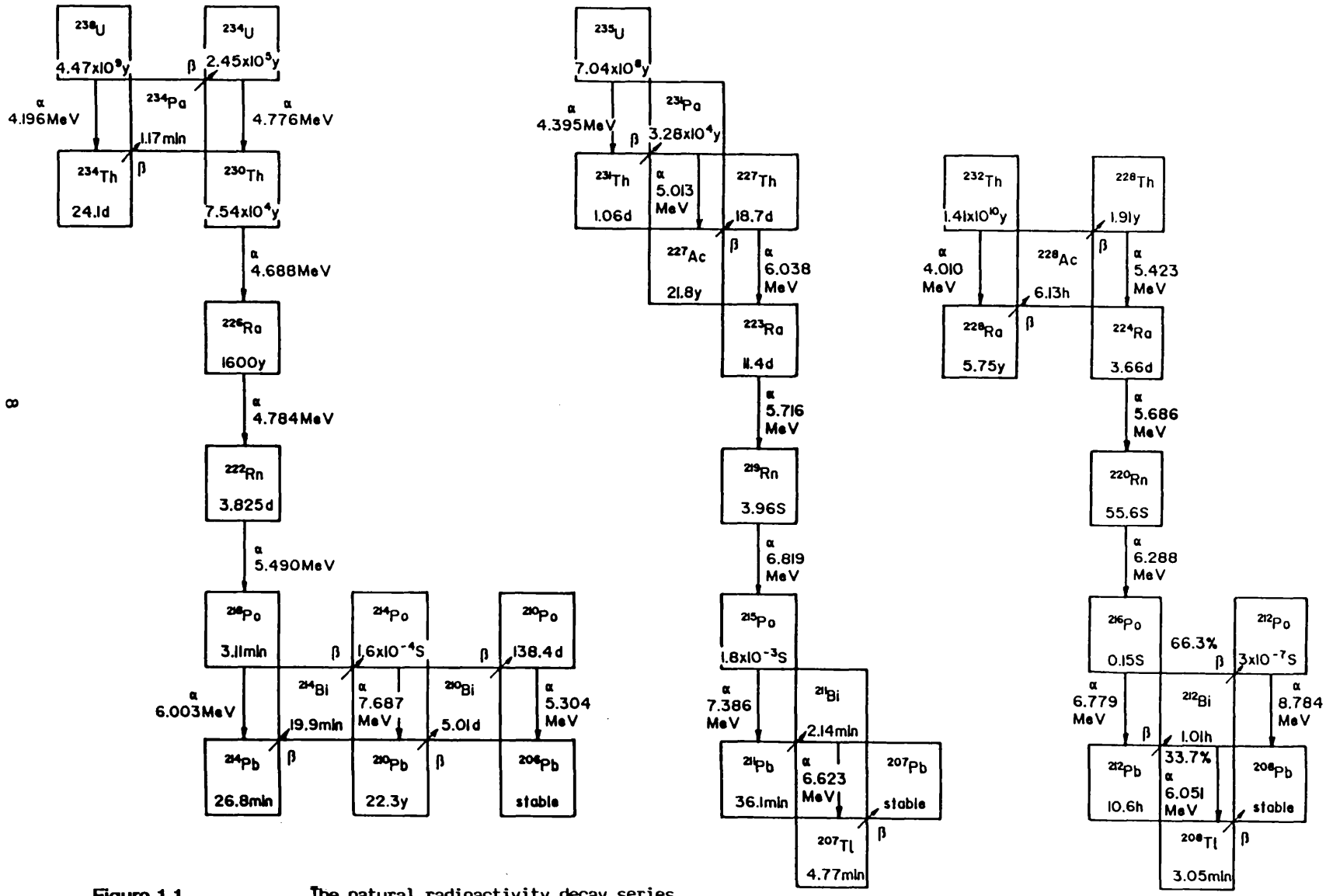

Figure 1.1 The natural radioactivity decay series

$$e^{\lambda_B t} dN_B + \lambda_B N_B e^{\lambda_B t} dt = \lambda_A (N_A)_o e^{(\lambda_B - \lambda_A)t} dt$$

This may be integrated at once, to yield

$$N_B e^{\lambda_B t} = \frac{\lambda_A}{\lambda_B - \lambda_A} (N_A)_o e^{(\lambda_B - \lambda_A)} + C \qquad (1.4)$$

since we are assuming that $N_B = 0$ when $t = 0$, we have:

$$0 = \frac{\lambda_A (N_A)_o}{\lambda_B - \lambda_A} + C$$

Eliminating C from equation (1.4), we obtain

$$N_B e^{\lambda_B t} = \frac{\lambda_A}{\lambda_B - \lambda_A} (N_A)_o (e^{(\lambda_B - \lambda_A)t} - 1)$$

and finally

$$N_B = \frac{\lambda_A}{\lambda_B - \lambda_A} (N_A)_o (e^{-\lambda_A t} - e^{-\lambda_B t})$$

In the case of more than two radioactive products in one chain reaction, the solution is given by the so called Bateman equation for a chain of X members with the special assumption that at $t = 0$, the pure parent substance only is present, that is, that $(N_B)_o = (N_C)_o \ldots = (N_X)_o = 0$. The general solution for the number of nuclei of the Xth product at t, N_X, is

$$N_x = C_A e^{-\lambda_A t} + C_B e^{-\lambda_B t} + C_C e^{-\lambda_C t} + \ldots C_x e^{-\lambda_X t}$$

where,

$$C_A = \frac{\lambda_A \lambda_B \lambda_C \ldots \lambda_{X-1} (N_A)_o}{(\lambda_B - \lambda_A)(\lambda_C - \lambda_A) \ldots (\lambda_X - \lambda_A)}$$

$$C_B = \frac{\lambda_A \lambda_B \lambda_C \ldots \lambda_{X-1} (N_A)_o}{(\lambda_A - \lambda_B)(\lambda_C - \lambda_B) \ldots (\lambda_X - \lambda_B)}$$

$$C_C = \frac{\lambda_A \lambda_B \lambda_C \ldots \lambda_{X-1} (N_A)_o}{(\lambda_A - \lambda_C)(\lambda_B - \lambda_C)(\lambda_D - \lambda_C) \ldots (\lambda_X - \lambda_C)}$$

Secular equilibrium is observed when the decay constant of the parent nucleus is much less than that of the daughter, (ie. the parent half life is much greater than that of its daughter).

Thus, if a radionuclide (A) having decay constant λ_A decays into nuclide B which has decay constant λ_B then these are said to be in secular equilibrium if the half life of A is much longer than B in which case $\lambda_A \ll \lambda_B$

$$A \xrightarrow[\lambda_A]{} B \xrightarrow[\lambda_B]{} C$$

If N_A and N_B are the number of atoms of A and B respectively at any time t, then the rate of decay of A is the rate of formation of B. Hence this condition of equilibrium of radionuclides can be expressed in the following equation:

$$\frac{N_A}{N_B} = \frac{\lambda_B}{\lambda_A} \text{ or } \lambda_A N_A = \lambda_B N_B$$

When the half life of a parent radionuclide is slightly greater than that of its daughter (ie. λ_A is slightly less than λ_B), a state of so called transient

equilibrium is reached. That is, after a certain time the ratio of the numbers of atoms and consequently, the ratio of the disintegration rates of parent and daughter become constant, so that:

$$\frac{N_A}{N_B} = \frac{\lambda_B - \lambda_A}{\lambda_A}$$

As a consequence of the state of transient equilibrium ($\lambda_B > \lambda_A$) the sum of the parent and daughter disintegration rates in an initially pure parent fraction goes through a maximum before transient equilibrium is achieved.

In the case where the half life of the daughter exceeds that of the parent (in which case $\lambda_A > \lambda_B$), no equilibrium is attained at any time. If the parent is made initially pure from the daughter, then as the parent decays the amount of daughter increases, passes through a maximum, and then decays at its own characteristic rate. The total activity in this case does not increase to a maximum (Friedlander et al, 1981).

The decay and growth of radionuclides in serial decay processes is of major importance in the natural decay series in natural systems and also in some cases involving manmade radionuclides such as the decay of ^{241}Pu to ^{241}Am.

1.1.3 Interaction of Radiation with Matter

a. Introduction

The following section provides a description of the basic aspects of the interaction of radiation with matter, a topic which is of fundamental importance in

this work since (a) the radiation detection methods used rely upon the quantitative observation of the effects of the interaction of radiation with matter and (b) an understanding of radiological aspects of environmental pollution with radionuclides, and the safe handling of radionuclides in the laboratory require a knowledge of the interaction of radiation with matter.

In a perfect vacuum, all forms of radiation will continue to move indefinitely, unless the particle is unstable. In solid, liquid or gaseous media, however, all forms of radiation lose energy and are eventually absorbed through a variety of different mechanisms. The processes by which alpha, beta and gamma radiations interact with matter all basically involve interaction with electrons, but show considerable variation in detail as discussed below.

b. Interaction of alpha radiation with matter

Alpha particles, being heavy and doubly charged, lose all of their energy within a short range in passing through matter. They interact with atomic electrons through a Columbic process which results in excitation and ionization of the atoms. The removal of electrons from atoms of the absorber by the incident particle is called primary ionization and the energy imparted to the electrons in the primary ionization process is often sufficient to cause further ionization, known as secondary ionization. In each ionization event affecting an originally neutral atom of the stopping material, a free negative electron and a residual positive ion are formed and alpha particles give rise to intense ionization with, for example, some 2000 to 6000 ions mm^{-1} produced along the path of an alpha particle in air, depending on the velocity of the

particle. The term ion pair means the residual positive ion and its negative counterpart regardless of whether the electron is free or attached. The energy required to produce an ion pair in any material is greater than the ionization potential of the atoms of that material and the additional energy is used in the excitation of the atoms and dissociation of the molecules of the medium.

The interaction of alpha particles with matter is generally expressed in terms of the energy loss per unit path length (also known as the specific ionization or stopping power) and the total range of the particle. In a given medium the specific ionization is expressed mathematically as dE/dX and can be derived from the general function relating specific ionization to the energy, charge and mass of an ionizing radiation particle:

$$-\frac{dE}{dX} = \frac{4\pi^4 eC^2}{mv^2} NC \ln \frac{2mv^2}{I}$$

where,

C = charge of the particle

v = velocity of the particle

m = mass of the particle

N = number of absorber atoms per unit volume

I = the effective ionization potential of the atom absorber

e = charge of the electron (Friedlander et al, 1981)

Alpha particles have very high values for specific ionization and consequently they have a very low penetrating power. The maximum distance which alpha particles travel in matter is known as the range and the alpha particle absorption curve for monoenergetic alpha particles as a function of distance of penetration of an absorber is flat, with no reduction in the number of alpha particles until a certain range is reached, at which point, there is a sharp decrease in the number of alpha particles over a very short distance ie. the alpha particles all travel approximately the same distance. The distribution of the observed ranges for alpha particles is Gaussian about the average range. Alpha particles have ranges of only a few centimetres in air at STP and are totally stopped by a thick sheet of paper. (Harvey, 1969; McKay, 1971; Friedlander et al, 1981).

The intensity of ionization produced by alpha radiation has important implications in radiobiology and in the analytical techniques which must be used for determination of alpha emitters. For example, when attention is focused on the absorbing medium, as in radiobiology, the short range of alpha radiation means that external alpha radiation does not in general pose a health hazard since alpha particles emitted from an external source will almost certainly be absorbed by air or by clothing before they can interact with people, and the outer dead layer of human skin in fact provides a substantial degree of protection for the inner living layers. In contrast, alpha radiation is very dangerous in the context of an internal radiation hazard, since the particles can interact with the living cells of the body and this results in severe tissue damage over the length of the alpha particle range. A further consequence of the very short range and high specific ionization of alpha particles is that

the success of alpha spectroscopy measurements is highly dependent upon chemical separation in order to selectively remove the alpha emitting nuclides from the bulk of the sample and from any interfering alpha emitting nuclide in the sample. The chemical separation methods commonly used in connection with alpha spectroscopy measurements are discussed in detail in section 1.1.5 and include co- precipitation with selected scavenger elements, solvent extractions, ion-exchange and electrodeposition techniques, the object in all cases being to achieve a highly selective separation with a high chemical yield. A chemical tracer (or spike) is normally added at the start of these procedures to monitor the yield and counting efficiency.

Once again, due to the short range of alpha particle radiation, an extremely thin, source of minimum mass on a perfectly flat planchette is the ideal aim in alpha spectroscopy to avoid loss of energy by self absorption and to achieve optimum resolution (Lally and Glover, 1984).

c. Interaction of beta radiation with matter

Beta particles are electrons and, as a consequence of their mass differences, the velocity of a beta particle is much greater than that of an alpha particle of the same energy. This fact, in conjunction with the singly charged nature of beta particles, results in a reduced efficiency for Columbic interactions of β^- particles with electrons and the specific ionization of beta particles is therefore much less than that of alpha particles. Such interactions involving beta particles, give rise to the ionization and excitation of the atoms in their path and the initial energy of beta particles is generally dissipated in a large number of

interactions, each of which gives a small energy loss, of the order of several electron volts, before the particle is finally brought to rest. The difference in specific ionization between alpha and beta radiations is illustrated by the fact that an alpha particle of energy 3MeV produces specific ionization of about 50000 ion pairs cm^{-1} in air at STP, whereas a beta particle of the same energy only produces about 50 ion pairs cm^{-1} under the same conditions (Pentreath, 1980). The ranges of beta particles in air extend from a few centimetres to several metres depending upon the particle energy and in aluminium, ranges of up to a few millimetres are observed (Friedlander et al, 1981).

Unlike alpha particles, beta particles can undergo a high degree of scattering and occasionally a high degree of energy loss in individual ionization events so that beta particles do not travel in a straight line through an absorber. Beta radiation attenuation in an absorber is therefore complex but an exponential absorption as a function of distance is in fact observed.

As beta particles pass through matter, some of the particles will occasionally pass close to the nucleus of an atom and the strong attractive force between the nucleus and the beta particle will cause acceleration of the particle and a sharp deviation from its original path. Energy loss in this process results in the emission of a photon of electromagnetic radiation known as Bremsstrahlung. The photons emitted have a spectrum with the maximum photon energy being equal to the kinetic energy of the incident beta particles and high atomic number absorber nuclei are more efficient than light nuclei in producing Bremsstrahlung.

As with alpha radiation, the nature of the interaction of beta radiation with matter has important implications for radiological considerations and for radioanalytical methods required for the analysis of beta emitters. Thus since the range of beta particles in air can be up to several metres and an energetic beta particle will penetrate human tissue to a depth of one centimetre or more, beta radiation represents an external, as well as an internal, health hazard.

In beta spectroscopy generally, the source of beta activity does not necessarily have to be thin, since self absorption effects are much less than for alpha radiation. Increasing the source thickness for very thin β^- sources can, in fact, increase the counting rate due to scattering of beta particles out of the sample plane and into the detector. After reaching a maximum of about 1.3 times the counting rate obtained from a massless source, however, the counting rate decreases as self absorption effects become dominant.

Because the beta particle energy spectrum is continuous for any given beta emitting nuclide, a high degree of chemical separation is, however, required to give a chemically pure source and for the same reason, yield tracers cannot generally be used in beta analysis.

Beta analysis can be a highly sensitive technique with very low limits of detection, but due to the difficulties involved in beta activity measurements, gamma spectroscopy is often used if possible as an alternative to beta spectroscopy eg. ^{137}Cs is a beta emitter but gamma spectroscopy is commonly used for its determination in samples with moderate to high specific activities (Harvey, 1969), although for very low specific activities, the more sensitive beta analysis is required (McKay, 1971; Yarwood, 1973;

Livingston and Bowen, 1978; Sholkovitz and Mann, 1984).

d. Interaction of gamma radiation with matter

Gamma radiation consists of high energy photons of electromagnetic radiation. These photons have a very low probability of interaction with the atoms they encounter in their path, giving rise to very low values for specific ionization and, when passing through an absorber, they retain their initial energy until they eventually interact by one of the following mechanisms:

i. The photoelectric effect

In this case, the photon transfers all of its energy to one of the inner bound orbital electrons in an atom of the absorber and absorption of the gamma photon energy (E_γ) causes ejection of the electron as a photoelectron with energy (E_e). The total absorption of the photon energy can only occur for a bound electron because the nucleus is essential for conserving momentum. Thus a free electron cannot absorb all the energy of a gamma photon to become a photoelectron.

The process is favourable for atoms of large atomic number and the probability of this effect is approximately proportional to Z^5 of the absorber. The effect is also more efficient for lower photon energies.

Energy is conserved in the photoelectric process according to:

$$E_\gamma = E_e + E_b$$

where,

E_γ = gamma photon energy

E_e = energy of photoelectron

E_b = binding energy of electron

The ejected electron is effectively a beta particle and causes further secondary ionization as described above for beta radiation.

ii. Compton scattering

This process involves an interaction between a gamma photon and an electron (which in this case can be either bound or free) and results in absorption of only part of the photon energy by the electron, leaving a scattered gamma photon of reduced energy. The electron is ejected from the atom in which it was initially contained and gives rise to secondary ionization as described for beta radiation. The probability of this effect depends only upon the number of free electrons available, and so is approximately proportional to the Z value of the absorber. Except for the highest and lowest energies the probability of this interaction does not depend markedly on photon energy. Once again, energy is conserved in this process according to:

$$E_\gamma = E_i + E_e + E_b$$

where,

E_i = energy of scattered gamma photon and other symbols are as defined above (Adams and Dams, 1970; Friedlander et al, 1981).

iii. Pair production

This effect can only occur for gamma photons of energy greater than 1.022MeV and involves the disappearance of photons in the process of creating a positron-electron pair. Each electron has a rest mass energy equivalence of 0.511MeV and the electron pair carries off the remainder of the incident photon's energy as kinetic energy. Pair production is always followed by annihilation of the positron by combination with an electron, resulting in the emission of two 0.511MeV gamma photons, known as annihilation radiation. The probability of this effect is proportional to Z^2 of the absorber and increases only logarithmically with increasing photon energy.

The electrons ejected in each of the three processes described above give rise to secondary ionization and detection of this ionization forms the basis for gamma spectroscopy measurements. As a result of the variations of the efficiency of these three processes as a function of photon energy and Z-value of the absorber, the photoelectric effect is predominant for low values of photon energy and for large values of atomic number of the absorber. Compton scattering is most efficient for intermediate photon energies and intermediate atomic number of the absorber, while pair production is dominant for high photon energy and large values for the atomic number of the absorber.

The interaction of gamma radiation with matter results in an exponential attenuation of the number of photons with distance of penetration:

$$I_d = I_o e^{-\mu d}$$

where,

I_o = the incident intensity

μ = the absorption coefficient

I_d = the intensity transmitted through a distance d.

A given thickness of material will therefore reduce the intensity of the gamma radiation by a constant factor. The thickness required to reduce the intensity by a factor of two is called the half-value thickness, and similarly, the thickness to reduce the intensity to one tenth of the original intensity is known as the tenth-value thickness.

High energy gamma rays can penetrate several centimetres of lead while the absorption of gamma radiation in air at standard temperature and pressure (STP) is negligible compared with those of alpha and beta particles.

Because of the dependence of the photoelectric effect on atomic number of the absorber, lead is by far the preferred shielding material for gamma radiation of photon energy less than 100keV. For higher energy photons, the photoelectric effect is not so dominant, but lead is still the most practical option for shielding material in general. The very low specific ionization of gamma radiation means that, while it must still be considered in the context of internal exposure, it is most often an external radiation hazard. The distance of an absorber from an external radiation source has a very important influence on the radiation dose, since the dose received is proportional to the number of photons incident on unit area of the absorber. In general terms, the radiation dose received at distance, d, from a point source is

proportional to $1/d^2$. So that if, for example, the distance is increased by a factor of two, the number of photons falling on unit area of the absorber is reduced by a factor of four.

As a result of the very low values of specific ionization for gamma rays, self absorption of gamma radiation is much less pronounced than in the case of alpha or beta radiation and source preparation for gamma spectroscopy measurements is completely different from that of alpha or beta spectroscopy. In the case of gamma counting, chemical separation and thin source preparation are not usually necessary, and thick sources can often be used in direct gamma spectroscopy analysis. This is relatively easy, requiring only homogenization of the sample and use of a well defined gamma detection efficiency. The dependence of photoelectric absorption of gamma photons on Z^5 of the absorber means that particular care must be taken to avoid variations in the average Z-values of samples or, if such variations do occur, to take account of them by use of appropriate standards.

1.1.4 Radiation Detection Methods

a. Introduction

The following section provides a summary of the basic principles of radiation detection methods, with particular emphasis on alpha and gamma spectroscopy which were the main instrumental methods used in this study. Solid state nuclear track detectors, which were used in a subsidiary part of the project to determine the distribution of alpha emitting nuclides in sediment samples, are also discussed in some detail. Many standard texts provide detailed coverage of these subjects and the following material was drawn largely

from works by Price (1964); Adams and Dams (1970) and Friedlander et al (1981).

The general principle underlying methods for detection of nuclear radiation is that, whatever the form of the radiation, it gives up some, or all, of its energy to the medium of the detector (as described in detail in the preceeding section) by ionizing it directly (ie. primary ionization), by causing the emission in it of primary ionization electrons which in turn produce further ionization called secondary ionization, or by excitation of electrons. The ionization or electron excitation produced is then detected by one of the following methods:

i. the charge may be collected directly by the application of a potential difference to the detector (eg. gas ionization and semiconductor detectors).

ii. light photons emitted during electron de-excitation may be detected by a photomultiplier tube (eg. scintillation detectors).

iii. the radiation particle may leave a trail of ionized atoms in the detector medium resulting either in "permanent" damage or transient reactions (eg. solid state nuclear track detectors or bubble chambers).

Historically, a variety of detector types, such as gas ionization detectors and scintillation detectors have been used for the detection of alpha and gamma radiation (Adams and Dams, 1970; Friedlander et al, 1981) but for most present research purposes, the semiconductor materials Ge or Si are used as the detector.

Although gas ionization detectors and scintillation detectors were not used in this project, a brief description of the operating principles and properties of these detectors is presented below for completeness.

The two most common types of gas ionization detectors are the Geiger and proportional counters both of which have the same basic construction, namely a glass tube containing a concentric metal tube acting as a cathode and a central metal wire acting as an anode. The tube is generally sealed and contains an inert gas such as argon as the detection medium. The gas in the Geiger and proportional counters is an insulator so that no current flows when a potential difference (lower than the discharge voltage for the gas) is applied across the electrodes. However, interaction of ionizing radiation with the gas produces electron-positron ion pairs and this allows a transient electrical current to flow. The electric field in these detectors causes acceleration of the electrons towards the anode and thus gives amplification to the pulse by collisions between the accelerated electrons and the gas molecules, resulting in further ionization. An increase of the pulse size by up to 10^6 times can be achieved in this way in Geiger counters but the output signal is a function of the individual tube and is not related to the radiation energy. In contrast, the output pulse from a proportional counter requires further amplification but is proportional to the energy of the radiation.

Geiger counters can be used for the detection and counting of radiation from alpha, beta and gamma decays when measurement of the energy of the particles is not required and low background proportional detectors are highly useful devices for the analysis of beta

emitters. The low density and consequent low efficiencies of these devices for detecting gamma radiation along with their poor resolution means that they are, however, of limited value for alpha and gamma analysis.

Detectors based upon the scintillation process are amongst the most commonly used instruments for radiation detection. In the scintillation process, the radiation energy causes promotion of electrons to excited levels in an inorganic crystal or in an organic molecule. The number of electrons promoted is proportional to the radiation energy and almost instantaneous de-excitation of these electrons results in the emission of light photons with an intensity proportional to the original radiation energy. The light photons are collected at the photosensitive cathode of a photomultiplier tube and cause the ejection of photoelectrons from the cathode. These photoelectrons are accelerated by the applied potential field towards the first of a chain of electrodes (called dynodes) where they are multiplied by secondary emission from the dynode. Repetition of this process down the dynode chain gives a voltage pulse which is finally collected at the anode. The amplification in the photomultiplier tube is highly linear so that the resulting pulse height is proportional to the incident radiation energy.

NaI(Tl) crystals, which consist of NaI with a deliberately added impurity of 0.1 to 0.2% of Tl to provide suitable energy levels to facilitate the scintillation process, are the most commonly used type of inorganic scintillation detector. The high density ($3.7 g\ cm^{-3}$) of NaI and the high Z value of iodine mean that these crystals have a high stopping power for gamma photons and are consequently efficient gamma

radiation detectors. NaI(Tl) crystals provide relatively inexpensive gamma detectors but they have limited resolution, with the best available resolutions for the 662keV gamma ray of ^{137}Cs being about 7% (Full Width at Half Maximum) (FWHM). This severely limits the usefulness of these detectors for complex gamma spectroscopy.

Liquid scintillation detectors probably represent the optimum detection method presently available for beta radiation detection. In this technique, the sample is dissolved in a solution along with an organic molecule which acts as the scintillator. In the liquid scintillation process, the solvent is the main stopping medium for the radiation and must be chosen to give efficient energy transfer to the scintillating solute and to have little light absorption. Liquid scintillation counters have a low efficiency for gamma radiation detection and very poor resolution and poor energy transfer in alpha radiation detection and have consequently found limited application, to date, for these purposes. The latest generation of liquid scintillation counters offering low backgrounds, pulse shape analysis and Multi Channel Analyser (MCA) capability may, to some extent, change this situation in the future.

Semiconductor detectors are now the most common type of devices used for research involving alpha and gamma spectroscopy and they present a number of distinct advantages for this purpose. In describing the use of semiconductors as radiation detectors it is useful to consider initially some of the basic properties of the semiconductors themselves.

A semiconductor is a material which has electrical properties intermediate between those of a conductor

and an insulator. The electrical properties of materials can conveniently be described using the band theory (Adams and Dams, 1970) of electron energies and in this model, the electrons are considered to occupy energy bands separated by a so called "forbidden" energy region. The upper band is the "conduction band" and any electrons occupying this band are mobile under the influence of an applied potential difference and so contribute to the electrical conductivity of the material. The lower band is the "valence band" where electrons are immobile since they are bound to specific atomic sites. In a conductor, the conduction band is permanently partially filled so that electron mobility is always possible. In an insulator, or a semiconductor at absolute zero temperature, the conduction band is virtually empty and the valence band is filled so that electron mobility is consequently not possible. The energy gap between the conduction and valence bands in insulators is too large (5eV or more) to allow electron promotion from the valence to the conduction band by thermal excitation. In a semiconductor, however, the gap is small (of the order of 1eV) and the electrons can cross the forbidden region following thermal excitation. The number of electrons in the conduction band increases with temperature according to the relationship.

$$N_e = f(T)\ e^{-Eg/kT}$$

where, (Adams and Dams, 1970)

N_e = the number of electrons in the conduction band

Eg = energy band gap

f(T) = temperature dependent function giving the number of possible positions of excited electrons

k = Boltzmann's constant

T = absolute temperature

The properties of a semiconductor therefore tend towards those of an insulator at low temperatures where the conduction band has a low level of occupancy and towards those of a conductor at high temperatures where there is a high electron occupancy of the conduction band.

Semiconductor materials are classed as being one of two types depending upon their degree of purity. Thus, very high purity materials which exhibit true semiconductor properties are classed as intrinsic semiconductors. In many cases, however, trace impurities are present at concentrations high enough to alter the electrical properties of semiconductors and such substances are classed as extrinsic semiconductors. A further subdivision of extrinsic semiconductors into n and p types, depending on the nature of the impurities, is also applied. Thus the group IV elements Ge and Si, which are the most useful semiconductors in the context of radiation detection, are tetravalent and atoms in their lattice consequently form covalent bonds with four adjacent atoms. If a group V element (eg. P), having five electrons in its outermost shell, occurs as an impurity and replaces a Ge or Si atom in the lattice then four covalent bonds will be satisfied leaving the fifth valence shell electron of the group V element unbonded. The energy level of this extra electron will lie in the forbidden region just below the conduction band as it is very lightly bound to the impurity site. The separation of

its energy level from the conduction band is very small about (0.1eV) and even as the result of thermal excitation, the electron can pick up sufficient energy to migrate to the conduction band leaving a net positive charge (hole) at the impurity site in the lattice. Under an applied electric field a current will flow due to the motion of these electrons in the conduction band and this type of material, containing an electron donor impurity, is called an n-type semiconductor. In contrast, p-type semiconductors are produced by the presence of electron acceptor atoms in Ge or Si. Thus if a trivalent group III element (eg. B) occurs as an impurity and occupies a Ge or Si lattice site then only three bonds will be saturated at this site, leaving one bond unsaturated. The energy level of an electron satisfying the fourth bond will be just above (~0.1eV) the Ge or Si valence band such that thermal excitation in the crystal can easily raise the electron from the valence band to this energy level. After accepting the electron, the group III element atom will become negatively charged and the lattice site from which the electron migrated will become a positive hole. Under an applied voltage a current will flow in such a material due to the motion of the positive holes.

On the basis of their electrical properties, semiconductors therefore have the potential to be used as radiation detectors provided they can be obtained with sufficiently few electrons in the conduction band that the material will normally be an insulator. Under these conditions, interaction of ionizing radiation with the semiconductor will promote electrons to the conduction band giving rise to a charge pulse proportional to the radiation energy, (ie. solid state analogues of gas ionization detectors). In some cases, suitable detectors can be produced from intrinsic

semiconductor material but in others modification of extrinsic semiconductor material is necessary to produce suitable detector properties, as discussed in the appropriate sections below.

b. Gamma spectroscopy

Semiconductor detectors are widely used for gamma spectroscopy research purposes and Ge, in particular, presents an attractive option for gamma detection since; (a) it has a high density (5.33g cm^{-3}) and with a Z value of 32 has a reasonable efficiency for photoelectric absorption of gamma photons and (b) it can be used to produce very high resolution detectors as discussed below.

Within the last few years improvements in manufacturing technology have meant that intrinsic Ge of suitable purity (impurity concentration of 10^{10} atoms cm^{-3}) has become available in sufficient quantities to allow the commercial production of gamma radiation detectors in the form of High Purity Ge Crystals (HP Ge). At liquid nitrogen temperature (77°K) these crystals contain so few electrons in the conduction band that they can be used directly as gamma radiation detectors by the application of a potential difference of several thousand volts across the crystal. Intrinsic Ge detectors of various types and sizes are available for different gamma spectroscopy applications and the catalogues produced by the commercial manufacturers provide an excellent source of up to date information on the operation and potential uses of these devices.

Some typical geometries of "state of the art" intrinsic Ge detectors are shown in Figure 1.2a. The basic type of intrinsic Ge detector is the coaxial detector which consists of a cylinder of high purity Ge with a diffuse

Li (n-type, 0.5mm thick) contact on the outer face and an evaporated gold (40mg cm^{-2}) or ion implanted B (p-type contact) on the rear surface of a coaxial well to provide the electrical contacts for the application of the high voltage across the active region. The interaction of photons within the active region produces charge carriers which are swept by the electric field to their collecting electrodes where a charge sensitive pre-amplifier converts this charge into a voltage pulse proportional to the energy deposited in the detector. A schematic diagram of a typical coaxial Ge detector is shown in Figure 1.2b. The crystal is contained under vacuum in a protective aluminium can and is maintained at its operating temperature by contact with a copper rod, the other end of which is immersed in a Dewar of liquid nitrogen.

The electronic modules required to generate a gamma spectrum from a Ge detector are shown in Figure 1.3, and consist of a bias voltage supply, a pre-amplifier, a spectroscopy amplifier, an analogue to digital convertor (ADC) and a multichannel analyser (MCA). The function of each of the modules is briefly described as follows.

The detector bias supply provides a voltage to the detector to effect charge pulse collection. For high resolution spectroscopy applications the bias supply must be well regulated (typically 0.001 to 0.002% variation in output) and stable, with extremely low ripple and noise content. The voltage supply for an intrinsic Ge detector would typically be used to apply a bias of several thousand volts and, in order to

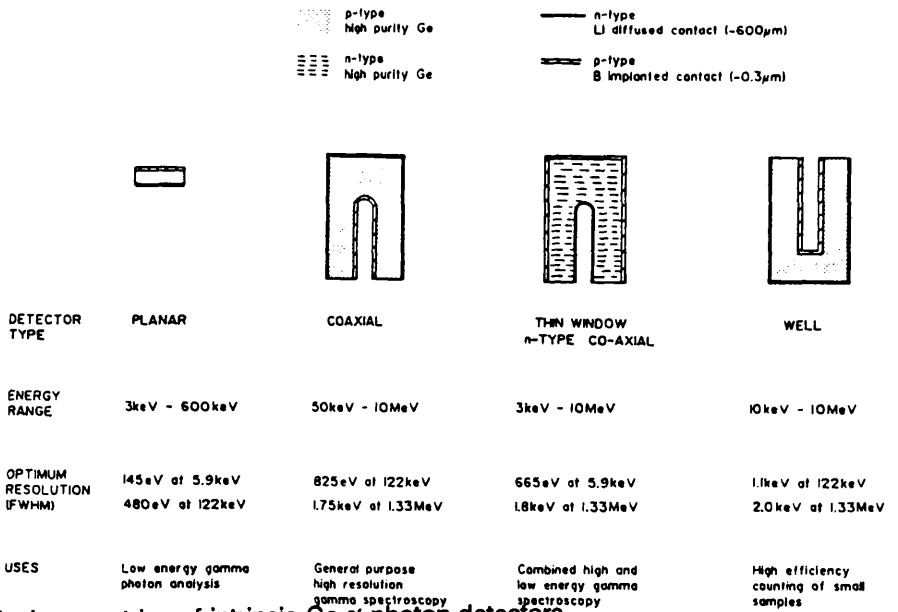

Figure 1.2a Typical geometries of intrinsic Ge γ-photon detectors

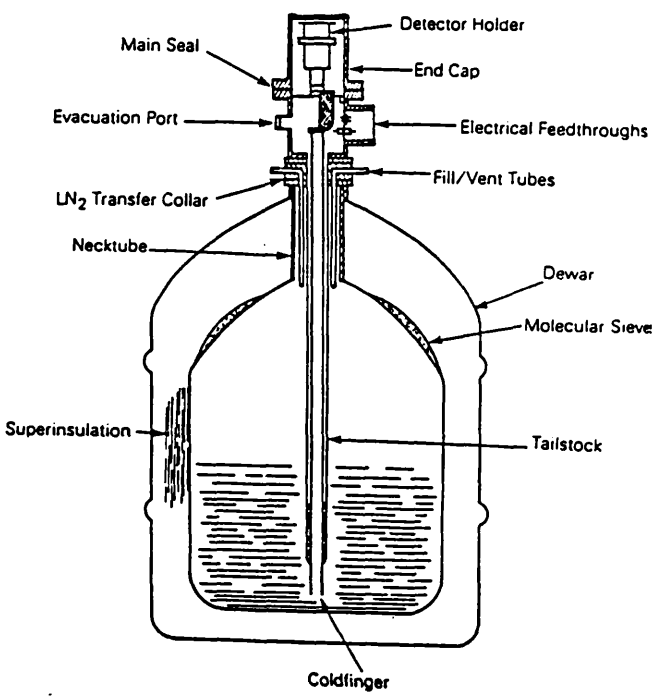

Figure 1.2b Schematic diagram of the construction of an intrinsic Ge detector

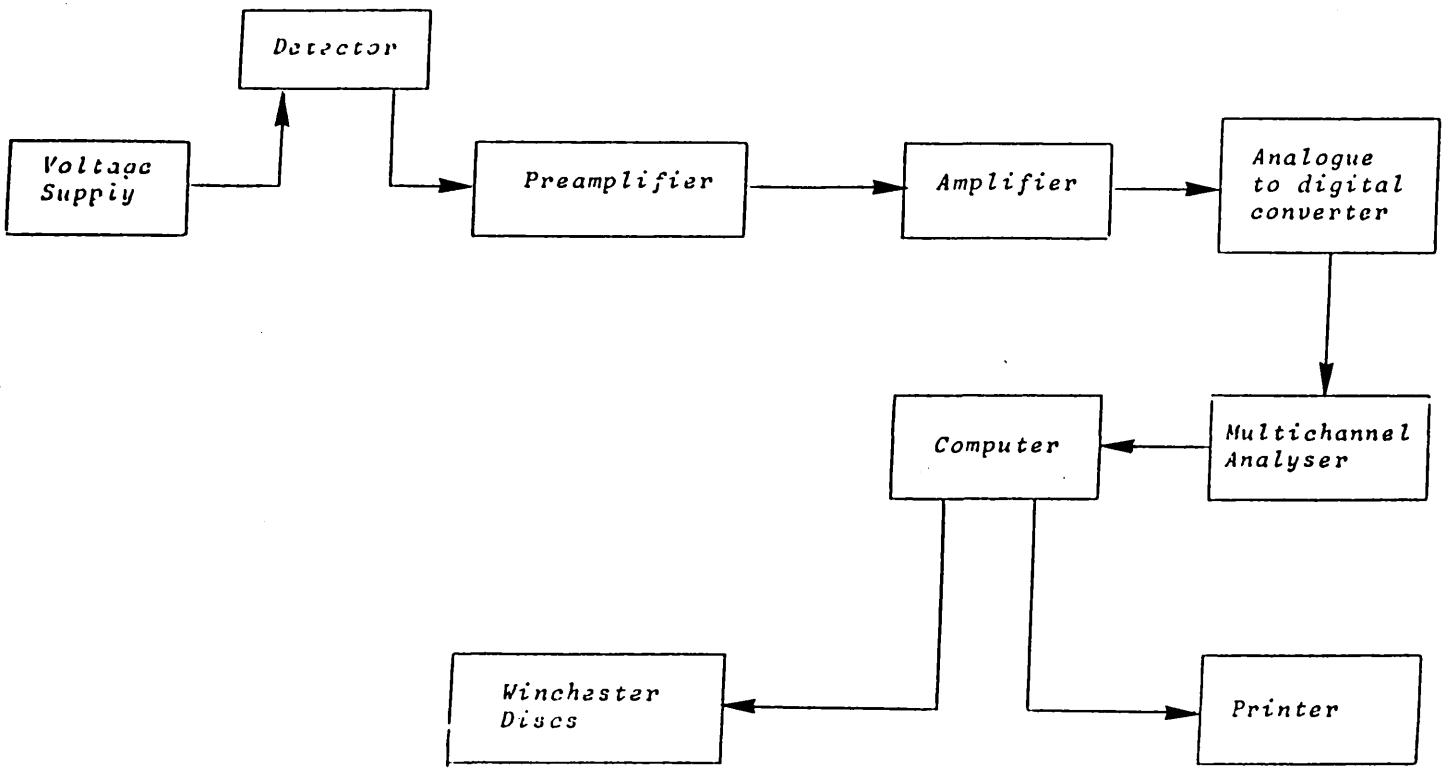

Figure 1.3: The main components of a typical gamma spectroscopy system

protect the field effect transistor (FET) which is incorporated in the input stage of the pre-amplifier, it is necessary to apply this voltage slowly. The charge sensitive pre-amplifier integrates the total charge produced in the detector into a voltage pulse. The pre-amplifier is mounted as close as possible to the detector to maximise the signal to noise ratio by avoiding unnecessary input capacitance of the interconnecting cables. The pre-amplifier is also an impedance matching device between the high impedance of the detector and low impendence of the pulse processing amplifier stage.

The spectroscopy amplifier accepts pulses from the pre-amplifier for shaping and amplification. The amplifier performs near Gaussian pulse shaping and the amplification factor (gain) used is typically in the range 10 to 100 and can be accurately adjusted using coarse and fine grain controls. The amplifier has a base line restorer to reduce the output voltage to zero when the pulse is received and a pole/zero cancellation circuit is also included to prevent under or over shoot of the pulses.

The ADC converts the amplitude of the voltage pulse from the spectroscopy amplifier into a digital number, with a high degree of proportionality again being achieved. Thus the overall function of the system is to generate a series of digital pulses which are proportional in size to the original gamma photon energies deposited in the crystal. The performance characteristics of an ADC are determined by its conversion gain, conversion speed, linearity and dead time. Conversion gain is the number of channels into which pulses are divided and a high conversion gain (4096/8192) is necessary in a high resolution gamma spectroscopy system. Conversion speed is the time

required to digitise the pulse and modern ADC's can provide conversion speeds of about 22μsec. During this time, no other pulse can be accepted and the system is therefore said to be "dead". The analysers compensate for this by counting for "live-time" periods such that for any given counting period, the actual time elapsed or "real-time" is equal to the sum of "live-time" plus the total "dead-time" during the counting period. Linearity, which is the deviation from the average channel or address, must be as low as possible, about 0.025% being a typical performance.

The digital pulses from the ADC, each representing an individual gamma photon energy, are transmitted to the MCA and are stored at locations in a "memory" (channel number) proportional to the input voltage of the pulse. Each channel represents an increment of the energy of the voltage pulse and consequently an increment in the gamma photon energy. The number of counts in each channel therefore represents the number of gamma photons of a defined energy that have interacted with the crystal. The data in the "memory" of an MCA can also be displayed in the form of an energy spectrum on a cathode ray tube. An MCA generally has the capability of acquisition, storage, display, readout and interpretation of the pulse data for gamma energy.

A source with a number of gamma emissions of known energy is used to define the linear relationship between channel number and gamma energy.

The typical energy range of gamma photons that can be analysed using a standard coaxial Ge detector is from about 30keV to more than 10MeV and the resolution (FWHM) at 122keV is typically in the range of 0.9 to 1.2keV while at 1332keV, FWHM values of 1.8 to 1.9keV are readily obtained. The energy resolution of a

detector for a radiation of a particular energy is mathematically expressed as full width of the peak at half its vertical maximum (FWHM). The smaller the FWHM, the better the resolution and vice versa. Resolutions obtained by Ge detectors are much better than those of NaI(Tl) scintillation detectors, as a result of the small amount of energy required for the formation of an electron-hole pair in the Ge detector which is approximately one hundredth the energy expended in the production of one photoelectron at the photocathode of a NaI(Tl) detector. Thus, since the resolution is governed by the spread on the number of charge carriers, given by the square root of the number of charge carriers, Ge detectors have substantially better resolution than NaI(Tl) detectors. The efficiency of Ge detectors is conventionally quoted relative to the efficiency of a 3" x 3"NaI crystal, in each case for detection of photons of energy 1.33MeV from a standard ^{60}Co source at a distance of 25cm from the end cap of the detector and relative efficiencies of up to about 100% can be obtained for coaxial detectors.

The gamma spectra produced by semiconductor (and NaI(Tl)) gamma detectors are the direct result of the interaction of gamma radiation with the material of the detector as discussed in section 1.1.3 (ie. photoelectric effect, Compton scattering and, for photons of energy greater than 1.022MeV, pair production). The energy lost in these discrete processes is transferred to electrons which are absorbed in the detector causing ionization and electron excitation. The photoelectric effect is the mode of interaction which generates the peaks used for analysis in gamma ray spectroscopy by deposition, in this case, of the energy of the photoelectron plus X-rays from the atom which lost the photoelectron. The

full peak which is also called the "photopeak" therefore appears in the gamma spectrum with a size which is proportional to the energy of the incident gamma rays.

Compton scattering gives rise to electrons with a continuous distribution of energies which are absorbed in the detector to give the so called "Compton continuum" extending from zero energy up to a maximum energy corresponding to the maximum energy imparted to the electrons in the Compton interaction, represented in the spectrum by the Compton Edge.

Annihilation of the positron produced in the pair production process gives rise to two gamma rays of energy 0.511MeV called annihilation radiation and a peak of this energy generally also appears in gamma spectra and is called the annihilation peak. One or both of the annihilation gamma photons may escape from the detector without interaction, in this case the gamma spectra may show single or double escape peaks at energies 0.511MeV or 1.022MeV respectively below the photopeak.

Other peaks which can also appear in gamma spectra include; sum peaks due to coincident detection of two gamma rays emitted by a source; the "backscatter peak" at 0.2 to 0.25MeV, due to gamma rays from the source which have undergone Compton scattering at a large angle with the surrounding material; characteristic X-rays of high Z value shielding materials such as lead.

A schematic diagram of a gamma spectrum showing some of the typical features described above is shown in Figure 1.4.

A modification of the coaxial Ge detector is the reverse electrode coaxial Ge detector, which has the position of the electrodes reversed. Since the p-type contact is extremely thin compared to the n-type contact, the low energy response of the reverse electrode Ge detector is better than the conventional Ge detector and the use of an ultra-thin Be window can extend the useful energy range down to 5keV. These detectors therefore provide enhanced efficiency at low energy but still give efficiencies equal to conventional coaxial detectors at higher energy, along with the advantage of very high resolution.

The planar detector is another type of intrinsic Ge detector, in this case fabricated from a thin circular disk (5 to 15mm thickness) of Ge with a Li diffused (n-type) contact on the rear side and a surface barrier p-type contact on the other. This geometry is useful for detection of low energy gamma photons since it has a very low efficiency for high energy gamma photons and has very high resolution.

A final variation is the Ge well detector which provides a high efficiency since the sample counting geometry approaches 4π. However, due to charge collection problems this type of detector gives generally poorer resolution ranging from 1.1 to 1.4keV at 122keV (FWHM) and greater than 2.0keV at 1.333MeV.

Intrinsic Ge detectors of this type have only become available at reasonable prices within the last few years and before the advent of these devices, suitable modification of extrinsic Ge had to be performed in order to simulate intrinsic semiconductor conditions. For gamma spectroscopy purposes, this was achieved in the Lithium drifted Germanium detector (or Ge(Li) detector) and, although now obsolescent, such detectors

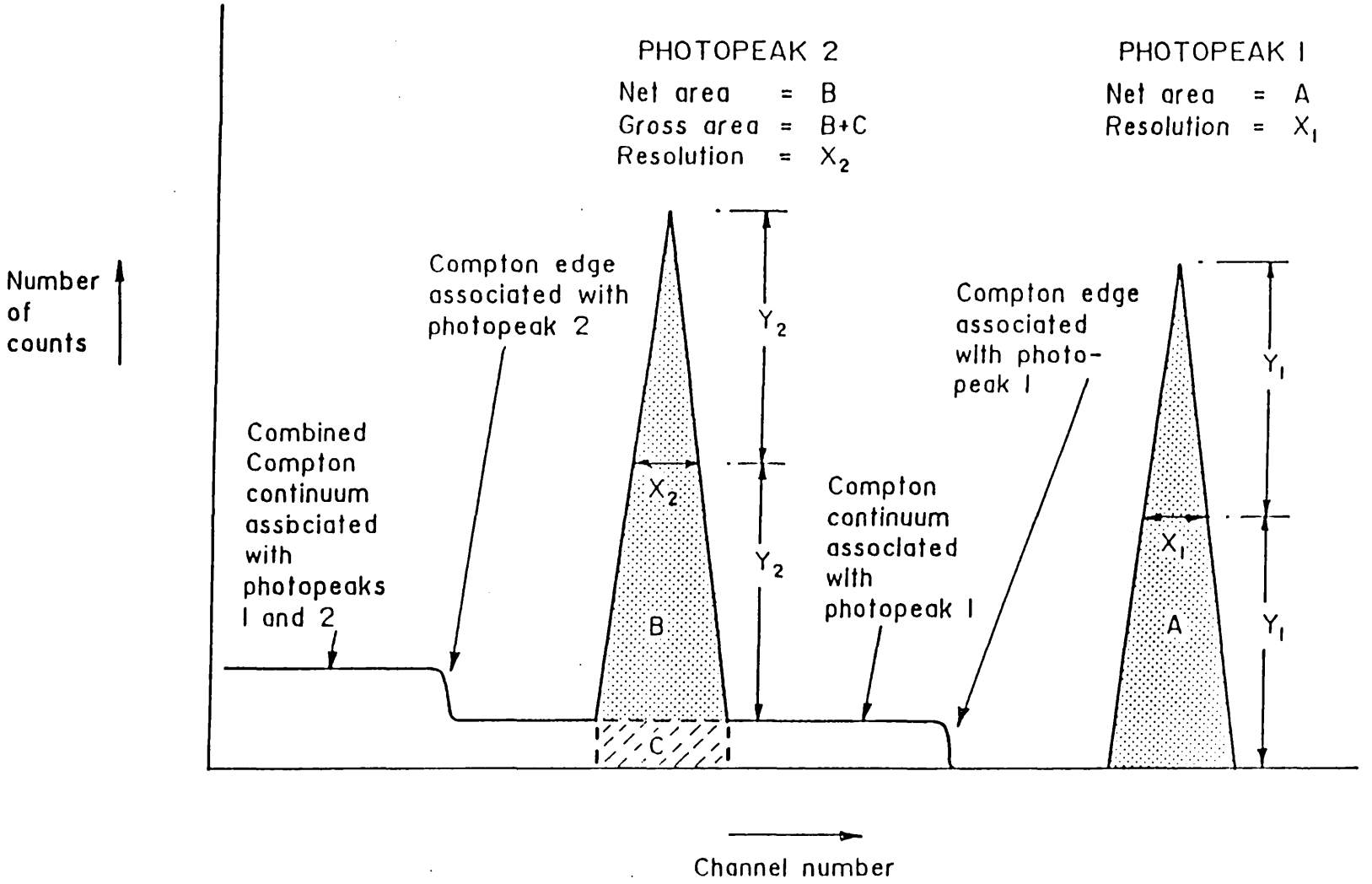

Figure 1.4: Schematic diagram showing the main features of a γ-spectrum

are still widely used in gamma spectroscopy research applications. In Ge(Li) detectors, defects in p-type Ge are compensated by the deliberate addition of Li to the crystal. In the Li addition process, Li-metal is coated on the side of the Ge-crystal and is diffused into the bulk material by heating to 400°C. This creates an n-type region near the exposed surface of the p-type semiconductor by pairing of Li atoms with p-type defects so that the Li 2s-electron is added to eliminate the defect and the Li^+ ion remains as an immobile species in an interstitial lattice position.

A p - n junction is thus formed and a reverse bias is applied across the junction to increase the depth of the compensated zone, which is depleted in charge carriers and is of very high resistivity. The crystal is then cooled to liquid nitrogen temperature, thus immobilizing the Li^+ ions, and must be permanently maintained at this temperature to preserve the Li drifted structure. The excess Li at the surface of the original p-type semiconductor converts the surface into an n-type layer which is used as an electrical contact.

The principle of operation of Ge(Li) detectors is basically the same as that described above for intrinsic Ge detectors, and involves the collection of the charge produced as electron-hole pairs by the interaction of ionizing radiation (gamma photons in this case) with the Ge. Ge(Li) detectors provide gamma detection performances approaching, but generally poorer than, those of intrinsic Ge detectors. However, Ge(Li) detectors have the major disadvantage that any warming of the crystal will destroy its properties whereas when voltage is removed from intrinsic Ge detectors, they can safely be allowed to warm to room temperature.

Typical resolutions (FWHM) obtained for Ge(Li) detectors are in the range 1.8keV to 2.0keV at 1332keV and the useful energy range which can be studied extends from about 50keV to 10MeV.

c. Alpha spectroscopy

Alpha particle detection is much less complex than gamma ray detection because alpha particle paths are more clearly defined and they deposit all of their energy, by a single dominant mechanism, directly within a small region of the detector as a consequence of their very high specific ionization. Semiconductor detectors are also used for alpha particle detection, but the detectors differ significantly from those used for gamma radiation detection in that they are very thin and are operated at room temperature. Si surface barrier detectors are the most common devices for alpha spectroscopy and they provide excellent properties namely: (i) high energy resolution (ii) high efficiency (iii) low background (iv) negligible interaction with beta and gamma radiations.

A surface barrier detector consists of a thin wafer of Si containing a junction between p-type and n-type sections. The density of electrons and holes is uniform in both the n- and p-type Si except near the junction where electrons from the n-region diffuse into the p-region and conversely holes from the p-type Si migrate into the n-region. The loss of negative charge, and gain of positive charge by the n-type Si in conjunction with the reverse situation for the p-type, eventually results in an equilibrium situation with a net positive charge on the n-side and net negative charge on the p-side of the interface. Under these conditions, a potential barrier (of about 0.5V)

is established across the interface thus preventing any further net charge transfer on either side. The junction is therefore a region of very low density of charge carriers ie. a depletion layer which exhibits a high electrical resistance. The p - n junction can be exploited for the detection of charged particles by the application of a reverse bias voltage (ie. positive on n, negative on p). This extends the depth of the depletion zone, giving a volume of Si containing virtually no charge carriers so that no current flows under the influence of the reverse bias. However, ionization produced in the depletion layer by alpha particles depositing their energy will produce electron-hole pairs that will be swept away by the applied potential, constituting a charge pulse that can be amplified and detected.

For alpha spectrometric measurement the output pulse from the detectors must be proportional to the energy of the alpha particle, which is only possible when the total energy of the particle is deposited in the depletion layer. It is therefore essential that the depth of the depletion layer should extend to the front surface of the detector ie. there should be no dead layer to reduce the energy of the particle before entering the sensitive volume of the detector. The depth of the depletion layer is related to the bias voltage by the expression:

$$d = \sqrt{KP\ (V + Vi)}$$

where,

d(cm) is the depletion depth

P (Ωcm) is the resistivity of n-type Si

V and Vi (volts) are the applied and natural potential difference respectively

K is a constant equal to 3.2×10^{-9} for n-type Si

For 5000Ωcm n-type Si, the depth of the natural depletion layer is 30μm and it can be extended up to as much as 5000μm by the application of the reverse bias. In alpha spectroscopy the ideal situation is achieved when the alpha particle is totally stopped but the depletion depth is low enough to present a negligible efficiency for other forms of ionizing radiation and this is achieved by a depletion depth of about 100μm.

In the production of a surface barrier detector, a p-type oxide layer is formed on one surface of a thin slab of n-type material by exposure to air. The manufacture process involves etching of the surface of the n-type Si wafer and evaporative deposition of a thin layer (40μg cm^{-2}) of gold on to it under oxidizing conditions to provide an electrical contact on the front face. On the other face, evaporated Al (40μg cm^{-2}) is used to form the electrical contact (Figure 1.5). In addition to the conventional surface barrier detector described above, modified alpha spectroscopy detectors are now available which offer improved performance in many areas. For example, passivated implanted planar Si detectors have recently been developed with ion implanted entrance windows which are stable, rugged and cleanable and have thicknesses less than those of Si surface barrier detectors. The leakage current is typically 0.1 to 0.01 of that of the Si surface barrier detector and this type of detector also offers improved alpha energy resolution and higher efficiency for low level alpha spectroscopy. Improved

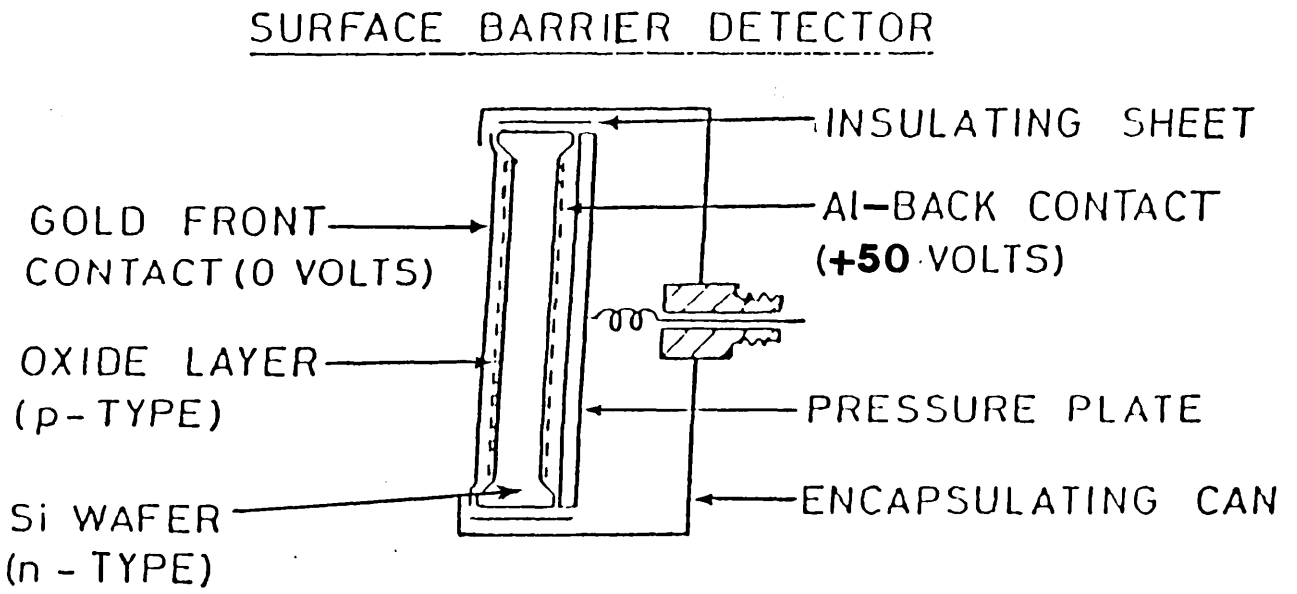

Figure 1.5: The construction of a surface barrier detector

surface barrier detectors with Al front contacts are also now available which share some of the passivated implanted planar Si detector's advantages over the old Si surface barrier detector ie. good resolution, high efficiency and capability of being cleaned.

The electronic system required for alpha spectroscopy is essentially similar to that already described for gamma spectroscopy and consists of the detector, connected to a bias voltage supply, pre-amplifier, spectroscopy amplifier, ADC and MCA as shown in Figure 1.3.

In alpha spectroscopy it is necessary to count the source in a vacuum chamber at reduced pressure to prevent degradation of the alpha particle energies by interaction with air since significant energy loss occurs with path lengths of only a few mm of air.

In an alpha spectroscopy system, the walls of the vacuum chamber prevent any external alpha radiation interacting with the detector and the small volume of the depletion zone gives a negligible efficiency for detection of other forms of radiation. Alpha spectroscopy systems therefore have very low background count rates. The resolution which is obtained in alpha spectroscopy varies as a function of the area of the surface barrier detector, with smaller detectors giving better resolution, and the typical range of resolution available extends from about 12keV to 40keV FWHM at 5.5MeV. Surface barrier detectors present a 2π counting geometry thus giving a maximum theoretical detection efficiency of 50% but, in practice, detection efficiencies in the range 20 to 30% are normally achieved. Since chemical separation of the nuclides being analysed is performed and thin sources are produced, typically by electrodeposition methods

(section 1.1.5), alpha spectra generally contain well resolved peaks separated by a zero, or near zero level baseline, giving relatively simple conditions for analysis of the spectrum.

d. Solid state nuclear track detectors

Solid state nuclear track detectors (SSNTD's) are used as the radiation detectors in an extremely simple and relatively cheap technique for the measurement of alpha particle radioactivity and the technique may be used for the investigation of the distribution of alpha emitting nuclides in samples. The method involves placing a sample containing alpha particle emitters in contact with a sheet of plastic (or other dielectric material eg. mica) for a suitable period of exposure, during which each alpha particle that interacts with the detector creates a narrow, intense ionization trail resulting in a track of damage on an atomic scale recorded in the detector. These damage tracks are developed to an extent where they are visible in an ordinary optical microscope by treatment with suitable chemical reagents such as sodium hydroxide solution (Hamilton and Clifton, 1981). These reagents rapidly and prefentially attack damaged areas of the tracks and much less rapidly remove the surrounding undamaged matrix (Fleischer et al, 1975). Certain concentrations of sodium hydroxide or mineral acid solutions are commonly employed for the etching process and suitable selection of the reagent concentrations, the etching time and temperature are extremely important in order to produce suitably etched tracks. For example, suitable etching conditions established by Hamilton and Clifton (1981), Fews and Henshaw (1984) and Kershaw et al (1986) involved exposure of the plastic to a 6.0M sodium hydroxide solution at 75°C for about 3 hours.

A wide variety of dielectric solid state nuclear track detectors are available in different types, thicknesses and sizes and one of the most useful for alpha track analysis is the plastic CR39, which is the polymerization product of the oxydi-2, 1-ethanedyl di-2-propenyl ester of carbonic acid (Fleischer et al, 1975; Hamilton and Clifton, 1981; Durrani and Bull, 1987). Hamilton and Clifton (1981) reported that most other plastic dielectric detectors suffer physical disadvantages relative to CR39, in particular with respect to inhomogeneity and anisotropy. CR39 is highly suitable as an alpha particle track detector since it is available in a wide range of thicknesses (0.08 to 1.3cm), has an abrasion resistance similar to glass, a specific gravity of 1.32 at 25°C, a refractive index of 1.505 at 20°C and is isotropic and homogeneous with respect to its ability to record ionizing radiations from alpha particles. Cross linking after radiation damage of chemical bonds does not occur, hence effective track resolution is enhanced compared with many other plastic detectors (Hamilton and Clifton, 1981; Durrani and Bull, 1987). CR39 is also resistant to most solvents except strong bases and highly oxidizing acids.

Solid state nuclear track detectors are widely used in many research fields including environmental radioactivity studies. For example, Hamilton (1981) used CR39 in studying alpha particle radioactivity of hot particles in suspended marine particulates, sediments and some forms of biota from the Esk estuary in Cumbria, north west England. Kershaw et al (1986) also used CR39 detectors to study hot particles in Irish Sea sediments.

1.1.5 Chemical Separation and Source Preparation Techniques in Alpha Spectrometry

a. General Principles of Separation Techniques

As indicated in previous sections, the requirements of source preparation vary for alpha, beta and gamma radiation detection. Thus, while thick sources can be used for gamma spectroscopy (often without chemical processing) and thick sources of pure chemical species can be used for beta analysis, the very high specific ionization associated with alpha emitters requires the separation of virtually massless sources to avoid alpha particle energy attenuation within sources. The accurate measurement of low-levels of alpha emitting radionuclides usually requires their complete separation from the sample matrix and from other alpha emitting nuclides in the sample. A separation scheme for analysis of an alpha emitting nuclide typically involves one or more processes such as solvent extraction, co-precipitation or ion exchange and the choice of method depends both on the nature of the sample and on the radionuclides to be determined.

The following discussion deals with general aspects of the special requirements of separation techniques for alpha emitting radionuclide analysis, with particular emphasis on the alpha emitting species involved in this study (uranium, thorium, plutonium and polonium). Also, particular emphasis will be placed on soil and sediment sample materials since they formed the central part of this work.

The first requirement in the analysis of alpha emitting nuclides in materials such as soils and sediments is the removal of organic material and in order to achieve

this, the sample is generally heated in a furnace at high temperature (450°C to 550°C). The second requirement is to obtain the elements of interest in solution in the presence of a yield tracer spike which is an isotope of the element being analysed but which is not present in the sample (eg. ^{232}U, ^{229}Th, ^{236}Pu), in order to equilibrate the spike with the nuclides in the sample. This is achieved by addition of the spike or internal standard to the ashed sample followed by acid digestion and leaching or by total dissolution of the sample using mineral acids such as hydrochloric, nitric and hydrofluoric acids (Talvitie, 1971; Wong, 1971; Hetherington, 1978; Lally and Eakins, 1978; Volchok and Planque, 1982).

Once the sample has been obtained in a liquid form, the next step is to remove the nuclides of interest from the matrix of interfering elements and the analytical techniques described below are commonly used for this purpose.

b. Co-precipitation techniques

This technique is defined as the precipitation of one substance in conjunction with one or more other substances. The co-precipitation method is usually used to isolate micro-quantities of radionuclides from large volumes of solutions. In the separation of alpha emitting nuclides, this technique can, for example, be used to quantitatively precipitate trace quantities of uranium, thorium and plutonium as hydroxides, carbonates, phosphates, oxalates, fluorides or iodates.

U^{4+} can be co-precipitated as the fluoride or phosphate from relatively strong acid, while U^{6+} phosphate is co-precipitated only from very weak acid solution (pH 5.0 to 6.0). Also, when co-precipitating U^{4+} with

hydroxides at pH 6.0 to 7.0, using ferric hydroxide as a carrier, the ammonia used must be free of carbonate, otherwise some of the uranium will remain in solution as the stable anionic carbonate complex, (Korkisch, 1969; Wong, 1971).

Thorium can also be co-precipitated as a hydroxide by adding ammonia at pH 5.5 to 6.0 and using ferric hydroxide as a carrier. Instead of ammonia, various other reagents may be used which provide an approximately constant and suitable pH for hydrolytic precipitation of thorium, (Katz et al, 1986).

A wide range of plutonium co-precipitation procedures with inorganic carriers is available and plutonium can be isolated in the form of hydroxides, fluorides and phosphates and the appropriate carrier is selected according to the elements interfering and the oxidation state of the plutonium, (Katz et al, 1986).

c. Solvent extraction techniques

This technique is a partitioning process based on the selective distribution of substances in two immiscible phases, normally an organic and an aqueous solution. The solvent extraction, or liquid - liquid extraction can be achieved either by extraction of the element to be separated into the organic phase, or by extraction of the interfering elements leaving the element to be separated in the aqueous phase. This technique has been widely applied to the extraction of uranium, thorium and plutonium from large numbers of interfering elements. When employing solvent extraction techniques, the most important considerations are the selection of a suitable organic solvent and the recovery of the solute from the organic extract. Recovery can be achieved by distillation, evaporation

or back extraction techniques. Amines, ketones and phosphates are the major three groups commonly used as extractants (Butler, 1965; McDowell et al, 1974; Reynolds and Scott, 1975; Volchok and Planque, 1982). Solvent extraction separations are mainly dependent for their successful operation upon the distribution ratio of the species between the organic and aqueous phase. Distribution ratios are influenced by the pH and salt concentration of the aqueous phase. Best selectivity in solvent extraction techniques can be achieved by accurately controlling the pH of the solution and addition of chelating agents such as Tri-n-butylphosphate (TBP), Thenoyltrifluoroacetone (TTA) and Ethylenediamine tetra-acetic acid (EDTA).

Uranium extraction using TBP as the organic phase and nitric acid as the aqueous phase is widely used due to the properties of the TBP such as (a) the relatively high distribution coefficients obtainable, (b) its non-volatility over a very wide temperature range, (c) its chemical stability and (d) its very low solubility in water. Furthermore, the use of EDTA in the extraction of uranium by TBP has proved very successful as the separation of uranium from almost all other elements is made possible. Also uranyl nitrate $[UO_2(NO_3)_3]^-$ can be extracted into organic liquids from nitric acid solutions after it has reacted with chelating agents such as TTA which is one of the most widely used. For example, uranium forms a complex with TTA which can be extracted from aqueous solutions of pH 3.0 or higher using 0.15 to 0.50M TTA in benzene, (Lally, 1982). Thorium, iron and rare earths are also co-extracted in this process, but Khopar and De (1960) have reported that the addition of EDTA and control of the solution pH to 6.0 improves the selectivity of uranium extraction.

Thorium, like uranium can be extracted with many organic solvents. The separation of thorium from uranium can be achieved by extracting with TBP in hydrochloric acid solution, (Korkisch, 1969). TTA in benzene or toluene is frequently used for thorium extraction and the extraction is best performed in nitric, hydrochloric or perchloric acid solutions. Ko and Weiller (1962) reported that extraction of thorium using TTA at pH 1.0 to 2.0 gives a good separation of thorium from uranium, aluminium, alkali metals and rare earths.

Plutonium can also be extracted using liquid - liquid extraction methods with different aqueous and organic reagents and Cleveland (1970a) has reported many different schemes which have been adopted for environmental plutonium analysis. The three major groups of extractants used for plutonium analysis are the same as those described above for the other actinides, namely phosphates, ketones and amines. The most widely used phosphate is di-2-ethylhexyl, (Butler, 1965; McDowell et al, 1974), while TTA is the most common ketone (Reyonlds and Scott, 1975; Volchok and Planque, 1982) tridodecylamine, tri-isooctylamine and other amines are used for plutonium extraction from other actinides and rare earths (Moore, 1958; Butler, 1965; Veselsky, 1976; Singh et al, 1979).

d. Ion exchange techniques

Ion exchange represents one of the most efficient and selective techniques for the separation of trace elements in analytical applications and separation techniques based on ion exchange are widely used in the analysis of radionuclides.

The term ion exchange is generally used to mean the

exchange of ions of like charge between a solution and a solid, highly insoluble body in contact with it. Ion exchange resins are synthetic, high molecular weight organic polymers containing a large number of functional groups which, in the ionic form, act as labile ions. These fixed ions are capable of exchanging with mobile ions in the surrounding liquid medium, without any major physical changes taking place in the structure of the resin. The most common forms of resin matrix available are the cross linked polystyrene and phenolic types, each of which is available with a variety of functional groups in both the cationic and anionic forms. In general the positive or negative charge produced by the fixed ions in an ion exchange resin is exactly neutralised by the charges on the counter ions. These active ions are cations in the case of cation exchange resin and anions in an anion exchange resin. Thus a cation exchange resin consists of a matrix containing fixed anions in contact with a solution containing active cations, while an anion exchange resin has matrix cations counter balanced with active anions (Korkisch, 1969; Minczewski et al, 1982). The general cation exchange reaction in an exchange resin is:

$$(ResA^-)\ B^+ + C^+\ (soln.) \longrightarrow (ResA^-)\ C^+ + B^+\ (soln)$$

The exchange reaction on cation exchange resin is best performed using a low concentration of acid, so that a high acid concentration can be used to achieve desorption of the metal from the resin either by mass action or, alternatively, desorption can be affected by decreasing the concentration of C^+ ion in solution by use of a complexing agent (Minczewski et al, 1982; Singh et al, 1984). The reaction with the ion exchange resin is reversible, so that by passing a solution containing B^+ ions through the product, the C^+ ions may

be removed from the resin and the original form is thus regenerated.

On the other hand the general anion exchange reaction is:

$$(ResA^{+})\ B^{-} + C^{-}\ (Soln.) \longrightarrow (ResA^{+})\ C^{-} + B^{-}\ (soln)$$

Anion exchange resins of the strongly basic type are, like the strongly acidic cation resins, completely ionized and hence can be used in a wide range of pH values. Adsorption of anions on strong base anion exchange resins is usually performed at high acid concentrations, while desorption occurs at low acid concentrations.

Ion exchange techniques provide a particularly powerful tool for chemical separation in the analysis of actinide elements. Thus, methods based upon ion exchange are commonly used for the separation of uranium, thorium and plutonium from each other and from other actinides, (Hyde, 1960; Grindler, 1962; Coleman, 1965; Minczewski, 1982) and to achieve the high degree of isolation of the actinide elements from the sample matrix required to produce suitably thin sources for alpha spectroscopy. Separations of uranium and plutonium are commonly performed by their adsorption on strong base anion exchange resins from either sulphuric or hydrochloric acid solutions, while the separation of thorium can be achieved either by its adsorption on a strong acid cation exchange resin or by anion exchange in a nitric acid medium.

A review of some applications of ion exchange techniques in actinide analysis is presented below:

i. Cation exchange

Uranium

A number of applications involving the separation of uranium from various sample matrices using cation exchange resins have been reported in the literature (Korkisch, 1969; Lally, 1982; Minczewski, 1982), but such methods are used less frequently than anion exchange for the analysis of uranium since most common cation exchange resins show only limited selectivity towards the uranyl ion. A higher degree of selectivity of uranium separation is obtained by the use of sulphuric acid than by using nitric or hydrochloric acid, since uranium is one of the few elements which forms stable anionic sulphate complexes (eg. $[(UO_2\ (SO_4)_2]^{2-}$ and $[UO_2\ (SO_4)_3]^{4-}$) and these can be eluted preferentially from a resin containing other elements (Grindler, 1962; Strelow et al, 1965).

In hydrochloric acid media, uranium cannot be separated clearly from many divalent and trivalent metal ions using cation exchange, because several of these elements form, like uranium, anionic chloride complexes, resulting in reduced adsorption on the cation exchange resins (Lally, 1982; Paunescu, 1986).

Separation of uranium from pure nitric acid solutions using cation exchange is poor because in this medium uranium, as well as many other metal ions, forms no complex (or only very unstable anionic nitrate complexes), especially at low nitric acid concentration. Low values for distribution coefficients are thus generally

obtained for uranium adsorption on cation exchange resins in sulphuric, nitric and hydrochloric acid media, and consequently the selectivity of uranium separation by cation exchange is low. Enhanced selectivity of uranium separation on cation exchange resins can be obtained by the use of an aqueous - organic solvent mixture containing hydrohcloric acid (Strelow et al, 1971; Katz et al, 1986).

Thorium

Thorium is adsorbed well onto strongly acidic cation exchange resins from each of hydrochloric, sulphuric and nitric acids. At constant molarity, the adsorption of thorium onto strongly acidic cation exchange resins is highest in hydrochloric acid and lowest in sulphuric acid. This is due to the fact that thorium does not form an anionic chloride complex in pure hydrochloric acid solutions but anionic complexes are formed in both nitric and sulphuric acid media. The separation of thorium in hydrochloric acid solutions with concentrations in the range 1.0 to 4.0M, allows this element to be isolated selectively from all metal ions which have smaller distribution coefficients than thorium (Sackett et al, 1958; Hyde, 1960).

Other media which can be used for the cation exchange separation of thorium from other elements include dilute nitric and sulphuric acids and ammonium chloride solutions (Korkisch, 1969). Thorium is also very strongly absorbed by cation exchange resins from organic solvent - water mixtures containing dilute mineral acids such as hydrochloric acid and nitric acid (Strelow et al,

1965).

In order to elute thorium from strongly acidic cation exchange resins, eluants such as 3.0M sulphuric acid and 0.5M oxalic acid have been used and of these 5.0M sulphuric acid is probably the most suitable, giving nearly quantitative (95%) elutions (Korkisch , 1969). At lower or higher concentrations of sulphuric acid the percentage of thorium eluted is considerably lower. The adsorbed thorium can also be recovered by ashing the resin and the resulting thorium dioxide can be dissolved in nitric acid containing a trace of sodium fluoride (Ahrland et al, 1975; Ivanovich and Harmon, 1982; Minczewiski et al, 1982).

Plutonium

Cation exchange mehtods are used less frequently than anion exchange for separation of plutonium from sample matrices, actinides or other metal ions. Plutonium in different oxidation states can be adsorbed well on cation exchange resins at low acid concentrations and is desorbed at high acid concentrations. However, many anions form neutral or anionic complexes with plutonium in all of its oxidation states, and plutonium may therefore be desorbed by reaction with anions of the acid, as well as by mass action displacement. The order of adsorbability of different oxidation states of plutonium on cation exchange resins is Pu^{4+} > Pu^{3+} > Pu^{6+}. The distribution coefficient values of plutonium on cation exchange resins show that the highest degree of plutonium adsorption occurs in nitric acid and the lowest in hydrochloric acid (Coleman, 1965; Ahrland, 1975; Lally, 1982).

ii. Anion Exchange

Methods based upon the anion exchange properties of actinides are frequently used to obtain highly selective separation of these elements from each other and from other interfering elements.

Uranium

The uranyl ion forms anionic complexes such as ($(UO_2\ Cl_3)^-$ and $(UO_2\ Cl_4)^{2-}$) in concentrated hydrochloric acid, and these complex anions can be adsorbed on strong base anion exchange resin with the efficiency of this adsorption increasing rapidly with increasing hydrochloric acid concentration. Many other metals also from anionic chloride complexes and hence are adsorbed along with uranium on anion exchange resins, but by varying the molarity of the hydrochloric acid, the isolation of uranium from these metal ions can be achieved (Korkisch, 1969). For example, Joshi and Ganguhly (1976) showed that uranium can be separated from a solution containing uranium, thorium and protactinium by loading the solution onto an anion exchange column in 12.0M hydrochloric acid. While uranium is adsorbed by the resin, thorium remains in cationic form and is not adsorbed from the aqueous medium and passes straight through the resin column. Protactinium is adsorbed but is preferentially eluted from the resin with 4.5M hydrochloric acid and finally uranium is eluted with 0.1M hydrochloric acid (Lally, 1982; Yamada and Tsunogai, 1983). A high degree of selectivity of uranium separation can be achieved in hydrochloric acid media by taking advantage of the different distribution coefficients on anion exchange resin exhibited by

ions in various oxidation states. For example, the radiochemical separation of U^{6+} and U^{4+} can be achieved from hydrochloric acid solution using anion exchange resin. Data reported by Grindler (1962) show that U^{4+} and U^{6+} are retained differently on anion exchange resin as a function of hydrochloric acid concentration. The above procedures were used by Cochran et al (1986) for analyses of samples of marine sediment and pore water and the results show that at 4M hydrochloric acid concentration, U^{6+} is quantitatively retained on the resin while U^{4+} passes through. Uranium and iron can also be separated on an anion exchange resin in chloride form if the iron is reduced to the divalent ferrous ion with ascorbic acid, ammonium iodide or hydrogen iodide (Cochran et al, 1986)

In pure nitric acid solutions U^{6+} is only weakly adsorbed on strong base anion exchange resins and maximum adsorption is obtained in the concentration range of about 6.0 to 8.0M nitric acid and with decreased sorption observed with an increase in the nitric acid concentration. This is probably caused by the instability of strongly basic anion exchange resins in concentrated nitric acid (Grindler, 1962; Korkisch, 1969; Lally, 1982). Anion exchange techniques which are based upon the separation of uranium in pure nitric acid media show very low selectivity compared to the uranium adsorption from nitrate salt solutions. Most metal ions which are not adsorbed on strongly basic anion exchange resins from pure nitric acid solutions are also not adsorbed in the presence of large amounts of nitrate salts, therefore the nitrate systems can be used for the quantitative separation of uranium from accompanying metal ions

and the uranium separations which can be achieved by using nitrates are often of very high selectivity (Korkisch, 1969; Katz et al, 1986). For example, in dilute nitric acid solutions which contain large amounts of soluble inorganic nitrates, uranium forms anionic nitrate complexes. For example, $[UO_2 (NO_3)_3]^-$ and $[UO_2 (NO_3)_4]^{2-}$ are readily formed at nitrate ion concentrations of 2M and 4 to 6M respectively and these complexes can be adsorbed on strong base anionic resins (James, 1967). Thus at a constant nitric acid concentration of 0.1M increasing the concentration of nitrate in the solution results in a rapid increase in the distribution coefficient of uranium. On the other hand, the distribution coefficient of uranium decreases if a constant concentration of nitrate is maintained but the molarity of nitric acid is raised (Grindler, 1962)

In dilute sulphuric acid solutions U^{6+} reacts with sulphate ions to form anionic sulphate complexes, with $[UO_2 (SO_4)_2]^{2-}$ being the dominant form and to a lesser extent $[UO_2 (SO_4)_3]^{4-}$. These sulphate complexes are strongly retained on strong base anion exchange resins in sulphate form. This adsorption is extremely high at low concentrations of sulphuric acid and decreases when the acid concentration is increased. The adsorption of uranium on strong base anion exchange resins is not only affected by the molarity of sulphuric acid but also by the concentration of sulphates. An increase of the sulphate ion concentration causes a decrease of uranium adsorption (Grindler, 1962; Korkisch, 1966).

For the elution of the uranyl sulphate complex adsorbed on strong base anion exchange resins,

dilute mineral acid solutions are mostly used. The efficiency of the various eluents depends upon two factors:

i. how effectively they can break up the sulphate complex and

ii. whether they can form anionic complexes with uranium.

For the complete elution of uranium the following eluents can be used: 0.25 to 2.0M nitric acid, 0.5 to 3.0M sulphuric acid, 0.25 to 1.0M hydrochloric acid and 1.0 to 2.0M perchloric acid. The most effective elution is obtained with perchloric acid because it readily destroys the uranyl complex and does not form anionic complexes with uranium (Korkisch, 1969; Lally, 1982).

Thorium

Unlike uranium, thorium is not adsorbed on strongly basic anion exchange resins from hydrochloric acid media since thorium forms no anionic chloride complexes. This fact is widely used to separate thorium from most monovalent and divalent elements in a concentration range of about 1.0 to 4.0M hydrochloric acid solution (Sackett et al, 1958; Strelow et al, 1965). This technique has also been successfully applied in the separation of thorium from other heavy elements and from fission product which do form anionic complexes in hydrochloric acid media (Lally, 1982; Minczewski et al, 1982).

In concentrated nitric acid, thorium forms a stable anionic complex $(Th\ (NO_3)_6)^{2-}$ which is

effectively adsorbed on strong base anion exchange resins from 5.0 to 10.0M nitric acid solutions (Korkisch, 1969; Lally, 1982). Reasonable selectivity can be obtained for the separation of thorium from other elements under these conditions and this separation technique is consequently the one which is most widely used for the anionic exchange separation of thorium (Katz et al, 1986)

The best eluents for desorption of thorium from strongly basic anion exchange resins are dilute solutions of mineral acids, which allow a rapid and quantitative elution, although it should be noted that thorium, like uranium, can be adsorbed on strong base anion exchange resins from dilute sulphuric acid solution (but with a much lower distribution coefficient than is observed for uranium), (Minczewski et al, 1982).

Plutonium

Plutonium in the oxidation states +4, +5 and +6 is strongly absorbed on anion exchange resins as anionic chloride complexes such as $(Pu\ Cl_5)^-$ and $(Pu\ Cl_6)^{2-}$ (Cleveland, 1970a, 1970b, 1979), but, in contrast Pu^{3+} is not adsorbed since it does not form anionic complexes in hydrochloric acid giving $(Pu\ Cl)^{2+}$ in 2.0 to 8.0M hydrochloric acid and $(Pu\ Cl_2)^+$ above 8.0M (Coleman, 1965; Marcus, 1966). Pu^{4+} is complexed even in very dilute hydrochloric acid solutions (0.3 to 0.4M) and the degree of complexing increases with increasing chloride ion concentration and above about 7.0M essentialy all the plutonium is in the anionic form (Grenthe and Noren, 1960). Generally the adsorption and desorption of plutonium can be achieved by varying the oxidation state, since lower oxidation states

show much lower distribution coefficients. In order to keep plutonium in the tetravalent oxidation state, and prevent its reduction to the non-adsorbed trivalent oxidation state, oxidizing agents such as nitric acid, sodium or ammonium nitrate can be used.

Similarly Pu^{4+} in nitric acid media forms anionic nitrate complexes like $[Pu(NO_3)_5]^-$ and $[Pu\ (NO_3)_6]^{2-}$ and plutonium is best adsorbed on strong base anion exchange resins as tetravalent ions from nitric acid solutions with molarities ranging from 6.0 to 10.0M and the maximum distribution coefficient of plutonium is observed at a nitric acid concentration of about 7.7M (Saito, 1984), with decreasing values being observed above this concentration due to the formation of $[HPu\ (NO_3)_6]^-$ and $[H_2Pu\ (NO_3)_6]$ (Ryan, 1960). Pu^{5+} is not adsorbed at all from nitric acid, while Pu^{6+} is very poorly complexed even in relatively high nitric acid concentrations, forming the anionic complex $[Pu\ O_2\ (NO_3)_3]^-$ only in 11.0M nitric acid (Cleveland, 1970a). The tetravalent state is the most stable oxidation state in nitric acid solutions, but it is sometimes necessary to condition plutonium to Pu^{4+} before proceeding with the ion exchange separation. This requires the reduction of all higher oxidation states to the trivalent oxidation state using suitable reducing agents, then Pu^{3+} is oxidized quantitatively to Pu^{4+} by addition of concentrated nitric acid or hydrogen peroxide.

Elution of Pu^{4+} from strong base anion exchange resins is best achieved by:

i. reducing plutonium to Pu^{3+},

ii. by reducing the nitrate concentration of the solution, or

iii. by adding an agent that forms a neutral or cationic complex with plutonium

Under these conditions plutonium can be separated from all or most other elements and this technique is so simple and effective that it has become one of the standard laboratory techniques for separation of plutonium (Cleveland, 1970a, 1979; Katz et al, 1986).

The final stage of actinide separation processes for alpha spectroscopy very often involves the electrodeposition of the radionuclide onto a stainless steel disc. In chloride solutions the electrodeposition mechanism involves a hydrochloric precipitate forming near to the cathode before being reduced to the metal and subsequently deposited on the cathode (Lally and Glover, 1984). A wide range of different electrolytes have been used for electrodeposition of actinide nuclides in either slightly acid or alkaline aqueous solutions. The electrolytes used for electrodeposition of actinides have been summarized by Rudran (1969) and Lally and Glover (1984), who indicate that the most commonly used electrolytes are ammonium salts including ammonium chloride, sulphate, oxalate and formate and these electrolytes have been used either singly or in various combinations. Low voltages of (12 to 20V) are usually used in the electrodeposition process with sufficient current capacity to give 300mA cm^{-2} of deposition area (Talvitie, 1971).

In the electrodeposition process, stainless steel discs

are generally used as the cathode and the anode is normally a platinum wire. The temperature must be controlled to avoid the loss of liquid and changing of pH, either by condensation of the vapour or by addition of cold distilled water. The time required for quantitative electrodeposition is generaly dependent upon the selected electrolyte and current capacity. Sources produced in this way are generally very thin and stable, giving suitable conditions for alpha spectroscopy measurement.

1.2 INTERTIDAL SEDIMENTS AND FLOOD PLAIN DEPOSITS

Almost all of the sediments in the oceans and the dissolved constituents in seawater are derived from weathering and erosion of continental rocks. The two main types of weathering are (1) physical weathering which is simply the fragmentation of rocks, for example by frost-shattering (when water freezes and expands in cracks), or by the cumulative effects of alternate heating and cooling, and (2) chemical weathering which is basically the decomposition of rocks through the reaction of surface water and ground water with rock- forming minerals, resulting in the formation of new minerals and the removal of material in solution. Weathering by biological agencies is mainly chemical, as many organisms secrete compounds that attack rocks. Some weathering by biological agencies is, however, physical; for example, the growth of plant roots in cracks can bring about physical fragmentation. The rate at which rocks become weathered depends on many factors, including climatic conditions, the strength, porosity and permeability of the rock, and the composition, size and shape of the constituent mineral grains. The dominant minerals of clastic, or detrital, sediments are those that are chemically the most stable at the Earth's surface and are physically the most resistant to abrasion. For example, the clay minerals are formed mainly by chemical weathering of feldspars and

ferromagnesium minerals in igneous and metamorphic rocks. All of the clay minerals are typically very fine grained and their crystal structure is such that they occur normally as flocks. Four main clay mineral groups are important in marine sediments namely: (1) Chlorite ($Mg_5Al_2Si_3O_{10}(OH)_8$). Chlorite can be released by physical weathering to form the clay component of sediments, but it can also be further modified or even destroyed by chemical weathering. As a consequence, chlorite is found mainly in sediments formed in cold high latitudes, where the weathering is predominantly physical and there is little chemical breakdown of minerals; (2) Kaolinite ($Al_2Si_2O_5(OH)_4$) which is formed mainly by the breakdown of feldspar, especially under warm and humid conditions, and is therefore found mainly in sediments whose source lies in equatorial regions; (3) Montmorillonite ($Al_2Si_4O_{10}(OH)_2.xH_2O$) which is formed mainly by chemical weathering and alteration of basic rocks, including volcanic ashes, though some results from the chemical alteration of other clay minerals; (4) Illite (K $Al_3Si_3O_{10}(OH)_2$) forms under a variety of conditions and so, unlike chlorites and kaolinites, is not characteristic of any particular latitude. The most abundant clay minerals found in the oceans belong to the Illite group. (Riley and Chester, 1976; Broecker, 1974).

Quartz (SiO_2) is the only common mineral of igneous and metamorphic rocks that is chemically stable at the Earth's surface as well as being comparatively resistant to physical breakdown. Detrital quartz therefore occurs commonly in marine sediments as sand.

In addition to these inorganic sources of sediments, the discarded shells of marine organisms can also constitute a significant source of material to marine sediments and organic matter can also occur as a significant component, particularly in nearshore and intertidal sediments.

Transportation of sediments to the ocean is mainly by water, but can also occur by wind and ice action in specific locations. The sediments of the intertidal zone in temperate latitudes are, in general, transported, sorted and distributed by water. The supply and distribution of intertidal sediments can change locally very rapidly on a seasonal or even diurnal timescale. Storms, floods or droughts can greatly affect the amount of sediments which are transported to the sea and distributed in the intertidal zone. The main sediment supply agencies in the intertidal zone are rivers which in fact provide the largest proportion of lithogenous solids to the oceans. About 90% of all sediments enter the oceans from the world rivers but river transported sediment has a wide range of particle size, and only a small proportion of material greater than 4μm in size reaches deep-sea areas directly. Thus most river borne sediment is initially deposited on the continental shelf and slope regions which act as intermediate sediment traps. Subsequently, these shelf and slope sediments may be transported to deep-sea locations by continental margin processes such as current action, sliding and slumping.

Currents, tides and waves are responsible for the dominant part of the kinetic energy of water in the intertidal zone and are therefore mainly responsible for sediment movement. Coastal currents, controlled by factors such as wind direction, shape and slope of the coastline and the Coriolis force, can result in significant sediment transport. Turbidity currents, involving the slumping of sediments down slopes, are important in the deep ocean but are less significant in the intertidal zone. Tides are also effective in sediment transport in the intertidal zone, with tidal currents reaching speeds of up to 1m s^{-1} in shallow waters. Waves are one of the most important agents of sediment transport in the intertidal zone and are generally responsible for resuspending sediment and thus allow sorting, especially by winnowing out the finer

particles which may then be deposited elsewhere. The longshore transport of sediment by waves striking a beach obliquely can be thought of as being due to either a wave-generated longshore current or the thrust component of the waves parallel to the beach. Waves can also transport sediment on and off-shore at different times, with high, steep waves tending to erode fine sand from beaches and transport it offshore, whereas low waves tend to move bars of medium sand shoreward. In waves of moderate size, suspended sediment is likely to be removed in this net offshore flow at mid-depths, whereas transport near the seabed will be onshore, because that is the direction of net bottom flow. Wind action is important in the transport of sediment to and from beaches. Some beaches are backed by sand dunes, formed by onshore winds transporting sand in the 100 to 500μm size range, which has been supplied to the beaches by waves. In most nearshore regions the input of lithogenous material to the sea by wind transport is very small relative to that from rivers. Thus the main influence of wind on the intertidal zone in temperate latitudes can be regarded as onshore transfer of material, particularly sand.

In summary, the main source of intertidal sediments is river-borne material consisting of detrital rock fragments, clay materials and quartz and the main mechanism of transport and sorting are waves and current action giving rise to physical sorting of the sediments. Intertidal sediments therefore consist of coarser and generally more heterogeneous material than deeper marine sediments.

True intertidal sediments may be considered as those deposits lying between the mean high and low water levels and which are subject to submergence by the sea on a twice daily basis. In addition, in some areas, the coastal zone may contain low lying flood plains which are subject to only very occasional incursion by the sea, often at times of

exceptional tides or under storm conditions. Thus these flood plain deposits may be submerged by seawater perhaps only one or two times per year. The sediment deposited in such areas is often composed of fine silt and, as a consequence of the transient influence of high salinity water, only a limited range of characteristic salt-resistant species of vegetation can survive in this zone. Generally trees do not occur and these salt marshes are often covered with salt resistant grasses, with the maximum high water mark being clearly delineated by a sharp transition to a different and more varied vegetation. Flood plain deposits of this type are often used for farming or other human activities and can thus represent a zone of direct human interaction with marine derived materials. Salt marshes represent a geochemically interesting environment in that sediment deposition often occurs under brackish conditions and once deposited, the marine derived sediments are subsequently exposed to markedly different geochemical conditions.

True intertidal deposits can be treated in general as simply being an extreme variety of marine sediments and the processes which normally affect marine sediments can be considered as also affecting intertidal sediments, although sometimes to a greater or lesser extent. The main differences between intertidal sediments and offshore marine sediments arise largely as a function of the often coarse particle size of intertidal sediments, the low and variable salinity of the water, the enhanced effects of irrigation produced by cyclical draining and transient exposure to air with possible partial drying.

The physical processes described above cause deposition, mixing, resuspension, movement and physical sorting of intertidal sediments. In addition to these influences, these sediments are also subject to a series of post-depositional effects which can be generally grouped under

the heading of diagenesis. These effects include physical processes such as compaction, chemical reactions and biological processes such as bacterial action and mixing. Diagenesis is therefore the result of a complex set of interacting influences involving the overlying water, the sediment, pore waters and the biological system and, as such, it is difficult to produce a rigorous definition for the overall process. Indeed it is hard to attribute a single cause to many of the observed effects and while the various processes are considered individually below it must be stressed that many of the influences will operate simultaneously. Diagenesis ultimately gives rise to solidified sedimentary deposits but the processes of relevance to intertidal sediments are those involved in the initial part of the process. In the following discussion, diagenesis will therefore be used in the context of "early diagenesis" as described by Berner (1980).

A summary of some of the more important aspects of diagenesis with respect to intertidal sediments is presented below. This summary is largely based upon the comprehensive reviews of the subject presented by Price (1976) and Berner (1980).

As mentioned above, many of the processes involved in diagenesis are inter-related, particularly those involving biological and chemical processes. It is therefore convenient to initially consider those processes which are dominantly physical in origin and then consider biological and chemical interactions.

Processes such as tidal and current action and waves have been discussed above in the context of sediment supply and movement. The major post-depositional effect of these processes is physical mixing of the sediment. Another physical process which is of major importance is compaction. This can be defined as the loss of water upward from the

pore water of any layer of sediment by the effect of increasing pressure due to overlying sediment. The effect of compaction is therefore to increase pressure, which can influence chemical reactions, and to cause an upward advective movement of pore water and any dissolved material.

The diffusion of ions or molecules in the pore water of sediment is a physical process which proceeds when a concentration gradient is established in the water. The diffusion laws governing the process are Ficks Laws of Diffusion, the one-dimensional forms of which are:

First Law: $$Ji = -D \frac{\partial Ci}{\partial x}$$

Second Law: $$\frac{\partial Ci}{\partial t} = \frac{\partial Ji}{\partial x} = \frac{\partial (D \frac{\partial Ci}{\partial x})}{\partial x}$$

For Constant D: $$\frac{\partial Ci}{\partial t} = Di \frac{\partial^2 Ci}{\partial^2 x}$$

where,

Ji = diffusion flux of component i in mass per unit area per unit time;

Ci = concentration of component i in mass per unit volume;

Di = diffusion coefficient of i in area per unit time;

x = direction of maximum concentration gradient.

A detailed discussion of the application of these equations to sediments is provided by Berner (1980).

Biological processes in the sediments have both physical and chemical consequences. For example, one of the most important physical results of biological activity in surface sediments is bioturbation, which is the mixing process resulting from the activities of benthic organisms in the sediments. Bioturbation occurs in several different ways. For example, some organisms, such as crabs and snails, mix surface sediment simply by crawling and ploughing through it whereas others, such as polychaete worms and bivalves, burrow into sediments and ingest the sediment particles. Such burrowing can extend to several tens of centimetres. Once their burrows are constructed, some organisms remain in them and flush the burrows with overlying seawater, thus bringing about enhanced exchange between porewater and overlying seawater in the process of irrigation.

The overall effect of bioturbation is complex and in attempting to describe the results of bioturbation, the simplest approach is to assume that rapid mixing of the sediment occurs throughout a zone within which there is a high level of biological activity, and that the sediment properties are uniform from the sediment-water interface down to this fixed depth of mixing. Bioturbation of pore water in nearshore sediment can exhibit seasonal variations and can be much more rapid than particulate bioturbation, (Sholkovitz and Mann, 1984; Goreau 1977). Aller (1977, 1980) suggested that enhanced pore water bioturbation is best described as the irrigation of burrows, and proposed an irrigation model to describe this process.

Chemical changes in near surface sediments are often intimately linked with biological processes and so it is best to consider the two together. Diagenetic changes taking place within sediments are obviously important in

determining the final nature of the sedimentary deposit and are also of major importance in controlling chemical fluxes between the sediments and the overlying seawater. Shallow water marine sediments and intertidal sediments often contain substantial amounts of organic matter and terrigenous detritus and are therefore often sites of intense chemical and biological activity. The dominant factors controlling diagenetic reactions are the sediment accumulation rate, the amount and type of organic matter present and the rate of consumption of organic matter by biological systems.

In most nearshore sediments bacteria and other living organisms are the most important agents responsible for the change in the physico-chemical character of the sediments. For instance, the pH and Eh at any position at depth within the sediment appear to be a function of the net balance between the types of bacteria, the amounts of metabolizable organic matter, the buffering capacity of the sediments and the diffusion rate of oxygen through the sediment. In this respect, much of the change in inorganic as well as organic constituents that occurs during burial is related directly, or indirectly, to the population and activity of organisms within a sediment. Respiration, photosynthesis and the decay of organisms cause changes in the carbon dioxide and ammonia content of sediment pore waters and thus are important in determining the pH of the interstitial waters. A thermodynamic model for the sequence of redox reactions involving elements, such as Mn, Fe, N, S, and C which may be applied to oxidation/reduction reactions during sediment burial has been suggested by Sillen (1966). In this model the oxidation of organic matter will supply electrons firstly to the lowest unoccupied electron level, ie. dissolved O_2 and then successively to the next highest level, eg. NO_3^-, NO_2^-, Mn^{4+} and so on, until the redox potential is sufficiently low for fermentation and reduction of SO_4^{2-} and CO_2 to take place. Many oxidation and reduction

reaction rates in the natural environment (such as certain metal-ion oxidations, oxidation of sulphide and sulphate reduction) are very slow but enzymes can act as redox catalysts for these reactions thus accelerating the process. In the enzyme catalysed process it is probable that several redox reactions take place simultaneously so that gradual changes in composition will occur as the redox potential of the system varies, rather than the stepwise ones which would be expected if thermodynamics was the sole controlling factor. All of the processes described above may occur simultaneously within the zone of bioturbation of intertidal sediment. Also, strong horizontal gradients in organic matter content can occur as the result of the presence of discrete organic remains in the sediment. Horizontal gradients in pore water composition are brought about by stirring and by irrigation of burrows with overlying seawater. The normal depth succession of deoxygenation, denitrification, sulphate reduction, and methane formation can therefore occur over short distances depending upon the local conditions in the sediment. The main elements influenced by redox processes in sediments are Fe and Mn and others involved are C, N, O, H, and S which are all closely linked to various biological processes.

In recent years diagenetic reactions involving manganese in marine sediment have attracted considerable attention. The dissolution, migration and precipitation of Mn phases in media of different pH and Eh are important in such studies. Many oxidising surface sediments become reducing when they are buried and reduction of Mn at some depth in the sediment can often be discerned by a colour change from brown oxidised surface sediments to grey coloured, reduced sediments. In nearshore sediments this colour change is usually well defined, and takes place in about the upper 5cm of the sediment (in oceanic sediments the thickness of oxidised layer may be substantially greater). Under highly oxygenated conditions Mn occurs only as insoluble Mn^{4+}

hydroxides or oxides but at depth, where reducing conditions prevail in the sediment, is converted to soluble Mn^{2+} ions. The concentration of soluble Mn^{2+} in sediment interstitial waters is controlled by two main factors: (1) the solubility of the sulphide and carbonate; (2) the upward movement of ions out of the reduced zone, and their reprecipitation as Mn^{4+} at, or near, the sediment-water interface. From diffusion controlled models the concentration of manganese and related elements in sediment interstitial waters would be expected to show an exponential increase with depth. This concentration gradient together with sediment compaction, will cause an upward movement of ions through the sediment. When conditions are favourable their reprecipitation may occur near the sediment-water surface. Deviations from the idealized pattern can be produced by reactions with anions and precipitation of $MnCO_3$ at depth in sediments has been observed both in deep ocean and nearshore situations (Manheim, 1976).

Manganese diagenesis is of importance in nearshore and intertidal areas. For example, Calvert and Price (1970) describe the formation of manganese nodules in Loch Fyne in the Clyde Sea Area and MacKenzie and Scott (1982a) provide manganese profiles for intertidal sediments from southern Scotland which show distributions characteristic of diagenetic reactions. Manganese diagenesis is of intrinsic scientific importance, but is also important since manganese deposits efficiently scavenge other species from seawater. eg. Aston and Stanners (1981) have shown that most of the plutonium in intertidal sediments in Cumbria is associated with the manganese oxide phase of the sediment. Thus, uptake of radionuclides in manganese oxide deposits provides a means of radionuclide removal from seawater to the sediment but, conversely, manganese diagenesis may result in associated changes in the speciation of radionuclides in sediments.

Flood plain deposits represent an extreme limit of marine influences and, in many cases, the source of sediments producing flood plain deposits and their main mechanism of transport can be similar to those of intertidal sediments. Flood plain sediments are, however, subject to markedly different geochemical conditions to those affecting true intertidal sediments and they are, in most ways, better regarded as soils. Thus, once flood plain material is deposited and the contained seawater drains from the system, the sediments are subsequently exposed to physical, chemical and biological weathering processes which are significantly different from those which normally affect true intertidal sediments. Flood plain deposits are exposed to air for most of the year and are therefore, at least on the surface, exposed to oxidizing condition. Also rain water, ground water, and river water draining through these sediments can cause many changes in their physical, chemical and biological conditions, notably giving a large reduction in their salt content. Physical sorting processes affecting flood plain deposits include mechanical processes such as expansion of water on freezing, growth of roots, river and ground water movement and marine floods. Chemical weathering also exerts a major influence on these sediments and the process can be regarded as the approach to chemical equilibrium of a system involving soil, air and water. The free availability of air and fresh water in flood plain sediments gives rise to considerably different Eh and pH conditions to those under which the sediments were initially deposited, resulting in differences in solubility and giving rise to changes in the chemical composition of soil minerals. For instance, the dissolution of carbon dioxide affects the pH of the soil solution and the solubility of soil carbonates. Carbon dioxide dissolves in water and rapidly establishes an equilibrium to form the weak acid H_2CO_3. In the soil, soluble salts such as sodium chloride, alkali and alkaline earth cations (mostly Na, K, Mg, Ca), the halides, sulphate and silica tend to remain in solution

and they are consequently carried down through the soil profile by percolating rainwater and ultimately are transported out of the system entirely (Bohn et al, 1979). In contrast, minerals which are resistant to chemical changes induced by soil conditions are accumulated near the surface unless any physical changes take place to remove them. The differences between the chemical conditions of flood plain and true intertidal sediments result in different biological populations in the two environments so that bioturbative sorting processes differ between the two, although the physical results of the processes (eg. mixing, enhanced irrigation) are often similar. Finally it should be noted that mixing and movement by physical processes is generally much less pronounced for flood plain sediments than for intertidal deposits.

The present study was concerned with intertidal sediments and flood plain deposits in south west Scotland and a considerable range of sediment types is found in the area with rocky shorelines containing gravel and shingle beaches, sandy beaches and fine silt and mud deposits in different areas. Extensive flood plain deposits occur along the shoreline of the Solway Firth and these are known locally as Merse deposits. Four main study sites were of interest in this work (Figures 1.6, 1.7, 1.8 and 1.9), namely:

a. Ardmore Bay

Ardmore Bay, which is situated on the north bank of the Clyde Estuary occupies an area of about 0.5km^2. There is no major river flowing directly into the bay so that any fresh water input is as direct runoff from the land or from the rivers Clyde and Leven. Saline water from the Atlantic Ocean and Irish Sea can reach the bay via the Firth of Clyde and the North Channel. The absence of a direct river input also means that the major source of sediment to the bay is from the Estuary. The surface sediments to the seaward end

of the bay consist of sand with a transition to a mixed deposit of sand and clay near shore. Ardmore Bay has a diverse biological population including eg. Arenicola marina, Talitrus Saltator and Crangon Vulgaris. The geochemistry of the sediments and their accumulation and mixing characteristics have previously been the subject of a detailed study by Ben-Shaban (1985).

b. Skyreburn Bay

Skyreburn Bay lying on the north coast of the Solway Firth in south west Scotland occupies an area of about 1.0km^2 on the northern side of the larger Fleet Bay. The bay consists of a highly heterogeneous mixture of silt, sand, shell fragments and detrital stones and rock fragments. Organic matter in the form of seaweed can also occur occasionally in high concentration. Only two narrow river channels flow into the bay.

The intertidal sediments of the bay support a diverse biological population including Arenicola marina and the Amphipod Corophium Volutator as well as large colonies of migrating birds (MacKenzie and Scott, 1982a).

c. The Merse Deposits of the Solway Firth

The merse deposits are relatively large areas composed mainly of fine silt, individually being as large as 9km^2 and covering a total area of about 70km^2 on the north Solway coast. The merse areas are covered with seawater only infrequently and the boundary of the merse is generally fairly clearly defined as the mean high water mark at the seaward extremity and a sharp transition from salt resistant grass coverage to trees and bushes at the landward end. Since the rivers draining into the Solway reach it over gentle gradients, they carry into it little material in

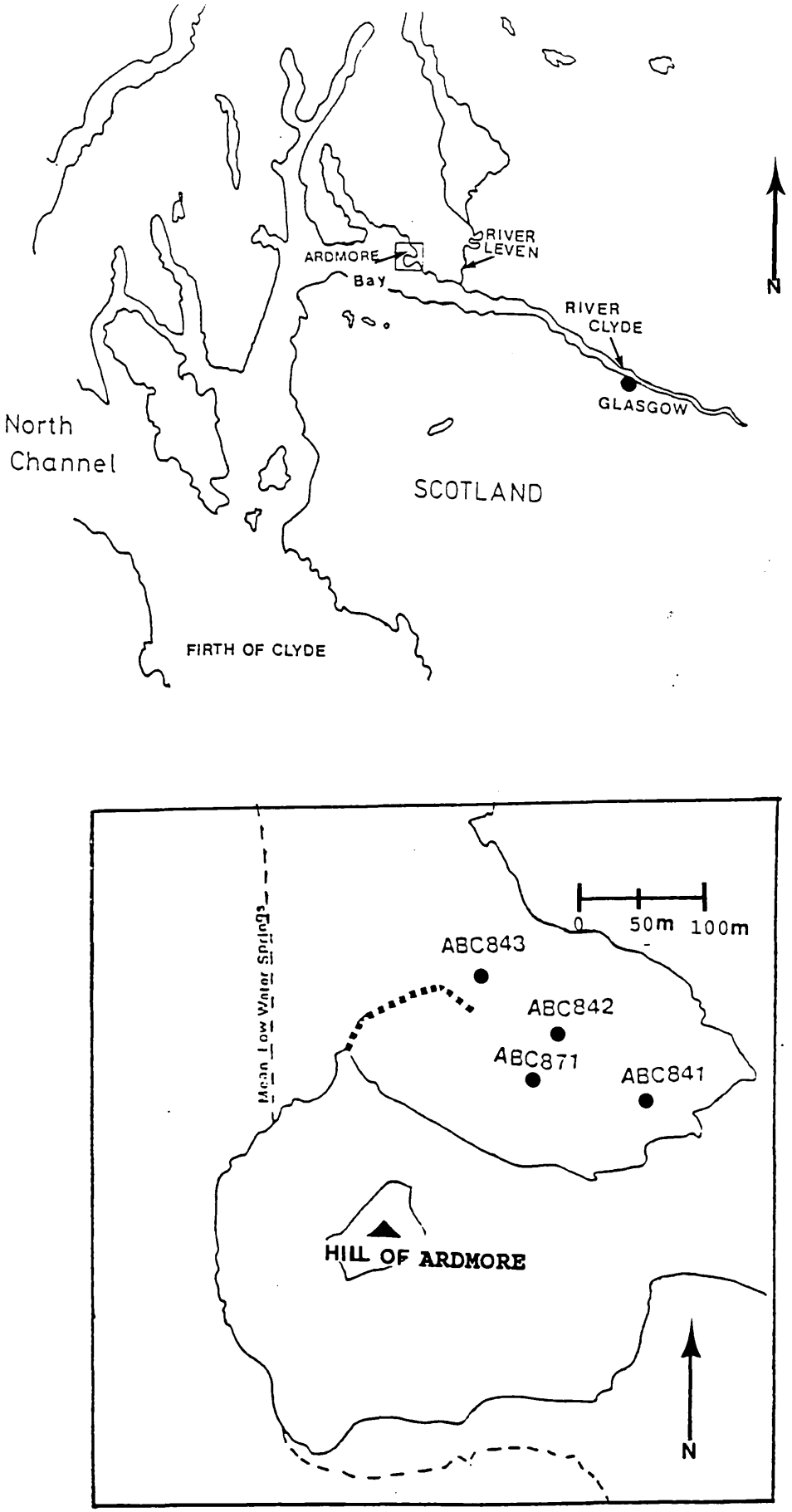

Figure 1.6 Maps of the Ardmore Bay sampling site

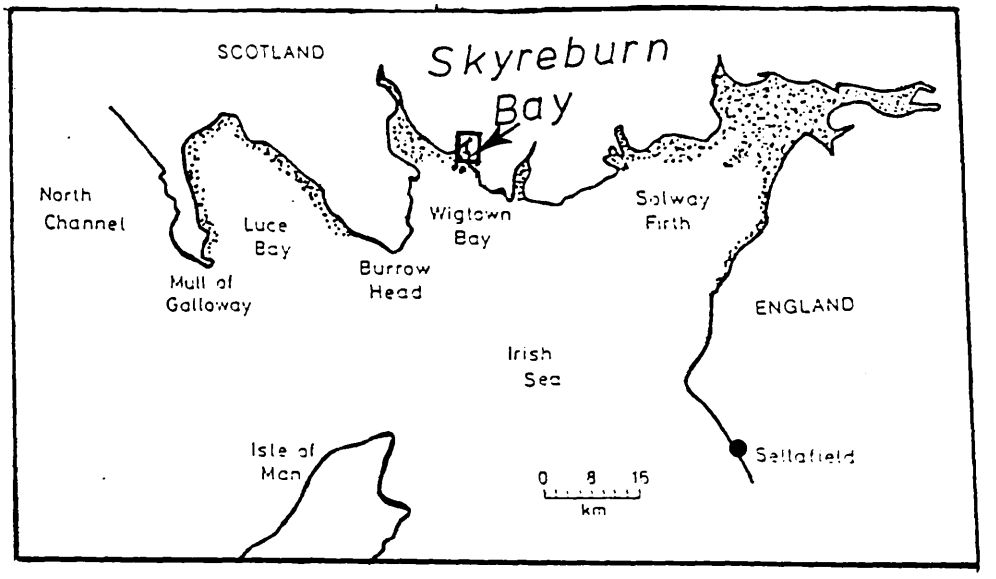

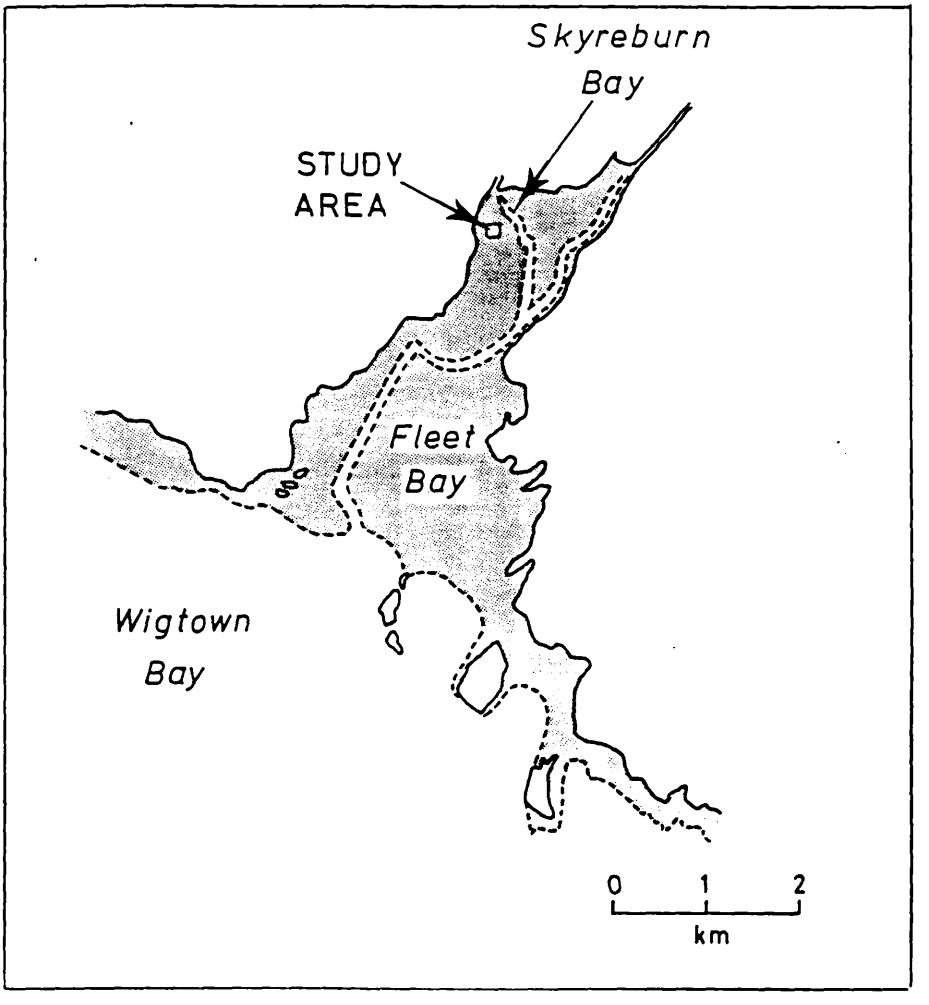

Figure 1.7 Maps of the Skyreburn Bay sampling site

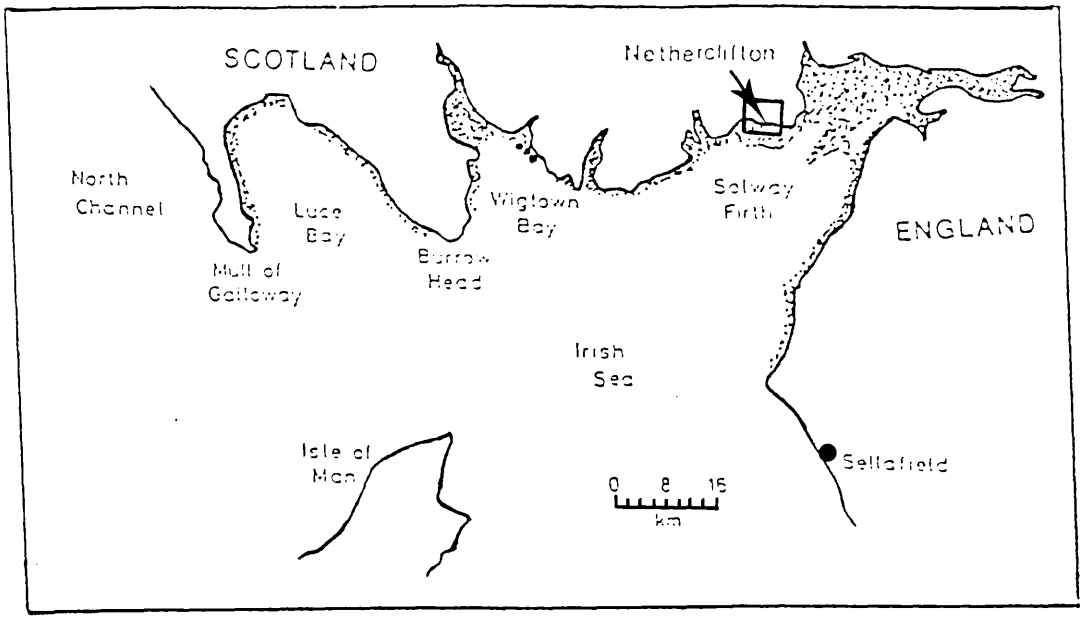

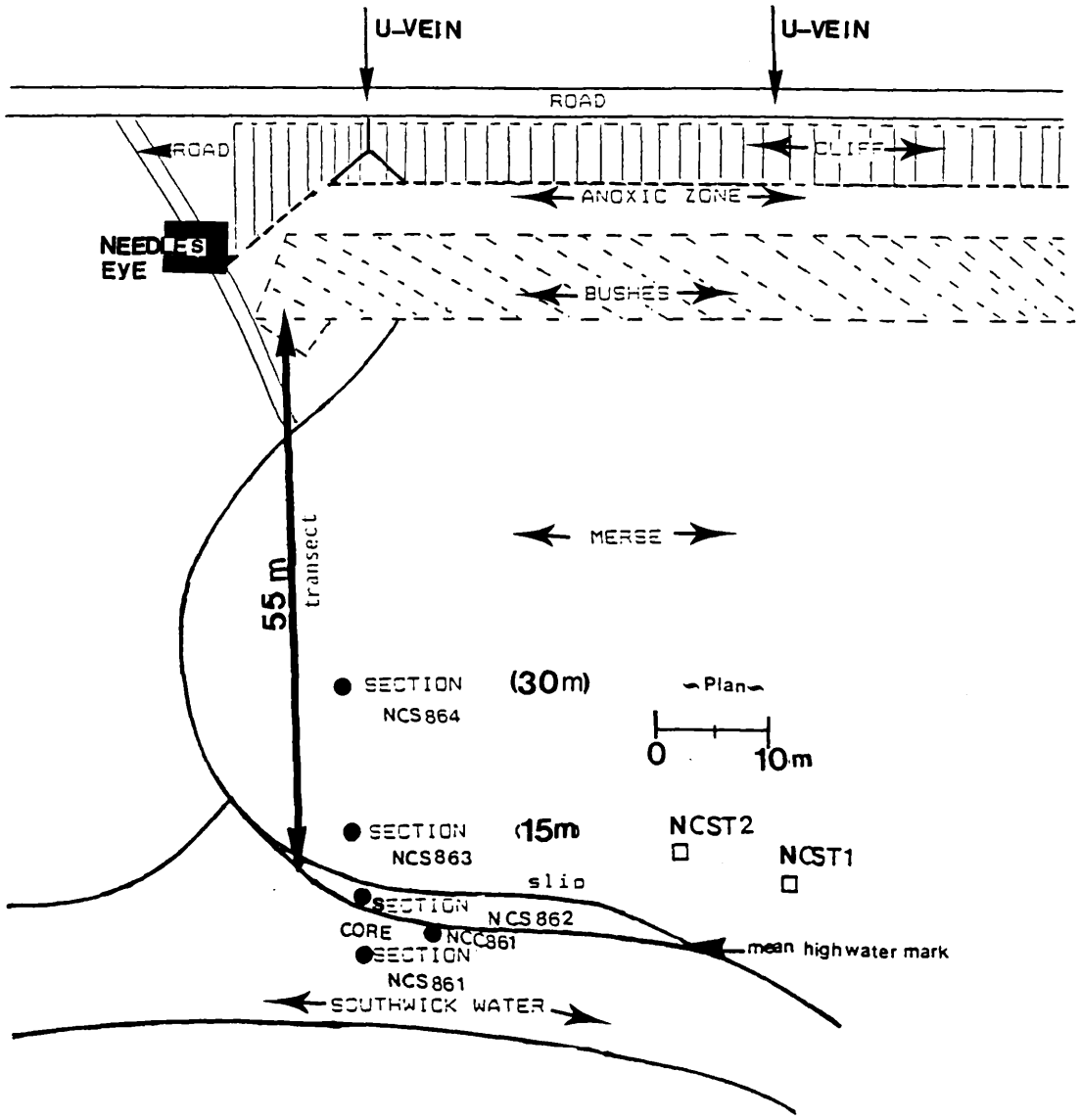

Figure 1.8 Maps of the Netherclifton sampling site

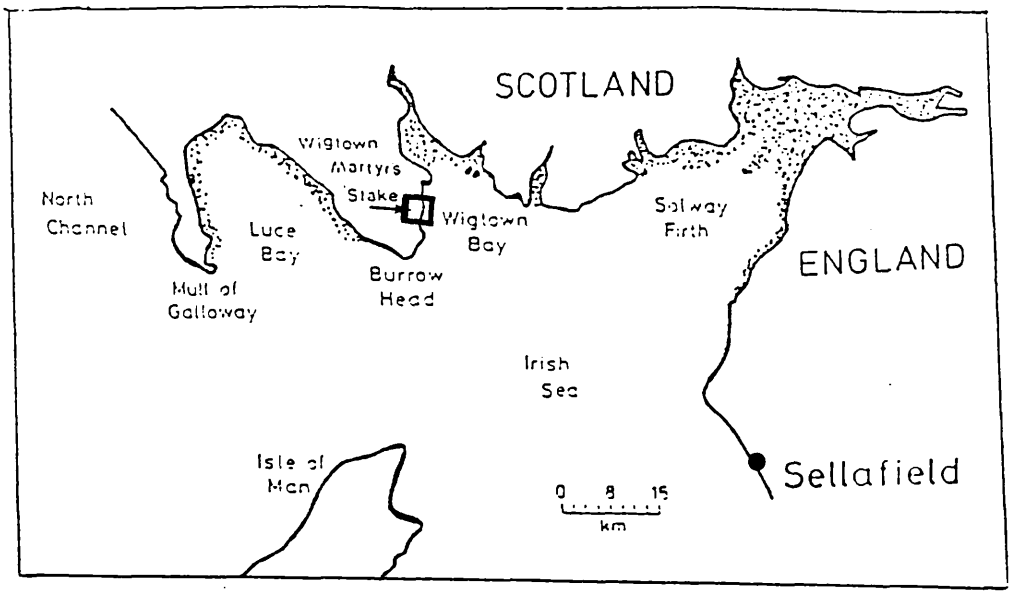

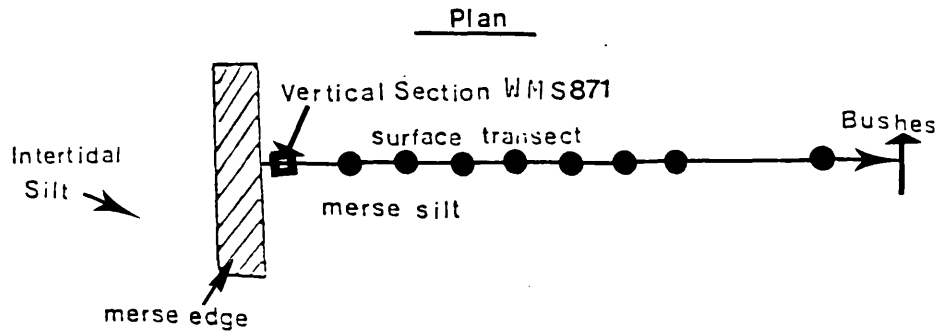

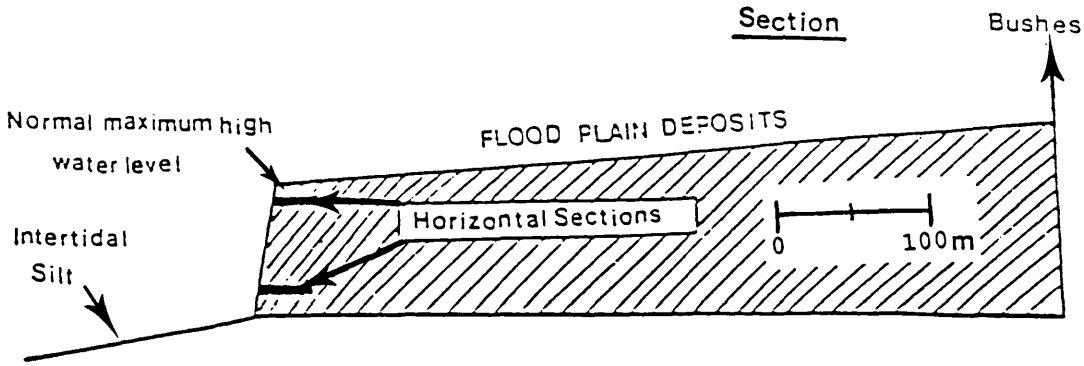

Figure 1.9 Map and schematic diagrams of the Wigtown Martyr's stake sampling site

suspension, at any rate during most of the year, and the merse deposits are in fact generally traversed by numerous small, deeply cut, meandering rivers. The merse sediments are very fine, with a high percentage of clay and silt believed to originate as the result of flocculation taking place when fine river borne material reaches salt water, and by onshore transfer of fine sediments of marine origin (Marshall, 1962a). The sediments are normally deposited during very high tides and storms and these clays, silts and sands are initially laid down in a highly saline system after which, drainage and the effects of rain water wash the soluble salts out of the soil (Chapman, 1960). The soil quality is such that in many areas, the merse deposits are used for grazing cattle and sheep and in some areas, such as the reclaimed Preston Merse (Steers, 1973), for agriculture.

Merse deposits develop quickly in the Solway and are soon colonized by plants. Algae are the first colonizers especially Vaucheria, Rhizochorium and Cladaphora and then the plants follow including Puccinellia, Salicornia, Planlains and Aster.

A common feature observed over many of the merse deposits are step features or terraces, generally a few tens of centimetres in height. Marshall (1962b) suggested that these are primarily erosion features caused by floods, heavy rainfall, sudden thaws in the hills, wind and tide movement.

1.3 RADIONUCLIDES IN THE MARINE AND COASTAL ENVIRONMENT

1.3.1 Introduction

Radionuclides are present in the environment both as purely natural species and as manmade pollutants resulting from human activity. The following sections

provide a description of the occurrence, distribution and geochemistry of selected radionuclides in the nearshore terrestrial and intertidal environments namely the natural radionuclides ^{238}U, ^{235}U, ^{234}U, ^{234}Th, ^{232}Th, ^{230}Th, ^{228}Th, ^{228}Ra, ^{226}Ra and ^{210}Pb and the manmade nuclides $^{239,240}Pu$, ^{238}Pu, ^{241}Am, ^{137}Cs and ^{134}Cs. A review is also provided of the use of these radionuclides as tracers of environmental processes.

1.3.2 General Occurrence and Distribution of Natural Radionuclides in the Marine and Coastal Environment

Natural radionuclides can be subdivided into (i) primordial radionuclides (and their decay products) which have half-lives of the same order of magnitude as the age of the earth (4.6×10^9y), (McKay, 1971; Henderson, 1982), and have been present since the time of formation of the earth and (ii) cosmic ray produced radionuclides which are continuously produced by the interaction of cosmic rays with the constituent gases of the upper atmosphere. Primordial radionuclides are distributed throughout the earth and oceans as a function of their geochemical properties, and a particularly interesting group of primordial radionuclides are ^{238}U, ^{235}U and ^{232}Th which are the parents of the three natural decay series, (Figure 1.1). As a consequence of the varying physical and chemical properties of the different members of these decay chains, separation of parent-daughter pairs can often occur during geochemical processes giving rise to disequilibrium situations which can, in suitable circumstances, be used to investigate natural processes as discussed in detail below. Cosmic ray produced radionuclides are generated mainly in the upper atmosphere from where they are dispersed as a function of their half-lives and geochemical properties and can

also be used as tracers of natural processes in selected cases. The cosmic rays consist of very high energy protons and alpha particles and they produce drastic reactions in any nuclei they strike in the atmosphere. The main reactions are with ^{14}N and ^{16}O, producing species such as ^{14}C, ^{3}H, ^{7}Be and ^{10}Be.

Natural radionuclides in the coastal and marine environment therefore occur both as primordial species and as cosmic ray produced nuclides which have half-lives that are long enough to allow their transport from the upper atmosphere to the surface of the oceans or continents. Primordial radionuclides give rise to the major part of the natural radioactivity of marine materials. Thus, for example, the β-emitting primordial radionuclide ^{40}K ($t_{½} = 1.26 \times 10^{9}y$) exhibits highly conservative behaviour and comprises more than 90% of the total natural radioactivity in seawater, with a relatively constant concentration of about 12Bq l^{-1}. ^{238}U is the most abundant of the uranium isotopes (99.27% abundance), (Ivanovich and Harmon, 1982), and its concentration in seawater is relatively constant at about 0.04Bq l^{-1} (Riley and Skirrow, 1975), making it the dominant alpha emitter in seawater. In contrast, ^{232}Th ($t_{½} = 1.39 \times 10^{10}y$) is present in seawater at a very low concentration of less than 3×10^{-7}Bq l^{-1} reflecting the generally very low solubility of thorium in natural waters.

^{40}K and the natural decay series nuclides also account for most of the natural radioactivity in the minerals and detrital rock fragments which constitute the sediments of the marine environment and the soils of the terrigenous environment.

A variety of mechanisms can contribute to the supply and transport processes affecting radionuclides in the

coastal terrigenous and nearshore marine environment. Some of the main processes are:

i. Rivers supply dissolved radionuclides such as uranium and radium in solution and insoluble species such as thorium and protactinium in their particulate load, giving a net transport of radionuclides from the land towards the sea. Many geochemical interactions take place in the river, estuarine and coastal systems and these processes may influence the transport of radionuclides through these environments by, for example, uptake of radionuclides on particulate material or release of radionuclides from the particulates in conditions of varying salinity and pH.

ii. The process of occasional flooding of low lying coastal plains with seawater can give rise to transport of radionuclides in the reverse direction to that produced by rivers. Thus seawater containing dissolved uranium and radium (and soluble manmade radionuclides) can interact with floodplain soils resulting in radionuclide deposition in these sediments. Marine particulate material containing radionuclides can also be transported onshore in this process.

iii. Soluble nuclides such as ^{226}Ra, ^{228}Ra and ^{222}Rn, which are produced within sediments and soils as the result of radioactive decay of their longer lived parents, can be transported into solution in sediment pore waters and groundwaters, either by recoil effects in the radioactive decay process responsible for

their production or by chemical leaching into the fluid phase after their formation (Cochran, 1982; Harmon and Rosholt, 1982). Depending upon the extent of their subsequent interaction with sediment or soil particles, appreciable quantities of these nuclides can be transported away from their source area by movement in overlying waters in seas and lakes or in groundwaters on land. Groundwater transport of radionuclides from the land towards the sea can thus act as a source of supply of radionuclides to coastal soils. The magnitude and efficiency of this process will vary with the Eh and pH of the groundwater, the presence of complexing agents and the efficiency of sorption processes. For example, Cowart and Osmond (1974) reported large variations of uranium concentration within a single aquifer and have interpreted these as being due to Eh-pH changes which cause precipitation of uranium from solution during flow.

iv. Decay of the relatively soluble isotopes of uranium, radium and radon in seawater and in groundwater provides a mechanism for in situ production of insoluble daughter nuclides, including ^{234}Th, ^{230}Th, ^{228}Th, ^{210}Pb and ^{210}Po, which rapidly become associated with particulate material and are efficiently taken up by sediments and soils.

v. ^{222}Rn emanates from continental rocks and soils to the atmosphere and thereafter decays to ^{210}Pb which is scavenged by precipitation and is deposited onto surface waters of the aquatic environment and onto the top layers

of soil on land.

vi. Wind blown particles and their associated radionuclides can enter the marine environment, constituting a source of sedimentatary material, but the importance of this mechanism is largely restricted to deep ocean situations.

1.3.3 Uranium and Thorium Geochemistry

The inter relationship between uranium and thorium in the environment means that it is convenient to consider the geochemistry of these elements together. The differing physical and chemical properties of the various descendants of ^{238}U and ^{232}Th in the natural series give rise to differences in solubility so that pronounced disequilibria are observed in natural waters. As a general rule it can be stated that uranium, radium and radon are soluble in most natural waters, while protactinium shows limited solubility and all of the other nuclides in the decay chains are essentially insoluble.

The contrasting geochemical behaviour of uranium and thorium with respect to solubility in natural waters can be used to illustrate some of the general principles of solubility control for different elements. The degree of solubility of any species in a given environment is dependent on a number of geochemical variables such as the Eh-pH conditions, its ionic potential, the availability and concentration of complexing ions, temperature and pressure. Of these various parameters, the dominant factor giving rise to the difference in solubility between uranium and thorium is the difference in their values of ionic potential, which is defined as the ratio of ionic

charge to ionic radius (Å) and which controls the degree of hydration, hydrolysis and complex formation of an ion in solution.

The ionic potential is a measurement of the electronegativity of the ion, since the smaller the radius of a positive ion and the higher its charge, the more acidic is its oxide, and conversely, the larger the radius and the smaller the charge, the more basic the oxide, (Mason, 1966; Mason and Moore, 1982). From the electrostatic viewpoint, the ionic potential is a measurement of the intensity of positive charge on the surface of the ion and this determines the magnitude of the repulsive force between the positive charge on the cation surface and the protons of water molecules attracted to it. Depending on the magnitude of the ionic potential, this effect can result in the precipitation of an insoluble hydroxide or the formation of a soluble oxyanion. Thus at very low ionic potential, simple hydration without hydrolysis occurs. If, however, the ionic potential is higher and the repulsion force between the surface charge of the cation and the protons in the co-ordinated water molecules is sufficiently great, some of these protons may be detached, thereby neutralising the charge on the central cation and resulting in insoluble hydroxide precipitation (ie. hydrolysis). With even higher repulsion force (ie. higher ionic potential), all of the protons can be expelled from the attached water molecules and an oxide is formed which, in turn, can form soluble complex ions. Ionic potential exerts a similar influence over particle reactivity of ions and a general pattern of behaviour with respect to hydrolysis and particle reactivity control of solubility is shown in Table 1.2. The controlling influence of ionic potential on the solubilities of U^{6+} and Th^{4+} is paralleled by a marked difference in

solubility of U^{6+} and U^{4+} with the former being fairly soluble whereas the latter shows a low solubility similar to Th^{4+}.

The relatively simple concept of ionic potential control of solubility thus gives a useful qualitative guide to the geochemical behaviour of different species. Consideration of ionic potential in conjunction with the effects of Eh and pH on speciation and the availability of suitable ligands can thus be used to rationalize the geochemical behaviour of different elements.

The differences in solubility and particle reactivity exhibited by uranium and thorium give rise to pronounced differences in transport processes affecting these nuclides, particularly in the near surface terrestrial environment and in surface waters of the aquatic environment where oxidizing conditions generally prevail.

Thus thorium is almost exclusively transported bound in insoluble resistate minerals or adsorbed on the surface of clay minerals and, even when some thorium isotopes such as ^{234}Th and ^{230}Th are generated in solution (by radioactive decay of ^{238}U and ^{234}U respectively), they are rapidly hydrolysed and subsequently removed from solution to the soils or sediments, (Broecker et al, 1973; Anderson et al, 1982a, b; Aller et al, 1980). In contrast, uranium may either move in solution as a complex ion or, like thorium, it can also be transported in detrital resistate phases.

ION	RADIUS (Å)	IONIC POTENTIAL	GENERAL SOLUBILITY CHARACTERISTICS
Cs^{+}	1.67	0.60	
Na^{+}	1.02	0.98	
Ra^{2+}	1.48	1.35	
Sr^{2+}	1.12	1.69	GENERALLY SOLUBLE
Eu^{2+}	1.17	1.71	
Mn^{2+}	0.83	2.41	
Fe^{2+}	0.78	2.56	- - - - - - - - - - - - - - - -
Co^{2+}	0.745	2.68	
Ac^{3+}	1.12	2.68	
Zn^{2+}	0.740	2.70	
Ni^{2+}	0.690	2.90	
Ce^{3+}	1.01	2.97	
Am^{3+}	0.98	3.06	
Eu^{3+}	0.947	3.17	
Sb^{3+}	0.76	3.95	GENERALLY INSOLUBLE
Th^{4+}	0.94	4.25	
Po^{4+}	0.94	4.25	
Ru^{3+}	0.68	4.41	
U^{4+}	0.89	4.49	
Ce^{4+}	0.87	4.60	
Pu^{4+}	0.86	4.65	
Fe^{3+}	0.645	4.65	
Co^{3+}	0.61	4.92	
Pb^{4+}	0.775	5.16	
Zr^{4+}	0.72	5.55	- - - - - - - - - - - - - - - -
Tc^{4+}	0.645	6.20	
Pa^{5+}	0.78	6.41	INTERMEDIATE SOLUBILITY
Np^{5+}	0.75	6.66	
Pu^{5+}	0.74	6.76	
Mn^{4+}	0.53	7.55	- - - - - - - - - - - - - - - -
U^{6+}	0.73	8.22	SOLUBLE
Pu^{6+}	0.71	8.45	

TABLE 1.2: Ionic Potentials for selected elements. (Appropriate to co-ordination number 6; based on data from Henderson, 1982 and Greenwood and Earnshaw, 1984)

Both elements exist in the 4+ oxidation state in primary igneous rocks and minerals, but uranium unlike thorium can be oxidized to the 5+ and 6+ oxidation states in the surface environment, with the oxidation of U^{4+} to U^{6+} being described by:

$$U^{4+} + 2H_2O \rightarrow UO_2^{2+} + 4H^+ + 2e^-, \quad E_o = 0.2V$$

Under oxidising aquatic conditions the 6+ oxidation state of uranium is the most stable and forms soluble uranyl complex ions which play an important role in uranium transport during weathering.

During chemical weathering uranium often forms stable carbonate complexes such as $[UO_2 (CO_3)_3]^{4-}$ in oxidizing aqueous environments at pH 6.0 or greater, with uranium mobilized in this way ultimately entering the marine environment after transport in groundwater and in river waters (Gascoyne and Schwarcz, 1982). In addition to carbonate, soluble uranium complexes are also formed with phosphate, sulphate, fluoride and silicate ions. The importance of organic materials in complexing uranium is well demonstrated by the work of Szalay (1964); Moskvin et al (1967a; b) and Schmidt-Collerus (1967) who have shown that humic materials in the form of peat and lignite will absorb uranium from groundwaters. Uranyl humates are insoluble in the pH range 2.2 to 6.0 with maximum uranium adsorption by humic acids taking place about pH 4.0 to 5.0, (Ivanovich and Harmon, 1982). Uranyl fulvates are insoluble in the pH range 6.0 to 6.6, therefore the possibility of uranium transport in solution and reprecipitation can be clearly seen for uranyl humates and fulvates in natural waters, due to small changes in pH conditions.

The parents of the two uranium decay series, ^{238}U and ^{235}U, are chemically equivalent and their isotopic abundance ratio in naturally occurring materials has not been found to deviate from $^{238}U/^{235}U = 137.5 \pm 0.5$, (Gascoyne and Schwarcz, 1982), with one important exception, being that of the Oklo natural reactor in Gabon (IAEA, 1978).

In contrast, relatively large scale fractionation of the isotopes ^{238}U and ^{234}U can occur in natural systems during rock-water interactions due to preferential leaching into solution of ^{234}U relative to ^{238}U. Three possible mechanism have been suggested by which this disequilibrium can be produced:

i *Leaching of ^{234}U from radiation damaged lattice sites*

Radioactive decay of the parent ^{238}U to ^{234}U involves one alpha and two beta particle emissions and the total process has the effect of damaging the crystal lattice around the product ^{234}U atom and rendering this section of the crystal more easily attacked by weathering agents. It has also been suggested that the ^{234}U atom is often displaced by recoil from its original site and becomes more loosely bound and consequently more accessible and easier to remove by corrosive fluids such as rainwater, groundwater and hydrothermal solutions, (Rosholt et al, 1963; Kigoshi, 1971; Hussain and Krishnaswami, 1980).

ii *Alpha recoil into solution*

In particular cases where an alpha particle is ejected into the body of a mineral during

the decay of an atom of ^{238}U which is located very close to the surface of the mineral, the recoil of the immediate daughter nuclide, ^{234}Th can result in its ejection into the aqueous medium surrounding the grain. Subsequent decay to ^{234}U, thus results in preferential removal of ^{234}U to solution relative to ^{238}U, (Fleischer and Raabe, 1978; Fleischer, 1980, 1982).

iii Oxidation

An additional effect thought to enhance the preferential leaching of ^{234}U from a damaged lattice site is oxidation during the decay process, either by removal of orbital electrons in the emission of alpha and beta particles, or by changes in available energy levels between the original and the dislocated sites. These process could result in an increase in oxidation state, from U^{4+} to the much more soluble U^{6+}, (Osmond and Cowart, 1976; Gascoyne and Schwarcz, 1982; Harmon and Rosholt, 1982).

Disequilibrium between ^{238}U and ^{234}U in the interaction of natural waters with rocks, soils and sediments has in fact, been found to be the rule rather than the exception, with considerable variations being observed in the $^{234}U/^{238}U$ activity ratio. Values of the $^{234}U/^{238}U$ ratio observed in groundwaters range from 0.5 to 12, (Ku, 1965; Thurber, 1962; Veeh, 1967; Petit et al 1985; Cochran et al, 1986).

Uranium transported in groundwater and in rivers is, therefore, generally preferentially enriched in ^{234}U and consequently the average $^{234}U/^{238}U$ activity ratio in

seawater is about 1.14, (Ku, 1966; Cochran, 1982). This excess of ^{234}U in solution in river water and groundwater has been documented by many workers (eg. Ku, 1965; Bhat and Krishnaswami, 1969; Turekian and Chan, 1971; Scott, 1982) with typical values of the $^{234}U/^{238}U$ activity ratio in river water being in the range 1.2 to 1.3. In contrast, rocks, soils and river sediments which have undergone rock-water interaction exhibit a deficiency in ^{234}U compared to ^{238}U. The $^{234}U/^{238}U$ activity ratio in river sediments is typically less than unity with, for instance, an average of 0.95 being reported by Osmond and Cowart (1976).

Thorium geochemistry is also characterized by isotope fractionation and particular disequilibrium situations are controlled by the chemical properties and half-lives of the nuclides involved and possibly, in some cases, by recoil effects as described above for uranium. For example, the formation of ^{228}Th from ^{232}Th involves the soluble intermediate radionuclide ^{228}Ra ($t_{½}$ = 5.75y) and ^{228}Th is found in ocean water with $^{228}Th/^{232}Th$ activity ratios ranging from 5.0 to 30 and $^{228}Th/^{228}Ra$ ratios of less than one. Moore (1967) reported a $^{228}Th/^{232}Th$ activity ratio of 1.4 for Amazon River water and 1.2 for Mississippi River water and concluded that the excess ^{228}Th had grown in from its parent ^{228}Ra in solution. Any small amount of thorium present in river water is undoubtedly removed quickly onto sediment particles, (Rosholt, 1982), and it is generally accepted that the ^{228}Th in solution in coastal marine waters has been generated in the water column by decay of ^{228}Ra, rather than by addition of thorium from rivers. The ^{228}Ra may come, in part, from river water or from diffusion out of the sediments on the sea floor. The influence of ^{228}Ra solubility is also evidenced in bottom sediments older than ten years or so, which are found to have $^{228}Th/^{232}Th$ activity ratios

of less than unity due to ^{228}Ra migration, (Koide et al, 1973; Ku, 1976; Carpenter, et al 1984). In river sediments the $^{228}Th/^{232}Th$ activity ratios are also often less than one, as illustrated by the work of Martin et al (1978) who reported $^{228}Th/^{232}Th$ activity ratios of 0.8 to 0.9 in sediments of the Charente River.

^{234}Th and ^{230}Th also have in situ sources in the aquatic environment as the result of the radioactive decay of their ^{238}U and ^{234}U parents respectively. ^{234}Th activity in ocean water is higher than that of all other thorium isotopes because of its production in solution by decay of ^{238}U and its short lifetime before further decay to ^{234}U. In contrast, ^{230}Th is present at very low activity in seawater and, for instance, Cochran (1982) reported an activity ratio of ^{230}Th to its immediate parent ^{234}U of about 6×10^{-4}, or less, in seawater. This activity ratio, when compared with the equilibrium value of 1.0 indicates that removal of ^{230}Th is rapid relative to its half-life (Broecker et al, 1973; Anderson et al, 1983a, b; Aller and De Master, 1984). The short lived ^{234}Th ($t_{½}$ = 24.1d) shows marked variations in seawater concentration over short distances and this is related to varying rates at which thorium is removed from the water to the particulate phase. Bhat et al (1969) showed that the $^{234}Th/^{238}U$ activity ratio decreases towards the coast. The same observation has been reported by Knauss et al (1978) for California coastal waters indicating that thorium is removed more rapidly in nearshore water with higher suspended particulate concentrations than in the open oceans. Bhat et al (1969) also studied the vertical distribution of ^{234}Th in the top 200m of the oceanic water column and they observed $^{234}Th/^{238}U$ activity ratios of less than unity in the top 100m, but with an approach towards equilibrium with increasing depth. Matsumoto (1975) also observed $^{234}Th/^{238}U$ activity ratios in the uppermost 200m of the

North Pacific water column ranging from 0.4 to 1.2 with an average value of 0.8, corresponding to a mean residence time for thorium of 0.4y. Brewer et al (1980) and Broecker et al (1973) have also calculated a mean residence time of thorium using open ocean data and, in these cases, values of about 0.7 years were reported. Similarly Kaufman et al (1981), used $^{234}Th/^{238}U$ activity ratios to calculate removal rates for thorium in the New York Bight area and the residence times derived varied from about 10 to 90 days, in agreement with the results of Li and Chan (1979). Sediment traps have also been used to evaluate the residence time of thorium in seawater and Spencer et al (1978) and Brewer et al (1980) have observed that the activity of ^{230}Th on the sediment particles increased with depth due to the constant uranium concentration of seawater and the fact that, as the particles sink, they scavenge progressively more ^{230}Th, there being no time for ^{230}Th decay during particle setting. In contrast, the ^{234}Th activity of the particles was reported to be essentially constant with depth, indicating that the scavenging of ^{234}Th onto the particles was balanced by its decay. Brewer et al (1980) concluded that there may be horizontal scavenging and transport processes which contribute to the removal of thorium isotopes from the water column.

In the estuarine environment, removal rates for thorium are very rapid. For instance, In Narragansett Bay, Santschi et al (1979) have shown concordancy for thorium removal rates calculated using $^{234}Th/^{238}U$ activity ratios of less than 0.3 and $^{228}Th/^{228}Ra$ activity ratios of less than 0.02 indicating a mean residence time for thorium of less than 10 days. This is in general agreement with the result of Aller and Cochran (1976), of less than 2 days, based on $^{234}Th/^{238}U$ disequilibrium in Long Island Sound.

1.3.4 ^{210}Pb Geochemistry

^{210}Pb ($t_{½}$ = 22.26y) is a member of the ^{238}U natural decay series (Figure 1.1) and is of major importance in studies of the mixing and accumulation characteristics and the geochemistry of recent sediments. Unsupported ^{210}Pb is supplied to surface sea water and to surface soils from the atmosphere by decay of the noble gas ^{222}Rn (and four short lived intermediate decay products) which is continuously supplied to the atmosphere by diffusion from soils and rocks, (Poet et al, 1972). The non-reactive ^{222}Rn remains in the atmosphere until it decays, but ^{210}Pb is rapidly removed to the land and sea surfaces by both dry and wet fallout.

With an ionic potential of 5.1, Pb^{4+} is highly reactive in the aquatic environment both with respect to hydrolysis and to uptake on solid surfaces and in consequence, it is dominantly associated with particulate matter. As a result, dissolved ^{210}Pb is essentially absent from river water, (Rosholt, 1982). An excellent illustration of the behaviour of ^{210}Pb in a river system, and evidence of the effects of varying geochemical conditions is provided by the detailed studies which have been performed on the Susquehannah River system. Thus, for example, Lewis (1977), reported the concentration of dissolved ^{210}Pb in natural river water of pH around 8.0 to be less than 1.7 x 10^{-4}Bq l^{-1}. In contrast, the same author reported that when reduced pH conditions were encountered as the result of acid mine water draining into the west branch of the Susquehannah River, the dissolved ^{210}Pb concentration was significantly higher, at 2.8 x 10^{-2}Bq l^{-1}. Under similar conditions of acid mine drainage into the Colorado River system, Rama et al (1961), reported an even higher value of 0.23Bq l^{-1} for

the dissolved ^{210}Pb concentration in the Colorado River water. On the basis of the Susquehannah River work it was concluded that, as long as the pH of the river water was 4.0 or less, measurable quantities of dissolved ^{210}Pb could be found in solution, confirming previous observations of similar effects of acidification in this system, (Benninger et al, 1975; Lewis, 1976; Lewis, 1977). Lower ^{210}Pb concentrations were again observed as the effect of acidification decreased and it was postulated that ^{210}Pb removal from solution was possibly related to the precipitation of iron and manganese, which occurs as the pH of the acid river water increases during mixing downstream. The rate of manganese removal from solution is slow in this system and Benninger et al (1975), observed that the zone in which manganese precipitation occurred extended a considerable distance down river from the point at which neutralization of the water occurred. They also observed that, at points in or below the region of manganese precipitation, ^{210}Pb was completely scavenged from solution onto suspended particles.

Organic matter in river bottom sediment may also absorb ^{210}Pb from solution, and the presence of organic matter in the sediment can also result in the development of reducing conditions which induce a continuous cyclical flux of dissolved Mn^{2+} and Fe^{2+} from the sediments to the overlying oxidizing river water where oxidation to insoluble Mn^{4+} and Fe^{3+} occurs, giving an enhanced scavenging potential. The presence of soil organic matter in river suspended particulates has also been identified as an important factor in the scavenging of ^{210}Pb from river water, (Benninger et al, 1975).

Organic matter is also of importance in the binding of ^{210}Pb in soils, and a strong positive correlation between ^{210}Pb content and organic matter concentration

in soil profiles has been reported by Benninger et al (1975) and Lewis (1977). Benninger et al (1975) have presented studies of ^{210}Pb distributions in soil and salt marsh profiles from Maryland and Pennsylvania, USA in which they observed that, within the analytical uncertainties, the soil and salt marshes investigated retained virtually all of the ^{210}Pb supplied to them from the atmosphere in cases where the ^{210}Pb is associated with the organic fraction of the soil. They also concluded that ^{210}Pb exhibited an extremely low mobility in the dissolved phase in the soils and salt marshes studied, probably because of the strong retention properties of soil organic matter.

In the marine environment, the supply of ^{210}Pb to the surface of the oceans and seas varies with distance from the continental land masses which form the dominant source of ^{222}Rn to the atmosphere. An in situ source of ^{210}Pb production also occurs in seawater as the result of the decay of dissolved ^{226}Ra through ^{222}Rn. The influence of this source on the flux of ^{210}Pb to underlying sediments is a function of the integrated ^{226}Ra activity in the water column and in coastal areas, at depths of less than 100m, it is much less significant than the atmospheric ^{210}Pb flux, (Turekian et al, 1977; Nozaki et al, 1980). In contrast, in the open oceans, the production of ^{210}Pb from ^{226}Ra in a 4 to 5km deep water column can be comparable to the atmospheric flux (Cochran, 1982).

In surface seawater, the ^{210}Pb activity varies significantly with geographic location and some of the factors influencing ^{210}Pb concentration include: variations in input from ^{226}Ra decay, the atmosphere and possibly upwelling; varying rates of removal onto particulates; and water residence time. For instance, nearshore waters have low ^{210}Pb concentrations and low

$^{210}Pb/^{226}Ra$ activity ratios as a result of the efficient scavenging of ^{210}Pb by the high level of particulate matter present in the water column. Thus Bruland et al (1974) observed $^{210}Pb/^{226}Ra$ activity ratios ranging from 0.10 to 0.39 in mid Gulf of California waters and Krishnaswami et al (1975) reported a range of values from 0.2 to 0.6 for the Santa Barbara Basin. These low $^{210}Pb/^{226}Ra$ activity ratios suggested rapid removal of ^{210}Pb onto sinking particles. Benninger (1978) found that the total (ie. solid and dissolved) ^{210}Pb in the waters of Long Island Sound was well correlated with the concentration of suspended particles and concluded that there was effectively no dissolved ^{210}Pb present.

In deep seawater the removal of ^{210}Pb from solution has been reported by Craig et al (1973) who observed $^{210}Pb/^{226}Ra$ activity ratios in the range 0.25 to 0.80 with an average of 0.5 in North Atlantic and North Pacific deep waters and concluded that the mean residence time of ^{210}Pb in the deep ocean is about 50y.

1.3.5 Applications of Natural Decay Series Nuclides to the Study of Coastal and Marine Processes

The disequilibria between parent-daughter pairs which occur in the natural decay series in the coastal and marine environment, as the result of differences in chemical behaviour as described above, have been widely used in the study of the mechanisms and rates of natural processes.

Two topics which have been successfully studied by use of natural decay series nuclides are water movement processes and sediment accumulation and mixing processes. The use of radionuclides in the study of sedimentary processes is of direct relevance to the present work and, while this study did not directly

involve investigation of water movement processes, this topic is of central importance to some aspects of the considerations of radionuclide transport investigated. The concepts appropriate to the use of natural decay series radionuclides in both of these applications are therefore illustrated below.

Water movement can be considered to take place by a combination of advective and diffusive processes and the distribution of any soluble radionuclide which decays with a half-life of the same order of magnitude as the timescale of the mixing process can, in suitable circumstances, be used to establish the rate of the process. Thus, for instance, the equation describing the radioactive decay of a nuclide as it moves vertically upwards away from a sediment source area purely by diffusive mixing is:

$$C_D = C_o\, e^{-kz} \qquad \text{(Berner, 1980)}$$

where C_o and C_D are the concentrations at two depths (or distances), and

$$k = \sqrt{\lambda / D_z}$$

where,

λ = the decay constant of the nuclide

D_z = the coefficient of vertical eddy diffusion

z = the depth interval.

In other circumstances, particularly in nearshore situations, advection can be the dominant process and the equation describing a situation with uniform

advection and with no mixing (dilution) or removal (ie. a closed unit of water) is simply the first order decay equation:

$$C_D = C_o e^{-\lambda t}$$

$$\text{But} \quad V = \frac{D}{t}$$

$$\therefore \quad C_D = C_o e^{-\frac{\lambda}{V} D}$$

$$\text{ie.} \quad C_D = C_o e^{-\beta D} \qquad (1.3)$$

where,

$$\beta = \frac{\lambda}{V}$$

C_o = concentration at distance zero

C_D = concentration at distance D

V = advection velocity

t = time

Such a "closed" situation will almost never occur in reality and, in general, removal of the radionuclide by uptake on suspended particulates and sediments and dilution as a result of mixing will both also occur. In the simplest case, it could be imagined that, for a unit of water moving at constant velocity, a constant fraction of the radionuclide would be removed from solution in a constant time (or distance). Thus,

combination of uniform removal to the sediment with (1.3) gives:

$$C_D = C_o\, e^{-\beta_1 D}$$

where,

$$\beta_1 = \beta + r$$

and r = removal coefficient

$$\text{ie. } C_D = C_o\, e^{-(\beta + r)D}$$

Similarly, the simplest case of mixing would involve a regular degree of dilution in a given time (or distance) so that combination of uniform dilution with (1.3) gives:

$$C_D = C_o\, e^{-\beta_2 D}$$

where,

$$\beta_2 = \beta + d$$

and d = dilution coefficient

$$\text{ie. } C_D = C_o\, e^{-(\beta + d)\, D}$$

Thus the simplest theoretical situation which could be generated to include advective movement with removal and dilution both occurring at a uniform rate is:

$$C_D = C_o\, e^{-\beta_3 D} \qquad (1.5)$$

where,

$\beta_3 = \beta + r + d$

$$\therefore \quad C_D = C_o\, e^{-(\beta + r + d)D}$$

In practice, this simple, uniform situation is unlikely to occur and variable rates will almost certainly be encountered for velocities, and for rates of removal and mixing. Moreover, advection is rarely totally dominant and diffusion must almost always be considered. Nevertheless, this simple type of calculation can be usefully employed, in suitable circumstances, to set boundary conditions for processes.

Soluble natural decay series radionuclides generated by decay of insoluble parents are particularly well suited as tracers of water movement, since they are dominantly added to the water at the interface with the sediments and undergo transport from these zones in accordance with prevailing advective and diffusive processes.

The timescale of processes of interest in the intertidal zone ranges from days up to about 10^3 years and a number of natural decay series radionuclides provide half-life and geochemical properties suitable for study of processes on this timescale.

Probably the most successful natural decay series radionuclides used in this context are the radium isotopes ^{228}Ra ($t_{½}$ = 5.75y) and ^{226}Ra ($t_{½}$ = 1.602 x 10^3y) which exhibit maximal concentration near the sediment-water interface and are virtually totally unsupported in solution by their thorium parents. These nuclides

have become well established tracers of rates and directions of seawater movement in open ocean systems. For instance, in the case of ^{228}Ra being transported away from the sediment interface, the diffusion equation presented above becomes

$$(^{228}Ra) = (^{228}Ra)_o \, e^{-kt}$$

where,

$$k = \sqrt{\lambda^{228}Ra/Dz}$$

(Moore, 1969; Broecker et al, 1977; Craig, 1980).

Decay during transport results in more rapid reduction of the activity of the short-lived ^{228}Ra relative to ^{226}Ra so that nearshore waters and deep ocean waters have high $^{228}Ra/^{226}Ra$ activity ratios and high absolute ^{228}Ra concentrations relative to open ocean water.

Insoluble radionuclides can be used in the study of sediment geochronologies in cases when an unsupported radionuclide is incorporated in an accumulating sediment. Under ideal circumstances (ie. an undisturbed post-depositional situation) decay of the radionuclide in the sediment will result in an exponential decrease in concentration with increasing depth from the surface. Such a distribution allows the age of any given layer of sediment to be calculated and thus allows the determination of sedimentation rates as described in detail below for ^{210}Pb. In the case of a sediment system in which post depositional mixing occurs, the radionuclide distribution can sometimes be used to study the mixing process. The diverse range of half-lives of the natural radionuclides present in

the oceans allows the study of marine and coastal processes over a timescale ranging from days up to about 10^6 years and many of the radionuclides with half lives of less than 10^3 years are potentially suitable for study of intertidal processes. Some useful natural decay series "chronometers" suitable for dating of environmental systems are shown in Table 1.3.

^{210}Pb ($t_{½}$ = 22.26y) can provide a suitable means of establishing chronologies and mixing patterns for recent marine and freshwater sediments, (Krishnaswami et al, 1971; Robbins and Edgington, 1975; Goldberg et al, 1977; Oldfield et al, 1978) since it is continuously supplied to most sediments unsupported by ^{226}Ra as a consequence of the processes described in section 1.3.4. If the input of ^{210}Pb to surface sediment is constant and closed system conditions apply to the sediment subsequent to its deposition then sediment chronologies extending up to a time limit of about 150 years can be established, (Goldberg and Bruland, 1974; Swan et al, 1982). This timescale is highly appropriate to the study of many of the processes affecting intertidal sediments and some soils, particularly in the context of pollution studies.

The use of atmospherically derived ^{210}Pb as a geochronological tracer was first proposed by Goldberg and Koide (1963), who applied the technique to permanently accumulating snow fields in Greenland glaciers. This work demonstrated that the flux of excess ^{210}Pb and the rate of ice accumulation had been fairly constant over the time interval dated.

Krishnaswami et al (1971) observed that excess ^{210}Pb, unsupported by ^{226}Ra, was present in sediment cores

"Parent"		"Chronometer"	
Nuclide	Half-life (y)	Nuclide	Half-life (y)
^{238}U	4.5×10^{9}	^{234}Th	0.066
^{228}Ra	5.6	^{228}Th	1.91
^{226}Ra	1.6×10^{3}	^{210}Pb	22.3
^{235}U	7.1×10^{8}	^{231}Pa	3.5×10^{4}
^{234}U	2.5×10^{5}	^{230}Th	7.5×10^{4}
		^{234}U	2.5×10^{5}

TABLE 1.3: Natural decay series radionuclides which can be used in chronology studies

from several European lakes and used the depth profiles of ^{210}Pb in the sediment to establish chronologies.

Under ideal circumstances for ^{210}Pb dating, the sediments are deposited in a regular layered sequence, each layer representing a particular time interval and being undisturbed after deposition. Such conditions generate ^{210}Pb profiles with an ideal exponential decrease with depth. However, the ^{210}Pb activity in many sediment profiles has been observed to exhibit a surface section which has a constant activity with depth. This constant activity of ^{210}Pb with depth can best be explained by considering a model in which the surface of the sedimentary column is assumed to be completely homogeneous as a result of rapid physical and/or biological reworking. Robbins and Edgington (1975) compared the depth distribution of ^{210}Pb activity with that of the benthic activity in Lake Michigan sediments and found a high degree of correlation between the depth of benthic activity and the depth of constant ^{210}Pb activity. Thus, greater than 90% of the benthic population was found within the zone of constant ^{210}Pb activity. Robbins and Edgington (1975) also concluded from their evidence that many sediment deposits were subject to rapid reworking by burrowing organisms and that the observed depth distribution of ^{210}Pb was a useful indicator of the extent of this mixing process. They moreover showed that sedimentation rates could be derived from the ^{210}Pb profile below the depth of the biological activity zone and developed a mathematical model to include the effects of biological disturbance, and to satisfactorily explain the observed ^{210}Pb activity profiles.

In the simplest form, this model involves four assumptions:

i. that there has been a constant flux of ^{210}Pb to the sediment,

ii. that there has been a constant rate of sediment accumulation,

iii. that there has been no post-depositional migration of ^{210}Pb within the sediment,

iv. that supported ^{210}Pb activity is constant with depth.

Under these conditions, in ideal (unmixed) sediment experiencing no compaction, the ^{210}Pb concentration profile should show an exponential decrease with depth and

$$A_t = A_o e^{-\lambda t}$$

where,

A_o = the activity of excess ^{210}Pb at time = 0 (surface)

A_t = the activity of excess ^{210}Pb at time t, corresponding to an accumulation depth D of sediment

Thus, since $t = \frac{D}{S}$

where,

S = the sedimentation rate in cm y^{-1}, and

D = the depth (cm)

a plot of ln A (x-axis) against depth (y-axis) should yield a straight line in which the slope corresponds to - λ/S, from which a value of S in can be derived.

Two different models can be used for age calculations using ^{210}Pb and these involve one of two assumptions; (i) constant initial concentration, which is essentially the model described above, (Robbins and Edgington, 1975), or (ii) constant rate of supply. The constant rate of supply method assumes that the flux of excess ^{210}Pb to the sediment is constant with time at a particular location but does not necessarily assume a constant rate of sediment accumulation, although if the sedimentation rate is constant the two methods yield identical results (Oldfield et al, 1978). In this method

$$\Sigma Ad = F \int_{\infty}^{td} e^{-\lambda} dt$$

where ΣAd is the total excess activity of ^{210}Pb from the surface to depth d and F is the flux of excess ^{210}Pb.

The method based on the constant initial concentration of excess ^{210}Pb has been the most widely used of these two approaches to ^{210}Pb dating.

The ^{210}Pb dating technique has been widely applied in studies of mixing patterns and accumulation rates of recent sediments in a diverse range of environments. The technique has probably been most successfully applied in the freshwater lacustrine environment, often in conjunction with the complementary method of dating using the 1963 bomb fallout peak of ^{137}Cs (Krishnaswami et al, 1971; Robbins and Edgington, 1975; Robbins et

al, 1978).

^{210}Pb techniques have also been successfully applied in the coastal marine environment where it has been observed that the ^{210}Pb activity in surface sediments is often constant to a certain depth due to the effects of physical processes and/or biological activity within the oxic zone, giving rise to mixing of the sediments. Thus, for example, Clifton and Hamilton (1979) have presented results showing a marked contrast between ^{210}Pb distributions in sediment cores from different locations in the Severn Estuary, in which the ^{210}Pb activity of cores from the St John's Lake and Swansea Bay areas were found to show a marked correlation with depth giving sedimentation rates of 0.17 and 1.14cm y^{-1} respectively. In contrast, no such correlation was found for samples from Bridgewater Bay and Newport Deep indicating that these latter sedimentary systems were either being accumulated at a very fast rate (greater than 10cm y^{-1}) or were unstable and subject to intense mixing. Similarly, Swan et al (1982) have observed that in different sea lochs of the west coast of Scotland, varying degrees of mixing affected the ^{210}Pb profiles. They reported a limited mixing zone of about 4 to 6cm in Loch Goil, below which a relatively good exponential decay of ^{210}Pb was observed indicating sedimentation rates of 6.0 and 3.5cm y^{-1} at two different locations, whereas in Gare Loch, intense mixing affected the ^{210}Pb distribution to a depth of 15cm below which a sedimentation rate of 1.5cm y^{-1} was observed.

The above treatment of bioturbation as giving rise simply to a homogenisation of the ^{210}Pb distribution within the oxic zone is regarded as an oversimplification by a number of authors who present a more complex treatment of the subject. Thus, in

situations with varying biological populations as a function of depth, the effects of bioturbation are treated as being analogous to a diffusion process (Berner, 1980). Alternatively, Carpenter and Beasley (1981) suggest that some benthic communities, living at specific depth horizons, can preferentially exchange surface water and sediment with water and sediment from the depth that they inhabit. This type of process means that organisms living below the oxic zone can influence bioturbative processes. Thus, for instance, *Chaeotopterus Variopedatus*, which is a polychaete annelid, worm, lives in a U-shaped burrow at depth of up to 25cm in the sediment. *Upogebia deltaura*, which is a reptant decapods worm is also found in places living at depths of up to 50cm in seabed sediments. Such organisms cause transport of seawater and sediments downwards (Aller, 1977, 1980; Williams et al, 1981) during their movement within the tube or tunnel in order to bring oxygen to themselves.

Compaction is an important physical process which also takes place in most near surface sediments. Compaction can be defined as a loss of water from a layer of sediment due to compression arising from the deposition of overlying sediment. The effects of compaction on ^{210}Pb profiles are discussed in detail by Swan et al (1982) and compaction is conventionally compensated for by expressing the depth in units of g cm^{-2} rather than cm.

In the intertidal zone, the sediments are often subject to highly intense physical and biological mixing, giving rise to generally deep mixed layers as discussed in section 1.2, with major effects on ^{210}Pb distributions. Thus, for example, MacKenzie and Scott (1979) reported constant excess ^{210}Pb activity to a depth of 18cm in an intertidal sediment profile from

Skyreburn Bay in south west Scotland, indicating total mixing of ^{210}Pb to this depth. Similarly, Ben Shaban (1985) reported constant excess ^{210}Pb activities to depths of 30cm in three profiles of intertidal sediment from Ardmore Bay in the Clyde Sea area of West Central Scotland, once again indicating the effects of major physical and biological mixing in this environment. Clifton and Hamilton (1982) reported a range of sedimentation rates between 0.24 and 1.9cm y^{-1} in conjunction with physical and biological mixed layers of about 10cm for profiles from 16 sites in the salt marsh region near Newbiggin on the Esk Estuary, north west England.

In general, ^{210}Pb dating is much less useful for determination of accumulation rates of deep sea sediments because of the slow deposition rates involved. However, ^{210}Pb can be used in this situation to study mixing processes (Borole et al, 1977).

^{210}Pb dating is not generally applicable to soils but in certain favourable circumstances it can be used. Benninger et al (1975) used ^{210}Pb profiles to study the atmospheric flux of heavy metals in soil and salt marshes of north central Pennsylvania and coastal Connecticut New Haven, USA.

The short-lived thorium isotopes ^{228}Th ($t_{½}$ = 1.913y) and ^{234}Th ($t_{½}$ = 24.1d) are also well established tracers of environmental processes operating over a timescale of days to a few years, and have considerable potential for applications in intertidal sediment and soil studies. Thus ^{234}Th is formed in sea and groundwaters by decay of its immediate primordial parent ^{238}U and, in common with other thorium isotopes, ^{234}Th is adsorbed

rapidly on particulate matter immediately after it is produced (Hussain and Krishnaswami, 1980). In the shallow marine environment ^{234}Th is often found in excess relative to ^{238}U in surface sediments in spite of its short half-life and ^{234}Th has been successfully used as a tracer in studies of sediment reworking and diagenesis in shallow water regimes (Ku and Glasby, 1972; Lalou and Brichet, 1980). In various studies (Aller and Cochran, 1976; Cochran and Aller, 1979; Aller et al, 1980) using ^{234}Th in particle reworking and diagenesis investigations in shallow water sediments from Long Island Sound and New York Bight, USA, it was concluded that the excess ^{234}Th is bound dominantly to very fine particles which may be resuspended by storms and currents, leading to a deficit of ^{234}Th activity in sandy sediments and an excess in muddy areas. Also ^{234}Th has been successfully used in deep ocean bioturbation studies and in euphotic zone production studies (Benninger et al, 1979).

Koide et al (1973) and Murray (1975) demonstrated the successful application of excess ^{228}Th techniques for dating recent sediments. Because of the short half-life of ^{228}Th the range of this method only extends to approximately 10 years.

The longer-lived thorium isotope ^{230}Th ($t_{½}$ = 7.52 x 10^4y) is also capable of being used as a chronometer, particularly in dating deep marine sediments by observation of the decay of excess ^{230}Th deposited as the result of the decay of ^{234}U in the overlying water column (Riley and Chester, 1976; Ku, 1976).

Assumptions of constant initial concentrations of excess ^{230}Th and post depositional "closed" conditions, analogous to those discussed above in detail for ^{210}Pb, are required in this method. The range of

applicability of this method is from about 10^4 years up to about 4 x 10^5 years (Lalou, 1982), putting it at the limit of the timescale for processes of interest in the intertidal environment, but providing some potential for application in soil studies.

^{234}U ($t_{½}$ = 2.48 x 10^5y) and ^{238}U ($t_{½}$ = 4.468 x 10^9y) in conjunction with ^{230}Th also provide geochemical properties suitable for numerous geochronological applications but these are generally in the timescale 10^4 to 10^6 years and, as such, are once again at the extreme limit, or beyond, the timescale of interest in intertidal and coastal soil situations. Nevertheless the general principles involved are of potential relevance to the present study with respect to the characteristic labelling of different materials via their $^{230}Th/^{234}U$ or $^{234}U/^{238}U$ activity ratios so a brief summary of some of the applications of these nuclides follows below.

Uranium mobility in groundwater can be used as the basis of the study of deposits in cases where uranium is laid down in excess of its daughter ^{230}Th. An excellent example of this technique is the $^{230}Th/^{234}U$ dating of carbonates in which, if it is assumed that the carbonate is free of ^{230}Th at the time of its formation, then at any subsequent time, the $^{230}Th/^{234}U$ ratio is given by:

$$^{230}Th/^{234}U = \frac{1 - e^{-\lambda_{230}t}}{^{234}U/^{238}U} + \left(1 - \frac{1}{^{234}U/^{238}U}\right) \frac{\lambda_{230}}{\lambda_{230} - \lambda_{234}} \left(1 - e^{-(\lambda_{230} - \lambda_{234})t}\right)$$

Ivanovich (1982).

The above equation illustrates the relationship between the $^{230}Th/^{234}U$ and $^{234}U/^{238}U$ activity ratios for closed systems of varying initial $^{234}U/^{238}U$ ratio. The dating range of this method is considered to be from about 7.5×10^4y up to 3.5×10^5 years and the above equation is often solved graphically by plotting the $^{234}U/^{238}U$ activity ratio against the $^{230}Th/^{234}U$ ratio. In this plot, isochrons are nearly vertical lines, whose slopes decrease with increasing age, and the ages are determined by interpolating between isochrons.

A second example of the use of uranium in chronological studies, applicable mainly to the marine environment, utilises the $^{234}U/^{238}U$ activity ratio in materials in which uranium is initially deposited with a $^{234}U/^{238}U$ activity ratio of greater than unity. The decay of excess ^{234}U towards secular equilibrium with its parent ^{238}U is described by the equation:

$$[A_t - 1] = [A_o - 1]\, e^{-\lambda_{234} t}$$

where A_o and A_t = initial and present $^{234}U/^{238}U$ activity ratios respectively.

The method, in general, can date samples from about 10^5 up to at least 10^6 years (Thurber, 1963; Thompson et al, 1975; Osmond and Cowart, 1976). The main disadvantage of this technique is the inherent difficulty associated with establishing the value of initial excess ^{234}U in many cases. In general, no reliable a priori assumption about the initial $^{234}U/^{238}U$ activity ratio can be made, thus limiting the applicability of the technique (Osmond and Cowart, 1976). The method, therefore, appears to be most applicable in the marine environment where the $^{234}U/^{238}U$ activity ratio is uniform in seawater (Ku et al, 1974).

Radioactive disequilibrium studies of the ^{238}U - ^{234}U - ^{230}Th system have been used to investigate the migration of thorium and uranium in soil systems as the result of rock weathering (Hansen and Stout, 1968) and to evaluate the patterns of evolutionary trends of thorium and uranium isotope ratios in soils during the early stages of alterations of the transported parent materials (Rosholt et al, 1966). Hansen (1965) developed a model for determining the age of soil development in the San Joaquin Valley and in the Sierra Nevada in California using the thorium-uranium system. Rosholt (1982) has investigated extensively the thorium-uranium isotopic system in several different sedimentary deposits, some of which include multiple depositional units of different ages. These deposits were collected from environments which varied in climate from arid to humid. From the results of these thorium-uranium isotopic analyses, a concept for dating the deposition of the various surficial sediments was developed. This model for dating, uranium-trend dating, does not require the standard closed system assumptions normally used in natural decay series studies. This open system dating technique consists of determining an isochron from analysis of three to ten samples from various soil horizons in a given depositional unit. The concentration and the isotopic ratios of ^{230}Th, ^{234}U and ^{238}U in each sample are required. These data are plotted in the form of $(^{234}U - ^{238}U)/^{238}U$ against $(^{238}U - ^{230}Th)/^{238}U$. Ideally, this yields a linear relationship in which the measured slope changes in a predictable way for deposits of increasing age and the rate of change of the slope is a function of the half-period of uranium flux in the local environment.

1.3.6 Geochemistry of the rare earth elements

The rare earth elements (La-Lu), although of generally low solubility in natural waters, are a particularly important group of elements in the study of geochemical processes as a consequence of their characteristic patterns of chemical reactivity and solubility. Reviews of REE geochemistry are provided in Henderson (1982; 1984). Although the rare earth elements were only used in a minor part of the present work to complement the radionuclide studies which formed the central theme of the project, it is useful to consider briefly some of the geochemical properties of these elements and the way in which they can be used in geochemistry.

The rare earth elements generally exhibit a low solubility and exist normally in the 3+ oxidation state. The 3+ oxidation state ions of the rare earth elements decrease in radius with increasing atomic number from 1.14 Å for La^{3+} to 0.85 Å for Lu^{3+}. This feature, known as the lanthanide contraction, is caused by the filling of f-orbitals such that with increasing electron occupancy of the f orbitals, the increasing effective nuclear charge produces an increased attraction on the outer electrons and results in an effective decrease in ionic radius. As a result of this decreasing ionic radius along the group, the ionic potentials of the 3+ ions show a corresponding increase and this affects the geochemical properties, such as solubility and reactivity, of these elements. For instance, La^{3+} and Ce^{3+} at the beginning of the series have ionic potentials of 2.6 and 2.8 respectively, the intermediate elements, Sm, Eu and Tb have respective ionic potentials of 3.0, 3.1 and 3.2 while Yb and Lu both have an ionic potential value of 3.5. This change in the ionic potential produces variations in the

chemical behaviour of the rare earth elements resulting in increasing reactivity and decreasing solubility along the series (c.f. Table 1.2).

The rare earth elements therefore show generally similar chemical properties to each other, with observed variations being accounted for by the decrease in ionic radius and corresponding increase in ionic potential along the group.

Two exceptions to this are Ce and Eu which can exist in the 4+ (ionic potential 4.6) and 2+ (ionic potential 1.7) oxidation states respectively (Elderfield and Greaves, 1982; Henderson, 1982, 1984). Any geochemical fractionation of the rare earth elements therefore generally involves separation of light from heavy rare earth elements or "anomalous" enrichment or depletion of Eu or Ce, and many rocks and minerals consequently exhibit highly characteristic rare earth element concentration patterns which can be used to distinguish materials from different source areas (eg Topping and MacKenzie, 1988).

Rare earth element data are often presented in graphical form in which the concentrations of the rare earth elements are normalized to the corresponding concentrations in a chosen reference material (ie the concentration of each rare earth element in the sample is divided by the concentration of the same rare earth element in the reference material). Such plots are usually presented as the logarithm of the normalized abundance against atomic number or atomic radius. This type of plot is commonly referred to as a Masuda-Coryell diagram after the workers who proposed this procedure (Henderson, 1984). One of the main advantages of this approach is that the abundance variations between rare earth elements of odd and even

atomic number is eliminated. The phenomenon of odd/even atomic number dependence of the rare earth element abundances arises because variations in the binding energy, and hence the stability, of a nucleus depends on whether the neutron number (N) and the proton number (Z) are odd or even. Those nuclei with even atomic number (both N and Z even) are the most stable whereas those with odd atomic numbers (both N and Z odd) are the least stable. A second advantage of presenting rare earth element data in normalized concentration plots is that enrichment or depletion of selected rare earth elements relative to the reference material are easily seen. Two reference materials commonly used for normalization of rare earth element data are (1) chondrite which shows the relationship between the rare earth element concentration pattern in the sample and that of the solar or cosmic abundance and (2), shale, which shows the relationship between the concentration of the rare earth elements in the sample and those of the earth's average crustal concentrations.

The relative abundance of individual rare earth elements is often similar in sediments derived from a common source rock although the absolute concentrations of the rare earth elements may vary between the different sediments. This arises because during the weathering process, a large fraction of the rare earth elements originally present in the rock do not enter solution at all but rather remain in the resistant minerals (eg clays). Moreover, any rare earth elements which do enter solution are generally subject to rapid removal by uptake in newly forming minerals, eg oxides of iron and manganese (Fleet, 1984). The rare earth elements can therefore pass from the original rock via weathering to deposition almost exclusively without taking part in any significant chemical fractionation processes.

The rare earth element content of sedimentary rocks varies markedly depending upon their composition. For instance, sandstones typically have low rare earth element concentrations relative to other sedimentary rocks (eg shales) as a consequence of the low rare earth element concentrations in the major constituent minerals of sandstone (eg quartz). In some sandstones, however, detrital grains of minerals such as apatite, clays or zircons (in which the rare earth elements have been concentrated by igneous processes) are present in high abundance and cause the sandstone to be rich in rare earth elements.

In contrast to sandstones, shales generally have high rare earth element concentrations since the bulk of the rare earth elements in eroded material are contained in the constituent fine clay minerals of shales. The rare earth element concentration patterns of most shales are very similar, being enriched in the light rare earth elements relative to the heavy rare earth elements when normalized to chondrites. The recognition of this similarity of rare earth element contents in most shales led to the use of shales for typifying sedimentary rare earth element abundances and for normalizing the rare earth element concentrations of sediments. This approach can therefore indicate whether or not a sediment has typical sedimentary rare earth element contents or can identify enrichments or deficiencies of single elements or groups of elements. During weathering, some dissolution of rare earth elements does occur and this can result in fractionation between the rare earth elements. In general, for low temperature processes, only a very minor proportion of the total rare earth element content of the rock goes into solution during solid/fluid interaction so that they have a generally

low level of mobility (Fleet, 1984). Moreover, during transport in solution, any changes in the solution chemistry could lead to re-precipitation of the rare earth elements in secondary minerals. For example Nesbitt (1979) observed variable fractionation of light and heavy rare earth elements during the weathering of a granodiorite in Victoria, Australia, depending upon the degree of alteration of the original rock and the groundwater pH.

The rare earth elements enter the marine environment mainly incorporated in particulate material, with only a small percentage of the total supply being in the dissolved phase (Fleet, 1984; Henderson, 1984). The rare earth element content of the detrital material entering the marine environment is generally similar to that of sediments, being enriched in the light rare earth elements relative to the heavy rare earth elements without any significant fractionation of any particular elements (Henderson, 1984).

The small fraction of the rare earth elements entering the oceans dissolved in river water are slightly enriched in both the light and the heavy rare earth elements relative to those of intermediate atomic number (Henderson, 1984). The enrichment of the light rare earth elements reflects the greater abundance of these in the continental crust, while, the enrichment of the heavy rare earth elements is probably related to the ability of these elements to form soluble complexes (Humphries, 1984).

The rare earth element patterns in seawater are similar to those of filtered river water (Fleet, 1984). The rare earth elements are very efficiently removed from solution immediately after entering the ocean resulting in a very short residence time of rare earth elements

in seawater. This is particularly so for Ce which shows a marked depletion compared to other rare earth elements in seawater which is not shown in river water (Fleet, 1984; Humphries, 1984). This is probably caused by Ce^{3+} entering seawater being oxidized to Ce^{4+} and precipitated from solution as CeO_2 (De Baar et al, 1985). In contrast, the other rare earth elements remain in the 3+ oxidation state and are lost from solution without further discernible fractionation (Henderson, 1982; 1984; Elderfield and Greaves, 1982).

Deep ocean sediments generally show rare earth element concentration patterns similar to those of seawater with the notable exception of the existence of a positive Ce anomaly for the sediment, but, as mentioned above a negative Ce anomaly for the water.

In the present work the sediments of interest are of recent detrital origin and these processes affecting the rare earth elements in the deep ocean are consequently of limited relevance. In contrast the geochemical characteristics of the potential source rocks of the sediment studied will be of major importance. In this context, one study of relevance is an investigation by Stephens et al (1985) of the rare earth elements in the Criffel pluton, a potential source rock for a number of the sediments investigated. This work revealed that the Criffel granite shows chondrite normalized rare earth element patterns with characteristic enrichment of light relative to heavy rare earth elements but with no significant Eu or Ce anomalies relative to chondrite.

1.3.7 Manmade Radionuclides in the Coastal and Marine Environments

In addition to natural radioactivity, manmade

radionuclides have also been present in the environment for more than 40 years, with the major sources being nuclear weapons testing and deliberate and accidental releases during nuclear power production operations.

This section provides a review of the major sources of manmade radionuclides to the coastal marine and near shore terrestrial environment, with particular consideration of the UK coastal environment. For ease of treatment, the various sources of manmade radionuclides to the UK environment are considered in the chronological sequence in which they influenced the environment, thus illustrating the evolution of contemporary levels and isotope ratios of radionuclide contamination.

The largest amount of manmade radionuclides so far released to the environment has in fact been from nuclear weapons testing and the major input from this source took place in the late 1950's and early 1960's. Some of the nuclear weapons tests took place within the ocean, giving rise to relatively high levels of localised radionuclide contamination. For instance, the highest concentrations of ^{90}Sr observed as the result of weapons testing have been recorded in north-western Pacific Ocean waters which received direct input from the earlier major series of weapons tests (Riley and Skirrow, 1975). The major portion of manmade radioactivity added to the oceans was, however, derived from atmospheric explosions. Bowen and Livinston (1980) reported that over 1.48×10^4 TBq of $^{239, 240}Pu$ has been deposited in the environment as the result of atmospheric weapons testing. Of this total, 1.11×10^4 TBq of plutonium is estimated to have been distributed on a worldwide basis as global fallout and at least 2.59×10^3 TBq has been deposited in local environments near test sites (Joseph et al, 1971; Bowen

and Livingston, 1980). It has also been estimated that about 1.26 x 10^6 TBq of ^{137}Cs had been introduced to the atmosphere by nuclear weapons testing prior to 1970 (Joseph et al, 1971). Little ^{241}Am was released directly during the testing period, but substantial quantities of ^{241}Pu were produced from this source and there has consequently been a growth of ^{241}Am activity. The inventory of ^{241}Am in soils is expected to become about equal to that of $^{239,240}Pu$ in the year 2010 (Holm and Persson, 1977; Bennett, 1978). Some of the main radionuclides present in weapons testing fallout are shown in Table 1.4, along with an estimate of the amounts of selected nuclides released to the environment from 1954 to 1970. The Atmospheric Test Ban Treaty was agreed in 1963 and no significant input from this source has occurred since then.

In addition to weapons testing fallout, a small, but significant release of plutonium as widespread atmospheric fallout occurred in 1964 when about 1kg (629 TBq) of the short-lived radionuclide ^{238}Pu ($t_{½}$ = 88Y) was released during the unplanned atmospheric burn up of a United States' Satellite with a nuclear auxiliary power system. This event increased the global environmental content of ^{238}Pu by a factor of three (Hardy et al, 1973) and gave rise to a $^{238}Pu/^{239,240}Pu$ activity ratio appropriate to the UK in 1964 of 0.05 (Joseph et al, 1971; Hardy et al, 1973; Cambray et al, 1982).

The result of the atmospheric testing of nuclear weapons has therefore been the global contamination of the environment at low level with radioactivity. In the marine environment, soluble species such as ^{137}Cs have remained largely in solution whereas insoluble species such as plutonium and americium have been incorporated to a large extent in the sediment (Hardy

Nuclide	Half-Life (y)	Decay Mode
^{3}H	12.35	ß
^{14}C	5730	ß
^{55}Fe	2.69	EC
^{60}Co	6.27	ß
^{129}I	1.57×10^{7}	ß
^{137}Cs	30.17	ß
^{238}Pu	87.71	α
^{239}Pu	2.41×10^{4}	α
^{240}Pu	6.57×10^{3}	α
^{241}Pu	14.36	ß

(a) Selected nuclides present in fallout with half lives greater than 1 year

Nuclide	Total production (T Bq)
^{137}Cs	7.8×10^{5}
^{90}Sr	1.3×10^{6}
^{241}Pu	8.9×10^{3}
$^{239, 240}Pu$	2.1×10^{2}

(b) Quantities of selected nuclides produced as fallout in the period 1954 to 1970

TABLE 1.4: Radionuclides in weapons testing fallout. (Data based upon Burton, 1975; Joseph et al, 1971; Hardy et al, 1973; Cambray et al, 1982)

et al, 1973, 1974; Edgington and Robbins, 1975; Livingston and Bowen, 1975, 1979; Santschi et al, 1983).

On land, soils also contain radionuclides deposited as fallout from atmospheric testing of nuclear weapons. In near surface explosions, most of the activity was trapped by condensing terrestrial material in the cloud and was deposited locally (Facer, 1980). The residence time of nuclear weapons debris in the stratosphere was found to be about 1 year (Perkins and Thomas, 1980) and this allowed substantial mixing and transport prior to deposition, which occurred mainly at the mid-latitudes in each hemisphere (Hardy et al, 1973). Rainfall is a major factor that influences the scavenging of fallout radionuclides from the atmosphere, and a relationship between the amount of rainfall and the total inventory of fallout radionuclides in the soil can be established at any given latitude (Hardy et al, 1973; Cambray et al, 1973, 1984; Eakins and Lally, 1984). For UK latitudes, it has been estimated that the inventory of $^{239,240}Pu$ is 55 Bq m^{-2} in the top 30cm of a soil profile, normalised to a rainfall of 1000mm y^{-1}. For ^{137}Cs the corresponding inventory in the top 30cm of soil is estimated to be 3.7 x 10^{3}Bq m^{-2} normalised to 1000m y^{-1} rainfall (Cawse and Horrill, 1986).

In most terrestrial ecosystems, the soil compartment holds about 99% of the plutonium inventory and 75% of the ^{137}Cs inventory (Dahlman et al, 1980; Little, 1980; Cawse and Horrill, 1986). Moreover, in soil profiles the radionuclides are generally held in the surface layers of about 30cm depth and such observations have been made in environments as diverse as the Nevada Test Site (Essington et al, 1976); West Germany (Jakubick, 1976); Japan (Yamamoto et al, 1980) and

West Cumbria, UK (Cawse, 1980).

In soils, particle size has an important influence on radionuclide concentrations and distributions and fine material, with very high surface area, tends to preferentially concentrate radionuclides. This phenomenon has been observed at several sites. For example, Muller (1978) has reported data showing that the <2μm fraction of Ohio soils was found to have specific activities of plutonium several times higher than bulk samples. At the Rocky Flats site, fine material has been found to be enriched in plutonium (Tamura, 1975) and in alluvial soils at Los Alamos, the <53μm fraction had specific activities ten times higher than 2-23mm material (Nyhan et al, 1976), but in this case, due to the particle size distribution of the soils, the majority of plutonium activity was held by particles of size greater than 105μm. Livens and Baxter (1988) have reported results for four soils from Cumbria in north west England, and they observed that in all these samples, the radionuclides were concentrated into the finer size fractions, with the <2μm particle size showing enrichments of plutonium from 1.5 to 40 times that in the bulk samples, of americium from 2 to 40 times and ^{137}Cs from 3 to 25 times.

In soils ^{137}Cs is strongly associated with fine clay minerals and two main mechanisms are involved in the fixation process. The first involves adsorption of ^{137}Cs on to non-selective sites at the edges of the clay crystal lattice but this does not result in permanent fixation and the radionuclide can be displaced by an excess of competitive cations eg. Na^+ and K^+ (Tamura, 1964). The second mechanism causes fixation in a permanent non-exchangeable form, mainly in micaceous clays that are depleted in K through

weathering and have an expanded lattice structure. The ^{137}Cs and other cations of similar ionic radii eg. K^+, Rb^+ and NH_4^+ may neutralise the negative charges within the clay lattice, causing the structure to collapse and trap the ions (Tamura and Jacobs ,1960). In contrast in the case of plutonium adsorption on soil particles, the mechanism involved is believed to be other than simple ion exchange. The availability of complexing ions such as organic matter, CO_3^{2-} and HCO_3^- is one of the most important factors in determining the degree of retention of plutonium by soil particles. The soil organic matter is capable of altering plutonium oxidation states, and can also produce complexation so that organic matter is able either to increase or decrease plutonium retention in the solid phase.

Manmade radionuclides taken up by soils can be associated with a number of notionally separate components of the soil such as the oxide coatings on mineral grains, the organic materials present and detrital mineral grains. A number of authors have utilized the technique of sequential leaching (McLaren and Crawford, 1973; Lally and Eakins, 1978; Muller, 1978) in an attempt to investigate such associations by the preferential dissolution of specific components of the soil by the use of selective solvents and reagents. While there has been recent criticism of this approach (Livens, 1985) it remains one of the few ways of investigating the solid phase speciation of radionuclides and it can give useful results. For instance, Cook et al (1984a, 1984b) used sequential extraction techniques to identify the geochemical association of plutonium in soil samples from the immediate environment of the Dounreay Nuclear Power Development Establishment, Caithness, UK using selective extractants. The selective extraction method

used was designed to determine the percentage of plutonium in the following forms; readily available, exchangeable and associated with specific adsorption sites, associated with organic matter as chelated complexes, co-precipitated with sesquioxides and finally, associated with the residual fraction. They found that the majority of the plutonium (about 65%) was associated with the organic matter fraction whereas only 28% was bound with the mixed oxides. In contrast, Muller (1978) suggested that about 70 to 90% of the plutonium in Ohio soils is associated with oxide phases.

Since the end of the period of major atmospheric testing of nuclear weapons, the major sources of manmade radionuclides to the environment of the UK have been planned, and accidental, discharges from nuclear industry facilities. Very small sources of radionuclides occur in discharges from other establishments such as hospitals, universities and conventional industrial facilities but they are of highly localised significance only and will not be considered here. The UK coastal marine environment has been particularly affected by authorized discharges from nuclear facilities and this has resulted in significant modification of radionuclide inventories and activity ratios in some areas, relative to those produced by atmospheric fallout.

In general, authorized releases of radionuclides to the environment at various stages of the nuclear fuel cycle constitute a much smaller source of radioactivity than fallout from weapons testing, but they are, however, essentially point source releases. Such discharges can therefore give rise to localised radioactivity concentrations which are higher than those produced from fallout and which generally

decrease rapidly with increasing distance from the source point. The species released as waste from the nuclear power industry are in general the same as those present in fallout, ie. transuranics, fission products and light activation products. In some cases, however, the isotope ratio for selected radionuclides in fallout is markedly different from that in nuclear power related waste and this can be used as an indication of the sources of environmental contaminants as described below. A particularly important example of this is the occurence of ^{134}Cs in nuclear industry waste (as an activation product) but not in weapons testing fallout.

Significant releases of nuclear industry radioactive waste have taken place since 1944, which marked the start of discharges of effluent from the Plutonium production plant in Hanford, Washington, USA to the north east Pacific Ocean via the Columbia River (Seymour, 1971). At present the three major sources of nuclear waste to the world ocean system are the nuclear fuel reprocessing plants at Trombay (India), Cap De La Hague (France) and Sellafield, formerly Windscale (UK) (Taylor, 1982; Bayer, 1983; MacKenzie and Scott, 1984), but reprocessing facilities are also planned to come into operation in the near future in Japan and West Germany.

In the context of the UK coastal and aquatic environment, there are 26 establishments recognised as discharging significant quantities of manmade radionuclides as shown in Figure 1.10. These consist of a series of nuclear reactors, fuel fabrication facilities, radionuclide production centres, military establishments and the two reprocessing facilities at Dounreay and Sellafield. The Sellafield discharge is, however, far larger than all of the other sources and has exerted a dominant influence in determining the

levels of radionuclide contamination in much of the UK coastal environment since the 1960's. Other discharges are of only local significance and in this context, possible local effects must be considered in the area of the present study as a result of releases from the nuclear reactors at Hunterston and Chapelcross, although, as shown in Table 1.5, these discharges are extremely small relative to the Sellafield discharge. The influence of these discharges is therefore very small in comparison to the Sellafield discharge and is of significance only in the immediate vicinity of the discharge point (Baxter et al, 1979; MAFF, 1983, 1984; MacKenzie and Scott, 1984).

The discharge from the Sellafield operation has in fact been of globally significant magnitude in the last 30 years, especially during the 1970's. The annual quantities of radionuclides discharged from Sellafield have shown marked variations with time, with a pronounced maximum in the mid 1970's, after which discharge levels were significantly decreased due to improvements in technology such as the use of skips containing Zeolite ion exchange resin (Taylor, 1982) and introduction of the SIXEP ion exchange plant (BNFL, 1981) to remove radionuclides from the waste liquids.

The discharge data for radiocaesium and plutonium isotopes and for ^{241}Am are shown in Table 1.6 and Figure 1.11, along with the cumulative totals allowing for radioactive decay and ingrowth of ^{241}Am as a consequence of the decay of ^{241}Pu.

The radionuclides in the liquid effluent discharged from Sellafield basically arise from two main sources: a) storage ponds, where the spent Magnox fuel elements are flushed with water prior to reprocessing and b) sea tanks, where the reprocessing wastes are held.

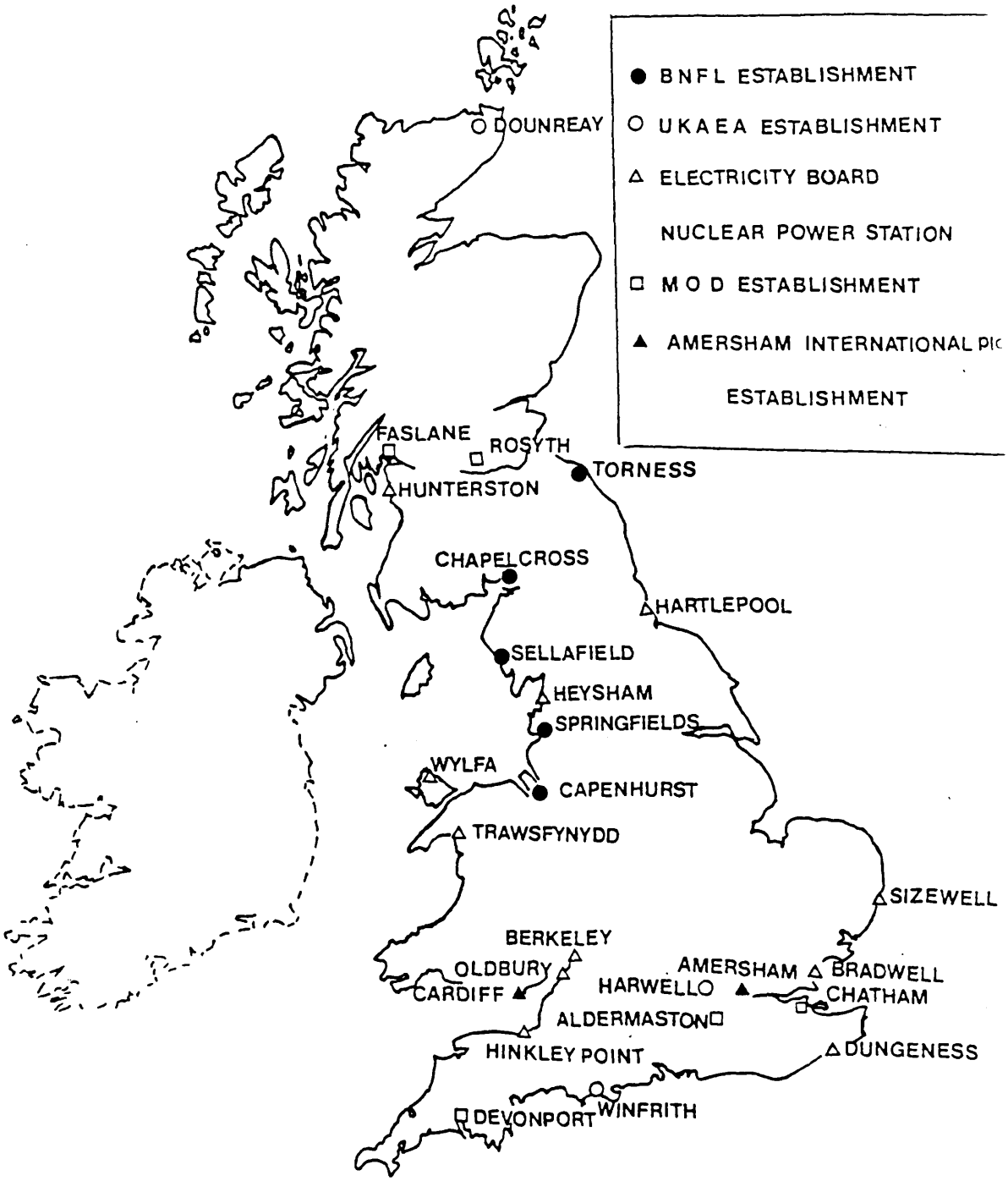

Figure 1.10 Map showing the main establishments discharging liquid radioactive waste to the UK aquatic environment

After a suitable storage period, these effluents from the storage ponds and sea tanks are monitored and are then neutralised by addition of alkali, after which they are discharged to sea at high tide via a pipeline (NEA, 1981; BNFL, 1982, 1984; Pentreath et al, 1985).

Nuclear fuel reprocessing is required to close the nuclear fuel cycle and allows recovery of uranium (depleted in ^{235}U) and plutonium isotopes including ^{239}Pu (BNFL, 1982, 1984). The reprocessing of the irradiated nuclear fuels at Sellafield initially involves stripping of the alloy casing from the fuel elements after which they are dissolved in nitric acid. Plutonium and uranium are extracted from the resulting solution in mixer/settler units using tributyl phosphate in odourless kerosene (TBP/OK). Following separation, the organic fraction, containing the uranium and plutonium, is back-extracted using ferrous sulphate as a reducing agent to remove plutonium, while uranium remains in the organic phase and is separated (Chesne, 1983). The bulk of the fission products are left in the aqueous residue from the first extraction, and these fission products are then concentrated and stored as high level waste solutions while lower level waste solutions are treated, neutralised with ammonium hydroxide and are then discharged to the sea (Hetherington, 1975; Pentreath et al, 1984).

^{137}Cs and ^{90}Sr are the major constituents of the beta/gamma fraction of the Sellafield waste, while the alpha activity in the discharge is mainly due to plutonium isotopes and ^{241}Am. Up to 1972 plutonium isotopes accounted for most of the alpha activity in the discharge but the reprocessing of more highly irradiated fuel after this date led to significant increases in the discharge of ^{241}Am, which accounted for

YEAR	CHAPELCROSS Total Activity	HUNTERSTON Total Activity
1970		
1971	0.78	0.81
1972		
1973	0.26	1.04
1974	0.26	2.59
1975	0.63	4.29
1976	1.18	5.88
1977	0.34	4.44
1978	2.8	2.42
1979	9.1	4.27
1980	0.32	13.7
1981	1.8	8.61
1982	4.1	8.92
1983	3.1	2.93
1984	0.48	2.84
1985	2.0	3.69
1986	-	1.63
1987	-	1.13

TABLE 1.5: Discharge data for Chapelcross and Hunterston (MAFF 1971-1987)

Units = TBq

Year	Cumulative ^{137}Cs	Cumulative $^{239,240}Pu$	Cumulative ^{241}Am	Discharge ^{137}Cs	Discharge ^{241}Pu	Discharge $^{239,240}Pu$	Discharg ^{241}Am
1957	138			138			
1958	387			249			
1959	460			73			
1960	494		0.14	34		2.9	
1961	534		0.45	40		3.9	
1962	575		1.1	41		6.9	
1963	589		2.1	14		8.6	
1964	693		3.5	104		10.6	
1965	802		5.4	110		10.8	
1966	983		7.7	181		10.8	
1967	1133	18.5	10.8	150		18.2	
1968	1504	49.1	15.2	372		30.7	
1969	1948	79.3	20.8	444		30.2	
1970	3102	113.9	46.8	1156		34.7	19.1
1971	4427	155.7	93.1	1327		41.8	37.7
1972	5716	212.9	183.8	1290	1902	57.3	79.5
1973	6484	278.5	307.9	769	2755	65.8	109.2
1974	10545	324.7	443.1	4065	1708	46.2	118.3
1975	15776	368.9	498.2	5236	1817	44.4	36.3
1976	20065	415.8	530.2	4294	1297	46.9	12.0
1977	24543	452.1	554.5	4483	981	36.3	3.7
1978	28631	510.1	584.9	4092	1773	45.7	7.9
1979	31193	559.5	616.4	2565	1494	37.5	7.8
1980	34159	586.7	648.4	2969	728	20.4	8.3
1981	36516	607.0	680.7	2359	596	15.3	8.8
1982	38516	627.7	710.3	2000	485	16.1	6.4
1983	39716	639.4	735.1	1200	331	8.7	2.2
1984	40150	650.6	759.5	434	345	8.3	2.3
1985	40475	654.0	782.3	325	81	2.6	1.6
1986	40493	656.7	803.9	18	63	1.3	
1987	40505	656.7	823.8	12		0.7	

TABLE 1.6: Quantities of selected nuclides discharged as low level liquid effluent from Sellafield in the period 1957 to 1987 (Cambray, 1982; MAFF, 1970-1988)
Units = TBq

Year	Discharges				
	$\frac{^{134}Cs}{^{137}Cs}$	$\frac{^{137}Cs}{^{239,240}Pu}$	$\frac{^{137}Cs}{^{241}Am}$	$\frac{^{241}Am}{^{239,240}Pu}$	$\frac{^{238}Pu}{^{239,240}Pu}$
1960		11.7			
1961		10.5			
1962		5.9			
1963		1.6			
1964		9.8			
1965		10.5			
1966		16.7			
1967		8.1			
1968		12.1		0.69	
1969		14.7		0.49	
1970	0.22	33.3	60.5	0.55	
1971	0.18	31.8	35.2	0.90	
1972	0.17	22.5	16.2	1.38	
1973	0.22	11.7	7.0	1.66	
1974	0.25	88.0	34.4	2.56	
1975	0.21	117.8	144.2	0.82	
1976	0.17	91.6	357.8	0.26	
1977	0.13	123.4	1211.6	0.10	
1978	0.10	89.7	518.0	0.17	0.27
1979	0.09	68.4	328.8	0.21	0.32
1980	0.08	145.8	357.7	0.40	0.34
1981	0.07	153.9	268.1	0.57	0.32
1982	0.07	124.6	312.5	0.40	0.29
1983	0.07	137.4	545.5	0.25	0.33
1984	0.08	52.2	188.7	0.28	0.31
1985	0.09	125.0	203.1		
1986	0.07		13.8		
1987	0.10		17.1		

TABLE 1.6: Continued

Year	^{137}Cs / $^{239,240}Pu$	Cumulative ^{137}Cs / ^{241}Am	^{241}Am / $^{239,240}Pu$
1960		3528.6	
1961		1186.7	
1962		522.7	
1963		280.5	
1964		198.0	
1965		148.5	
1966		127.7	
1967	61.2	104.9	0.58
1968	30.6	98.9	0.31
1969	24.6	93.7	0.26
1970	27.2	66.3	0.41
1971	28.4	47.6	0.60
1972	26.8	31.1	0.86
1973	23.3	21.1	1.11
1974	32.5	23.8	1.36
1975	42.8	31.7	1.35
1976	48.3	37.8	1.28
1977	54.3	44.3	1.23
1978	56.1	49.0	1.15
1979	55.8	50.6	1.10
1980	58.2	52.7	1.11
1981	60.2	53.6	1.12
1982	61.4	54.2	1.13
1983	62.1	54.0	1.15
1984	61.7	52.9	1.17
1985	61.9	51.7	1.20
1986	61.7	50.4	1.22
1987	61.7	49.2	1.25

TABLE 1.6: Continued

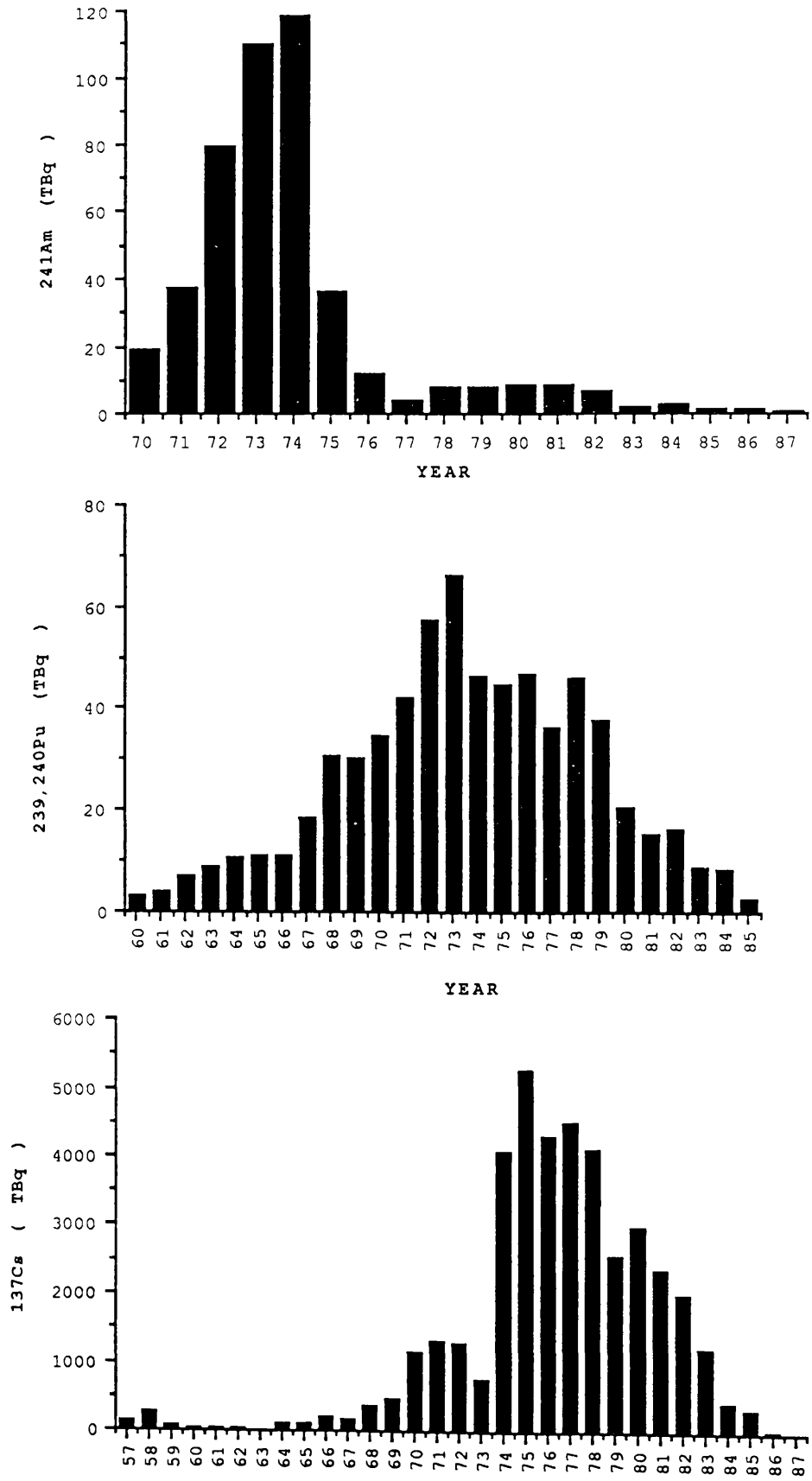

Figure 1.11 Temporal variations in the quantities of ^{137}Cs, $^{239,240}Pu$ and ^{241}Am discharged annually from Sellafield as low level liquid effluent (Cambray, 1982, MAFF, 1970-1988)

over 70% of the alpha activity discharged in 1974 (Hetherington et al, 1976; Smith et al, 1980).

The activity of the beta emitter ^{241}Pu in the discharge is many times greater than the activity from the alpha emitting plutonium isotopes. However, ^{241}Pu has a relatively short half-life (14.7y) and decays to the alpha emitter ^{241}Am according to the equation:

$$^{241}Pu \xrightarrow[14.7y]{\beta} {}^{241}Am \xrightarrow[433y]{\alpha} {}^{237}Np \xrightarrow[10^6y]{\alpha}$$

(Hetherington et al, 1976; Day and Cross, 1981). Thus, in addition to directly discharged ^{241}Am, ingrowth of this nuclide from ^{241}Pu present in the environment must also be considered.

The dispersion of radionuclides in the environment as a consequence of the Sellafield discharge is of fundamental importance in evaluating the radiological impact of the discharge and observation of the pattern and rate of dispersion of the radionuclides can provide a useful tracer for study of natural processes. The dispersion processes affecting different radionuclides are determined by their geochemical and biogeochemical behaviour in the environment and, as a consequence of the differences in their physico-chemical properties, radically different dispersion patterns are observed for different nuclides. This is clearly illustrated as outlined below by the differences in behaviour of americium, plutonium and caesium isotopes discharged from Sellafield, which constitute some of the most radiologically significant nuclides in the discharge and which are also central to the interest of the present work.

Most of the ^{137}Cs discharged from Sellafield to the

Irish Sea remains in the solution phase, while only a small fraction (about 5%) is retained in the Irish Sea Sediments (Miller et al, 1982; Jones et al, 1984, MacKenzie et al, 1987). The ^{137}Cs in solution is transported northwards and, after leaving the Irish Sea, is carried around the Scottish coast and then both south into the North Sea and north east into the coastal waters of Norway (Jefferies et al, 1973; Hetherington, 1976; Livingston and Bowen, 1977; Baxter et al, 1979; McKinley et al, 1981a,b).

In contrast to ^{137}Cs the major fraction (about 95%) of the plutonium and virtually all of the ^{241}Am discharged to the Irish Sea from Sellafield is lost from the water column to the sediments immediately after release, with much of the total discharge inventory of these species residing in a muddy area within 30km of the Sellafield pipeline (Hetherington, 1976; Livingston and Bowen, 1977; Aston and Stanners, 1981). The remaining 5% or so of the plutonium is retained in the aqueous phase and is transported in solution within the Irish Sea and around the Scottish coast and appears to behave as a relatively conservative element in the manner of ^{137}Cs (Jefferies et al, 1973; Hetherington et al, 1975, 1976). Subsequent to their incorporation in the sediments, plutonium and americium are subject to burial, mixing and transport from the initial point of deposition in accordance with the general sediment accumulation and transport processes operating in the area as discussed in detail below.

The pronounced differences in the geochemical properties of caesium, plutonium and americium therefore have a profound influence on the long term fate of these species in the Sellafield discharge and it is therefore useful to consider some of the factors of importance in determining their geochemical

behaviour.

A reasonably good general indication of the behaviour of a radionuclide with respect to aqueous phase solubility in the environment is given by the distribution coefficient (K_D) which, in this work, will be taken as

$$K_D = \frac{\text{Activity of nuclide/kg of solid phase}}{\text{Activity of nuclide/kg of aqueous phase}}$$

The term K_D in fact represents the net result of a complex set of reactions and although K_D values are widely used in the literature this complexity is not explicitly referred to in many publications. In order to understand the causes of nuclide distribution using the K_D concept, the following points must be borne in mind.

i. Natural waters contain particles of various sizes and mineralogies and with varying organic matter and skeletal material content. The organic matter may be living, partly decomposed or the residue of decomposition, while the skeletal matter may also be in various stages of formation or dissolution (Sholkovitz, 1983).

ii. The chemical composition, particle size distribution and suspended concentration of particles in coastal waters can undergo large spatial and temporal (eg. over a tidal cycle) variations in response to hydrographically controlled resuspension and deposition processes (Sholkovitz, 1979).

iii. In practice, the measurement of K_D values incorporates the effects of a suite of

geochemical, biochemical and sedimentological processes such as adsorption, desorption, remineralisation, precipitation, redox transformations, bioaccumulation, and ion exchange.

iv. For nuclides which exist in several oxidation states, each capable of having different solubility, complexing and adsorption properties, different K_D values will be appropriate to each oxidation state.

v. Variations in concentrations of ligands, such as phosphate, bicarbonate and organic substances in the aqueous phase, may alter the equilibrium.

vi. Equilibrium may not be reached in some conditions.

vii. Variations in temperature can affect K_D.

K_D is, therefore, a static form of a thermodynamic parameter which is governed by a set of complex and not necessarily interrelated processes, so the concept that K_D can be regarded as a rigorously defined equilibrium constant capable of predicting the concentration and fractionation of any nuclide in natural waters appears inherently too simple. Nevertheless, the use of K_D's does represent a useful, semi-quantitative method of describing and predicting radionuclide solubilities in defined systems.

K_D values defined by observation of the partitioning of pollutant radionuclides between the aqueous and solid phases in the environment are largely determined by the kinetics of sorption, and the mechanisms by which sorption of radionuclides onto sediment occurs can include direct retention by surface adsorption or

ion exchange and retention in the thin films of water, hydrated oxide or organic materials associated with particle surfaces. For instance, adsorption of plutonium and americium has been shown to be strongly associated with manganese or iron oxide films on the surface of sediment particles (Means et al, 1978; Muller, 1978). In addition to the above mechanisms, other parameters which can be of importance in controlling the uptake of radionuclides by sediment include, (a) salinity of the water, (b) pH and Eh of the system, (c) the ionic sorption capacity of the solid particles, (d) ionic potential and particle reactivity of the nuclide, (e) availability of complexing ions and chelating agents, and (f) oxidation states of the nuclide (Smith et al, 1980; Edgington, 1981; Sholkovitz, 1983; Sholkovitz and Mann, 1984; Assinder et al, 1985).

The limitations in the use of K_D values are illustrated by the observation that the K_D's derived by study of the initial sorption of pollutant radionuclides need not be appropriate to subsequent desorption reactions. Thus, for example, radiocaesium and plutonium (or americium) exhibit contrasting properties with respect to sorption behaviour, but once incorporated in the sediments, these radionuclides often show similarities in behaviour, eg. the behaviour of these nuclides, following their delivery to shallow water marine sediments of the north east coast of the USA has been shown to be chiefly a function of the sedimentary regime involved (Livingston and Bowen, 1979).

Caesium is the most electropositive element known and, with an ionic potential of 0.6, exists in aqueous solution entirely as the solvated monovalent cation. It is therefore highly soluble in seawater (ie. effectively exhibiting conservative behaviour) and

consequently has a long residence time (approximately 10^4 to 10^5 years) in open ocean waters (Brewer, 1975) and, even in coastal waters, where scavenging particle fluxes are greater, residence times of more than 10^2 years are observed (Swan et al, 1982).

K_D values for the partitioning of caesium between the particulate and aqueous phases in seawater have been reported in many publications, relating both to laboratory and field studies. For instance, Stanners and Aston (1981) reported K_D values for ^{137}Cs in the range 300 to 500 for partitioning between seawater or brackish water and Irish Sea sediments. Similarly, Baxter et al (1978) reported a value of 200 for the K_D of ^{137}Cs for seawater-sediment partitioning in the Clyde Sea Area in south west Scotland. A survey of the literature reveals that published laboratory and field values for the K_D of caesium under realistic environmental conditions in fact range from about 10^2 to 10^3 (Aston and Duursma, 1973; Duursma and Eisma, 1974; Pillai et al, 1975; Stanners and Aston, 1981), with K_D's derived from well-mixed water overlying coastal sediments lying at the lower end of this range (Swan et al, 1982). The K_D values calculated from tank experiments, may in fact be an order of magnitude higher than values calculated from field experiments due to the influence of environmental parameters such as salinity, temperature etc. (Stanners and Aston, 1981).

The mechanism of ^{137}Cs adsorption onto marine sediment has been found from tank experiments (Duursma and Eisma, 1974) to involve exchange with ions other than stable Cs^+. Most field and laboratory studies indicate that ^{137}Cs is strongly and preferentially adsorbed onto illitic clays probably by exchanging with K^+ ion (Tamura and Jacobs, 1960; Lomenick and Tamura, 1965;

Janne and Wahlberg, 1968; Lammers, 1968).

Tamura and Jacobs (1960) and Cheng and Hamaguchi (1968) have suggested that sorption of caesium onto clays can involve both "edge" and "interlayer" fixation Rapid uptake was suggested to favour the former process, with the latter resulting from the slower processes of diffusion of ions into interlayer sites causing a decrease in the interlayer distance and hindering desorption . This "two-step" adsorption processes was invoked by Stanners and Aston (1982) to explain the differential degree of retention of ^{137}Cs and ^{134}Cs shown by contaminated Ravenglass sediment. Thus, in laboratory experiments an observed preferential desorption (lower K_D) of ^{134}Cs was attributed to its more recent origin compared with the longer-lived ^{137}Cs which had been incorporated into the minerals in a more irreversible form (Stanners and Aston, 1982).

Apparently incompatible results have been reported for the degree of reversibility of radiocaesium sorption onto clays. Thus, in tank experiments, contaminated intertidal sediments from the Ravenglass Estuary near Sellafield showed about 30% desorption of radiocaesium into "clean" seawater in 10 days (Stanners and Aston, 1982). Ganapathy et al (1968) similarly reported a 10% desorption of ^{137}Cs from Bombay sediments after 50 days' exposure to seawater. Both studies suggest that a significant percentage of adsorbed ^{137}Cs is reversibly associated with the sediment. However, environmental evidence from studies of Cumbrian sediment by Aston and Stanners (1979) suggested that most of the radiocaesium is firmly bound to the sediment particles with a low affinity for desorption.

The solubility of plutonium in natural waters is dependent upon its oxidation state and the +5 and +6

forms with ionic potentials of 6.76 and 8.45 respectively are more soluble in natural waters then the lower oxidation states of +3 and +4 which have correspondingly lower ionic potentials of 3.00 and 4.65 respectively rendering them highly susceptible to hydrolysis and sorption onto particle surfaces as discussed in section 1.3.3 (Edgington and Robbins, 1975; Hetherington, 1978, Lovett and Nelson, 1978; Sholkovitz, 1983).

The chemical equilibrium of Pu^{5+} and Pu^{6+} with Pu^{3+} and Pu^{4+} in seawater is therefore continuously perturbed by removal of the less soluble lower oxidation states to the sediments (Lovett and Nelson, 1978). The low solubility of plutonium in seawater is reflected by its high K_D value of about 10^5. This can be compared with reported K_D values of 10^4 and 10^6 for uranium and thorium respectively.

In sediments (and soils), for all oxidation states of plutonium in the pH/Eh range of environmental interest, strong complexes are formed between plutonium and oxygen containing ligands such as (O^{2-}, OH^-, CO_3^{2-} and HPO^{2-}_4). Organic matter complexation with plutonium is also very important and the tendency for plutonium towards preferential sorption on the smaller grain size fraction of sediment is similarly well documented (Hetherington, 1975, 1978; Aston, 1980, Aston et al, 1981).

Under environmental conditions, americium exists virtually exclusively as Am^{3+} giving it an ionic potential of 3.06 and a consequently very low solubility (Edgington, 1981; Pentreath, 1981, Pentreath et al, 1984). The extremely low solubility of americium in aquatic environments is reflected in its very high K_D value of greater than 10^6 (Edgington,

1981). The higher K_D value of americium compared to plutonium is a consequence of variable oxidation state of plutonium in aquatic environments and the K_D values of the actinides in fact form a logical sequence when related to oxidation state (Rhodes, 1957; Anderson et al, 1982a, 1982b; Ivanovich, 1982). Typical K_D values of the elements associated with the present work are shown in Table 1.7. Due to its very high particle reactivity, americium is mainly associated with solid phase materials such as suspended particles (both biotic and abiotic), soils and sediments. For example, the americium discharged from Sellafield, has been shown to be immediately taken up by the sediments close to the point of discharge, being even more efficiently scavenged from solution than plutonium. Thus, soon after discharge into the Irish sea, americium undergoes a number of different chemical reactions such as co-precipitation, active uptake with biogenic material, association with particulate matter, precipitation on the surface of particles and adsorption or ion exchange with surface layers (Edgington, 1981). The general features of the environmental behaviour of americium were established by studies of weapons testing fallout and have been confirmed by studies of nuclear industry waste such as the Sellafield discharge. As discussed above ^{241}Am is produced by decay of ^{241}Pu and the distribution of ^{241}Am in the environment is therefore influenced both by its own geochemical behaviour and by that of ^{241}Pu. The implications of this for the Sellafield discharge have been discussed by Day and Cross (1981).

On the basis of the reported Sellafield discharges and considerations of radionuclide geochemistry and radioactive decay and growth, the localised area of fine silt in the north east Irish Sea (Figure 1.12) can be estimated to have contained about 6×10^2 TBq

Element	Recommended K_D values for coastal sediments
Na	1×10^0
Mn	2×10^5
Fe	5×10^4
Sb	1×10^3
Te	1×10^3
I	2×10^1
Cs	3×10^3
Ce	2×10^6
Sm	2×10^6
Eu	5×10^5
Tb	1×10^6
Dy	5×10^5
Tm	3×10^5
Yb	1×10^6
Hf	1×10^5
Ta	2×10^5
Pb	2×10^5
Po	5×10^7
Ra	5×10^3
Ac	2×10^6
Th	2×10^6
Pa	1×10^6
U	1×10^3
Np	5×10^3
Pu	1×10^5
Am	2×10^6

TABLE 1.7: K_D values for selected elements (IAEA, 1985)

each of $^{239,240}Pu$ and ^{241}Am and of the order of 10^3 TBq of ^{137}Cs in the mid 1980's (MacKenzie and Scott, 1984; MacKenzie et al, 1987). To put these numbers in perspective the ^{137}Cs represents about 1% of the world-wide ^{137}Cs environmental inventory due to nuclear weapons testing fallout (Holm and Persson, 1977;MacKenzie and Scott, 1984), and the corresponding figures for $^{239,240}Pu$ and ^{241}Am are about 7% and 30% respectively. Activities of an order of magnitude greater than those due to atmospheric fallout have in fact been detected in Irish Sea sediments at distances of up to 100km from the Sellafield discharge point (Smith et al, 1980) while close to Sellafield concentrations of up to 10,000, 2,300 and 2,000 Bq kg^{-1} are observed in silts for ^{137}Cs, $^{239,240}Pu$, ^{241}Am respectively (MAFF, 1981).

It is therefore evident that the behaviour of the fine sediment in this area greatly influences the fate and transport pathways of these radionuclides and a considerable research effort has been devoted to demonstrate the importance of these fine silts as a sink for radionuclides and to the study of the behaviour of these sediments. For instance, Hetherington et al, (1975) reported that the alpha activity per unit dry weight of intertidal sediment from Newbiggin on the Ravenglass Estuary near Sellafield, increased steadily with decreasing grain size from sand to clay. Similarly, later results for $^{239,240}Pu$ presented by Hetherington (1978) and for ^{241}Am, reported by James et al (1978), revealed the same trend. Smith et al (1980), in a comprehensive review of all the available data relating to the Sellafield discharges concluded that almost all the plutonium discharged from Sellafield is associated with the sea bed sediments, particularly the fraction less than 62.5μm in size. Jones et al (1984) also reported

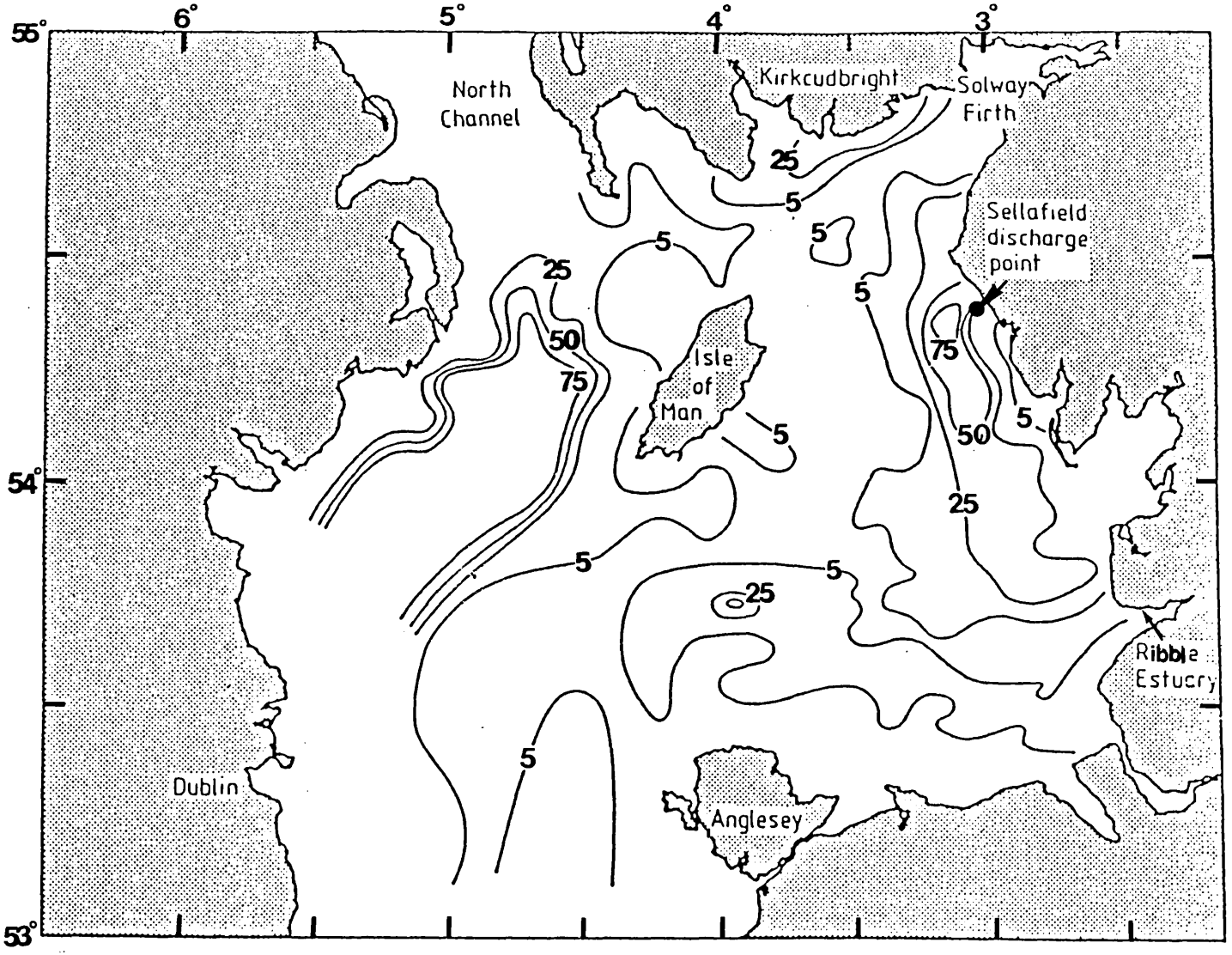

Figure 1.12 Distribution of sediment types on the bed of the Irish Sea (Miller et al, 1982)
(contours show average sediment particle size in % by weight of sediment less than 62 μm)

results for intertidal sediments from the Solway Firth, to the north of Sellafield, and once again observed that the highest activities were associated with the finest grained mud flat and salt marsh sediments. Further studies illustrating the major significance of fine grain sediments in the uptake of radionuclides have been reported for different locations within the Irish Sea by numerous workers, including Hetherington (1976, 1978), Hamilton (1980; 1981), Hamilton and Clifton (1981), Williams et al (1981), Dyer (1986) and MacKenzie et al (1987).

Considerable effort has been devoted to the study of the mechanism of uptake of radionuclides by these fine sediments and to post depositional redistribution of the radionuclides, which is controlled largely by the movement of the sediments themselves. Smith et al (1980) summarised several mechanisms by which radionuclides can be incorporated at depth in the sediments, namely (a) sedimentation in which particle associated activity is added directly to the sediment framework (b) diffusion from the overlying water column into the sediment porewater, which will clearly be limited in significance to soluble (low K_D) species, and (c) bioturbation, in which activity associated with the surface sediment, overlying water or suspended particulate matter is drawn down into the sediment by the action of the biota. Constant plutonium concentrations and activity ratios for sediment profiles in cores collected from the mud patch off the Cumbrian coast indicate that plutonium is incorporated into these sediments by mechanisms other than rapid accumulation and that bioturbation probably plays a major role (Kershaw et al, 1983). A similar conclusion was reported by Kershaw et al (1988a, 1988b) who used $^{234}Th/^{238}U$, $^{210}Pb/^{226}Ra$ and radiocarbon techniques to show that a very high degree of bioturbation and a low, or

negligible, sedimentation rate is applicable to these sediments.

Smith et al (1986) have also suggested that several different mechanisms may be of potential importance in removal of radionuclides from the fine sea bed sediments of the Irish Sea, including (a) erosion of the sediment surface, (b) diffusive transport from the sediment pore water into the overlying water column (which would only be of significance for low K_D species), (c) biological action, in which activity is ejected from the substrate into the overlying water, and (d) consolidation of the sediment, which effectively removes activity from the zone of bioavailability and possible redistribution. Clearly the latter mechanism would be highly advantageous with respect to minimising the radiological significance of the Sellafield discharge while the other mechanisms would be detrimental in this context.

Return of radionuclides from the sediment to the water column will occur as a result of the law of mass action when uncontaminated seawater (or seawater with a lower level of contamination) comes into contact with the contaminated sediments. Given the higher K_D values of plutonium and americium this will, however, give an insignificant release of these nuclides to the Irish Sea water from contaminated silt, although if the sorption of caesium was truly reversible and if a K_D of the order of 10^2 was applicable then there could be a detectable release of this nuclide.

In studies of oceanic sediment radionuclide profiles, in which fallout ^{137}Cs was observed at greater depths in the sediment than the corresponding $^{239,240}Pu$, Livingston and Bowen (1976, 1979) have suggested that diagenetically remobilised plutonium is preferentially

transported upwards in the sediment column by diffusion in the interstitial water, possibly in the form of soluble organic complexes, as a mechanism to explain the relative plutonium and caesium distributions. Clearly if such a process was to operate in the case of the highly contaminated Irish Sea sediments then there would be considerable potential for return of plutonium to the overlying waters. However, many workers have argued against the existence of a plutonium remobilisation process, including work done on Sellafield contaminated sediments by Hetherington (1976, 1978) and Aston and Stanners (1981). These authors attempted to match the Sellafield discharge data with observed plutonium distributions in intertidal sediment profiles and they concluded that any plutonium upward diffusion was negligible in this system, although it should be noted that, given the apparently high sedimentation rates applicable to these sediments, this system is an inherently insensitive area in which to attempt to observe diffusion effects over the short timescales appropriate to these studies. On the basis of plutonium concentrations, $^{238}Pu/^{239,240}Pu$ ratios and ^{137}Cs and ^{241}Am concentrations, plutonium immobility has also been advocated in Santa Barbara basin sediments, California, by Koide et al (1975) and in anoxic marine sediments by Carpenter and Beasley (1981).

In studies of plutonium concentrations in sediment pore waters from Irish Sea sediments Nelson and Lovett (1981) reported that plutonium is not mobile in the sediments receiving the discharge from Sellafield. Sholkovitz (1983) has, however, reinterpreted their plutonium pore water profiles to suggest that some remobilisation of the reduced form of plutonium in the Irish Sea sediments cannot be ruled out. In addition, Sholkovitz has carried out laboratory based pore water

studies (Sholkovitz, 1983) and complementary analysis of nearshore sediment pore waters for radiocaesium and plutonium (Sholkovitz and Mann, 1984), to investigate the possibility of plutonium remobilization. Whilst the reported levels of plutonium in pore waters were higher than those of the overlying water, there was no convincing evidence in this work that plutonium is subject to any significant diagenetic chemical changes in speciation. Furthermore, on the basis of the relative radiocaesium and plutonium porewater profiles, Sholkovitz concluded that downwards migration of ^{137}Cs was a much more likely explanation for the observed sediment profile distribution of these nuclides reported by Livingston and Bowen than upwards migration of plutonium. This conclusion is supported by work by Santschi et al (1983) and Edgington (1981) and is consistent with the observed solubilities in seawater and particle reactivities of radiocaesium and plutonium, which would favour relatively much greater pore water transport of caesium than plutonium.

The balance of evidence thus appears to suggest that negligible diagenetic remobilisation of plutonium occurs in a wide variety of marine sediments so that, in the case of the contaminated fine sediments of the Irish Sea, any concern over possible future dispersion of the contaminant radionuclides will be centred more or less entirely upon movement of the contaminated sediment particles themselves. Some of these fine sediments are in fact brought onshore by tidal action, waves and storm processes and are deposited in the intertidal zones of the Cumbrian coast and its associated estuaries and salt marshes (Hetherington, 1978; Aston and Stanners, 1981) and in corresponding areas of the Solway Firth (Jones et al, 1984). Two distinct types of environment, both of which were of

concern in the present study, are generated in this way, namely (a) truly intertidal areas which are inundated by the sea on a diurnal basis, and (b) salt marshes which are only subject to infrequent inundation, often during exceptionally high tides or as a consequence of storms.

Cores of intertidal sediments from different locations in the Irish Sea have been analysed by numerous workers in order to define the vertical distribution of Sellafield waste radionuclides in the sediments (eg. Hetherington, 1976, 1978; Aston and Stanners, 1979, 1981; Hamilton et al, 1981, 1983; Smith et al, 1980, 1986; Williams et al, 1981, Kershaw et al, 1983). A variety of distributions, depending upon the time and location of sampling, have been reported in these works, including radionuclide activities decreasing approximately exponentially with depth from the surface, subsurface activity maxima, and mixed surface sediment with uniform concentrations overlying sediment with decreasing concentrations at depth. The depth of penetration of the radionuclides has been found to vary from about 30cm to about 1 meter. Attempts have been made to relate the observed profiles to known variations in the Sellafield discharge pattern (as discussed more fully in section 1.3.7), and the general conclusion is reached in most of these publications that the profiles represent continuous sediment deposition with varied degrees of mixing at different locations.

An interesting feature of the Irish Sea sediment contamination is that "hot particles", (in the size range 100 to 300μm) containing very high concentrations of alpha emitters, have been reported by Hamilton (1980, 1981) and Hamilton and Clifton (1981) to be present in intertidal sediments from the Ravenglass

Estuary about 10km south of Sellafield. The transuranic radionuclides, plutonium and americium have been identified in these particles and Hamilton (1981) has suggested that they consist of magnesium hydroxide fragments derived from fuel elements in the Sellafield cooling ponds.

The overall transport mechanism (or mechanisms) affecting radionuclides discharged from Sellafield is of fundamental importance in determining the radiological significance of the discharge and the transport mechanism is initially controlled by the partitioning of the nuclides within the seawater/ sediment system close to the discharge point.

In general terms, radionuclide transport in this system will be dominated by one of two main mechanisms, namely (a) movement of soluble species in solution in seawater, and (b) particle associated movement of insoluble components. Thus, while the generally northwards transport of soluble Sellafield waste radionuclides, in accordance with the dominant direction of water flow in the Irish Sea, is well established, it has additionally been recognised that, with the much lower level of discharges from Sellafield applicable during the 1980's, the mud patch off Sellafield must now be regarded as a potential source of radionuclides rather than a sink, as it was generally considered in the 1970's. For example, MacKenzie et al (1987) have investigated the relative significance of the above two mechanisms in the transport of Sellafield waste radionuclides to the intertidal sediments of south west Scotland by relating the concentrations and the isotope and nuclide ratios of radiocaesium, plutonium and americium to possible source terms. The possible source terms considered were weapons testing fallout and Sellafield waste,

Results for sediments

Region	$\frac{^{137}Cs}{^{239,240}Pu}$	$\frac{^{241}Am}{^{239,240}Pu}$	$\frac{^{238}Pu}{^{239,240}Pu}$	$\frac{^{137}Cs}{^{241}Am}$
A	<10	>1	>0.2	<10
B	10-40	~1	~0.2	10-50
C	>40	<1	<0.2	>50

Source terms*

Source	$\frac{^{137}Cs}{^{239,240}Pu}$	$\frac{^{241}Am}{^{239,240}Pu}$	$\frac{^{238}Pu}{^{239,240}Pu}$	$\frac{^{137}Cs}{^{241}Am}$
particle associated Sellafield waste	1.9	1.04	0.24	1.8
soluble Sellafield waste	35	<0.28	0.31	>125
atmospheric fallout	56	0.23	0.05	240

TABLE 1.8: Radionuclide activity ratios for possible souces of contamination of Solway Firth intertidal sediments (Figure 1.13)

* Ratios appropriate to intertidal sediments in south west Scotland in 1984 - 1985, arising from the dominant sources (MacKenzie et al, 1987)

which was assumed to undergo rapid partitioning between the aqueous and sedimentary phases and was consequently treated as a two component system of soluble and particle associated species in this case. The characteristic values assumed for the source terms are shown in Table 1.8.

This work, in confirmation of other studies (eg. MAFF, 1982-1987; Kirby et al, 1983; Dyer, 1986), demonstrated that the manmade radionuclide content of intertidal sediments from the Solway Firth can be attributed almost entirely to Sellafield effluent and that the observed radionuclide ratios were compatible only with those of the particle associated source. Moreover, it was observed that in the Solway Firth intertidal sediments there was a strong linear correlation between the concentrations of ^{137}Cs, ^{241}Am and $^{239,240}Pu$ and their isotope and nuclide activity ratios were similar to those of the highly contaminated fine sediments close to Sellafield and to those of the time - integrated Sellafield discharge into the Irish Sea as shown in Tables 1.6 and 1.8. This observation of a linear correlation between the concentrations of these three nuclides over a distance of about 100km along the Solway coast was highly significant since, as discussed in detail in section 1.2.3 above, movement of a radionuclide by a combination of advection and diffusion away from a point source in conjunction with dilution and continuous removal to the solid phase would result in an exponential decrease in concentration with distance. The rate of exponential decrease would vary for radionuclides of different solubilities so that the activity ratio of two radionuclides with markedly different solubilities, such as ^{137}Cs and ^{241}Am, should also vary exponentially with increasing distance from the point source. Clearly this does not apply in the case of the Solway

intertidal sediments and the linear correlation reported for radionuclide concentrations in this area by MacKenzie et al can also be discerned in other intertidal areas of the Irish Sea (MAFF, 1982-1988). Based on the above observation MacKenzie et al (1987) concluded that in the mid 1980's dispersal of contaminated silt from a mixed reservoir further south in the Irish Sea was the dominant mechanism supplying manmade radionuclides to the intertidal sediments of the Solway coast. Moreover, a sharp discontinuity in radionuclide concentrations in the sediments at Burrow Head, (Figure 1.13) about 50km north-west of Sellafield was interpreted as indicating that the transport of the fine silt is less effective to the west of this point, with a limited spread of contaminated particles as far as the North Channel. There was no evidence in this work that this mechanism operates further north than the North Channel. Also, transport in solution was identified as supplying some of the radiocaesium to surface sediments between Burrow Head and the North Channel and as being the main means of transport of Sellafield waste radionuclides to areas north of this. Baxter et al (1989) and McDonald et al (1990) have, more recently, extended the hypothesis of MacKenzie et al for the transport of Sellafield radionuclides to the Solway region by analysis of offshore Irish Sea surface sediment and obtained very good agreement with the particle associated transport model.

In summary, considerable evidence exists showing the significance of the level of manmade radionuclide contamination of the fine silt in the Irish Sea and establishing patterns of movement of this material will be one of the main tasks which has to be performed in order to properly evaluate the long term radiological implications of the Sellafield discharge.

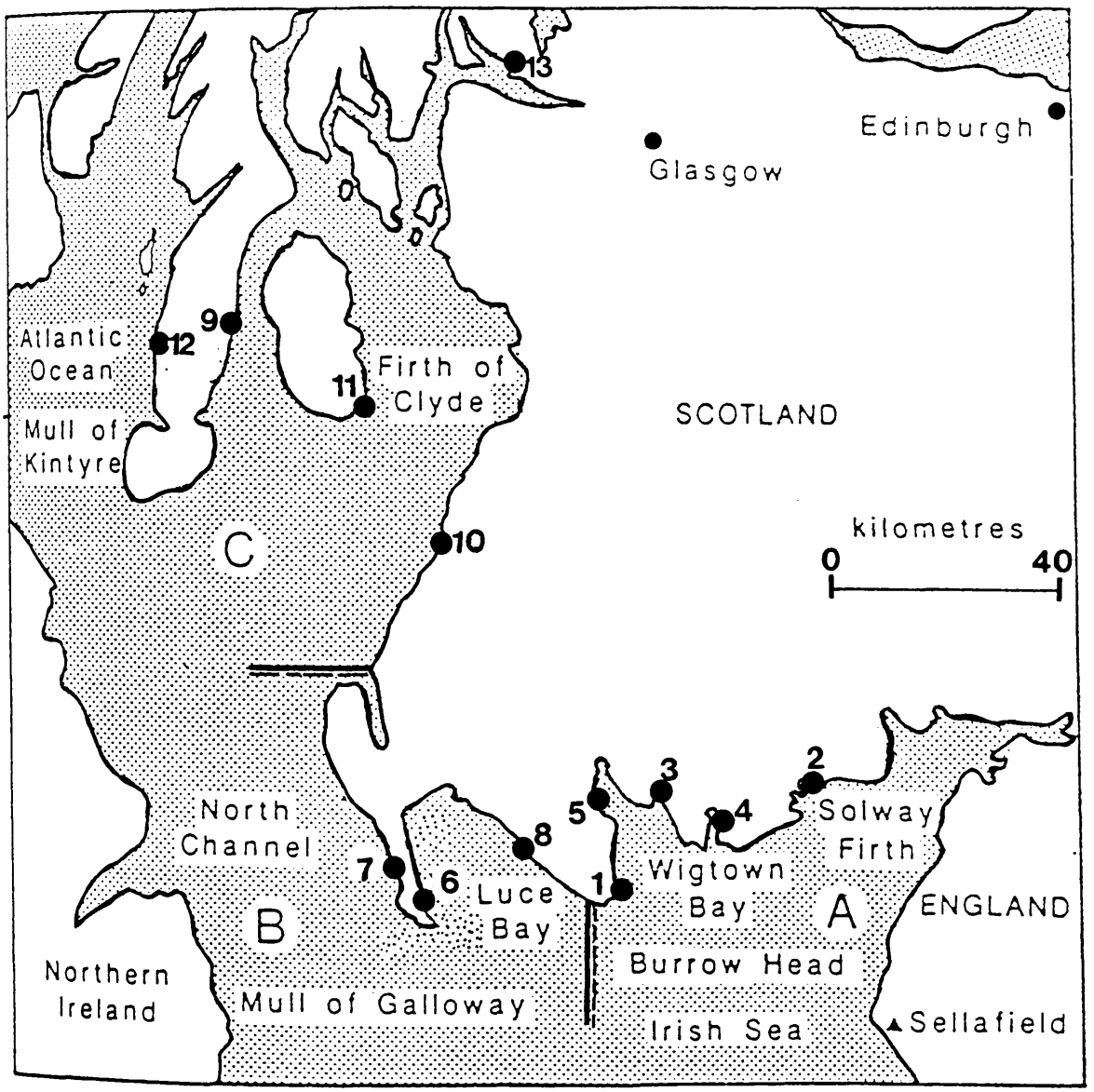

Figure 1.13 Map showing the locations of sampling sites for samples used for neutron activation analysis (Table 3.4). Also shown are Regions A,B and C as defined by MacKenzie et al (1987) with respect to northwards dispersal of Sellafield waste. (cf. Table 1.8)

Sellafield derived contamination can also be detected in more distant marine sediments (eg. Murray et al, 1978). For example, intertidal sediments from the Firth of Clyde on the west coast of Scotland and the Firth of Forth on the east coast of Scotland have much lower radionuclide concentrations than those of the Irish Sea but show isotope ratios consistent with a mixture of Sellafield waste and weapons testing fallout (MacKenzie and Scott, 1982b). Offshore marine sediments from the Firth of Clyde (Baxter et al, 1979; Swan et al, 1982) and from Loch Etive (McKay and Baxter, 1985; Williams et al, 1988) also show a dominant influence of Sellafield contamination.

The return of any marine discharged Sellafield waste to land could have implications for the overall population radiation dose from this source and it has been found that most of the coastal soils of west Cumbria contain elevated radionuclide concentrations for distances inland of 10km or more. In investigations of this contamination, workers from Harwell (Cambray and Eakins, 1980; Cawse, 1980; Pattenden et al, 1980) have established the extensive existence of an onshore transfer of marine discharged waste. Cambray and Eakins (1980) initially used the $^{238}Pu/^{239,240}Pu$ activity ratios and the total plutonium inventory in soil samples to identify the onshore transfer of marine discharged Sellafield waste in Cumbria. The total plutonium inventory in the soil was observed to be higher than expected from nuclear weapons fallout and $^{238}Pu/^{239,240}Pu$ ratio values of up to 0.18 clearly indicated a large Sellafield contribution to the plutonium concentration. They also observed that with increasing distance from the coast the $^{238}Pu/^{239,240}Pu$ activity ratio decreased from Sellafield dominated values towards fallout levels of 0.04. Similarly, a positive identification of onshore

transfer of Sellafield radionuclides was made by many workers on the basis of the $^{134}Cs/^{137}Cs$ activity ratio (Cambray and Eakins, 1980; Cawse, 1980, 1983, Cawse and Horrill, 1986; McDonald et al, 1990).

The onshore transfer of Sellafield radionuclides is more effective for plutonium and americium than for caesium and it has been shown that airborne particulate matter displays a higher ratio of $^{239,240}Pu$ to ^{137}Cs than is observed in Irish Sea seawater, suggesting either that sea spray is enriched with actinides or else that breaking surf generates particle-rich spray.

Further work in which muslin screens were used to trap particles from either side of the surf zone demonstrated that the resuspension of fine particulate material, followed by injection of the particles into the atmosphere in the surf zone is almost certainly the main mechanism responsible (Eakins et al, 1982).

The total effect of this onshore transfer has been estimated as having given rise to the movement of 0.1 and 2.0 TBq of $^{239,240}Pu$ and ^{137}Cs respectively from the sea to the land. Thus the effect represents only a very small, but nevertheless significant, fraction of the total Sellafield discharge.

McDonald et al (1990) investigated the onshore transfer of Sellafield discharged radionuclides in soil transects from different locations along the Solway Firth and they concluded that, while detectable levels of Sellafield effluent were found up to 500m inland, onshore transfer, analogous to that observed in Cumbria, is not significant in the Solway area.

The onshore transfer of radionuclides discharged to the sea from the Dounreay reprocessing facility at

Caithness has also been identified by Cook et al (1984a, 1984b). The maximum deposition of radionuclides in the soils in the Caithness environment corresponds to a level eleven times higher than the expected weapons testing fallout value. A small onshore transport of radionuclides has also been observed in the vicinity of the Cap de La Hague reprocessing plant in France (Fraizier et al, 1977).

The Sellafield derived contamination of the Irish Sea is one of the worst cases of radioactive contamination of the marine environment on a worldwide basis and the situation is therefore of considerable interest from a radiological viewpoint. The geochemical properties, half-lives and the nature of the radiations emitted by the discharged nuclides are all important aspects in assessing the effects of the waste disposal and are all required inputs for the process of critical pathways analysis which is performed to assess the maximum radiation exposure either of individuals or of groups in the population. Species with short half-lives (days or months) are generally removed by decay before significant human exposure can occur, except for locations close to the discharge point (eg. Cumbrian intertidal sediments). At the other extreme, special significance must be attached to very long lived nuclides because of their long mean residence time in the environment. Generally, the alpha emitting nuclides are not important in external exposure since total shielding is provided by a few centimetres of air or some tens of microns of any solid material. Alpha emitters are mostly of importance in the context of internal human exposure because alpha particles are highly ionising and produce intense damage along short tracks in tissue. Beta/gamma emitting nuclides, although still significant with respect to internal exposure, are of lower concern than alpha emitters

because the radiations involved are less highly ionising. However, the greater ranges of beta and gamma radiations mean that beta/gamma emitters are of more significance, in external exposure. Most radiological concern is therefore focused upon radionuclides with long half-lives, those which follow pathways resulting in internal exposure (particularly alpha-emitters) and beta/gamma emitters which are concentrated in environmental materials in close proximity to areas of human activity. The assessment of the radiological significance of nuclear waste discharges to the environment thus requires, in addition to a knowledge of the radiological properties of the nuclides, a detailed understanding of their geochemical behaviour and is consequently a subject of considerable complexity. The Sellafield discharge dominates the UK coastal marine situation and detailed discussion of the radiological importance of this and other sources of environmental radioactivity is presented in the series of monitoring reports of the Ministry of Agriculture, Fisheries and Food (eg. MAFF, 1973-1988) and in a number of review and specialist reports (eg. Pentreath, 1980; MacKenzie and Scott, 1984). In considering the radiological impact of radionuclide discharges, it is necessary to assess both the exposure to individuals in the critical group of people who are most exposed and exposure of the total population. In both cases, two critical pathways have been identified for the Sellafield discharged nuclides, and these are (a) the consumption of contaminated seafoods giving rise to internal exposure and (b) uptake of beta/gamma emitting nuclides in marine materials resulting in external exposure. The principal internal exposure pathway for Sellafield waste has been via the consumption of fish. Consumption of locally caught fish and shellfish is significant for a critical group of the Cumbrian

community, whereas commercial fish landings throughout western Europe give rise to the largest population exposure. The total population exposure is mainly due to ^{137}Cs, widely dispersed in the seas around the UK, whereas other radionuclides also become significant for fish and shellfish caught locally in the vicinity of Sellafield. As shown in Figure 1.11, the amount of ^{137}Cs discharged annually from Sellafield has been decreasing in recent years and is expected to fall to yet lower values (BNFL, 1981), so that the ^{137}Cs exposure pathway will probably result in a lower exposure in future. The principal external exposure resulting from Sellafield waste radionuclides results from the presence of gamma emitting nuclides in the sediments of the Cumbrian coast, in particular, the relatively highly contaminated intertidal deposits of the Ravenglass Estuary. The radionuclides responsible include ^{95}Zr, ^{95}Nb, ^{106}Ru, ^{144}Ce and radiocaesium. Up to 1979, the critical group for this external exposure pathway comprised fishermen working the salmon garth on the Ravenglass Estuary. Since then the use of the garth has declined and the critical group is now identified as fishermen living on-board ship in Whitehaven Harbour. Data for critical group exposure via both internal and external exposure during the period 1971 to 1988 are presented in Table 1.9 from which it can be seen that exposures are within the secondary ICRP limit of 5m Sv but not within the new recommended NRPB limit of 0.5m Sv for exposure as the result of the discharge from a single source (NRPB, 1987). If further discharges from Sellafield remain at present levels or less, then it is reasonable to assume that radiation exposure due to the consumption of fish will not be the most significant exposure pathway in future. Exposure from contaminated sediment by, for example, external exposure, transfer of activity from the sediment to organisms living within

Year	Internal committed effective dose equivalent (mSv y^{-1})		External committed effective dose equivalent (mSv y^{-1})
1974	-	-	0.35
1975	-	-	0.45
1976	2.20	-	0.40
1977	1.51	-	0.21
1978	1.28	-	0.19
1979	1.02	-	0.16
1980	1.20	1.95*	0.90
1981	2.30	3.45*	0.45
1982	1.70	2.70*	0.40
1983	1.45	2.25*	0.35
1984	0.54	0.84*	0.31
1985	0.49	0.73*	0.26
1986	0.12	0.34*	0.34
1987	0.1	0.33*	0.24

TABLE 1.9: Estimates of critical group exposure arising from the Sellafield liquid effluent discharge (a) internal exposure (b) external exposure (MAFF 1974-1988)

* Revised gut uptake factor

it or inhalation of resuspended sediment will therefore be likely to remain the major pathways. This, once again, illustrates the importance of establishing detailed models to describe any processes giving rise to movement of the highly contaminated fine sediments of the Irish Sea, particularly if such movement would result in transport of the radionuclides to areas of potential human contact such as intertidal areas and salt marshes.

In general, releases of radioactivity from nuclear industry installations such as Sellafield, are point sources of radioactive pollutants which affect only the local environment close to the discharge point. However, the Chernobyl reactor accident which took place in the Ukraine near Kiev on 26 April 1986 resulted in the injection of about 2×10^{18} Bq of fission and activation products into the atmosphere (Clark and Smith, 1988) with consequent deposition of fallout affecting significant areas of the northern hemisphere. The atmospheric plume of radioactivity from Chernobyl reached the UK on 2 May 1986 and the non-uniform geographical distribution of rainfall led to major variations in the distribution of the released radionuclides in different areas. A list of radionuclides detected in rainwater in south west Scotland as the result of Chernobyl fallout is shown in Table 1.10. The deposition inventories of Chernobyl ^{137}Cs observed in soil samples in Cumbria ranged from 10^2 to 10^4 Bq m^{-2}, illustrating the effects of sharp local variations in rainfall at the relevant time (Cambray et al, 1987; Clark and Smith, 1988). Chernobyl ^{137}Cs inventories and vertical distributions in soils from the Solway coastal region have been reported by Baxter et al (1989), who observed that in the top 15cm of the soil, the ^{137}Cs inventory ranged from 3×10^3 to 3.9×10^4 Bq m^{-2} and they therefore

Nuclide	Mode of Decay	Half-life
^{99}Mo	ß	66.02h
^{103}Ru	ß	39.35d
^{131}I	ß	8.04d
^{132}I	ß	2.29h
^{132}Te	ß	78.28h
^{134}Cs	ß	2.05y
^{137}Cs	ß	30 y

TABLE 1.10: Radionuclides detected in rainwater in south west Scotland (6 May 1986) as the result of Chernobyl fallout - SURRC Annual Report 1986-1987

concluded that on average, 86% of the ^{137}Cs inventory to 30cm depth is retained in the top 15cm.

In surface seawater of the Irish Sea in 1986 the ^{137}Cs concentrations as a result of Chernobyl fallout were reported by Mitchell and Steele (1988) to have ranged from 86 to 389 Bq m^{-3} whereas at depth in the water column of the Irish Sea, ^{137}Cs concentrations range from 92 to 370 Bq m^{-3}.

Of the radionuclides of interest in this study, only the radiocaesium was affected by the Chernobyl fallout. Moreover, the $^{134}Cs/^{137}Cs$ isotope ratio of the Chernobyl fallout had a highly characteristic value of about 0.55 (Devell et al, 1986; Fowler et al, 1987; Cambray et al, 1987; Aarkrog, 1988; Byrne, 1988; Mitchell and Steele, 1988; Clark and Smith, 1988; Bondietti et al, 1988). This ratio is markedly different to all of the other major sources of environmental radiocaesium, which provides a powerful tool for differentiation of the Chernobyl component from other contributions to radiocaesium contamination in any given environment.

1.3.8 Applications of Manmade Radionuclides as Tracers of Environmental Processes

Manmade radionuclides can be used, in complementary studies to those described above for natural radionuclides, in the investigation of environmental processes. In general, manmade radionuclides have been most widely and successfully used in studies of environmental processes in the aquatic environment. For example, soluble manmade radionuclides in seawater have much to offer in terms of defining rates and directions of seawater movement, while insoluble species can provide a powerful tool for the study of sedimentary process such as mixing and accumulation

and sediment movement.

A fundamental difference generally exists between the use of natural decay series and manmade radionuclides as tracers of environmental processes since the former are normally used in steady state systems which are in equilibrium, whereas manmade radionuclides rarely have a steady supply and are often not in chemical equilibrium situations in the environment. This difference in conditions must always be borne in mind when comparing natural decay series with manmade radionuclide distributions. The characteristics of the supply of manmade radionuclides to the environment can offer advantages eg. temporal variations are often large and can be used to establish time dependent patterns, also the source term can be relatively well defined in many cases.

Three of the most commonly used manmade radioelements employed as tracers of environmental processes are radiocaesium, plutonium and americium which exhibit markedly different geochemical properties as discussed above. These species were of central importance to the present study and, while other manmade radionuclides have been used as environmental tracers, only these three elements will be considered here.

As discussed in section 1.3.6, caesium is highly soluble in natural waters and exhibits only a very small tendency towards chemical or biological scavenging. Caesium therefore has a relatively long residence time (approximately 10^4 - 10^5 years) in open seawater (Brewer, 1980) and, even in coastal seawater where the concentration of particulate material is higher, the residence time is still greater than 10^2 years (Swan et al, 1982).

As a result of this soluble behaviour and suitable half-lives, the radiocaesium isotopes ^{134}Cs ($t_{½}$ = 2.1y) and ^{137}Cs ($t_{½}$ = 30y) are amongst the most useful manmade radionuclides in the study of both the rate and direction of coastal water movement and in surface ocean vertical mixing studies (Noshkin and Bowen, 1973; Broecker, 1974; Wilson, 1974; Baxter and McKinley, 1978; McKinley et al, 1981a, 1981b; Jefferies et al, 1982). Although the fraction of radiocaesium removed to the sedimentary regime is small, it is nevertheless significant, and radiocaesium has also been employed in numerous tracer applications in sedimentary studies, in particular in the investigation of mixing processes and accumulation rates (Krishnaswami et al, 1975; Goldberg and Bruland, 1974; Robbins and Edgington, 1975; Robbins et al, 1978; Aston and Stanners, 1979; MacKenzie, 1981; Stanners and Aston, 1981; MacKenzie and Scott, 1982; Clifton and Hamilton, 1982; Swan et al, 1982).

Both weapons testing fallout ^{137}Cs and nuclear waste, which contains ^{134}Cs and ^{137}Cs, have been used to study marine processes. In deep ocean applications, fallout ^{137}Cs has been used as a tracer for investigation of the mixing of surface waters with deeper oceanic water masses and has been used to derive vertical eddy diffusion coefficients (Broecker et al, 1966; Broecker, 1974; Bowen, 1977) and the resulting data have been shown to be compatible with those derived from other methods.

Radiocaesium released in effluents from nuclear industry facilities has also been highly successfully applied in investigations of more localized environments, particularly in near shore waters and estuaries (eg. McKinley et al, 1981; Jefferies et al, 1982; Livingston et al, 1982). Radiocaesium discharged

from Sellafield has been particularly useful in the study of coastal water movement around the UK. In this case ^{137}Cs and ^{134}Cs released from Sellafield into the Irish Sea can serve as "dye type" tracers of large scale seawater movement. The northwards transport of water out of the Irish Sea, around the west coast of Scotland, and into more distant areas such as the North Sea can thereby be followed (Jefferies et al, 1973). Assessment of North Sea circulation is also possible from assay of the diluted Irish Sea-derived component but is complicated in southern areas by the presence of another significant source of ^{137}Cs from the Cap de la Hague nuclear fuel reprocessing plant in France. The $^{134}Cs/^{137}Cs$ activity ratio has also been used to estimate the transit times of seawater away from Sellafield by making use of the different rates of decay of the radiocaesium isotopes. Wilson (1974) studied water movement and mixing processes in the St George's Channel at the southern end of the Irish Sea using ^{137}Cs present in this area as a consequence of discharges from Sellafield. He demonstrated a transit time of 8 -10 months for passage through the Liverpool Bay system giving an apparent velocity of about 200km y^{-1}. He also noted, however, that the mechanism of transport could be predominantly diffusive rather than advective, since tidal mixing is very strong in this region. McKinley et al (1981) have used Sellafield radiocaesium as a tracer to study the coastal currents in the region of the inner continental shelf of west Scotland, known as the Hebridean Sea. This areas is situated between Malin Head in the south west and the south coast of Skye in the north east. This study has given a transport rate of about 1.6km d^{-1} through the North Channel while the transport rate through the Hebridean Sea was considered to be faster at about 5km d^{-1}. The $^{134}Cs/^{137}Cs$ activity ratio observed in this study was effectively constant at

0.013 to 0.014 throughout the main plume in the Hebridean Sea during 1976 to 1977.

Baxter et al (1979) have shown that a significant fraction (about 30%) of radiocaesium discharged from Sellafield is carried via the dominant northwards water movement into the Clyde Sea Area and based upon matching the Sellafield discharge pattern with observed water concentrations Baxter et al (1979) and McKinley et al (1981) have also estimated that the radiocaesium transit time from Sellafield to the northern parts of the Clyde Sea Area is about 8 months. Radiocaesium provides an ideal water movement tracer in this system via the $^{134}Cs/^{137}Cs$ activity ratio, and the mean residence time for water in the Clyde Sea Area has been estimated at about 4 months, by matching observed seawater $^{134}Cs/^{137}Cs$ activity ratios with values in the Sellafield discharge (Baxter et al, 1979; McKinley et al, 1981).

The concentration of radiocaesium in waters of the Clyde Sea Area shows a high degree of spatial uniformity indicating rapid mixing within the system in general. An exception to this well mixed situation is observed in the fjord-like sea lochs where pulses of radiocaesium, arriving at the surface and then distributing vertically, demonstrated that water exchange follows a thermocline controlled pattern. McKinley and Baxter (1980) have studied the $^{134}Cs/^{137}Cs$ activity ratio profiles in Loch Goil on a monthly basis and have shown that the surface waters (less than 30m) undergo rapid exchange at all times. In the non-stratified state, the residence time of water in the loch is less than 1 month. Annual stratification in the period from August to December leads to restricted exchange through the pycnocline. Results for 1977 indicated that deep water residence times ranged from

3 months to 5 days depending upon the degree of stratification. Vertical eddy diffusion coefficients calculated for the stratified situation were reported to be in the range $7 \leq K_z \leq 25 cm^2 sec^{-1}$.

With a much lower solubility, plutonium has only been used infrequently (Murray et al, 1978; 1979) as a water movement tracer and, along with americium, is more commonly employed in the study of sedimentary processes. The small fraction of radiocaesium taken up by sediments can also be usefully employed in this context (Hetherington, 1975, 1976; Robbins and Edgington, 1975; Livingston and Bowen, 1979; MacKenzie et al, 1979; Bowen et al, 1980; Aston and Stanners, 1981a, 1981b; MacKenzie and Scott, 1982; Swan et al, 1982). These particle associated manmade radionuclides have been widely employed in sedimentary studies involving attempts to relate geographical distribution and sediment column distributions of these species to temporal variations in the Sellafield discharge. For instance, Hetherington and Jefferies (1974) used the plutonium isotope ratio $^{238}Pu/^{239,240}Pu$ in surface intertidal sites at distances of up to 20km from the Sellafield outfall point to suggest that the travel time for sediment borne activity over this distance is considerably less than one year. Waste radionuclides have also been used to investigate accumulation patterns in intertidal sediments of many areas within the Irish Sea. For example, Aston and Stanners (1979) reported a sedimentation rate of 6.7cm y^{-1} using the relationship between the $^{134}Cs/^{137}Cs$ activity ratio in sediment profiles from the Estuary of the River Esk in north west England and that of the Sellafield discharge. Aston and Stanners (1982) also reported sedimentation rates of 1.3 to 1.6cm y^{-1} for four cores of intertidal sediment from the Ravenglass Estuary by matching ^{241}Am profiles with the Sellafield discharge

historical record. In an extension of this work, relating to further sediment profiles from the Ravenglass Estuary, Stanners and Aston (1981) reported a range of sedimentation rates between 0.025 and 7.1cm y^{-1}. MacKenzie and Scott (1982) observed that both ^{137}Cs and $^{239,240}Pu$ profiles in intertidal sediments from Skyreburn Bay, in south west Scotland showed distinct sub surface maxima which could be related to the maximum in the amount of activity discharged from Sellafield in the mid 1970's, implying a sedimentation rate of about 3.5cm y^{-1} at this site. Also sedimentation rates of 1.6 to 6.4cm y^{-1} have been reported by Clifton and Hamilton (1982) by the use of $^{134}Cs/^{137}Cs$ activity ratios in sediment profiles from 16 sites in the salt marsh region near Newbiggin on the Esk Estuary, Cumbria.

Aston and Stanners (1981) also matched the Sellafield annual discharge rates and isotopic activity ratio of plutonium with concentrations of plutonium and $^{238}Pu/^{239,240}Pu$ ratios in profiles of intertidal sediment from the Ravenglass Estuary and they concluded that the presence of a buried peak in the plutonium activity within the sediment cores indicated that physical accumulation of contaminated sediment particles is the main mechanism controlling the plutonium distribution. They also argued that low values for the $^{238}Pu/^{239,240}Pu$ ratios observed at depth imply that the effects of physical mixing and chemical diagenesis are negligible. In this work, Aston and Stanners had to match the $^{238}Pu/^{239,240}Pu$ ratios of their cores with the values reported for this ratio by Hetherington (1978) for surface sediments collected between 1966 and 1975 from the River Esk Estuary since the isotopic activity ratio of the discharged plutonium was not measured during this period. The main assumption in this work was that the yearly collected surface sediments had the same

$^{238}Pu/^{239,\ 240}Pu$ ratio as the Sellafield discharged plutonium. This implies that the transit time to the estuary is fast (ie. months) and that recently contaminated sediments do not mix with older material, thereby modifying the isotopic ratios prior to deposition in the estuary. However, Aston and Stanners (1981) applied this activity ratio matching technique to intertidal sediment cores which were collected in 1978 and found that in order to explain the observed results they had to invoke a 2 to 3 year lag time between the discharge of plutonium from Sellafield and its deposition in the Ravenglass Estuary. The postulated existence of such a lag time, is incompatible with the above assumption that Hetherington's surface sediment data can be taken to represent the Sellafield discharge data and also requires the assumption of a constant accumulation rate over the depth of the profiles without any mixing. Similarly, the isotope activity matching technique led Aston and Stanners to estimate a lag time of 1.5 years for ^{134}Cs and ^{137}Cs. These lag times for plutonium and caesium appear very long compared with those reported for caesium isotopes by Jefferies et al (1973); Livingston and Bowen (1977); Baxter et al (1979); McKinley et al (1981) and Hetherington et al (1975), (1976).

In Clyde Sea Loch sediments Swan et al (1982) reported accumulation rates of 0.35, 0.6 and 1.5cm y^{-1} using similar techniques employing radiocaesium isotopes and these results were generally in good agreement with sedimentation rates derived from ^{210}Pb profiles.

2. EXPERIMENTAL

2.1 SAMPLE COLLECTION AND PRETREATMENT

Various types of sediment samples were collected during the course of this study and different sampling techniques were used which were appropriate to the individual sampling sites and the purpose of the analysis as follows.

2.1.1 Ardmore Bay

The objective of this part of the study was to establish the vertical distribution of manmade and natural radionuclides and selected stable elements in the sediments from different sections of the bay in an attempt to characterise the sediment geochemistry and accumulation and mixing characteristics. It was, therefore, necessary to obtain samples of the sediment from various depths, retaining their depth context and this was achieved by the conventional technique of manual insertion of plastic "drainpipe" tubes of internal diameter 5cm into the sediment. Thereafter the tubes, and contained sediment cores, were recovered by digging away the surrounding sediment, sealing the bottom of the tube by hand and then lifting it clear.

Experience showed that recovery of cores with lengths much in excess of about 50cm was impractical and coring tubes of a maximum length of 70cm were used both at this site and the others sampled in this way during the project.

Immediately after collection the cores were extruded from the top of the core tube, by pushing upwards from the base with a plastic plunger which acted as a piston, fitting closely inside the plastic tube. The cores were divided into 2cm vertical sections which

were transferred to clip seal polythene bags for return to the laboratory. Wet and dry weights of the samples were recorded. Four cores were collected from the locations shown in Figure 1.6. The first three cores were collected during 1984, while the fourth was collected in July 1987.

2.1.2 Skyreburn Bay

Vertical sediment cores were again required at this sampling site and the techniques used were as described above for Ardmore Bay except that 3cm vertical increments of the cores were taken in this case for purposes of comparison with previous cores studied from this site. The location of the sampling area is shown in Figure 1.7. Cores SBC831, SBC851 and SBC852 which were analysed in this work area were collected in July 1983, July 1985 and November 1985 respectively.

2.1.3 Surface Intertidal Sediments

The objective of this part of the study was to test the model of MacKenzie et al (1987) which describes the movement of particle-associated Sellafield waste radionuclides from the area close to the discharge point to the coast of south west Scotland. For direct comparison with the above work, intertidal sediment (from a depth of 0.5cm or less) was collected from different sites in south west Scotland in August 1987 as indicated in Figure 2.1. The individual samples, collected using a plastic scoop, were transferred into marked polythene bags and sealed. Upon return to the laboratory, wet and dry weights of the samples were recorded.

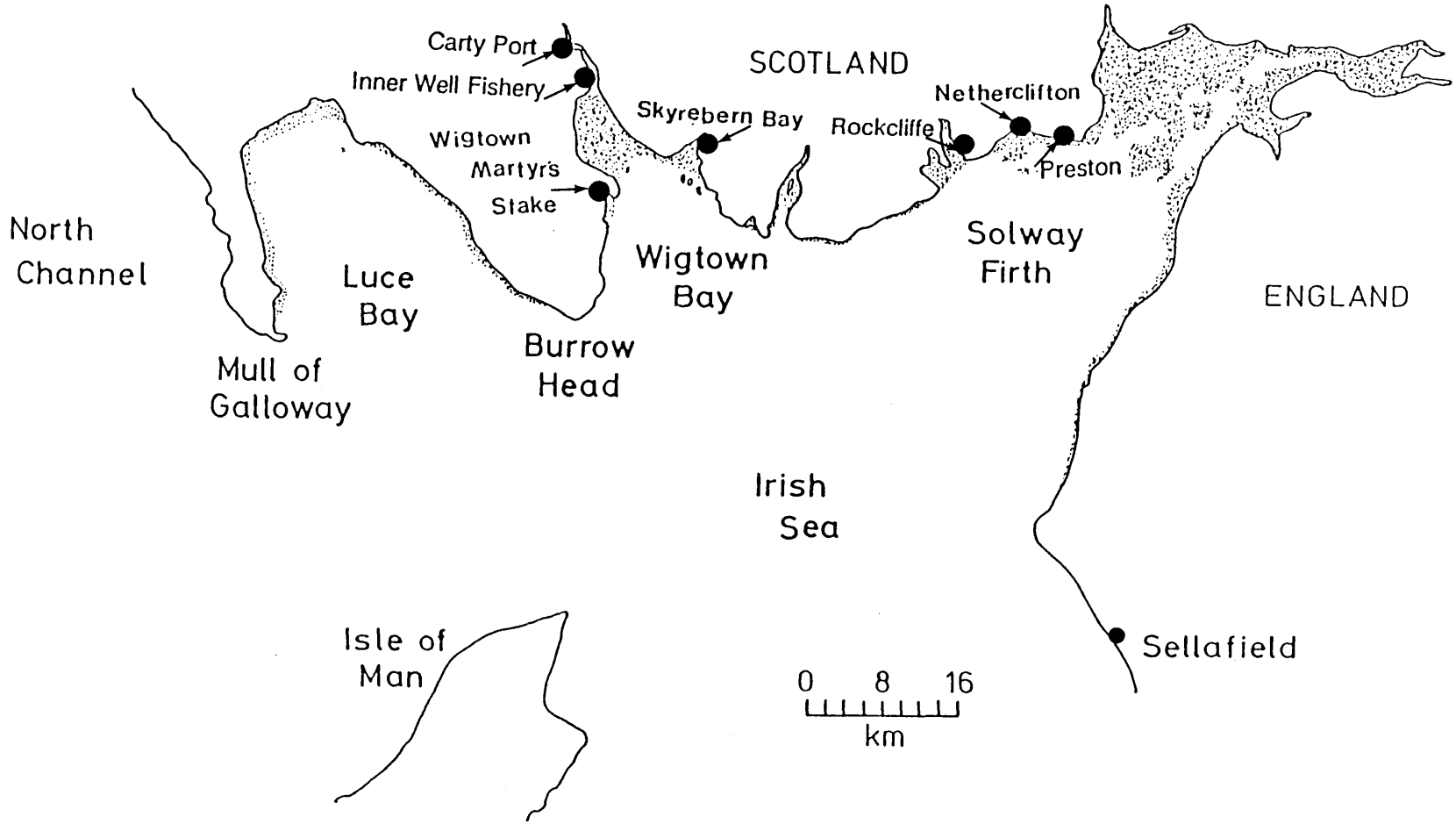

Figure 2.1 Map showing sampling sites from which surface intertidal sediment samples were collected in August 1987

2.1.4 Flood Plain Deposits

A number of related objectives applied in this section of the work dealing with the Solway Firth flood plain deposits, namely (a) to establish the mechanism of supply of manmade radionuclides to these areas, (b) to determine the vertical distribution of radionuclides within the sediment, (c) to evaluate the total inventory of the manmade radionuclides in the merse sediments and, thereby, to attempt to quantify the magnitude of the onshore transfer of Sellafield waste radionuclides to this area, and (d) in the case of the Netherclifton location only, to investigate uranium and thorium movement and deposition. Two merse sites were studied, namely Netherclifton and Wigtown Marytr's stake. Samples were collected from the Netherclifton site during March 1986 from the locations shown in Figure 1.8. Similarly, samples were collected from Wigtown Martyr's stake in August 1987 from the locations shown in Figure 1.9.

The following sampling techniques were employed to achieve the above objectives:

i. Vertical profile samples from the merse deposits were collected by digging pits with a spade and cleaning a vertical face of the pit using a trowel. Sections of area 10 x 10cm and depth 5cm were then removed down a vertical section in the face of the pit. The samples were placed in marked plastic bags and sealed for return to the laboratory with pretreatment as described above. Pits of this type were dug at 4 locations at the Netherclifton site, while at Wigtown Martyr's stake, the natural edge of the merse occurred as a step of depth 1.5m and the face of the deposit was cut back to give a vertical profile which was

sampled as above.

ii. Samples for total radionuclide inventory evaluation were obtained by cutting 10 x 10cm areas in depth increments 0 to 15cm and 15 to 30cm at the locations shown in Figure 1.8, for Netherclifton and along a 50m transect at Wigtown Martyr's stake as shown in Figure 1.9.

Surface samples (top cm of silt) were collected at Netherclifton every 5m along the line shown in Figure 1.8.

iii. Two horizontal sections were dug into the natural edge of the merse deposit at Wigtown Martyr's stake. The two profiles were collected at depths of 0 to 5cm and 70 to 75cm relative to the Merse surface and 12 samples from each profile were recovered over horizontal distances of 0 to 11cm with a sampling increment of 1cm and at 20 to 21cm. A schematic diagram of these profiles is shown in Figure 1.9.

iv. A sediment pit section and a sediment core were collected from the intertidal area of the Netherclifton site to characterise the concentration and nuclide ratios of manmade radionuclides. The collection techniques and pretreatment of the pit and the core profiles were similar to those described above for the merse deposit pits and the intertidal cores of Ardmore and Skyreburn Bays respectively.

2.2 INSTRUMENTAL ANALYTICAL METHODS

2.2.1 Direct Gamma Spectroscopy Analysis of Sediment Samples

As discussed in section 1.1.4 direct gamma spectroscopy analysis can be applied to the determination of specific activities of gamma emitting radionuclides in environmental materials without any chemical processing of the samples in suitable cases. This technique was adopted for the analysis of radiocaesium isotopes and ^{241}Am in this work. Beta counting is not a viable alternative for determination of the radiocaesium isotopes as a consequence of the continuous nature of β^- spectra and the complex spectra consequently obtained. In the case of the ^{241}Am analysis, radiochemical separation followed by alpha spectroscopy does offer a viable alternative method with a superior limit of detection to direct gamma counting. However, the radiochemical separation of americium is particularly difficult as a result of its chemical similarity to aluminium and the rare earth elements. As a result, the chemical methods commonly used are complex and time consuming and often give low and variable yields (Williams, 1985; Holm and Fukai, 1977 ; Holm et al, 1979). Thus, since the activities of ^{241}Am in the sediment in the main area of interest were suitable for analysis by direct gamma spectroscopy, this technique was adopted as being more appropriate and less time consuming than alpha spectroscopy for analysis of the samples.

The detector used for direct gamma spectroscopy analysis in this work was an EG and G Ortec 80cc Ge(Li) detector of resolution 2.0keV at 1333keV. This crystal was highly suitable for analysis of radiocaesium isotopes and had also been previously demonstrated

(Williams, 1985) to be superior for determination of ^{241}Am than a planar detector which was also available and had a better resolution but much lower efficiency than the 80cc Ge(Li) detector. The shielding arrangement used for the detector is shown in Figure 2.2 and this arrangement gave rise to gamma spectra with negligible background photopeaks and low compton continuum levels in the region of interest. The crystal was connected via appropriate amplification circuitry, as discussed in section 1.1.4, to an EG and G Ortec 7032 analyser interfaced to a DEC 11/73 computer equipped with two 30 Megabyte Winchester discs and dual 400 kilobyte floppy discs for data storage and processing. A spectrum size of 4096 channels was used to cover the energy range of approximately 0 to 2MeV and spectra were analysed using the standard EG and G Ortec software package, GAMMA2. The photopeaks used for analysis of ^{134}Cs, ^{137}Cs and ^{241}Am were 604keV, 662keV and 59.9keV respectively (Table 1.1).

The samples of sediment and soil analysed were prepared as fine homogeneous powders (using grinding with a mortar and pestle if required) and samples of weight approximately 100g were accurately weighed into polythene containers of standard size which were reproducibly positioned directly on the top face of the aluminium end cap of the detector. Samples were analysed for at least 16 hours to obtain suitable counting statistics for the peaks of interest and longer counts were employed for lower activity samples.

Two types of calibration were necessary in order to obtain meaningful specific activity results from the spectra produced using the Ge(Li) detector, namely an energy calibration and a detection efficiency calibration. Energy calibration is a relatively straightforward procedure and simply requires the

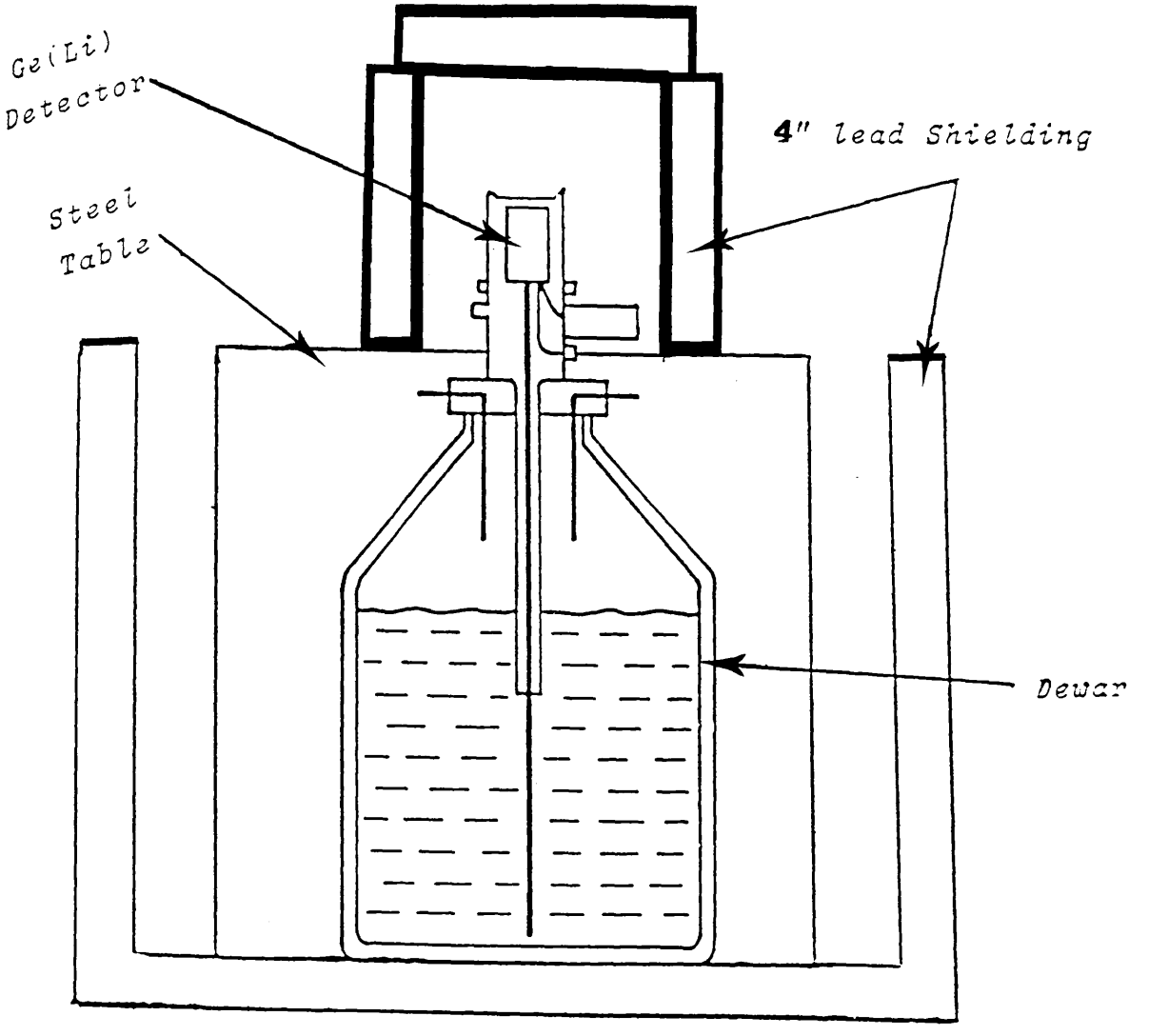

Figure 2.2 Shielding arrangements for a low background gamma spectrometer

analysis of a spectrum produced from a suitable source giving gamma photons with known energies in the appropriate range of interest. This type of energy/channel number calibration was regularly carried out for the 80cc Ge(Li) detector using a standard sealed solid source of ^{226}Ra. A typical data set for calibration of the detector is shown in Table 2.1, and the highly linear nature of the calibration can be seen in Figure 2.3.

A regression analysis was performed on each set of calibration data using the E G and G Ortec programme ENC2 which generates a calibration file for the detector defining the energy-channel number relationship. This file was stored on disc and was automatically used in the peak search and analysis programme.

Under normal circumstances, the detector was highly stable and showed negligible drift of peak positions over long time periods. Occasionally, however, periods of instability of the detector were experienced, characterized by pronounced loss of resolution and major and erratic jumps of several hundred channels in peak position. No obvious cause of this instability was identified and the transient existence of this fault condition reinforced the necessity for careful checking of peak shape, resolution and position in each spectrum recorded both visually on the MCA screen and on the gamma spectrum printout.

The efficiency E for detection of gamma radiation is defined as:

$$E = \frac{C}{DI} \times 100\%$$

CHANNEL	ENERGY (keV)
359	186
467	242
570	295
679	352
1176	609
1482	768
2160	1120
2387	1238
3401	1765

Table 2.1: Typical calibration of the 80cc detector using ^{226}Ra as a standard source

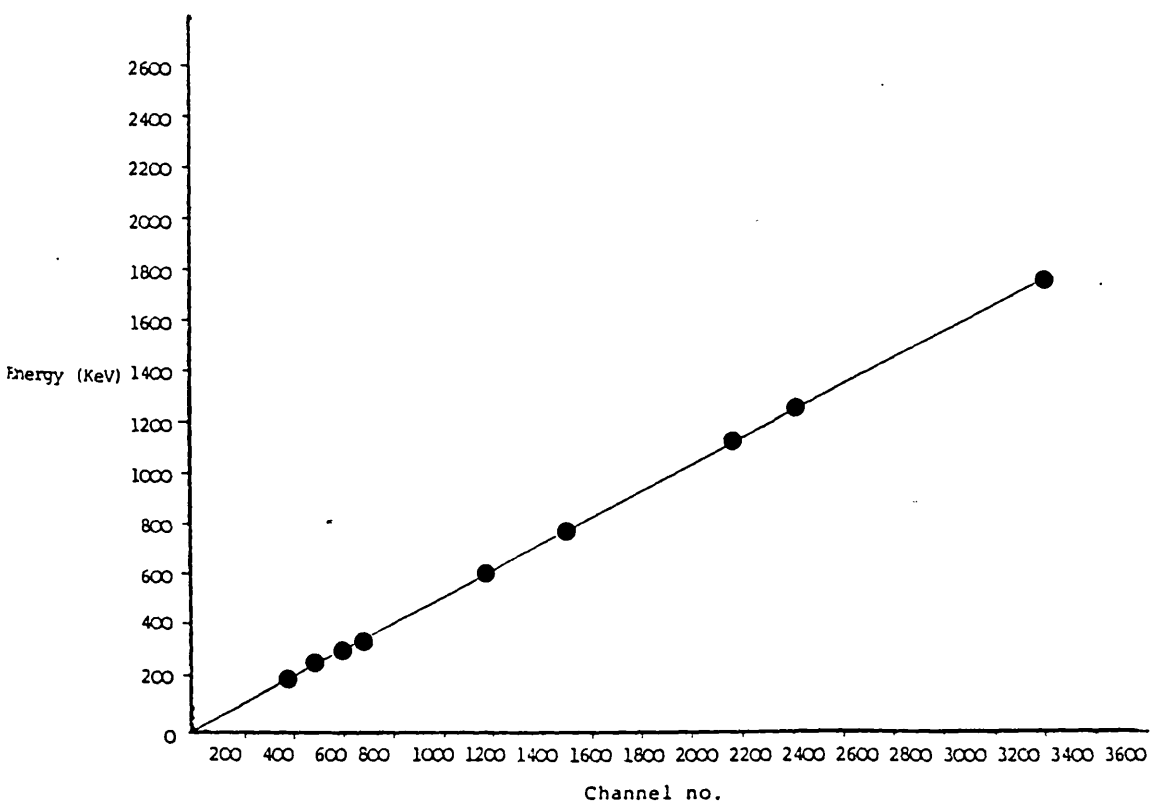

Figure 2.3: ^{226}Ra calibration of the 80cc Ge(Li) detector

where:

C = observed photopeak counting rate

I = intensity of the gamma emission

D = absolute disintegration rate of the source.

For a given source, the detection efficiency varies with the distance between the source and the detector according to:

$$E \alpha \frac{1}{d^2}$$

where:

E = counting efficiency

d = distance between source and detector.

Thus careful definition of the source counting geometry is essential in order to obtain good precision in gamma spectroscopy. The use of relatively large sources of varying chemical composition in the case of direct gamma spectroscopy analysis of sediments can present a problem since self absorption of the gamma radiation within the source can be significant. Moreover, the absorption process can be complex since it is sensitive to variations in (a) relative efficiency of the three possible mechanisms by which gamma photons interact with matter as discussed in section 1.1.3 (namely photoelectric effect, compton scattering and pair production), (b) photon energy, and (c) the z-value of the absorber material.

The detection efficiency calibration was performed

using standards prepared by dropwise addition and drying of known activities of ^{134}Cs, ^{137}Cs and ^{241}Am tracers to materials which resemble the sample composition. Two contrasting types of materials were analysed, namely silts (and other dominantly inorganic sediments) and organic soils. SiO_2 was used for detection efficiency calibration to simulate the silts and other inorganic sediments since its density and average Z-value are similar to those of the sediments. Similarly, powdered cellulose was used for efficiency calibrations for the organic soils since it provides a suitable density and average Z-value for this purpose. For intermediate deposits containing a mixture of organic and inorganic components, appropriate mixes of SiO_2 and cellulose were used in the efficiency calibration. These standards were counted in the same geometry as the samples, that is in the same shape of container filled to the same height, and from the observed counting rates the energy-detection efficiency relationship for a given geometry was found. Typical efficiency calibrations of the 80cc Ge(Li) detector using a 50/50 mixture, 100% of cellulose and 100% of SiO_2 are shown in Table 2.2, for ^{134}Cs, ^{137}Cs and ^{241}Am in each case.

The precision of the direct gamma counting technique was established by repeated analysis of a given sample. A sample of Solway Firth intertidal silt was selected as a suitable reference material and two sets of precision analysis were performed. In the first set, a sample of weight 134.5g was analysed on 15 separate occasions and the analytical data produced are shown in Table 2.3, indicating a precision of 1.6% for the ^{137}Cs analysis and 4.8% for the ^{241}Am. This approach does not allow for sample heterogeneity and to indicate the effects of this, a further set of 15 analyses of the same bulk silt were performed, in each case

Height (cm)	^{137}Cs (100% Clay) ε(%)	^{137}Cs (50% Clay + 50% Cellulose) ε(%)	^{137}Cs (100% Cellulose) ε(%)
1	1.263±0.028	1.142±0.022	1.344±0.024
2	0.978±0.019	0.937±0.016	0.975±0.016
3	0.788±0.013	0.778±0.012	0.803±0.013
4	0.675±0.011	0.673±0.010	0.695±0.010
5	0.588±0.009	0.589±0.009	0.611±0.009
6	0.509±0.008	0.527±0.008	0.546±0.008
7	0.447±0.007	0.463±0.007	0.503±0.007

(a)

Height (cm)	^{134}Cs (100% Clay) ε(%)	^{134}Cs (50% Clay + 50% Cellulose) ε(%)	^{134}Cs (100% Cellulose) ε(%)
1	1.668±0.070	1.583±0.062	1.903±0.072
2	1.343±0.052	1.287±0.048	1.408±0.051
3	1.097±0.041	1.075±0.039	1.176±0.042
4	0.929±0.033	0.936±0.034	1.010±0.035
5	0.811±0.029	0.825±0.039	0.885±0.031
6	0.720±0.026	0.730±0.025	0.796±0.028
7	0.637±0.023	0.645±0.023	0.731±0.026

(b)

Height (cm)	^{241}Am (100% Clay) ε(%)	^{241}Am (50% Clay + 50% Cellulose) ε(%)	^{241}Am (100% Cellulose) ε(%)
1	2.650±0.238	2.255±0.237	2.810±0.346
2	1.716±0.142	1.721±0.151	2.100±0.220
3	1.267±0.105	1.363±0.116	1.618±0.163
4	1.070±0.084	1.130±0.096	1.352±0.131
5	0.907±0.069	0.957±0.077	1.138±0.110
6	0.761±0.059	0.821±0.067	1.049±0.097
7	0.716±0.054	0.779±0.061	0.938±0.091

(c)

TABLE 2.2: Analytical data for calibration of the detection efficiency for ^{134}Cs, ^{137}Cs and ^{241}Am by direct γ spectroscopy for sources of varying height and composition

Sample	^{137}Cs	^{241}Am
STD 1	557±21	250±29
STD 2	553±20	262±29
STD 3	560±20	254±29
STD 4	551±20	255±29
STD 5	549±20	268±29
STD 6	548±20	288±31
STD 7	537±20	290±32
STD 8	573±20	288±32
STD 9	554±20	275±31
STD10	537±20	269±30
STD11	543±20	266±29
STD12	551±20	264±29
STD13	545±20	262±29
STD14	554±20	280±31
STD15	547±20	272±31
Mean	551±9	Mean 269±13
Rel Error	1.6%	Rel Error 4.8%

TABLE 2.3: Analytical data for 15 repeat analysis of a single sample of silt for ^{137}Cs and ^{241}Am by direct γ spectroscopy

Sample weight = 134.5g; Height = 6cm; On contact with 80cc GeLi detector, counting time = 10,000sec
Units = Bq kg^{-1}

selecting a different subsample of weight approximately 100g from the total bulk sediment of about 1.5kg weight. The results of this experiment are shown in Table 2.4 and, as expected, the precisions of 2.2% for ^{137}Cs and of 6.4% for ^{241}Am are poorer than those obtained in the preceding experiment, but the small difference between the two suggests that sample heterogeneity does not pose a problem in this study. The results of this experiment also indicate that the counting statistics applicable in the analysis represent the main limitation on the precision that can be obtained in the analysis.

The accuracy of the technique was not evaluated since no suitable standard reference material was available in SURRC at the time of analysis.

2.2.2 Neutron Activation Analysis

Instrumental neutron activation analysis was used to determine the concentrations of a range of stable elements in selected sediment samples in order to provide additional geochemical information for parts of this study. In this technique, samples of the sediment and appropriate standards are exposed to a flux of thermal neutrons in a nuclear reactor. Neutron capture by the constituent atoms of the sample and standard produces radioactive species and, in suitable cases, β^- decay of the radioactive products also gives rise to the emission of gamma radiation which can be detected using gamma spectroscopy techniques as described in section 1.1.4. Comparison of the gamma spectra of the samples with that of the standard allows the calculation of element concentrations in the samples. The following equation applies to the induced activity of any species X produced as the result of neutron capture by a stable element Y.

Sample	^{137}Cs Bq kg^{-1}	^{241}Am Bq kg^{-1}
STD 1	546±25	252±38
STD 2	528±24	271±41
STD 3	523±24	279±41
STD 4	544±25	295±43
STD 5	548±24	312±44
STD 6	521±23	287±41
STD 7	526±24	289±41
STD 8	528±23	288±42
STD 9	546±24	255±36
STD10	545±25	287±42
STD11	551±26	259±40
STD12	549±23	291±42
STD13	526±22	294±42
STD14	555±27	310±41
STD15	523±22	269±40
Mean	537±12	Mean 283±18
Rel Error	2.2%	Rel Error 6.4%

TABLE 2.4: Analytical data for 15 repeat analysis of a bulk silt for ^{137}Cs and ^{241}Am by direct γ-spectroscopy

Sample weight = about 91g; Height = 4cm; On contact with 80cc GeLi detector, counting time = 10,000sec

$$A_X = N_Y \sigma_Y \phi (1 - e^{-\lambda_x t})$$

where:

A_X = the induced activity of X

N_Y = the number of atoms of Y in the sample

σ_Y = the thermal neutron capture cross section of Y

ϕ = the neutron flux

λ_X = the decay constant of X

t = the irradiation time

(De Soete et al, 1972).

In principle, this equation can be used in absolute activation analysis so that by measurement of A_X and knowledge of the values of σ_Y, ϕ, λ_X and t , it is possible to calculate N_Y. In practice, however, the difficulty in determining A_X and the uncertainties associated with the other parameters means that comparative activation analysis is normally used and the count rates of selected photopeaks in the gamma spectra of samples and standards are used to derive the sample elemental concentrations. Ideally, the standard should be of a very similar composition to the samples and should be of the same dimensions and density (Adams and Dams, 1970; De Soete et al, 1972).

In the present work, a chemically well characterized, homogeneous clay was used as the primary standard in the instrumental neutron activation analysis. This

clay was originally characterized in an interlaboratory study organized by the National Museum of Antiquities of Scotland and will be referred to as "Edinburgh Standard Clay". The IAEA standard reference materials "soil 5" and "soil 7" were used to check the accuracy of the neutron activation analysis work.

All irradiations were performed using the Scottish Universities Research and Reactor Centre (SURRC) UTR-300 research reactor which, at full power of 300kW, provides a neutron flux of about 3 x 10^{12}n cm^{-2} sec^{-1} in the core area. The main irradiation facilities of the reactor are shown schematically in Figure 2.4, and irradiations in this work were all performed using the central vertical stringer (cvs) which is used for irradiation of large samples or for irradiations lasting more than 1 hour. In the irradiation process, about 0.2g each of the samples, standard and reference materials were accurately weighed into clean, high purity polythene vials of volume 1ml which were then sealed and were placed in a graphite container which was lowered through an access hole in the reactor top shielding into an irradiation position in the centre of the reactor core.

Small variations occur in the neutron flux experienced by individual samples during the irradiation and in order to compensate for this effect, flux monitors of iron wire (of weight approximately 0.1g and 99.5% purity) were attached to all of the sample and standard irradiation vials. In addition, the vials were then wrapped in aluminium foil as a secondary containment in case of vial rupture or partial melting as a consequence of heating during irradiation. The sample identification code was also marked on the aluminium foil rather than on the vials themselves in order to prevent any blank contribution from the marker pen ink.

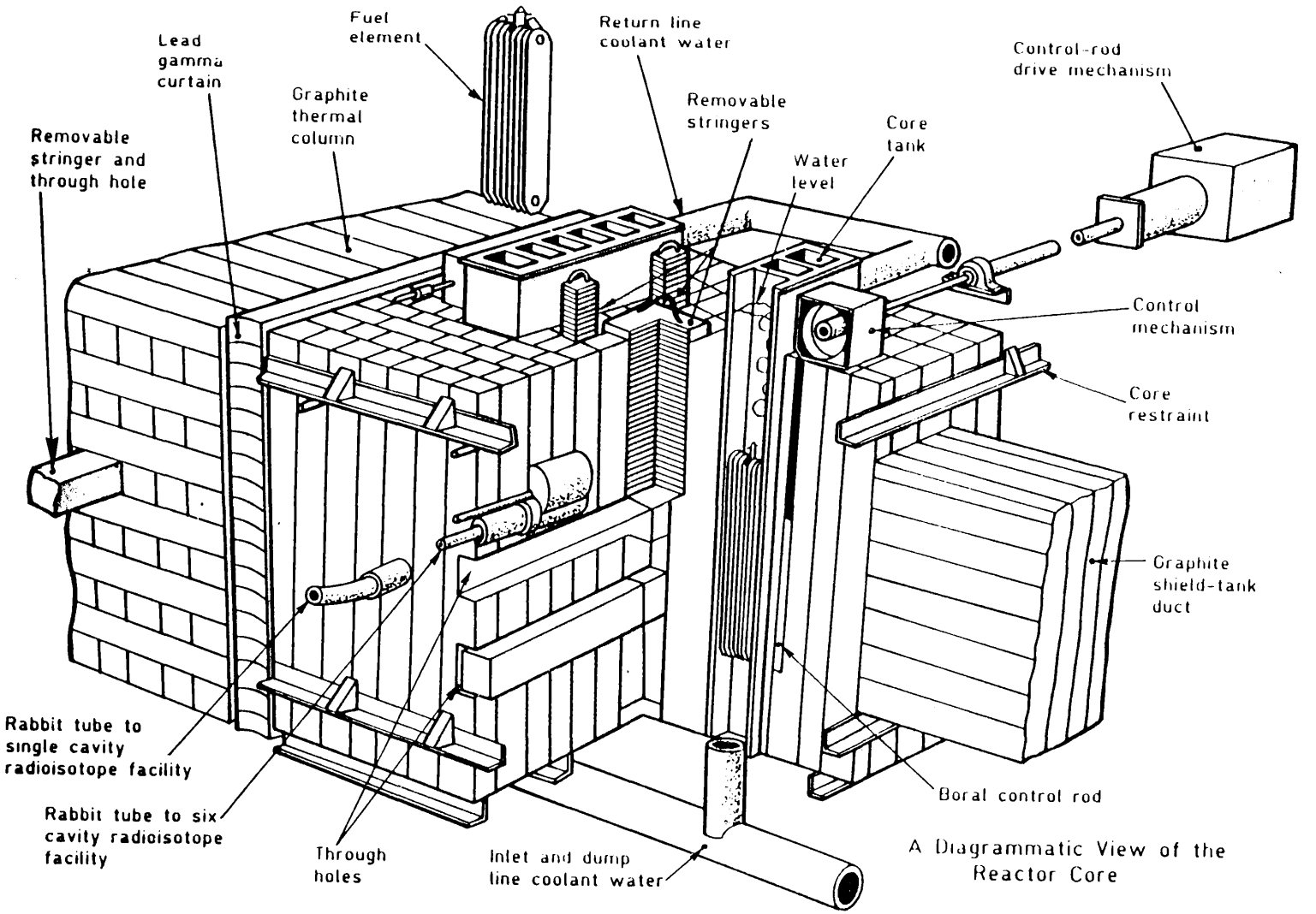

Figure 2.4 Schematic diagram showing the irradiation facilities in the UTR-300 research reactor

Batches of 10 samples along with the Edinburgh standard clay, soil 5 and soil 7 were packaged together in aluminium foil and were irradiated for 6 hour periods in this way. After a decay period of 3 days, during which the samples were kept in the SURRC isotope store to allow decay of excess short-lived radioactivity, the samples and standards were, with appropriate precautions, radiologically safe to handle. After carefully unwrapping the aluminium foil the vials were wiped clean of surface contamination and were transferred to suitably labelled polythene bags and stored behind lead shielding prior to counting. The iron flux monitors were also recovered and transferred to labelled polythene bags and stored with the samples until required for counting. All of the clean-up operations of the irradiated samples were carried out in the SURRC hot chemistry laboratory and a laboratory coat, overshoes and disposable gloves were worn for this process.

The radiation dose rate from each batch of samples and from individual samples was monitored using a calibrated dosemeter and all operations were carried out in accordance with the SURRC safety rules.

Two series of counts were performed after the 6 hour irradiation. The first series, carried out 3 days after irradiation, consisted of 1 hour counts with the samples accurately and reproducibly positioned in a sample holder at a height of about 10cm above an intrinsic Ge or Ge(Li) detector in order to achieve a suitable dead time and the elements detected are shown in Table 2.5. The dead time for counting of a given source can be reduced by increasing the distance between the source and detector since the counting efficiency varies as $\frac{1}{d^2}$ where d is the distance of the source from the detector (Newton et al, 1972). Thus

Element	Irradiation time	Delay time before counting	Radionuclide detected	Half-life	Gamma energy keV
Na	6 hours	3 days	^{24}Na	15.0 hours	1368.7
Al	10 seconds	3 minutes	^{28}Al	2.31 minutes	1780.0
K	6 hours	3 days	^{42}K	12.4 hours	1524.0
Sc	6 hours	3 weeks	^{46}Sc	83.8 days	889.2
Cr	6 hours	3 weeks	^{57}Cr	27.8 days	320.08
Mn	10 seconds	3 hours	^{56}Mn	2.576 hours	846.78
Fe	6 hours	3 weeks	^{59}Fe	45.1 days	1099, 1291
Co	6 hours	3 weeks	^{60}Co	5.26 years	1173.23, 1332.48
Rb	6 hours	3 weeks	^{86}Rb	18.66 days	1078.0
Sb	6 hours	3 weeks	^{124}Sb	60.3 days	1691.0
Cs	6 hours	3 weeks	^{134}Cs	2.05 years	795.8
La	6 hours	3 days	^{140}La	40.22 hours	1596.2
Ce	6 hours	3 weeks	^{141}Ce	33 days	145.44
Eu	6 hours	3 weeks	^{152}Eu	13 years	344.2, 1408.1
Sm	6 hours	3 days	^{153}Sm	4.68 hours	103.23
Tb	6 hours	3 weeks	^{160}Tb	73 days	215.6, 879.3
Lu	6 hours	3 weeks	^{177}Lu	6.7 days	208.36, 112.97
Hf	6 hours	3 weeks	^{181}Hf	42/4 days	133, 482
Ta	6 hours	3 weeks	^{182}Ta	115.0 days	1221.4
Th	6 hours	3 weeks	^{232}Pa	1.41 years	311.9

TABLE 2.5: Irradiation and counting data for instrumental neutron activation analysis

by increasing this distance, fewer counts are recorded and the dead time is correspondingly reduced. Careful definition of the source counting geometry is essential in order to obtain good precision in gamma spectroscopy (Adams and Dams, 1970). Therefore, activation analysis samples were held in a plastic holder which could be located at various heights above the detector in an aluminium support to give a suitable dead time. Spectra recorded in the 1 hour counts were dominated by species with half-lives in the range of tens of hours up to a few days. The lower activities of longer-lived activation products cannot in general be detected until the shorter-lived species decay to a large extent and the samples and standard can be recounted in a position close to the detector. The second series of counts therefore consisted of 16 hour counts with the samples held in a plastic mount in contact with the detector can and were performed approximately three weeks after irradiation. The elements detected in this way are listed in Table 2.5.

The slight variations in neutron flux experienced by samples during irradiation can be corrected for by assuming that the specific activity induced in the flux monitor for each sample is proportional to the neutron fluence experienced by the sample. Thus the iron wires were counted in a standard geometry and the specific activity of ^{59}Fe calculated at a defined reference time in each case. The observed gamma spectroscopy results for the various elements analysed were, during subsequent computer based calculations, normalised to an average flux based upon the flux monitor results.

Element concentrations were calculated from the peak search programme results using the SURRC activation analysis programme NAA (Harris, 1987). This programme takes the output file from the Ortec GAMMA 2 programme

directly from disc and performs a conventional activation analysis calculation based upon the equation

$$\frac{\text{weight of Y in sample}}{\text{weight of Y in standard}} = \frac{\text{count rate of X in sample}}{\text{count rate of X in standard}}$$

(Adams and Dams, 1970; Friedlander et al, 1981).

This programme corrects all observed count rates to a defined reference time, corrects for decay during counting, and allows inclusion of a priori errors to allow for uncertainties in counting geometry (with a value of 2% being used for a priori errors in this case), weight etc, and systematic errors to allow for flux variations. The final results are expressed as concentrations in "ppm".

The results for analysis of the IAEA reference materials are shown in Tables 2.6 and 2.7, and indicate a generally satisfactory accuracy and reproducibility for the method. This confirms previous, more detailed, evaluation of this technique at SURRC (Topping and MacKenzie, 1987).

2.3 RADIOCHEMICAL ANALYSES

In selecting analytical separation techniques for alpha spectroscopic analysis of ^{210}Pb via ^{210}Po, and for analysis of plutonium, uranium and thorium isotopes, it was first of all necessary to decide whether partial or total sample dissolution was required, since the sediments consist of (a) authigenic components (organics, carbonates, Fe/Mn oxides, and any other recent mineral growths) and (b) detrital minerals such as quartz and clays (section 1.2) and the different radionuclides are associated with different components of the sediment. Thus, of the nuclides of interest, unsupported $^{210}Pb/^{210}Po$ and plutonium isotopes are

Element	Observed Concentration (μg/g)	Certified Average Concentration (μg/g)
Na%	2.1±0.1	1.9
K%	2.0±0.3	1.9
Sc	18.5±0.6	14.8
Cr	34.0±1.6	28.9
Fe%	5.1±0.1	4.5
Co	16.4±0.6	14.8
As	121.0±10	93.9
Br	6.0±0.8	5.4
Rb	140.0±10	138
Sb	17.6±3.3	14.3
Ba	477.0±4.5	562
Cs	66.7±3.0	56.7
La	31.7±1.7	28.1
Ce	55.0±2.0	59.7
Eu	1.6±0.1	1.2
Sm	6.0±0.2	5.4
Tb	1.1±0.02	0.7
Yb	1.9±0.2	2.2
Lu	0.3±0.03	0.3
Hf	7.0±0.3	6.3
Ta	1.0±0.09	0.8
Th	12.8±0.5	11.3
U	3.5±0.7	3.2

TABLE 2.6: Observed concentrations (derived by INAA) and IAEA reference values for SOIL5

Element	Observed Concentration (1) μg/g	Observed Concentration (2) μg/g	Certified Concentration μg/g
Na%	2.4±0.1	2.3±0.09	2.3 - 2.5
K%	1.2±0.08	1.2±0.02	1.1 - 1.2
Sc	8.8±0.3	8.4±0.2	6.9 - 9.0
Cr	75.0±3.0	64.0±2.4	49 - 74
Fe%	2.6±0.1	2.7±0.1	2.5 - 2.6
Co	8.1±0.3	8.6±0.3	8.4 - 10.1
As	14.6±2.9	16.6±2.0	12.5 - 14.2
Rb	58±4.0	44.0±3.0	47 - 56
Sb	1.9±0.3	1.8±0.3	1.4 - 1.8
Ba	164.0±17.0	98.0±10.0	131 - 196
Cs	5.0±0.2	5.1±0.2	4.9 - 6.4
La	29.8±1.2	29.4±1.2	27 - 29
Ce	52±1.9	46.0±1.6	50 - 63
Eu	1.0±0.06	1.0±0.05	0.9 - 1.3
Sm	5.5±0.2	5.4±0.2	4.8 - 5.5
Tb	0.8±0.07	0.5±0.05	0.5 - 0.9
Yb	2.4±0.2	2.0±0.2	1.9 - 2.6
Lu	0.3±0.01	0.3±0.01	0.1 - 0.4
Hf	4.5±0.3	3.9±0.2	4.8 - 5.5
Ta	0.8±0.06	0.9±0.06	0.6 - 1.0
Th	8.6±0.2	7.8±0.3	6.5 - 8.7
U	2.6±0.4	2.8±0.4	2.2 - 3.3

TABLE 2.7: Observed concentrations (derived by INAA) and IAEA reference values for SOIL7

associated with the authigenic phase whereas uranium and thorium isotopes occur in both the authigenic and detrital phases. Consequently, uranium and thorium analyses required total sample dissolution while unsupported $^{210}Pb/^{210}Po$ and plutonium isotope analyses only required dissolution of the authigenic components.

A variety of sample weights was required for the different analyses and, on the basis of experience, weights of 10, 15 and 5g of dry sediment were taken respectively for the analysis of $^{210}Pb/^{210}Po$, plutonium and uranium/thorium.

The requirements for rigorous chemical separation and source preparation in alpha spectroscopy are discussed in detail in section 1.1.5, and the first stage in the purification process for all of the above nuclides, except ^{210}Po, involved furnacing at 450°C to destroy organic matter. The loss of weight on ignition (LOI) was used as an indication of the organic content of the samples (Chu, 1971; Talvitie, 1971; Wong, 1971; Hetherington, 1978; Lally and Eakins, 1978). Furnacing was not employed for ^{210}Po analysis since loss by volatilization could occur if this technique was used (MacKenzie and Scott, 1979).

The elements were then chemically extracted from the ashed residue (or finely divided sediment in the case of ^{210}Po) using an isotope yield tracer which was added at the start of the extraction in all cases. The yield tracers used in this study were ^{208}Po, $^{232}U/^{228}Th$ and ^{236}Pu for the analysis of ^{210}Pb, uranium/thorium and plutonium isotopes respectively. The specific activities of the spike solutions were selected to give suitable amounts of the tracer in 0.1ml aliquots which were dispensed using an automatic pipette. The spike activities used were 1.1, 1.04 and 0.29 Bq respectively of ^{208}Po, $^{232}U/^{228}Th$ and ^{236}Pu. The ashed residue or sediment was initially gently immersed in distilled water in a teflon beaker after which about 20ml of 12M hydrochloric acid was

carefully added and the samples were covered and left until reaction between the acid and any carbonate material present had ceased. The samples were then taken to near dryness on a hotplate after which they were digested with 10-20ml portions of concentrated nitric and hydrochloric acids separately and then with a mixture of 50% (V/V) hydrochloric acid/nitric acid (aqua regia) in order to totally dissolve the authigenic components. Thereafter the samples were taken to near dryness and the soluble components were leached into 9M hydrochloric acid.

The dissolution process for ^{210}Po and plutonium isotopes was complete at this stage and the sample solutions were filtered and taken immediately for analysis or were stored in polythene bottles prior to analysis.

In the case of uranium/thorium analysis further digestion using 40% hydrofluoric acid was employed to effect decomposition of silicates and quartz giving rise to removal of Si by volatilization as SiF_4. The samples were then dissolved in 9M hydrochloric acid, with further aqua regia/HF digestion of any residue until total dissolution was obtained. The total acid leachings were stored in plastic bottles prior to analysis.

2.3.1 ^{210}Pb Analysis

^{210}Pb analysis was effected indirectly by spontaneous deposition of its grand-daughter ^{210}Po ($t_{½}$ = 138.4d) onto copper foil followed by alpha spectroscopy determination of the deposited activity and assumption of secular equilibrium between ^{210}Pb and ^{210}Po to derive the ^{210}Po content of the samples (^{226}Ra in the leach solutions was below the limit of detection by gamma spectroscopy so no subtraction of a supported ^{210}Pb component was performed).

The deposition of ^{210}Po on Copper is a relatively simple technique with the only significant complication being that ^{210}Bi is also deposited on the foil. In the case of copper foils, the ^{210}Bi can be rapidly and totally removed by washing the foil with cold distilled water from a wash bottle, whereas the widely used alternative method of using Silver foils also gives ^{210}Bi deposition but, in this case, it cannot be washed off with cold water.

^{210}Po deposition onto $1cm^2$ copper foils, glued to a mylar backing, was carried out using 30ml of 9M hydrochloric acid sediment leaching solution to which was added 20ml hydroxylamine hydrochloride solution (35% W/V) to prevent deposition of iron on the foils. The solution was then made up to a volume of approximately 100ml with distilled water and the copper foil was suspended in the solution with stirring on a magnetic hotplate. The temperature was held in the range 90 to 95°C over a period of 30 minutes, with the solution volume being maintained by addition of distilled water as required, during which time about 80% recovery of ^{210}Po was achieved. Longer plating times gave greater recoveries but also gave rise to thicker sources with consequent loss of resolution in the alpha spectra. The copper foil was then recovered and washed with distilled water, dried and counted for alpha activity using a surface barrier detector spectroscopy system, the principles of operation of which are discussed in detail in section 1.1.5. The system used in the present work consisted of two EG & G Ortec surface barrier detectors of area $450cm^2$ in individual, commercially produced, vacuum chamber units which also incorporated bias supply pre-amplifier, amplifier and biased amplifier electronics. The alpha source was mounted on a platform beneath the silicon surface barrier detector, as close as possible to the

detector in order to obtain maximum counting efficiency. The resolution of the detector was 22keV full width at half maximum (FWHM) but in practice, poorer resolution was obtained as a result of the finite source thickness, with typical ^{210}Po resolution being about 60keV. This resolution is adequate to resolve the ^{210}Po and ^{208}Po alpha energies of 5.305MeV and 5.114MeV respectively. Spectra were recorded on an EG & G Ortec 7032 Analyser via a mixer/router with 1024 channels being used to cover the energy range from about 4 to 10MeV.

The counting times employed were normally about 16 hours or longer, depending on the activity of the source. These detectors have near zero inherent background.

The calculation of the results from the spectrum data is straightforward, involving the equation:

$$A_{sample} = \frac{I_{sample}}{I_{tracer}} \times A_{tracer}$$

where:

A = activity

I = peak integral.

2.3.2 Plutonium Analysis

Coprecipitation of plutonium from the acid leaching solution using ferric hydroxide as a scavenger was carried out by the careful addition of concentrated ammonia solution until production of a persistent dense brown precipitate occurred in the pH range 8.0 to 9.0. The natural Fe in the sample was sufficient for this

purpose without addition of further Fe. The precipitate, containing the plutonium, was separated from the solution containing many of the matrix elements of the sample by centrifugation. The precipitate was washed twice with distilled water before redissolution in concentrated nitric acid, after which the solution was taken to dryness on a hotplate. This step was repeated at least three times in order to ensure the oxidation of plutonium from the +3 oxidation state to the +4 oxidation state. The sample was then redissolved in about 50ml 9M hydrochloric acid prior to the ion exchange separation procedure.

Anion exchange was used for the isolation of plutonium using Bio Rad AG1-X8 anion exchange resin of 100 - 200 mesh. A resin column of height 6cm and cross section area $1cm^2$ was preconditioned by passing two 20ml portions of 9M hydrochloric acid through it after which the 9M hydrochloric acid solution containing the plutonium was passed through. In 9M hydrochloric acid, all plutonium is essentially held on the resin in the forms $(Pu\ Cl_5)^-$ and $(Pu\ Cl_6)^{2-}$ (Cleveland, 1970a; b; 1979), whilst potentially interfering species including radium, thorium and americium pass through the column with the sample solution. Iron and uranium are also held on the resin under these conditions. The column was then washed with two 10ml portions of 9M hydrochloric acid before the elution of plutonium with 2 x 20ml portions of 1.2M hydrochloric acid, each containing about 5ml of 1.0M ammonium iodide solution. This process involves the reduction of plutonium by I^- to the +3 oxidation state which cannot form anionic complexes in hydrochloric acid media and is, therefore, not held by the resin. The eluting solution was evaporated to dryness and the iodine was removed by oxidation by addition of nitric acid and taking the sample to dryness. This step was repeated as necessary

until all I^- was removed from the sample. This stage is of crucial importance since, if any traces of I^- remain, low plutonium yields are obtained. The sample was then redissolved in 8M nitric acid prior to a second anion exchange separation, this time using a Bio Rad AG1-X8 column of the same dimension as above, but preconditioned with 8M nitric acid. Under these conditions plutonium is adsorbed onto the resin whereas iron and uranium pass through the column without adsorption. The column was then washed twice with two 10ml portions of 8M nitric acid. Finally, the plutonium was removed by elution of the column using two 20ml portions of 1.2M hydrochloric acid, each containing about 5ml 1.0M ammonium iodide solution. I^- was removed once again by evaporation and addition of nitric acid prior to electrodeposition.

The plutonium isotopes were redissolved in about 8 drops of concentrated hydrochloric acid and about 40ml of 3.75% (W/V) ammonium chloride solution was added to give a solution from which the plutonium was electrodepositioned onto a 2.5cm diameter stainless steel disc. The electrodeposition was carried out using an electrolysis cell which consists of a cylindrical perspex body, 6cm in diameter and 10cm in depth, together with a brass base. A perspex support holds a platinum wire anode in the centre of the cell, while the stainless steel disc itself acts as the cathode, being firmly fixed in the centre of the base and sealed from the plating solution by use of a teflon coated rubber ring fitted between the planchette and the cell body. The copper base of the cell acts as a sink for the heat produced during the plating process and is also fitted with a locating pin for an electrical contact from the electrolysis power supply (Hallberg et al, 1960).

Electrolysis was carried out for 45 minutes at a voltage of 15V and fixed current of 3A, with the solution volume being maintained by addition of distilled water if necessary. At the end of the deposition, immediately before the voltage supply is switched off, the solution is made alkaline by addition of about 2ml of concentrated ammonia solution to prevent redissolution of the deposited plutonium and the source is removed, rinsed with distilled water then ethanol and dried for alpha spectroscopy.

The calculation of ^{238}Pu activity uses the same form of equation as given above for the ^{210}Po calculation. A combined $^{239,240}Pu$ activity was calculated from the results since the alpha spectroscopy method cannot resolve the energies of these two isotopes (^{239}Pu = 5.157MeV, ^{240}Pu = 5.168MeV).

The typical recovery of plutonium in this procedure was in the range 85 to 95% and typical sources gave resolutions of about 60keV (FWHM) which was good enough to resolve the energies of plutonium isotopes other than ^{239}Pu and ^{240}Po (Table 1.1). A counting time of 16 hours was normally used.

The accuracy and precision of the plutonium analytical method assessed by analysis of an IAEA reference marine sediment and an in-house reference clay respectively. The results, shown in Table 2.8, indicate a satisfactory degree of accuracy and a precision of 2.4% for the plutonium analysis.

2.3.3 Uranium/Thorium Extraction

In the uranium/thorium analysis, it was necessary to use a single sample for determination of the isotopic concentration of both elements in order to derive

Sample Reflect	LOI %	^{238}Pu Bq kg^{-1}	$^{239,240}Pu$ Bq kg^{-1}	$\frac{^{238}Pu}{^{239,240}Pu}$
STD 1	3.7	25.4±2.1	161±6	0.16
STD 2	3.6	25.8±2.2	166±7	0.16
STD 3	3.8	26.0±2.2	166±7	0.16
STD 4	3.4	25.5±2.3	162±6	0.16
STD 5	3.4	25.9±2.4	163±6	0.16
STD 6	3.9	26.0±2.4	167±8	0.16
STD 7	3.4	26.1±2.5	164±7	0.16
STD 8	3.6	25.4±2.3	164±6	0.15
STD 9	3.6	25.4±2.0	162±5	0.16
STD10	3.7	25.6±1.9	166±8	0.15
STD11	3.2	25.7±1.9	168±8	0.15
STD12	3.7	27.1±2.5	171±8	0.16
STD13	3.4	25.3±1.9	159±8	0.16
STD14	3.5	25.9±2.3	162±6	0.16
STD15	3.4	25.9±2.4	161±6	0.16
STD16	3.3	26.1±2.4	167±7	0.16
STD17	3.7	26.5±2.5	170±9	0.16
STD18	3.2	26.4±2.3	163±6	0.16
STD19	3.1	25.2±2.0	159±6	0.16
STD20	3.8	25.4±1.9	157±5	0.16
STD21	3.9	25.6±1.8	154±5	0.17
STD22	3.9	26.3±1.8	163±7	0.16
STD23	3.0	26.2±1.8	169±8	0.15
STD24	3.4	25.3±1.9	164±8	0.15
	Mean	25.8±0.5	Mean 164±4	
	Rel Error	1.8%	Rel Error 2.4%	

TABLE 2.8a): Analytical data for assessment of the precision of the plutonium analysis by replicate analysis of a bulk sample of Solway silt

sample weight = approx 5g
counting time = 16h

	^{238}Pu	$^{239,240}Pu$
Observed values	11±1	25±2
Certified values	9±1	21±3

TABLE 2.8b): Analysed data and reference values for analysis of IAEA standard for plutonium

Units: Bq kg^{-1}

useful $^{230}Th/^{234}U$ ratios, since even in finely powered, well mixed sediment, some degree of heterogeneity still exists and this can give rise to additional errors in this ratio if different subsamples are used for uranium and thorium assay.

The spike used throughout this study for uranium/thorium analysis was an "equilibrium" solution containing $^{232}U/^{228}Th$. This spike is in fact in transient equilibrium so that the ^{228}Th activity was 1.03 times the ^{232}U activity. Complication also exists with the use of ^{228}Th as the yield tracer due to the presence of natural ^{228}Th in the samples. The assumption was made that the natural ^{232}Th in the sample is in secular equilibrium with the natural fraction of ^{228}Th and the peak integral of ^{232}Th was subtracted from the total peak integral of ^{228}Th leaving the ^{228}Th tracer counts.

Many of the general features of the uranium/thorium analysis procedure are similar to those of the plutonium method described above. Thus the first step in the uranium/thorium method involved the coprecipitation of these elements using concentrated ammonia to precipitate ferric hydroxide as a carrier. The hydroxide precipitate was washed with distilled water, dissolved in concentrated hydrochloric acid and adjusted to 9M in hydrochloric acid for anion exchange separation using Bio Rad AG1-X8 resin in the chloride form (6cm x $1cm^2$ column preconditioned with 2 x 20ml portions of 9M hydrochloric acid). This stage achieves the separation of uranium from thorium since uranium is strongly held by the resin under these conditions, whereas thorium passes through the resin. The resin was washed through with two 20ml portions of 9M hydrochloric acid and the complete hydrochloric acid solution plus washings which have passed through the

resin were retained for thorium analysis as described below. The uranium was then eluted using 2 x 50ml portions of 1.2M hydrochloric acid, after which the eluting solution was taken to dryness and the residue redissolved in 9M hydrochloric acid for a second anion exchange purification step which was carried out in the same way. Since the samples of interest in this work contained plutonium in many cases, it was necessary to remove the plutonium from the uranium at this stage. This was achieved by taking the solution to dryness, re-dissolving the residue in 10M HNO_3 and passing the solution through a column of AG1X8, preconditioned with 10M HNO_3. Under these conditions the plutonium is retained but the uranium passes through. The column was washed with 10ml of 10M HNO_3 and the washing and uranium solution were taken to dryness. The residue was re-dissolved in 9M HCl and iron was extracted using solvent extraction into di-isopropyl ether. Thereafter the solution was taken to dryness, redissolved in about 9 drops concentrated hydrochloric acid plus 40ml of 3.75% (W/V) ammonium chloride solution for electrodeposition. The electrodeposition of uranium was carried out using the same deposition cell and conditions as described for plutonium.

The solution which had passed through the chloride form AG1-X8 resin contained the thorium and was taken to dryness then redissolved in concentrated nitric acid and a second coprecipitation of thorium was performed by addition of concentrated ammonia to precipitate $AL(OH)_3$ at pH 8 to 9 using the natural aluminium in the sample as a carrier for thorium. It is essential at this stage to remove all Cl^- from the sample and the precipitate was washed twice with distilled water, with vigorous shaking of the sample to totally disaggregate the precipitate in each case to avoid physical trapping of Cl^- in the precipitate. After this, the precipitate

was redissolved in concentrated nitric acid and the thorium coprecipitation with $Al(OH)_3$ was repeated. The precipitate was washed twice with distilled water and then redissolved in the minimum volume of concentrated nitric acid. The acid concentration was then adjusted to 10M and the solution was passed through a 6cm x $1cm^2$ column of Bio-Rad AG1-X8 anion exchange resin preconditioned with 20ml of 0.1M nitric acid then with 2 x 20ml of 10M nitric acid. Under these conditions, the thorium is held by the resin in the $[Th(NO_3)_6]^{2-}$ form. Elution of the thorium was achieved by passing 2 x 20ml portions of 0.1M nitric acid through the column. The solution was then take to dryness prior to electrodeposition as described above for plutonium and uranium.

Calculation of the various isotope activities used the form of equation given above for ^{210}Po.

Resolution of about 60keV was normally obtained in both the uranium and thorium analyses, readily resolving the uranium and thorium peaks in the spectra (Table 1.1). Uranium yields in the process were typically about 100% while thorium yields were approximately 60%. Counting times in both cases were at least 16 hours.

The accuracy of the technique was evaluated by analysis of the Canadian Centre for Metrology Standard reference sandstone DL-1a with the observed and reference values being shown in Table 2.9. The relatively good agreement verifies that the method provides a suitable degree of accuracy.

2.4 SEQUENTIAL LEACHING OF URANIUM

A sequential leaching scheme based upon that of Cook et al

	^{238}U	^{234}U	^{230}Th
Observed values	1435±26	1426±26	1415±35
Certified values	1400	1400	1400

TABLE 2.9: Analytical results for uranium and thorium analysis of reference sandstone DL-1a along with CANMET (certified values) (CANMET, 1983)

Units: Bq kg^{-1}

(1984b) was employed in the investigation of the geochemical association of uranium in samples from soil and intertidal profiles collected in March 1986 from the Netherclifton Merse area.

Representative subsamples of wet sediment of weight approximately 10g were accurately taken from the upper half and the lower half of each vertical profile and, because of limitations in the capacity of available apparatus, each sample was further subdivided into about 2.5g aliquots for sequential extraction. In each case, the appropriate extracts were combined after the leaching to give a sample representing the leaching of 10g of material. The 2.5g subsamples were subjected to the following extractions, giving the geochemical associations indicated.

a. Readily available uranium

Extraction of uranium in this case was achieved by addition of 10ml portions of 0.05M calcium chloride solution. The centrifuge tubes were tightly sealed and placed on an end-over-end shaker for 16 hours. The mixtures were then centrifuged at 3000 rpm for 20 minutes after which the supernatant liquid was decanted off and the sediment residues were washed 3 times with approximately 10ml distilled water portions followed by centrifugation each time. These washing solutions were combined with the calcium chloride solution and the total solution was filtered through a Whatman No. 44 filter paper. The filtered solution was acidified, spiked with ^{232}U tracer and evaporated to dryness. The solid thus produced was redissolved in 9M hydrochloric acid prior to uranium analysis as described above, using anion exchange separation followed by electrodeposition of the uranium to produce a suitable source for alpha spectroscopy.

b. Exchangeable uranium

The sediment residues from the above extraction were shaken with 10ml portions of 0.5M acetic acid for 16 hours. The mixtures were then centrifuged and the acetic acid solution was filtered, spiked, acidified, taken to dryness and redissolved in 9M hydrochloric acid. The isolation of uranium was performed as above.

c. Uranium associated with organic matter

In this extraction the sediment residues from the acetic acid extraction were shaken for 16 hours with 37.5ml portions of 0.1M tetra sodium pyrophosphate. The mixture was then centrifuged and the supernatant solution was filtered, spiked, acidified, evaporated and redissolved in 9M hydrochloric acid for uranium analysis.

d. Uranium occluded or co-precipitated with sesquioxides

The extraction in this case was carried out by shaking the sediment residues from previous extractions with 50ml portions of 0.1M oxalic acid/0.175M ammonium oxalate. The extractant solution was treated as for the pyrophosphate leach.

e. Residual uranium

The remaining uranium was extracted by the total dissolution of the sediment residue from the previous extractions. This was achieved using hydrochloric, nitric and hydrofluoric acids, as described above.

2.5 ALPHA PARTICLE TRACK STUDIES

Solid state nuclear track detection was used in this work to investigate the distribution of alpha emitting nuclides

in merse sediment samples from the Solway coast, with CR-39 plastic being employed as the alpha particle track detector (Fleischer et al, 1975; Hamilton, 1981; Hamilton and Clifton, 1981). 100cm^2 sections of CR-39 were cut for use with corresponding sources of sediment selected from section NCS862 at the Netherclifton sampling site. The primary objective of this part of the work was to investigate whether or not "hot particles" (Hamilton 1981) were present in these sediments and the established techniques developed by Hamitlon for investigation of this phenomenon were employed. The sources were prepared by distributing the sediment finely on a flat surface of heavy duty paper (Benchkote) covered with a thin layer of water soluble adhesive. Excess sediment was shaken from the source, after which the CR-39 detector was placed in contact with the flat surface of the sample. The source and detector were held firmly together, without moving, in the dark for a period of 5 to 7 months in order to record a sufficient number of alpha particle tracks. The detector was then separated from the sample and was washed with distilled water to remove any sediment particles adhering to it.

The next stage of the procedure involved developing the alpha tracks by etching for about 5 hours in 6.0M sodium hydroxide solution containing a small amount of surfactant (Decon) at 70°C in a water bath (Hamilton, 1981). After this time the detector surface assumes a slightly cloudy appearance and care must be taken to avoid over etching of the plates. The detector was then placed in a bath of slightly acidified distilled water to neutralize the sodium hydroxide over a period of 5 to 10 minutes at room temperature. The detector was then rinsed with distilled water and dried with soft tissue and transferred to a plastic bag for storage prior to examination.

A conventional transmission microscope with a magnification

of X200 was used for analysis of the alpha track distribution.

3. RESULTS

The analytical data obtained is this work are presented in Tables 3.1 to 3.25 and are depicted graphically in Figures 3.1 to 3.23 in the following sequence.

Tables 3.1 and 3.2; Figures 3.1 and 3.2: Ardmore Bay samples; radionuclide results

Tables 3.3 and 3.4: Surface intertidal samples from various locations in South West Scotland; radionuclide and neutron activation analysis results

Tables 3.5 to 3.7; Figures 3.3 to 3.6: Skyreburn Bay samples; radionuclide results

Tables 3.8 to 3.18; Figures 3.7 to 3.15: Netherclifton samples; radionuclide results

Tables 3.19 to 3.24; Figures 3.16 to 3.24: Wigtown Martyr's stake samples; radionuclide results

Table 3.25: Netherclifton and Wigtown Martyr's stake; neutron activation analysis

Radionuclide specific activities are expressed in units of Bq kg^{-1} throughout and the quoted uncertainties are based upon propagated 1σ statistical uncertainties.

The inventory results are expressed in units of Bq m^{-2} and the activation analysis results in units of ppm unless otherwise stated. The uncertainties quoted for the instrumental neutron activation analysis data are based upon 1σ counting statistics plus a priori and systematic errors as described above.

Depth cm	ABC841 ^{210}Pb	ABC842 ^{210}Pb	ABC843 ^{210}Pb
0-2	2.9±0.3	3.8±0.3	6.5±0.7
2-4	2.7±0.2	4.0±0.3	6.4±0.4
4-6	2.6±0.2	4.5±0.4	5.8±0.3
6-8	2.2±0.2	3.7±0.4	5.8±0.4
8-10	2.4±0.2	7.1±0.6	7.7±0.4
10-12	2.5±0.2	7.4±0.6	7.3±0.3
12-14	2.4±0.1	9.6±1.0	10.1±0.5
14-16	2.6±0.2	NA	6.1±0.2
16-18	2.5±0.2	8.8±0.8	5.4±0.2
18-20	2.6±0.3	9.9±0.5	5.6±0.2
20-22	2.4±0.2	9.7±1.1	5.7±1.7
22-24	2.6±0.2	11.0±1.5	7.6±0.2
24-26	2.7±0.2	12.3±0.7	11.2±0.7
26-28	2.4±0.2	13.0±0.6	10.4±0.3
28-30	2.2±0.2	13.8±0.6	8.7±0.3
30-32	2.1±0.2	12.9±0.8	11.4±0.5
32-34	1.4±0.2	10.8±1.1	6.0±0.5
34-36	NA	NA	9.9±0.5
36-38	NA	NA	13.3±0.9

TABLE 3.1: ^{210}Pb concentrations in samples from three cores of Ardmore Bay intertidal sediment, March 1984 (Figure 1.6)

NA = Not Analysed
Units = Bq kg^{-1}

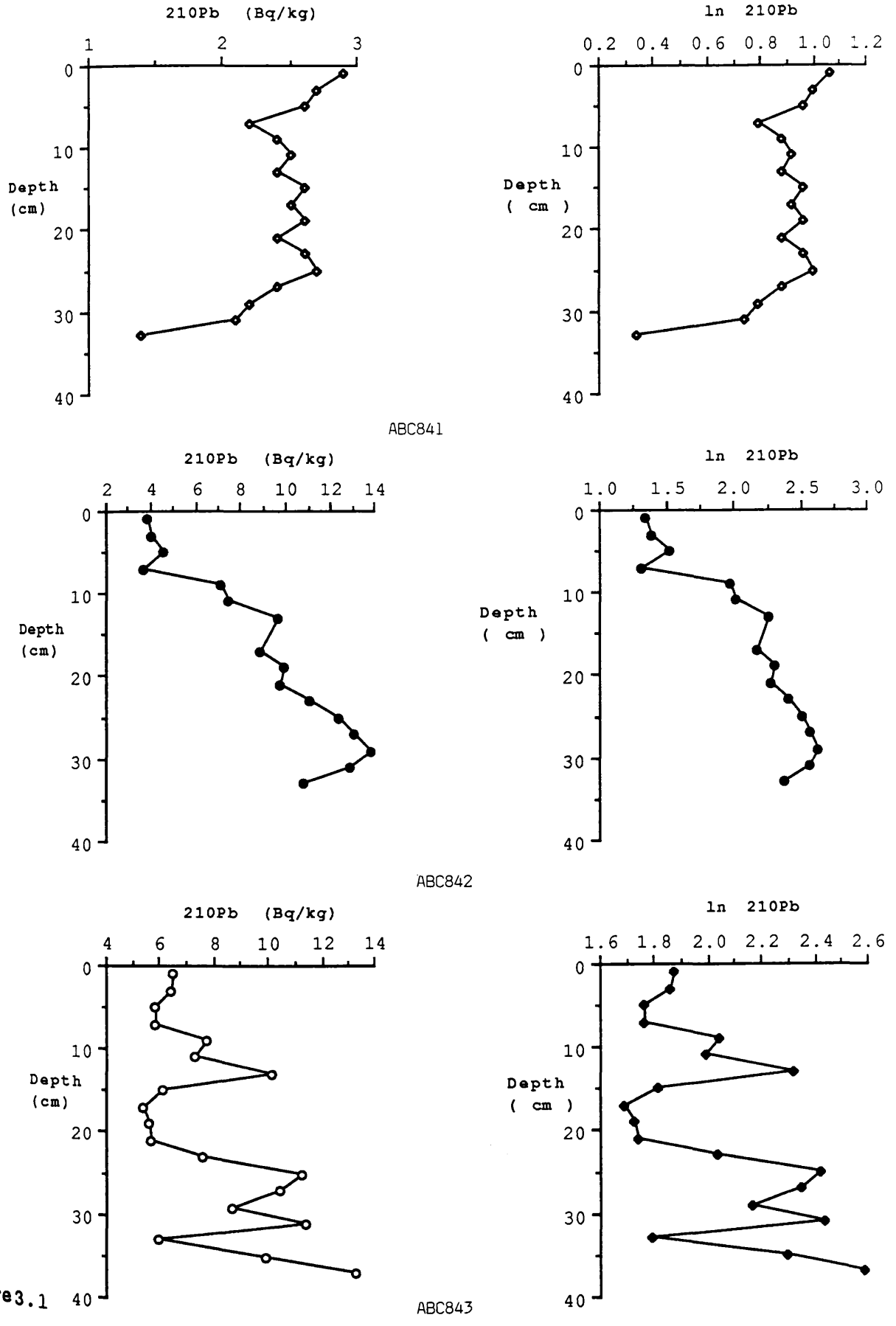

Figure 3.1 Plot of (excess ^{210}Pb) and ln (excess ^{210}Pb) versus depth from intertidal sediment cores ABC841, ABC842 and ABC843 from Ardmore Bay

Depth cm	Dry/Wet %	^{134}Cs	Total ^{137}Cs	Chernobyl ^{137}Cs	non Chernobyl ^{137}Cs	Total $\frac{^{134}Cs}{^{137}Cs}$	Chernobyl $\frac{^{134}Cs}{^{137}Cs}$
0-2	80	6.0±1.2	47±5	18	29	0.13	0.33
2-4	80	3.2±1.5	37±5	10	27	0.09	0.33
4-6	80	4.0±1.7	48±5	12	36	0.08	0.33
6-8	80	1.6±0.2	110±9	5	105	0.02	0.33
8-10	74	BDL	96±7	-	96	BDL	
10-12	75	BDL	65±6	-	65	BDL	
12-14	75	BDL	46±5	-	46	BDL	
14-16	74	BDL	48±4	-	48	BDL	
16-18	69	BDL	29±4	-	29	BDL	
18-20	76	BDL	13±3	-	13	BDL	
20-22	73	BDL	8±2	-	8	BDL	
22-24	74	BDL	8±2	-	8	BDL	
24-26	74	BDL	BDL	-	BDL	BDL	

TABLE 3.2: Radiocaesium concentrations and activity ratios in samples from core ABC871, Ardmore Bay, July 1987 (Figure 1.6)

BDL = Below Detection Limit
Units = Bq kg^{-1}

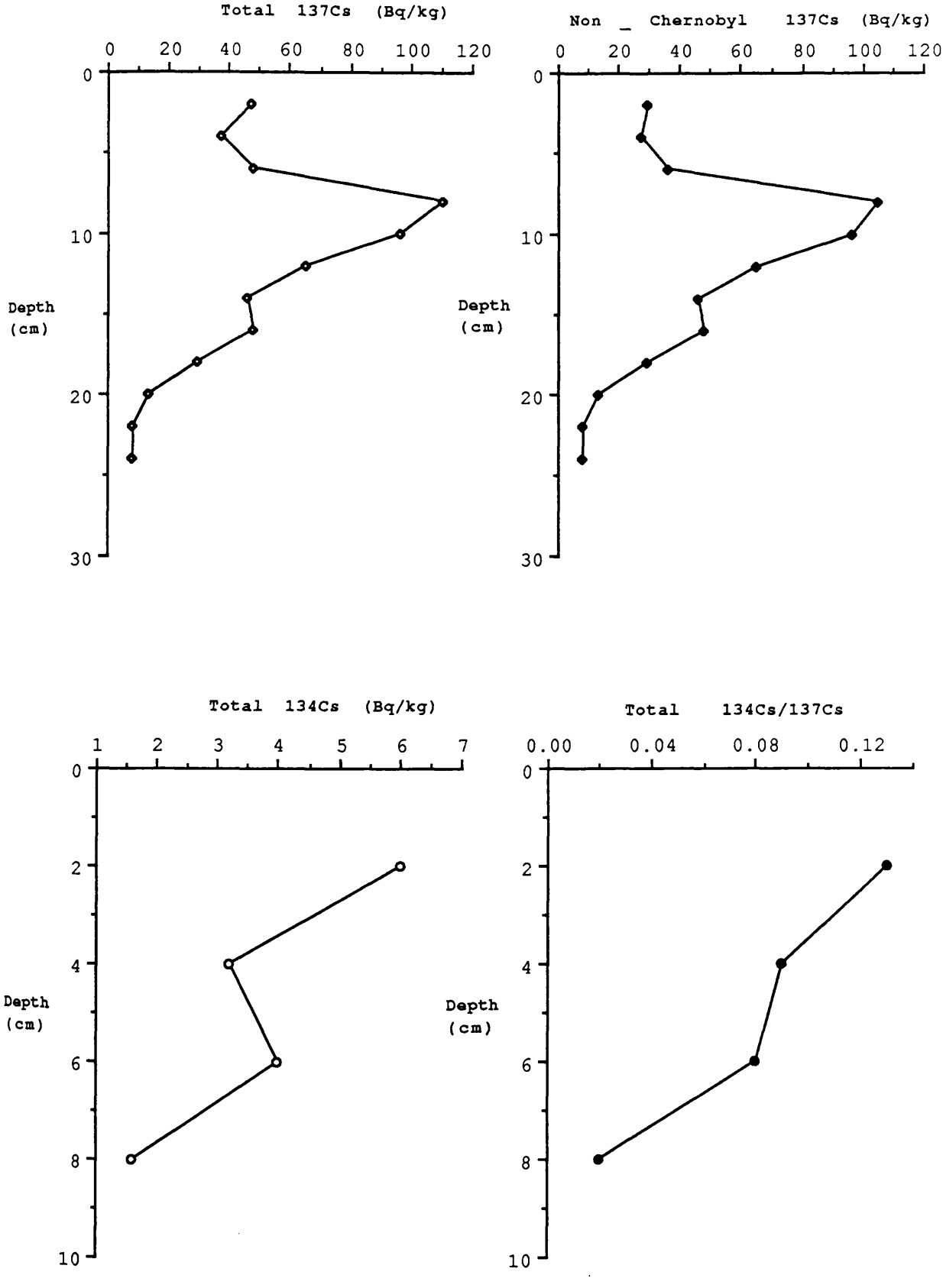

Figure 3.2 Plots of total ^{137}Cs and residual (non-Chernobyl) ^{137}Cs concentrations and ^{134}Cs results for intertidal sediment core ABC871 from Ardmore Bay

Sample Location	^{134}Cs	^{137}Cs	^{241}Am	^{238}Pu	$^{239,240}Pu$	$\frac{^{134}Cs}{^{137}Cs}$	$\frac{^{137}Cs}{^{241}Am}$	$\frac{^{137}Cs}{^{239,240}Pu}$	$\frac{^{241}Am}{^{239,240}Pu}$	$\frac{^{238}Pu}{^{239,240}Pu}$
Rockcliffe (sand)	BDL	266±7	BDL	7.9±0.7	31±2	BDL	BDL	8.6	BDL	0.25
Preston (sand)	BDL	150±5	BDL	4.2±0.3	21±1	BDL	BDL	7.1	BDL	0.20
Wigtown Martyr's Stake (silt)	7.3±0.6	371±10	154±14	28.7±1.2	119±8	0.02	2.4	3.1	1.3	0.24
Carty Port (silt)	18.0±2.1	606±15	219±19	24.4±1.0	98±5	0.03	2.8	6.2	2.2	0.24
Inner Well Fishery (silt)	40.1±3.6	596±15	323±27	85.5±3.8	372±14	0.07	1.8	1.6	0.9	0.16
Netherclifton (1) (silt)	2.4±1.3	615±21	137±16	16±1.6	86±6	0.004	4.5	7.2	1.6	0.19
Netherclifton (2) (silt)	7.4±2.6	233±13	58±12	NA	NA	0.03	4.0	NA	NA	NA
Skyreburn Bay (sand)	6.4±1.6	328±11	33±7	4.0±0.4	17±1	0.02	9.9	19.3	1.9	0.24
Skyreburn Bay (sand)	BDL	352±13	125±15	NA	NA	BDL	2.9	NA	NA	NA
Skyreburn Bay (sand)	3.2±0.9	229±9	51±10	NA	NA	0.01	4.5	NA	NA	NA

TABLE 3.3: Radionuclide concentrations and activity ratios in intertidal samples from different locations in south west Scotland, August 1987 (Figure 2.1)

NA = Not Analysed
BDL = Below Detection Limit
Units = Bq kg^{-1}

SAMPLE	Na %	K %	Sc	Cr	Fe %	Co	As	Br	Rb	Sb	Ba
Region A											
1. Isle of Whithorn	1.3±0.05	1.4±0.1	6.5±0.2	89±3	1.9±0.06	7.4±0.3	BDL	42±3.0	70±5	1.0±0.2	367±28
2. Kipford	1.2±0.05	1.3±0.1	5.8±0.2	76±3	1.7±0.05	8.0±0.3	7.9±0.9	22±1.6	74±4	0.7±0.1	386±26
3. Skyreburn Bay	1.1±0.04	1.3±0.1	6.6±0.2	102±4	1.9±0.07	7.7±0.3	7.7±0.9	14±1.2	74±5	0.8±0.1	352±27
4. St Mary's Isle	1.1±0.05	1.3±0.1	8.5±0.3	293±11	2.6±0.09	8.3±0.3	9.2±0.9	19±1.5	78±5	1.1±0.2	398±28
5. Wigtown	1.1±0.05	1.4±0.1	8.5±0.3	118±4	2.5±0.08	10.1±0.4	10.5±1.1	27±2.0	82±6	1.1±0.2	365±29
Region B											
6. Drummore	0.7±0.03	0.8±0.07	2.6±0.09	21±0.8	0.8±0.02	3.0±0.1	2.7±0.8	11±0.7	25±2	0.5±0.1	132±11
7. Port Logan	0.8±0.03	0.6±0.07	3.4±0.1	69±2	0.9±0.03	3.6±0.1	2.6±0.8	6±0.5	31±2	0.4±0.08	158±13
8. Port William	1.4±0.05	1.2±0.1	7.9±0.3	205±8	2.0±0.07	8.3±0.3	4.7±0.8	20±1.5	63±4	0.9±0.1	414±30
Region C											
9. Ardnacross	1.2±0.04	0.6±0.1	1.5±0.05	7±0.3	0.5±0.01	1.9±0.09	3.1±1.0	6±0.6	13±1	0.2±0.05	80±7
10. Girvan	1.3±0.04	0.6±0.07	7.2±0.2	371±14	1.9±0.06	9.3±0.3	3.5±1.0	9±0.7	25±2	0.6±0.1	157±15
11. Kildonon	0.7±0.03	1.2±0.2	5.0±0.2	17±0.7	0.8±0.02	2.4±0.1	2.9±0.9	18±1.1	35±3	0.2±0.05	297±23
12. Mull of Kintyre	1.0±0.04	0.6±0.07	1.5±0.05	6±0.4	0.6±0.02	1.4±0.08	3.4±1.0	13±0.9	17±1	0.2±0.05	88±9
13. Ardmore Bay	6.7±0.02	1.0±0.06	2.2±0.06	42±2	1.0±0.03	3.7±0.2	NA	NA	38±4	0.3±0.02	NA

TABLE 3.4: Neutron activation analysis results for surface intertidal sediments from various locations in south west Scotland (Figure 1.13)

Units ppm unless otherwise indicated

N A = not analysed

SAMPLE	Cs	La	Ce	Eu	Sm	Tb	Yb	Lu	Hf	Ta	Th	U
Region A												
1. Isle of Whithorn	2.2±0.2	21±1.0	44±2	1.0±0.08	3.8±0.1	0.5±0.05	2.3±0.1	0.4±0.02	9.6±0.4	0.7±0.07	7.1±0.3	2.1±0.2
2. Kipford	2.4±0.1	18±0.8	39±1	0.8±0.05	3.4±0.1	0.7±0.07	2.0±0.09	0.3±0.01	7.6±0.3	0.8±0.06	6.6±0.2	2.1±0.2
3. Skyreburn Bay	2.4±0.1	24±1.0	54±2	1.0±0.06	4.4±0.2	0.8±0.08	2.6±0.1	0.3±0.01	12.1±0.5	0.9±0.07	8.9±0.3	3.1±0.3
4. St Mary's Isle	2.4±0.1	57±2	128±5	1.7±0.1	9.3±0.3	1.3±0.1	5.8±0.2	1.0±0.04	45.8±1.8	1.5±0.1	22.0±0.8	6.0±0.4
5. Wigtown	3.4±0.2	27±1.0	56±2	1.2±0.09	4.9±0.2	0.6±0.06	2.8±0.1	0.5±0.02	12.4±0.5	0.8±0.09	9.0±0.3	2.6±0.2
Region B												
6. Drummore	0.6±0.05	7.4±0.4	13±0.5	0.3±0.02	1.4±0.05	0.1±0.02	0.9±0.1	0.1±0.004	1.6±0.07	0.2±0.02	2.3±0.11	1.1±0.1
7. Port Logan	0.9±0.06	9.4±0.4	15±0.5	0.4±0.02	1.7±0.06	0.2±0.04	1.1±0.2	0.4±0.02	6.5±0.3	0.9±0.08	13.9±0.5	3.4±0.3
8. Port William	1.6±0.1	21±0.9	49±2	1.0±0.07	3.7±0.1	0.8±0.08	2.8±0.1	0.4±0.02	21.1±0.9	0.8±0.07	8.5±0.3	2.5±0.3
Region C												
9. Ardnacross	0.3±0.04	5.1±0.2	7±0.2	0.3±0.02	0.9±0.03	0.05±0.01	0.9±0.1	0.1±0.004	2.0±0.08	0.3±0.03	1.4±0.05	1.4±0.2
10. Girvan	0.5±0.07	9.9±0.5	17±0.6	0.5±0.03	1.9±0.07	0.3±0.05	1.0±0.1	0.1±0.005	2.8±0.1	0.3±0.03	2.5±0.09	1.5±0.5
11. Kildonon	0.7±0.06	8.0±0.4	12±0.5	0.5±0.03	1.5±0.02	0.1±0.002	0.8±0.1	0.2±0.008	2.9±0.1	0.2±0.02	1.9±0.07	1.2±0.2
12. Mull of Kintyre	0.3±0.04	10.0±0.5	15±0.5	0.4±0.02	1.7±0.06	0.3±0.05	1.0±0.1	0.3±0.01	4.5±0.2	0.8±0.07	8.7±0.3	1.5±0.5
13. Ardmore Bay	1.1±0.1	14.0±0.8	37±1.0	0.9±0.04	3.0±0.09	0.5±0.1	NA	0.4±0.02	7.4±0.4	0.4±0.07	NA	NA

TABLE 3.4 continued:

Depth cm	LOI %	^{134}Cs	^{137}Cs	^{238}Pu	$^{239,240}Pu$	^{241}Am	^{210}Pb	$\frac{^{134}Cs}{^{137}Cs}$	$\frac{^{238}Pu}{^{239,240}Pu}$	$\frac{^{137}Cs}{^{239,240}Pu}$	$\frac{^{137}Cs}{^{241}Am}$	$\frac{^{241}Am}{^{239,240}Pu}$
0-3	0.8	6.4±1.6	328±11	4.2±0.4	17±1	33±7	943±91	0.02±0.005	0.25±0.03	19.3±1.5	9.9±2.1	1.9±0.4
3-6	1.2	9.1±1.8	290±10	4.0±0.3	16±1	32±8	793±75	0.03±0.006	0.25±0.03	18.1±1.7	9.1±2.3	2.0±0.5
6-9	2.2	11.1±2.4	1029±29	22.2±2.1	98±7	272±32	754±57	0.01±±0.002	0.23±0.03	10.5±0.8	3.8±0.5	2.8±0.4
9-12	25.3	15.9±3.4	1480±40	39.0±3.7	179±12	425±48	514±36	0.01±0.002	0.22±0.03	8.3±0.5	3.5±0.4	2.4±0.3
12-15	7.9	38.5±7.0	4045±109	155.5±10.3	695±21	1408±150	485±32	0.01±0.002	0.22±0.02	5.8±0.2	2.9±0.3	2.0±0.2
15-18	1.5	4.5±1.7	406±13	6.8±0.7	35±3	61±11	226±16	0.01±0.004	0.19±0.03	11.6±1.1	6.7±1.2	1.7±0.3
18-21	2.6	3.2±1.2	300±10	6.0±0.5	31±2	45±8	146±10	0.01±0.004	0.19±0.03	9.7±0.7	6.7±1.2	1.5±0.3
21-24	3.6	BDL	324±10	4.2±0.3	42±3	83±12	128±10	BDL	0.10±0.02	7.7±0.6	3.9±0.6	2.0±0.3
24-27	4.8	BDL	251±9	2.9±0.2	55±4	105±17	98±8	BDL	0.05±0.005	4.6±0.4	2.4±0.4	1.9±0.3
27-30	3.2	BDL	133±7	2.2±0.2	27±2	36±8	125±8	BDL	0.08±0.008	4.9±0.4	3.7±0.8	1.3±0.3
30-33	2.2	BDL	83±5	1.7±0.2	30±2	27±9	144±9	BDL	0.06±0.008	2.8±0.3	3.1±0.7	0.9±0.2

TABLE 3.5: Radionuclide concentrations and activity ratios for samples from Skyreburn Bay intertidal sediment, core SBC831, November 1983 (Figure 1.7)

BDL = Below Detection Limit
Units = Bq kg^{-1}

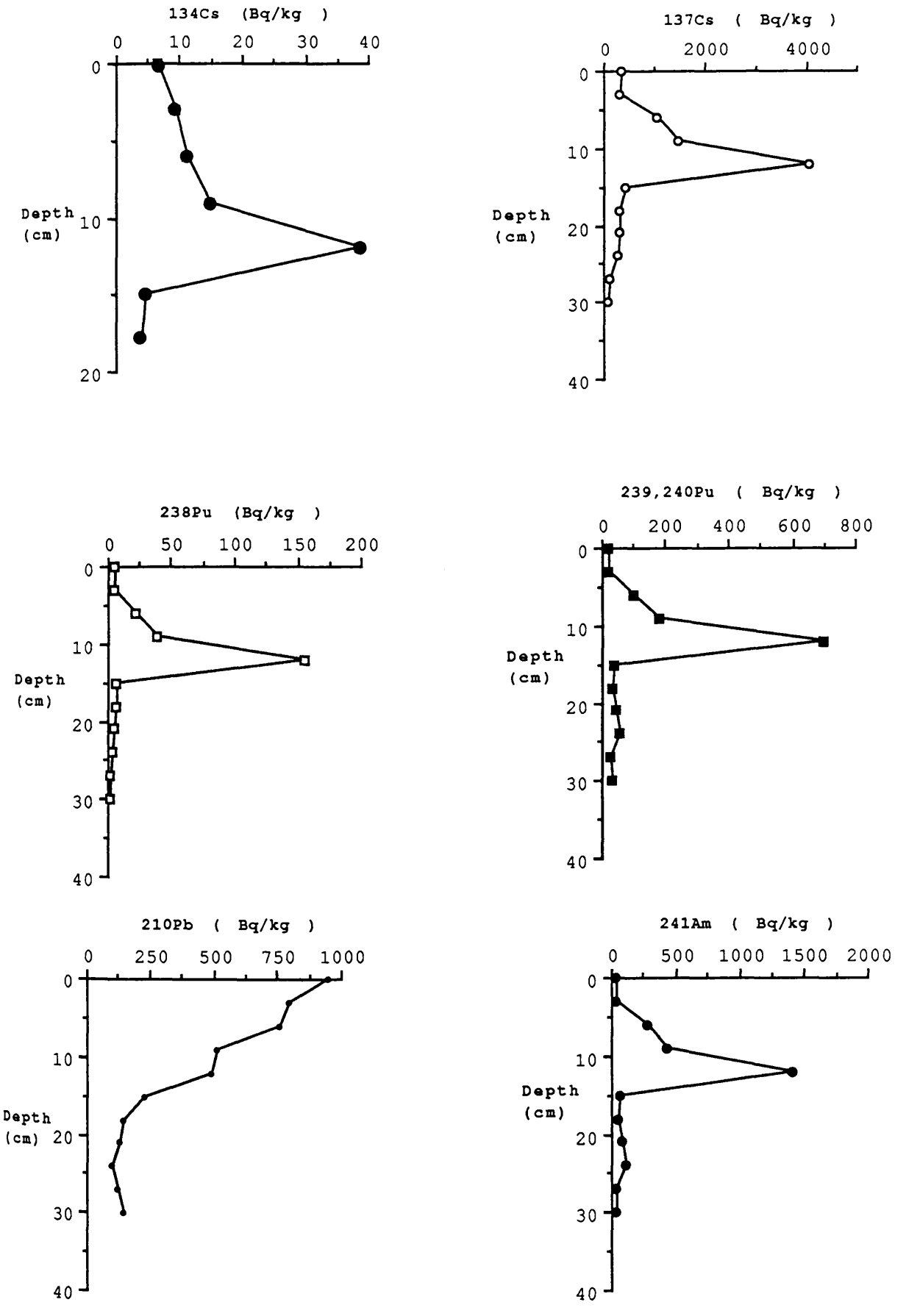

Figure 3.3 Radionuclide concentration profiles for core SBC831, Skyreburn Bay

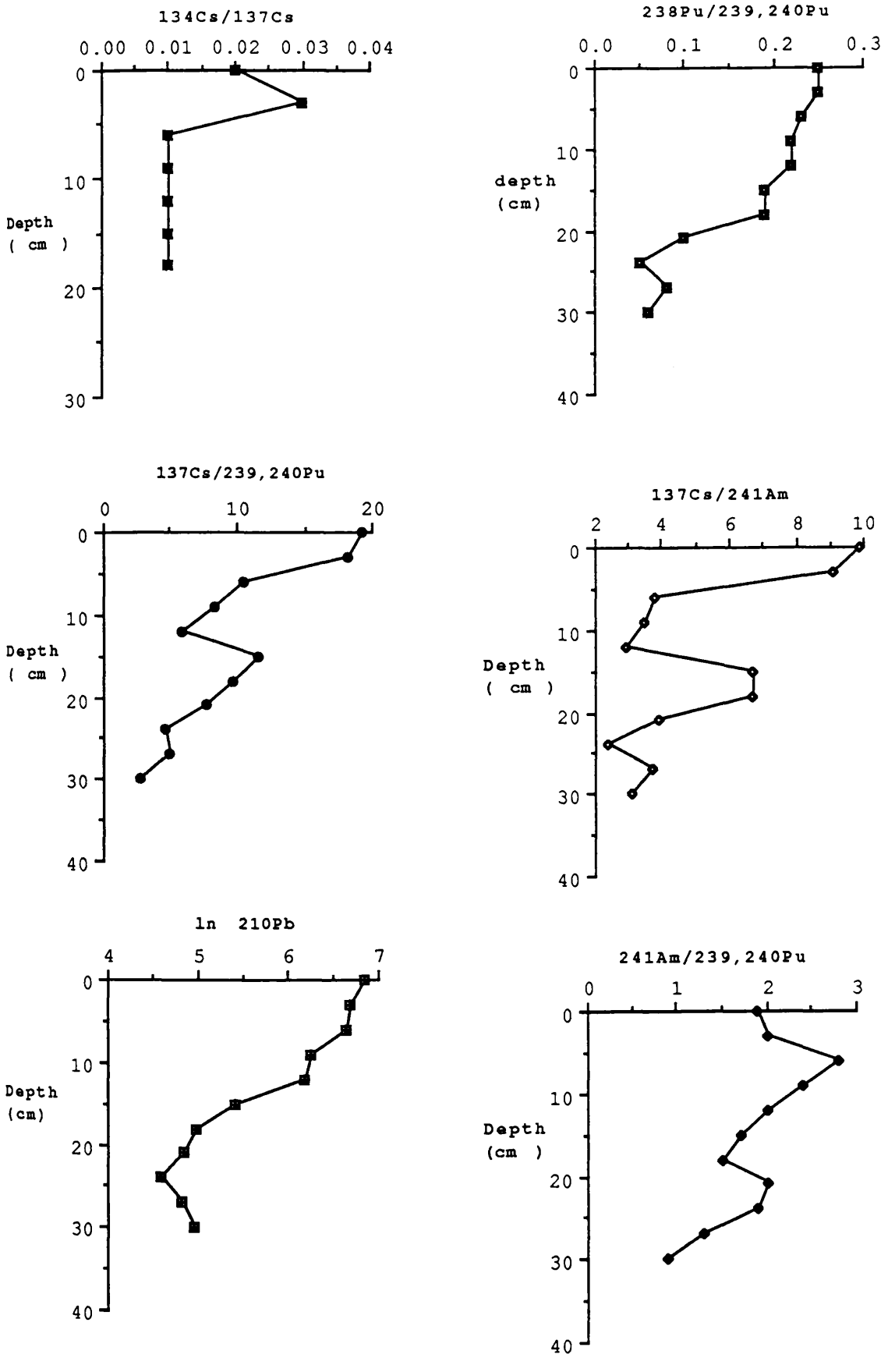

Figure 3.4 ln ^{210}Pb and radionuclide activity ratio profiles for core SBC831, Skyreburn Bay

Depth cm	Dry/Wet %	^{134}Cs	^{137}Cs	^{241}Am	$\frac{^{134}Cs}{^{137}Cs}$	$\frac{^{137}Cs}{^{241}Am}$
0-3	79	3.2±0.9	229±9	51±6	0.014±0.004	4.5±0.6
3-6	81	2.5±1.6	194±10	32±4	0.013±0.008	6.1±0.8
6-9	84	BDL	172±8	18±2	BDL	9.6±0.8
9-12	74	BDL	171±8	19±2	BDL	9.0±1.0
12-15	74	BDL	171±8	BDL	BDL	BDL
15-18	70	BDL	128±5	BDL	BDL	BDL
18-21	70	BDL	127±5	BDL	BDL	BDL
21-24	80	BDL	69±4	BDL	BDL	BDL
24-27	80	BDL	44±3	BDL	BDL	BDL
27-30	80	BDL	38±3	BDL	BDL	BDL
30-33	80	BDL	24±2	BDL	BDL	BDL
33-36	77	BDL	20±2	BDL	BDL	BDL
36-39	79	BDL	10±1	BDL	BDL	BDL
39-42	77	BDL	14±1	BDL	BDL	BDL

TABLE 3.6 : Radionuclide concentrations and ratios in samples from Skyreburn Bay, intertidal sediment core SBC851, July 1985 (Figure 1.7)

BDL = Below Detection Limit
Units = Bq kg^{-1}

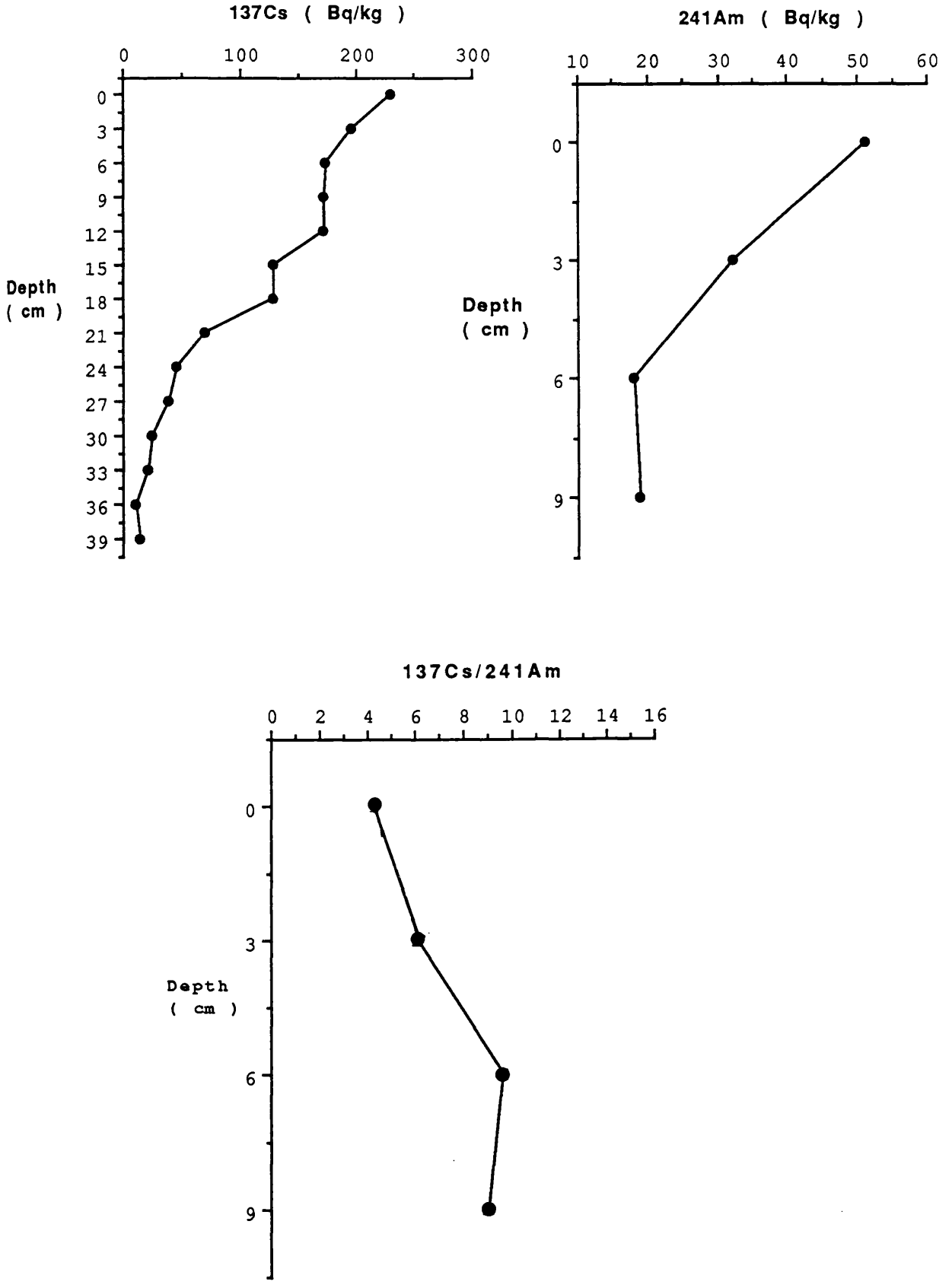

Figure 3.5 Radionuclide concentration and $^{137}Cs/^{241}Am$ activity ratio profiles for core SBC851, Skyreburn Bay

Depth cm	Wet/Dry %	^{134}Cs	^{137}Cs	^{241}Am	$\frac{^{134}Cs}{^{137}Cs}$	$\frac{^{137}Cs}{^{241}Am}$
0-3	71	BDL	362±13	125±22	BDL	2.9±0.5
3-6	72	BDL	251±12	62±14	BDL	4.1±0.9
6-9	76	BDL	275±12	89±18	BDL	3.1±0.6
9-12	82	BDL	272±11	93±17	BDL	2.9±0.5
12-15	80	BDL	427±17	88±18	BDL	4.9±1.0
15-18	77	BDL	269±11	113±25	BDL	2.3±0.5
18-21	73	BDL	627±23	611±100	BDL	0.9±0.1
21-24	78	BDL	525±25	356±60	BDL	1.5±0.3
24-27	82	BDL	419±17	208±37	BDL	2.0±0.4
27-30	81	BDL	192±9	90±21	BDL	2.1±0.5
30-33	81	BDL	150±8	59±15	BDL	2.5±0.6
33-36	71	BDL	135±8	BDL	BDL	BDL
36-40	75	BDL	51±5	BDL	BDL	BDL
40-43	74	BDL	21±2	BDL	BDL	BDL
43-46	76	BDL	31±3	BDL	BDL	BDL

TABLE 3.7: Radionuclide concentrations and ratios in samples from Skyreburn Bay intertidal sediment core SBC852, November 1985 (Figure 1.7)

BDL = Below Detection Limit
Units = Bq kg^{-1}

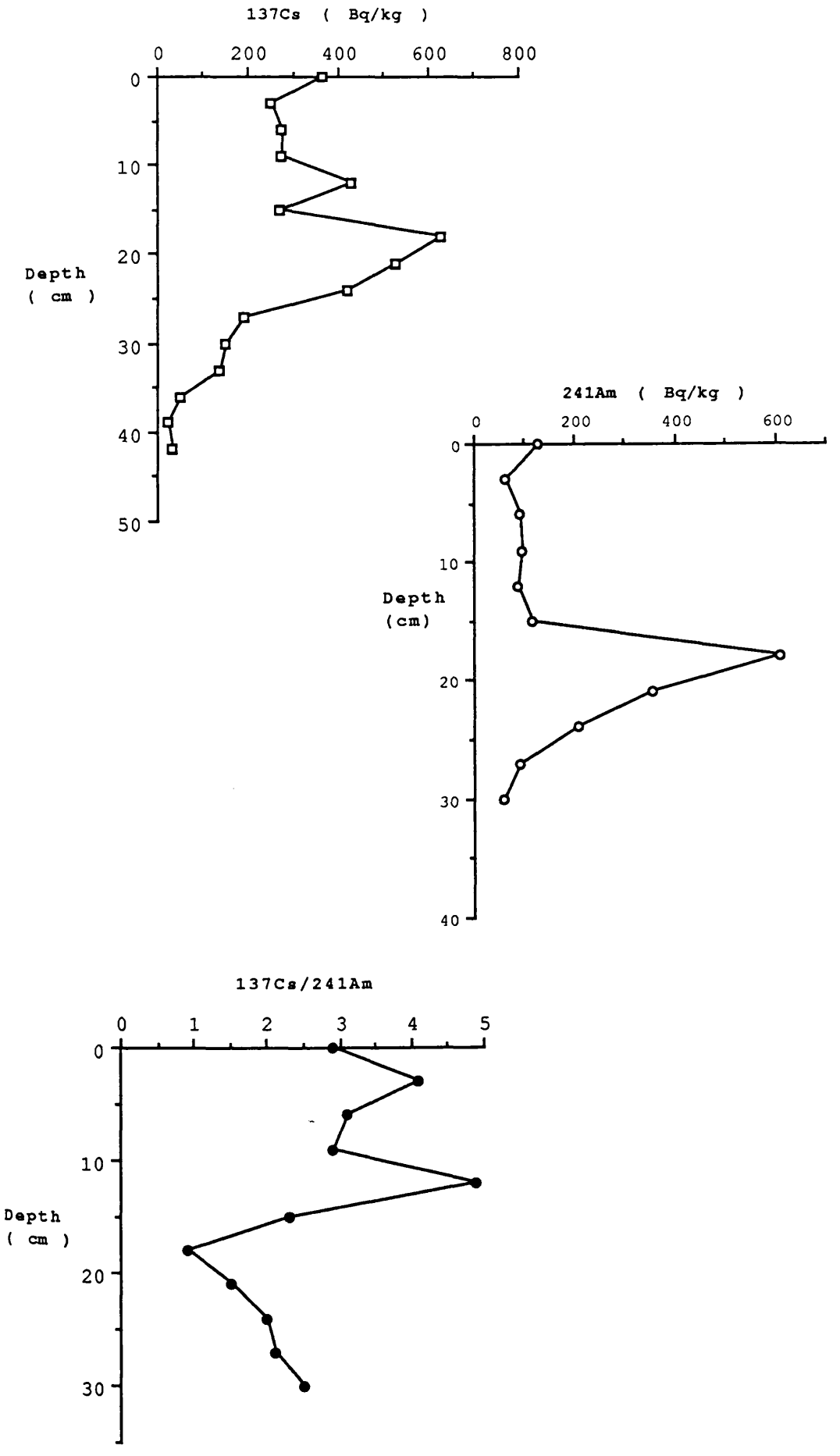

Figure 3.6 Radionuclide concentration and $^{137}Cs/^{241}Am$ activity ratio profiles for core SBC852, Skyreburn Bay

Distance m*	Dry/Wet %	LOI%	^{134}Cs	^{137}Cs	^{238}Pu	$^{239,240}Pu$	^{241}Am	$\frac{^{134}Cs}{^{137}Cs}$	$\frac{^{238}Pu}{^{239,240}Pu}$	$\frac{^{137}Cs}{^{239,240}Pu}$	$\frac{^{137}Cs}{^{241}Am}$	$\frac{^{241}Am}{^{239,240}Pu}$
0	71	4.6	9.7±2.1	804±25	41±4	206±16	206±28	0.012±0.003	0.20±0.02	3.9±0.3	3.1±0.3	1.3±0.2
5	69	4.3	9.6±2.6	746±24	35±3	155±10	222±24	0.013±0.004	0.23±0.02	4.8±0.3	3.4±0.4	1.4±0.2
10	57	9.6	16.7±2.4	1945±57	55±3	254±14	419±42	0.009±0.001	0.22±0.02	7.7±0.5	4.6±0.5	1.7±0.2
15	52	11.9	16.1±2.5	2371±69	53±3	297±15	486±49	0.007±0.001	0.18±0.01	8.0±0.5	4.9±0.5	1.6±0.2
20	46	17.2	22.1±2.9	3347±95	75±6	378±29	700±68	0.007±0.001	0.20±0.02	8.9±0.7	4.8±0.7	1.9±0.2
25	44	17.0	15.4±2.5	1952±5	59±5	304±22	548±55	0.008±0.001	0.20±0.02	6.4±0.5	3.6±0.5	1.8±0.2
30	39	21.6	12.9±2.4	2135±62	47±4	195±12	419±45	0.006±0.001	0.24±0.02	11.0±0.7	5.1±0.6	2.1±0.3
35	27	40.2	14.3±3.2	1961±61	34±3	167±12	304±35	0.007±0.002	0.20±0.02	11.7±0.9	6.5±0.8	1.8±0.2
40	15	60.4	13.3±3.6	1532±51	34±3	130±9	236±35	0.009±0.002	0.26±0.03	11.8±0.9	6.5±1.0	1.8±0.3
45	14	76.6	19.1±5.5	1549±54	NA	NA	159±30	0.013±0.004	NA	NA	10.2±2.0	NA
50	14	60.0	9.7±3.7	845±31	13±1	60±4	81±19	0.011±0.004	0.22±0.02	14.2±1.1	10.4±2.3	1.4±0.3
55	30	28.4	BDL	144±8	2±0.4	12±1	BDL	BDL	0.16±0.03	12.5±2.7	BDL	BDL

TABLE 3.8: Radionuclide concentrations and activity ratios for samples from a surface transect, Netherclifton, March 1985 (Figure 1.8)

NA = Not Analysed
BDL = Below Detection Limit
Units = Bq kg^{-1}
* = Distance inland from mean high water mark

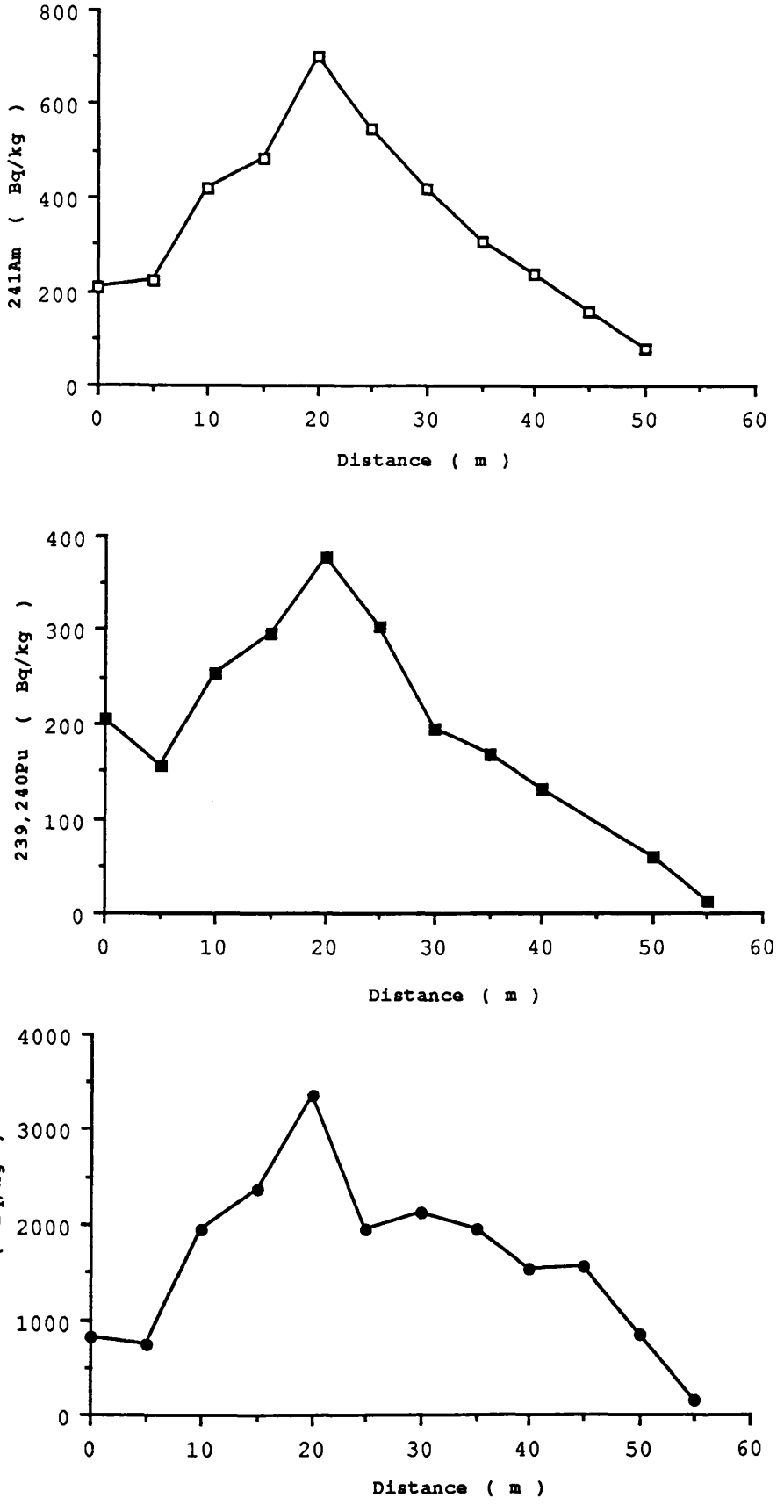

Figure 3.7 Plot of radionuclide concentration versus distance for Netherclifton surface transect samples

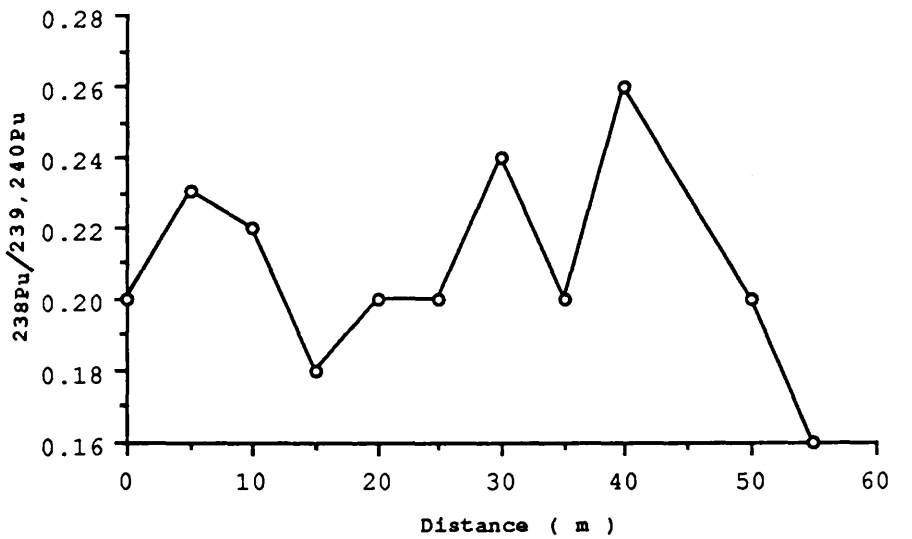

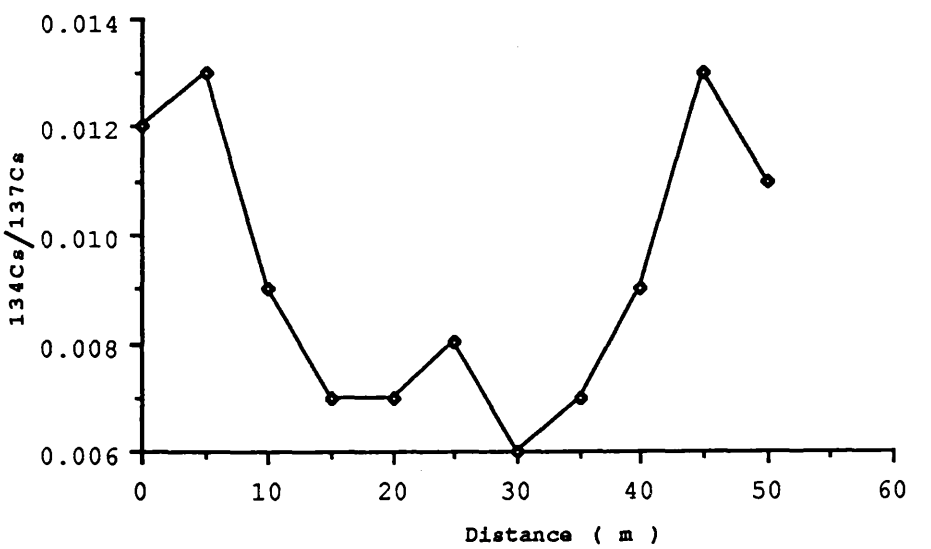

Figure 3.8 Plots of isotope activity ratios versus distance for Netherclifton surface transect samples

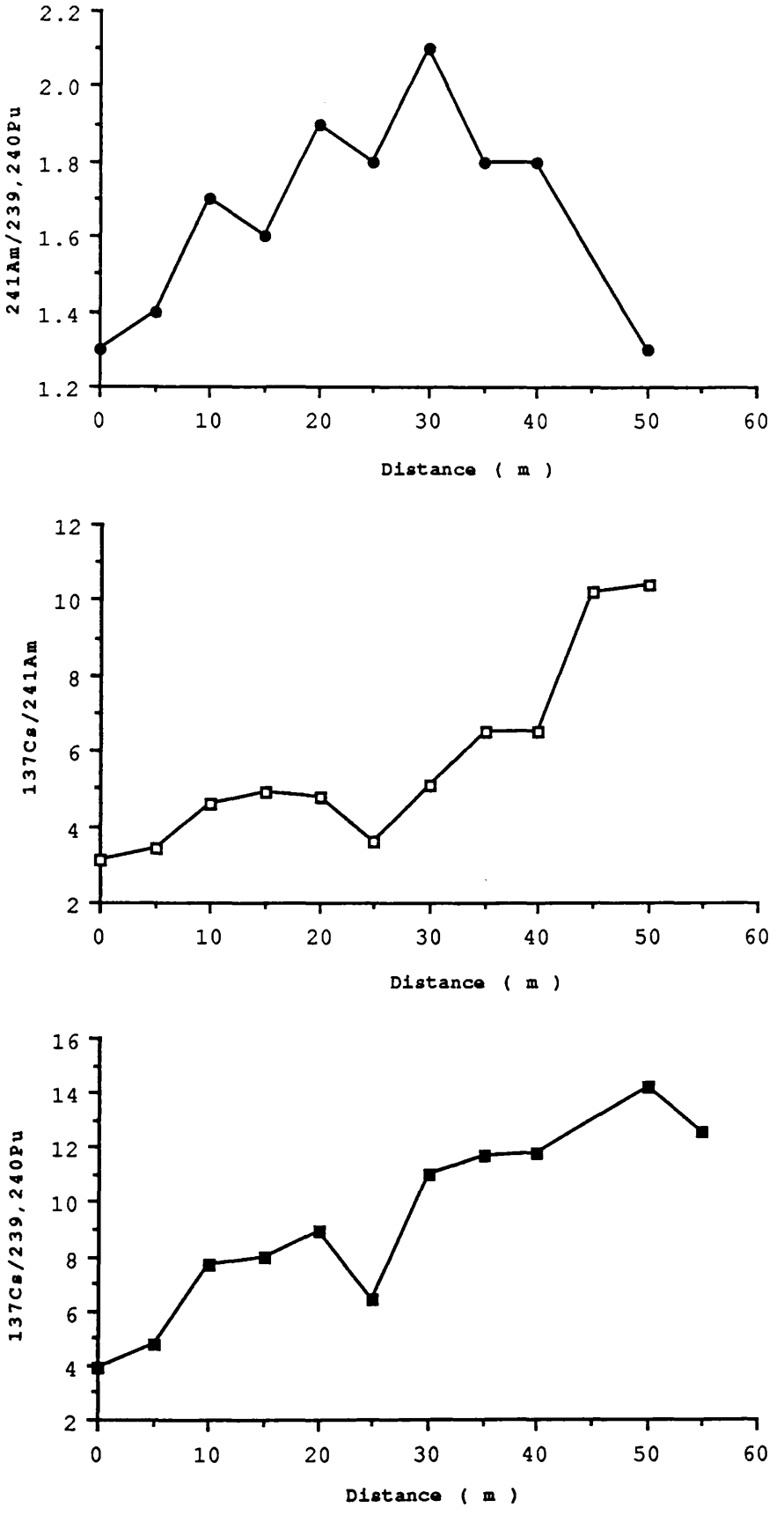

Figure 3.9 Plots of nuclide activity ratios versus distance for Netherclifton surface transect samples

Sample	^{134}Cs	^{137}Cs	^{238}Pu	$^{239,240}Pu$	^{241}Am
(a) 0-5cm					
NCST1	4.1×10^2	6.1×10^4	2.0×10^3	1.1×10^4	1.6×10^4
NCST2	2.8×10^2	2.7×10^4	1.1×10^3	6.3×10^3	6.7×10^3
(b) 15-30cm					
NCST1	BDL	5.9×10^3	31	2.7×10^2	7.7×10^2
NCST2	BDL	1.1×10^3	BDL	BDL	3.1×10^2
(c) 0-30cm					
NCST1	4.1×10^2	6.7×10^4	2.0×10^3	1.1×10^4	1.7×10^4
NCST2	2.8×10^2	2.8×10^4	1.1×10^3	6.3×10^3	7.1×10^3

TABLE 3.9: Radionuclide inventories in merse silt samples, Netherclifton, August 1987, (a) 0-15cm depth, (b) 15-30cm depth and (c) 0-30cm depth (Figure 1.8)

Units Bq m^{-2}

Depth cm	Dry/Wet %	LOI %	^{134}Cs	^{137}Cs	^{238}Pu	$^{239,\ 240}Pu$	^{241}Am	$\frac{^{134}Cs}{^{137}Cs}$	$\frac{^{238}Pu}{^{239,240}Pu}$	$\frac{^{137}Cs}{^{239,\ 240}Pu}$	$\frac{^{137}Cs}{^{241}Am}$	$\frac{^{241}Am}{^{239,\ 240}Pu}$
0-2	76	2.0	2.4±1.3	615±21	16.0±1.6	86±6	137±16	0.004±0.02	0.19±0.02	7.1±0.6	4.5±0.5	1.6±0.2
2-4	76	2.2	2.9±1.3	307±11	8.2±0.9	76±5	93±12	0.009±0.004	0.11±0.01	4.0±0.3	3.3±0.4	1.2±0.2
4-6	76	1.6	BDL	175±7	6.2±0.8	74±5	92±12	BDL	0.08±0.01	2.3±0.2	1.9±0.3	1.2±0.2
6-8	75	1.5	BDL	117±6	5.0±0.7	70±5	90±12	BDL	0.07±0.009	1.7±0.1	1.3±0.2	1.3±0.2
8-10	75	1.3	BDL	114±5	10.2±1.2	84±6	130±15	BDL	0.12±0.02	1.4±0.1	0.9±0.1	1.5±0.2
10-15	77	1.7	BDL	88±5	3.0±0.5	58±5	72±10	BDL	0.05±0.009	1.4±0.1	1.2±0.2	1.2±0.2
15-20	77	1.0	BDL	74±4	4.0±0.5	49±3	51±8	BDL	0.08±0.01	1.4±0.1	1.4±0.2	1.1±0.2
20-25	76	1.4	BDL	71±4	1.6±0.3	32±3	36±7	BDL	0.05±0.009	2.0±0.2	2.0±0.4	1.1±0.2
25-30	76	1.5	BDL	17±2	BDL	5±0.8	BDL	BDL	BDL	3.3±0.7	BDL	BDL
30-35	77	1.9	BDL	12±2	BDL	4±0.3	BDL	BDL	BDL	3.2±0.6	BDL	BDL
35-40	78	1.6	BDL	8±2	BDL	3±0.3	BDL	BDL	BDL	2.9±0.9	BDL	BDL
40-45	75	1.4	BDL	9±2	BDL	3±0.3	BDL	BDL	BDL	2.9±0.8	BDL	BDL
45-50	77	1.7	BDL	9±2	BDL	7±1	BDL	BDL	BDL	BDL	BDL	BDL

TABLE 3.10: Radionuclide concentrations and activity ratios for samples from section NCS861, Netherclifton, March 1986 (Figure 1.8)

BDL = Below Detection Limit
Units = Bq kg^{-1}

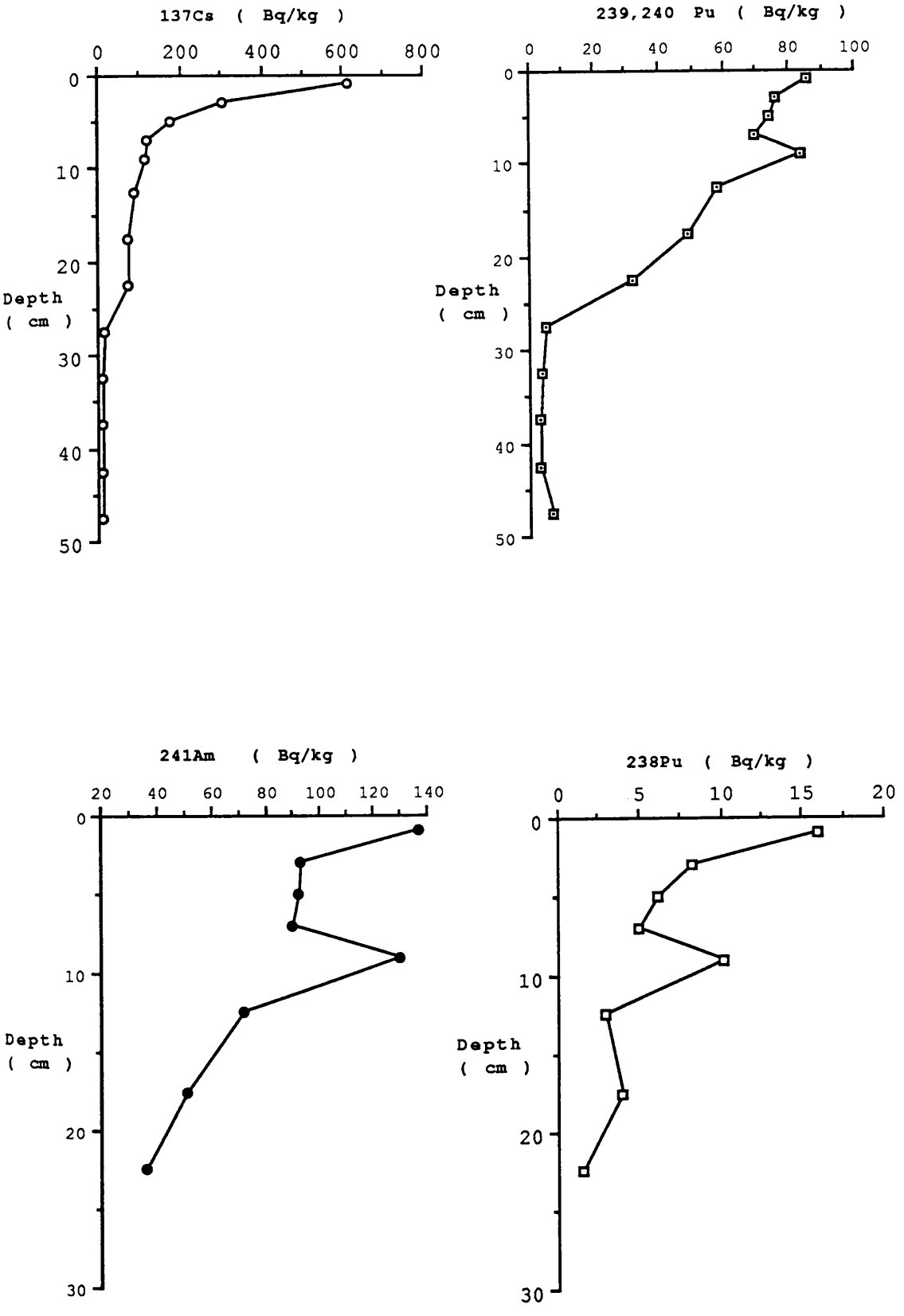

Figure 3.10 Radionuclide concentration profiles for samples from section NCS861, Netherclifton

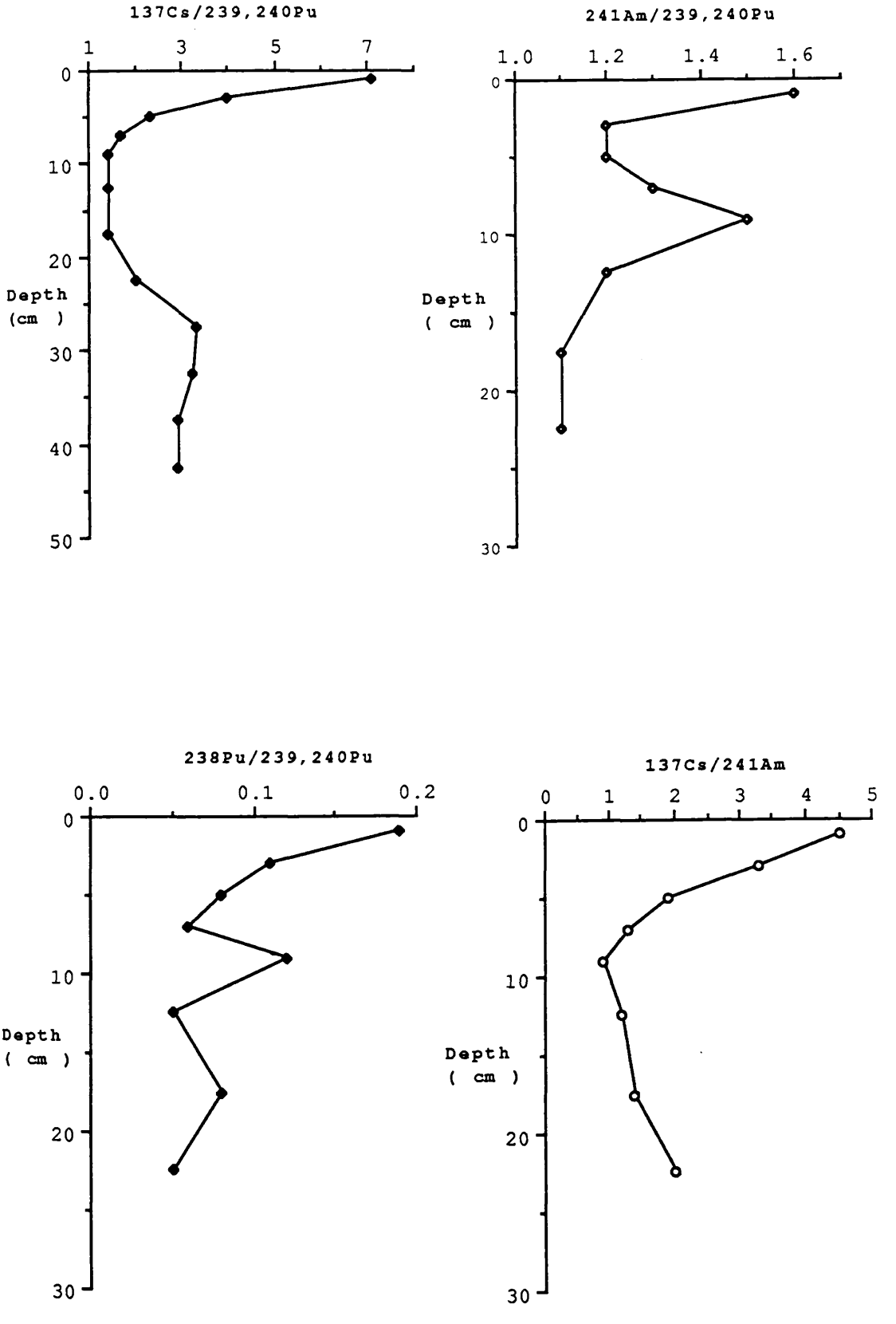

Figure 3.11 Radionuclide activity ratio profiles for samples from section NCS861, Netherclifton

Depth (cm)	Dry/Wet %	^{134}Cs	^{137}Cs	^{241}Am	$\frac{^{134}Cs}{^{137}Cs}$	$\frac{^{137}Cs}{^{241}Am}$
0-2	75	7.4±2.6	233±13	58±12	0.03±0.010	4.0±0.9
2-4	75	5.5±2.5	301±15	79±14	0.02±0.009	3.8±0.7
4-6	75	7.4±2.4	361±17	106±16	0.02±0.007	3.4±0.5
6-8	77	7.3±2.5	289±15	69±14	0.03±0.010	4.2±0.9
8-10	76	5.2±2.3	281±14	79±14	0.02±0.009	3.6±0.7
10-12	77	6.6±2.6	259±14	61±12	0.03±0.011	4.2±0.9
12-14	76	6.9±2.3	259±13	56±11	0.03±0.010	4.7±1.0
14-16	75	7.2±2.3	288±14	67±12	0.03±0.010	4.3±0.8
16-18	76	5.6±2.3	309±15	87±14	0.02±0.008	3.5±0.6
18-20	75	3.9±2.3	335±16	101±16	0.01±0.010	3.3±0.5
20-22	73	5.2±2.3	288±14	85±14	0.02±0.009	3.4±0.6
22-24	75	3.4±2.3	280±14	71±13	0.01±0.007	4.0±0.8
24-26	76	7.4±2.2	245±13	66±12	0.03±0.009	3.7±0.7
26-28	77	4.6±2.0	290±14	71±12	0.02±0.009	4.1±0.7
28-30	75	6.3±2.3	297±15	89±14	0.02±0.007	3.4±0.6
30-32	75	5.6±2.4	311±15	88±14	0.02±0.009	3.6±0.6
32-34	74	11.9±3.1	296±15	89±15	0.04±0.010	3.3±0.6
34-36	75	6.2±2.4	293±14	81±14	0.02±0.008	3.6±0.6
36-38	76	1.4±0.7	281±14	82±13	0.01±0.005	3.4±0.6
38-40	73	3.1±1.2	327±14	81±14	0.01±0.004	4.1±0.7
40-42	74	10.5±2.8	544±24	122±18	0.02±0.005	4.5±0.7
42-44	71	13.4±3.0	1204±45	245±30	0.01±0.002	4.9±0.6

TABLE 3.11 : Radionuclide concentrations in samples from core NCC861, Netherclifton, March 1986 (Figure 1.8)

Units = Bq kg^{-1}

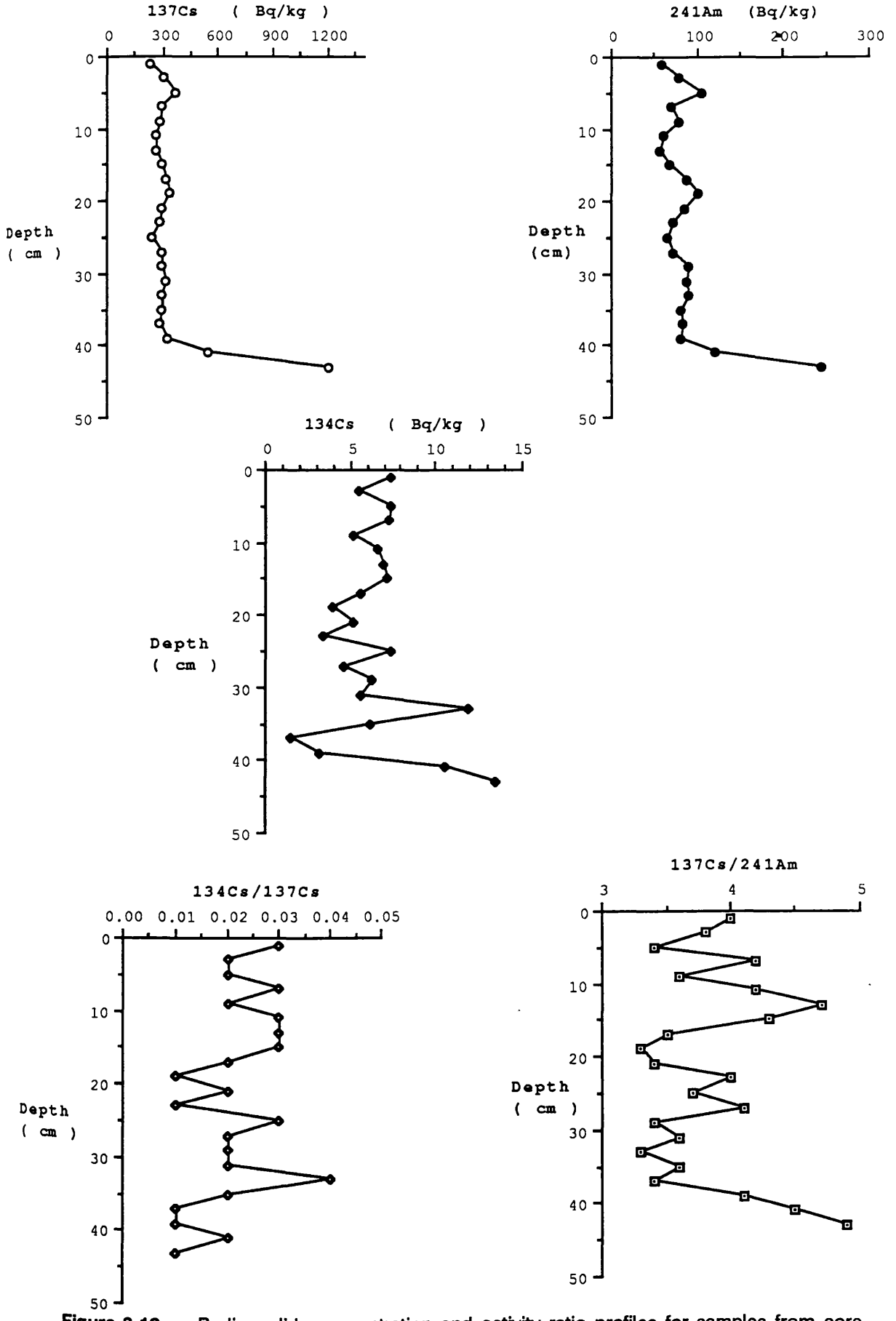

Figure 3.12 Radionuclide concentration and activity ratio profiles for samples from core NCC861, Netherclifton

Depth cm	Dry/Wet %	LOI %	^{134}Cs	^{137}Cs	^{238}Pu	$^{239,240}Pu$	^{241}Am	^{210}Pb	$\frac{^{134}Cs}{^{137}Cs}$	$\frac{^{238}Pu}{^{239,240}Pu}$	$\frac{^{137}Cs}{^{239,240}Pu}$	$\frac{^{137}Cs}{^{241}Am}$	$\frac{^{241}Am}{^{239,240}Pu}$
0-2	71	6	11.4±2.0	821±26	42±4	206±9	287±30	36±2	0.014±0.003	0.20±0.02	4.0±0.2	2.9±0.3	1.4±0.2
2-4	76	5	10.8±2.0	572±19	28±2	146±3	185±20	22±2	0.019±0.004	0.20±0.01	3.9±0.2	3.1±0.4	1.3±0.1
4-6	74	5	12.1±1.8	655±21	21±2	99±4	183±20	21±1	0.018±0.003	0.21±0.01	6.6±0.3	3.6±0.4	1.8±0.2
6-8	75	5	8.2±1.7	681±22	31±2	132±4	183±21	23±1	0.012±0.003	0.23±0.02	5.1±0.2	3.7±0.4	1.4±0.2
8-10	73	6	13.2±2.0	1084±33	57±7	232±12	279±29	31±1	0.012±0.002	0.23±0.03	4.7±0.3	3.9±0.4	1.2±0.1
10-15	73	6	10.0±1.8	1118±34	49±3	219±9	288±30	27±1	0.008±0.002	0.22±0.02	5.1±0.3	3.9±0.4	1.3±0.1
15-20	73	6	12.7±2.0	1667±49	50±5	234±13	334±34	34±1	0.007±0.001	0.21±0.02	7.1±0.4	5.0±0.5	1.4±0.2
20-25	73	7	12.6±1.9	1716±50	60±5	291±11	356±36	36±2	0.007±0.001	0.21±0.02	5.9±0.3	4.8±0.5	1.2±0.1
25-30	73	6	12.0±2.0	1871±55	83±7	400±18	464±46	33±1	0.006±0.001	0.21±0.02	4.7±0.3	4.0±0.4	1.2±0.1
30-35	74	6	12.4±2.3	1801±53	50±7	215±9	402±40	31±2	0.007±0.001	0.23±0.03	8.4±0.4	4.5±0.5	1.9±0.2
35-40	73	6	10.9±2.2	2152±63	71±5	335±10	464±46	30±1	0.005±0.001	0.21±0.02	6.4±0.3	4.6±0.5	1.4±0.1
40-45	75	5	9.3±1.8	1549±45	58±5	267±13	364±37	28±1	0.006±0.001	0.22±0.02	5.8±0.3	4.3±0.5	1.4±0.2
45-50	74	4	10.0±2.1	2023±59	84±7	390±12	543±53	28±2	0.005±0.001	0.21±0.02	5.2±0.2	3.7±0.4	1.4±0.1
50-55	74	6	16.6±2.6	2826±80	92±10	473±20	647±62	33±2	0.006±0.001	0.19±0.02	6.0±0.3	4.4±0.4	1.2±0.1
55-60	75	4	9.8±1.8	1747±51	50±5	274±11	496±48	23±1	0.007±0.001	0.18±0.02	6.4±0.3	3.5±0.4	1.4±0.1
60-65	74	4	7.6±1.7	1871±55	78±9	415±19	750±71	26±1	0.004±0.001	0.19±0.02	4.5±0.2	2.5±0.2	1.8±0.2
65-70	74	5	4.8±1.5	1491±44	89±8	493±23	859±80	25±2	0.003±0.001	0.18±0.02	3.0±0.2	1.7±0.2	1.8±0.2
70-75	75	5	BDL	734±24	73±5	396±11	732±69	22±2	BDL	0.18±0.01	1.8±0.1	1.0±0.1	1.7±0.2
75-80	77	4	BDL	489±17	69±5	395±12	601±57	25±1	BDL	0.17±0.01	1.2±0.1	0.8±0.1	1.8±0.2
80-85	76	4	BDL	441±15	40±3	290±11	361±36	29±2	BDL	0.14±0.01	1.5±0.1	1.2±0.1	1.5±0.2
85-90	76	4	BDL	453±16	34±4	261±10	320±33	24±1	BDL	0.13±0.02	1.7±0.1	1.4±0.2	1.2±0.1
90-95	77	3	BDL	393±13	23±4	218±9	242±26	22±1	BDL	0.10±0.02	1.8±0.1	1.6±0.2	1.1±0.1
95-100	76	4	BDL	247±9	14±3	157±7	128±16	19±1	BDL	0.09±0.02	1.5±0.1	1.9±0.2	0.8±0.1

TABLE 3.12: Radionuclide concentrations and activity ratios for samples from section NCS862, Netherclifton, March 1986 (Figure 1.8)

BDL = Below Detection Limit
Units = Bq kg^{-1}

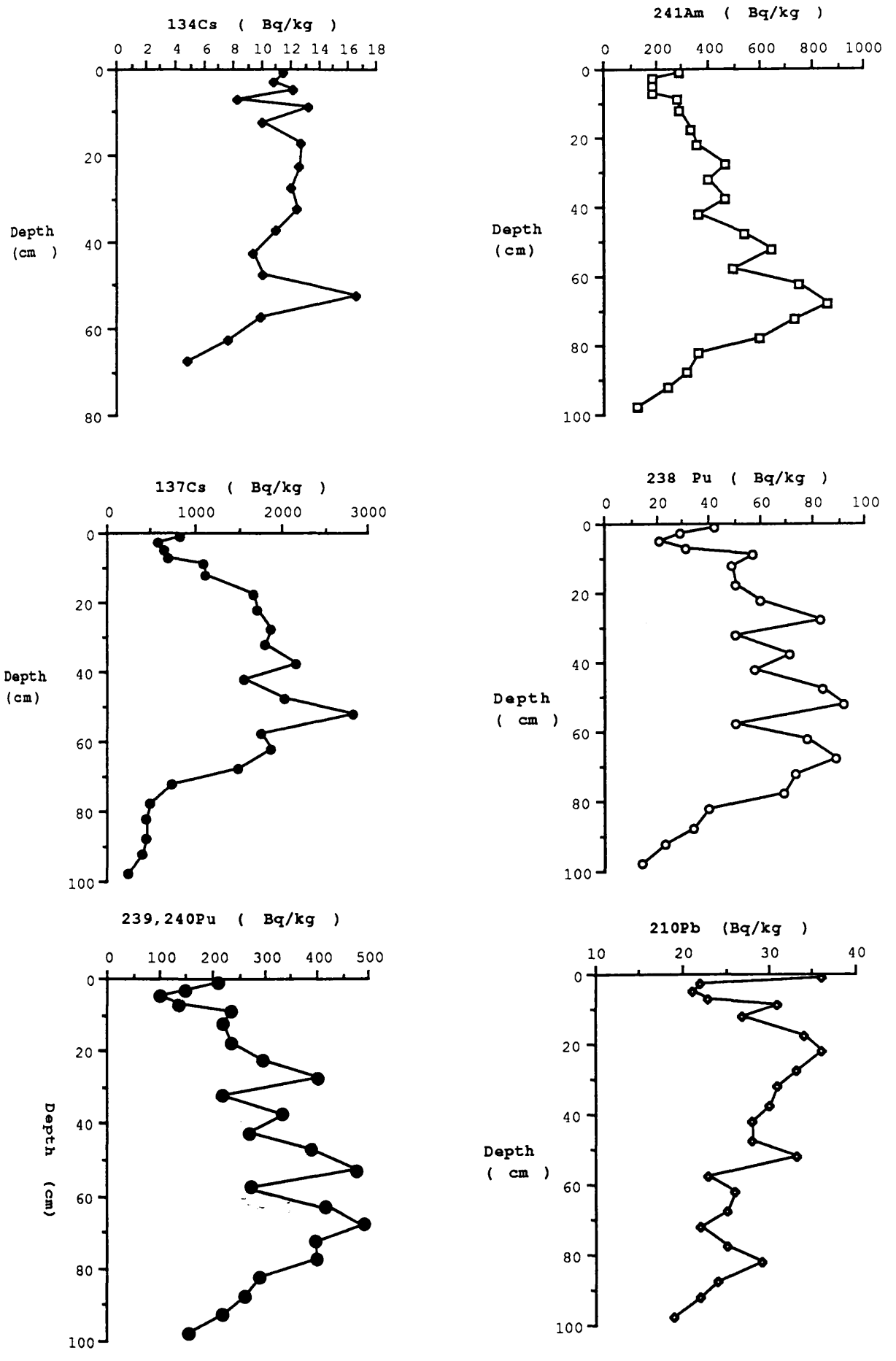

Figure 3.13 Radionuclide concentration profiles for section NCS862, Netherclifton

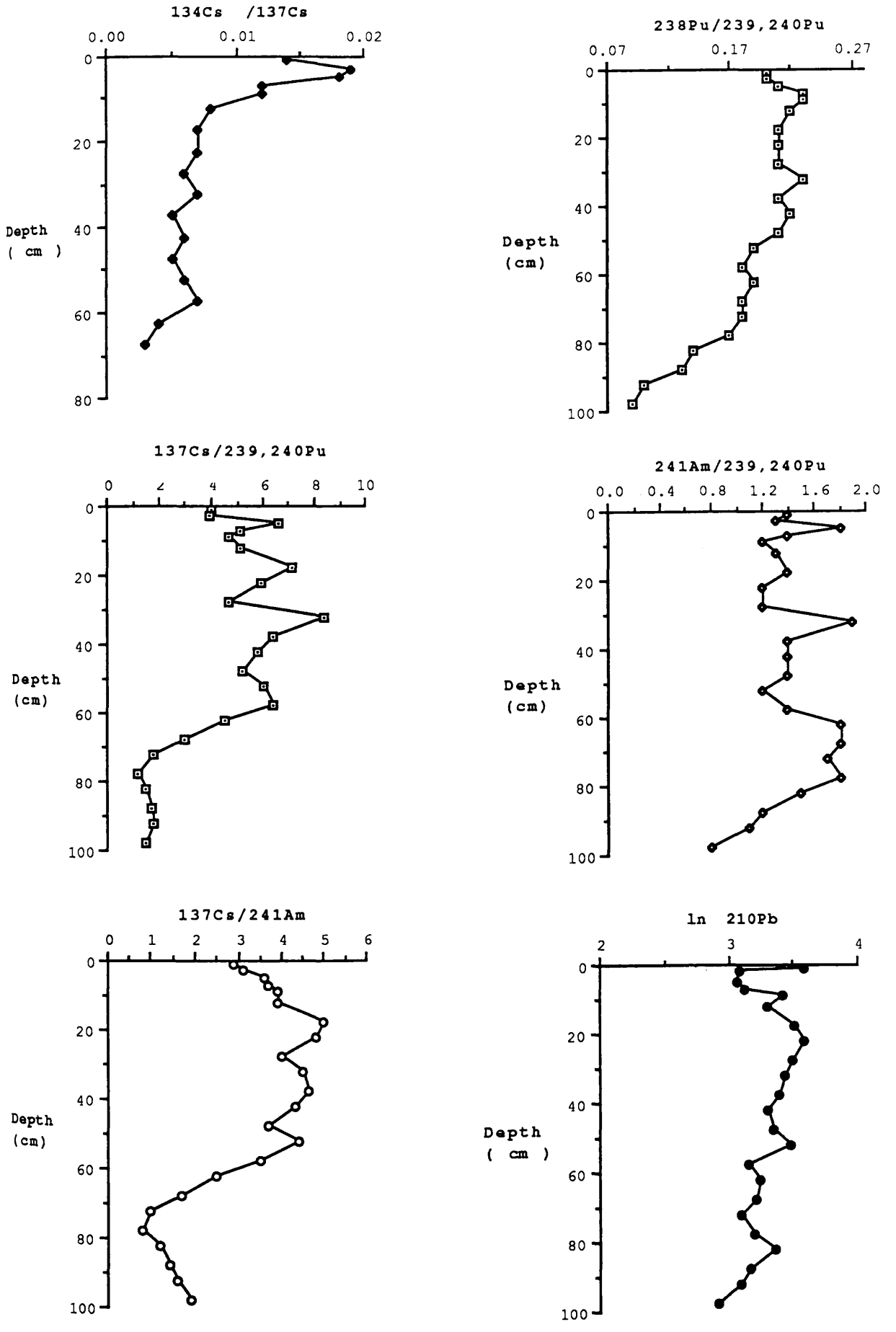

Figure 3.14 Radionuclide activity ratio profiles for section NCS862, Netherclifton

Depth cm	Dry/Wet %	^{134}Cs	^{137}Cs	^{241}Am	$\frac{^{134}Cs}{^{137}Cs}$	$\frac{^{137}Cs}{^{241}Am}$
0-2	58	12.2±2.4	1641±49	309±32	0.007±0.001	5.3±0.6
2-4	59	9.4±2.0	1715±51	638±62	0.006±0.001	2.7±0.3
4-6	64	8.2±3.3	342±13	58±9	0.02±0.008	5.9±0.9
6-8	72	BDL	93±5	BDL	BDL	BDL
8-10	81	BDL	20±3	BDL	BDL	BDL
10-15	74	BDL	BDL	BDL	BDL	BDL

TABLE 3.13 : Radionuclide concentrations in samples from section NCS863, Netherclifton, March 1986 (Figure 1.8)

BDL = Below Detection Limit
Units = Bq kg^{-1}

Depth (cm)	Wet/Dry %	LOI %	^{134}Cs	^{137}Cs	^{238}Pu	$^{239,240}Pu$	^{241}Am	$\frac{^{134}Cs}{^{137}Cs}$	$\frac{^{238}Pu}{^{239,240}Pu}$	$\frac{^{137}Cs}{^{239,240}Pu}$	$\frac{^{137}Cs}{^{241}Am}$	$\frac{^{241}Am}{^{239,240}Pu}$
0-5	42	21	6.3±0.3	956±31	20.2±2.0	134±5	190±23	0.007±0.002	0.15±0.016	7.1±0.4	5.0±0.6	1.4±0.2
5-10	58	12	3.3±0.5	40±4	2±0.6	13±1	2±0.6	0.08±0.01	0.15±0.05	3.1±0.4	20.0±0.6	0.2±0.06
10-15	63	11	BDL	9±3	BDL	BDL	BDL	BDL	BDL	3.0±0.4	BDL	BDL
15-20	64	9	BDL	BDL	BDL	BDL	BDL	BDL	BDL	BDL	BDL	BDL

TABLE 3.14 : Radionuclide concentrations and ratios in samples from section 4, Netherclifton, March 1986 (Figure 1.8)

BDL = Below Detection Limit
Units = Bq kg^{-1}

Distance Inland from Mean High Water Level (m)	^{238}U	$\frac{^{234}U}{^{238}U}$	^{232}Th	^{230}Th	$\frac{^{230}Th}{^{234}U}$
0	18.2±0.5	0.89±0.03	22.4±0.8	35.8±1.9	2.21±0.13
5	24.2±0.7	1.08±0.04	19.3±0.8	30.9±1.7	1.18±0.07
10	27.8±0.5	0.89±0.02	17.7±0.6	28.7±1.7	1.16±0.07
15	23.2±0.5	1.00±0.03	25.3±0.8	38.1±2.3	1.65±0.10
20	33.8±0.9	0.98±0.04	24.2±0.8	42.4±2.7	1.28±0.09
25	29.7±0.4	0.99±0.02	18.5±1.0	35.7±2.5	1.21±0.09
30	45.5±2.2	1.03±0.07	16.1±0.5	28.6±1.9	0.61±0.05
35	35.5±1.7	1.06±0.05	12.6±1.5	22.4±1.5	0.60±0.05
40	49.4±2.4	0.99±0.07	9.8±0.2	27.1±1.8	0.55±0.05
45	1078±46	1.00±0.06	8.0±0.2	21.6±0.7	0.020±0.001
50	219±4	1.01±0.03	12.0±0.2	49.3±1.6	0.22±0.01
55	218±4	1.01±0.02	20.2±1.2	126.0±5	0.57±0.02

TABLE 3.15: Natural decay series radionuclide concentrationsand activity ratios for a 55m transect running from the Southwick water towards Netherclifton (figure 1.8)

Units = Bq kg^{-1}

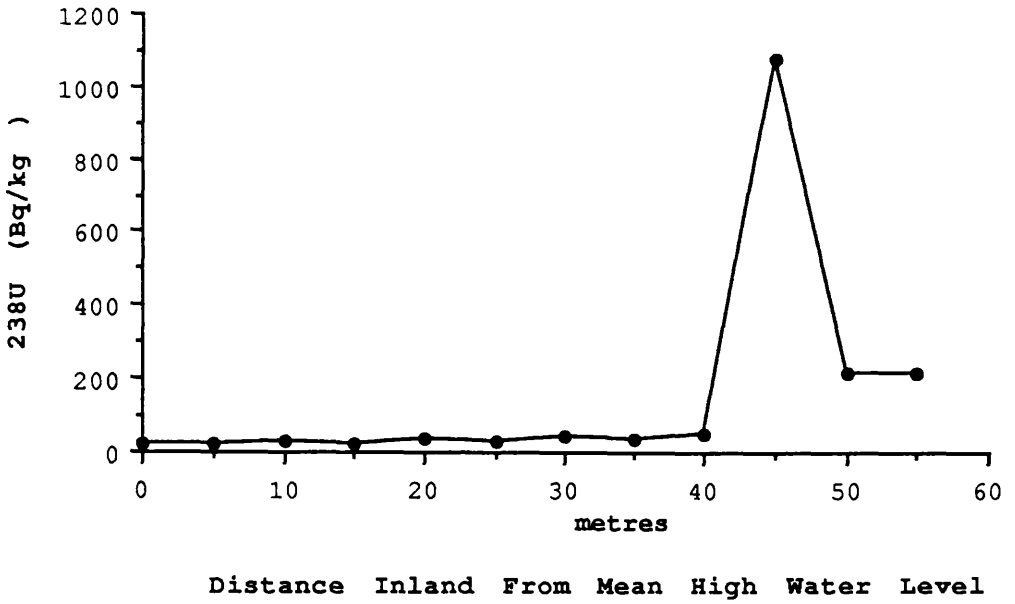

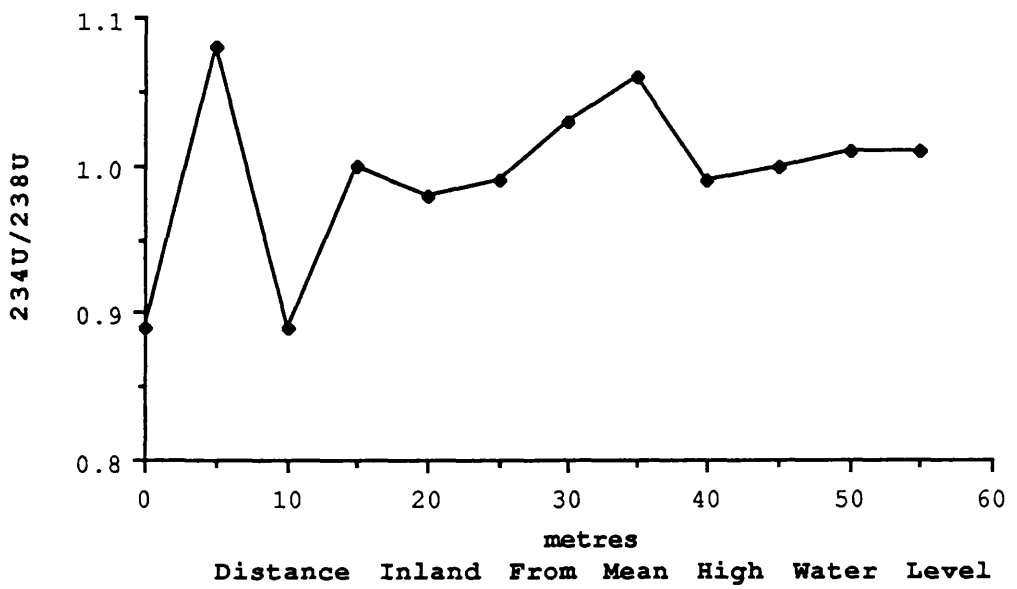

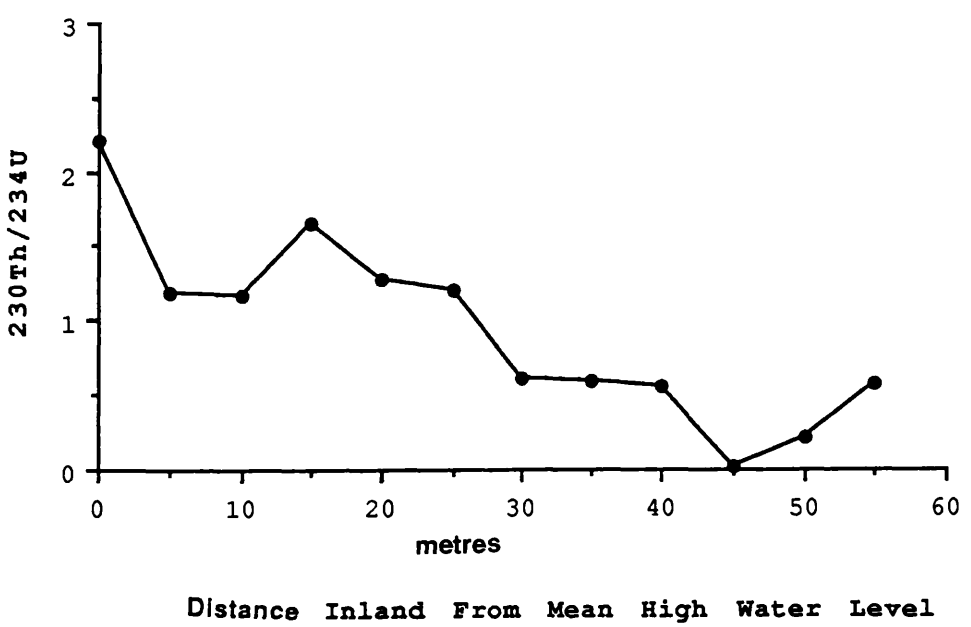

Figure 3.15 ^{238}U concentration, $^{234}U/^{238}U$ and $^{230}Th/^{234}U$ plots for Netherclifton surface transect samples

Sample	^{238}U	^{234}U	$\frac{^{234}U}{^{238}U}$	^{232}Th	^{230}Th	$\frac{^{230}Th}{^{234}U}$
Intertidal Section NCS861						
Surface	15.5±0.4	13.8±0.8	0.89±0.06	16.3±0.8	17.0±0.8	1.23±0.09
25cm	12.5±0.7	13.6±0.8	1.09±0.09	12.0±0.6	17.6±0.9	1.29±0.10
50cm	11.8±0.5	10.8±0.4	0.92±0.05	12.3±0.3	13.1±0.3	1.21±0.05
Merse Section NCS862 (7.5m)						
Surface	13.9±0.4	13.0±0.3	0.94±0.03	17.5±0.5	28.0±0.7	2.15±0.07
50cm	16.8±0.5	14.9±0.3	0.89±0.03	16.8±0.6	28.7±0.7	1.93±0.06
100cm	15.9±0.6	15.4±0.3	0.97±0.04	17.5±0.6	27.1±0.6	1.76±0.06
Merse Section NCS863 (15m)						
Surface	20.2±0.7	18.5±0.5	0.92±0.04	16.0±0.6	28.3±0.8	1.53±0.06
50cm	19.7±0.6	17.5±0.5	0.89±0.04	18.5±0.9	17.8±0.4	1.02±0.05
100cm	14.7±0.5	14.6±0.3	0.99±0.04	17.8±0.9	16.4±0.7	1.12±0.06
Merse Section NCS864 (30m)						
Surface	33.8±1.2	33.5±0.9	0.99±0.04	20.5±0.6	36.8±1.2	1.10±0.05
25cm	19.9±1.2	20.1±1.2	1.01±0.09	21.7±1.0	23.4±1.0	1.16±0.09
55cm	47.3±3.0	43.2±2.8	0.91±0.08	18.0±1.0	16.0±0.8	0.37±0.3
Irish Sea						
Surface Sediment	18.8±0.9	18.3±0.8	0.97±0.05	20.3±1.6	34.9±2.3	1.91±0.15

TABLE 3.16: Uranium and thorium concentrations and activity ratios for selected samples from Netherclifton Merse sections (Figure 1.8) plus a sample of surface slit from the north eastern basin of the Irish Sea.

Units = Bq kg^{-1}

Sample	% of Uranium Associated with Different Soil Components				
	Available	Exchangeable	Organics	Oxides	Residual
Intertidal Section NCS861					
Surface	0	4.5	4.0	7.6	83.8
100cm	0	5.4	6.6	8.7	79.2
Merse Section NCS862					
Surface	0	4.6	0	10.9	84.5
100cm	0	4.0	47.3	6.0	42.7
Merse Section NCS864					
Surface	0.5	0	7.0	81.6	10.7
55cm	0.25	3.2	2.0	20.2	71.3

TABLE 3.17 : Uranium association with different soil fractions for samples from Netherclifton Merse and intertidal sections (Figure 1.8)

Depth (cm)	Number of hot particles per field of view	Number of discrete (ie non hot particle) general alpha tracks per field of view
0-2	3	110
8-10	2	115
20-25	4	206
40-45	3	139
45-50	6	241
50-55	4	196
55-60	3	214
60-65	6	256
65-70	3	178
70-75	3	193
75-80	6	244
80-85	5	215
95-100	7	205

TABLE 3.18: Alpha particle track density produced in CR-39 plastic by samples from section NCS862, Netherclifton

Distance (m)*	^{134}Cs	^{137}Cs	^{238}Pu	$^{239,240}Pu$	^{241}Am	$\frac{^{134}Cs}{^{137}Cs}$	$\frac{^{238}Pu}{^{239,240}Pu}$	$\frac{^{137}Cs}{^{239,240}Pu}$	$\frac{^{137}Cs}{^{241}Am}$	$\frac{^{241}Am}{^{239,240}Pu}$
0	20±2	415±11	11±0.9	45±2	54±7	0.05±0.005	0.24±0.01	9.2±0.5	7.7±1.0	1.2±0.2
50	16±2	773±19	27±1.5	145±3	175±17	0.02±0.003	0.19±0.01	5.1±0.2	4.4±0.5	1.2±0.1
100	21±2	1000±24	29±2.0	171±6	240±21	0.02±0.002	0.17±0.02	5.8±0.6	4.2±0.4	1.4±0.2
150	30±3	1173±27	38±2.9	209±7	303±26	0.03±0.003	0.19±0.02	5.6±0.2	3.9±0.2	1.5±0.1
200	32±3	1278±30	39±2.5	217±6	300±28	0.03±0.003	0.18±0.01	5.9±0.2	4.2±0.4	1.4±0.1
250	82±5	1461±32	48±2.8	263±5	399±33	0.06±0.004	0.18±0.01	5.6±0.2	3.7±0.3	1.5±0.1
300	30±3	1346±29	43±4.1	239±12	418±34	0.02±0.002	0.18±0.02	5.6±0.3	3.2±0.3	1.7±0.2
500	34±3	1542±34	46±3.1	259±7	422±35	0.02±0.002	0.18±0.01	6.0±0.2	3.7±0.3	1.6±0.1

TABLE 3.19a: Radionuclide concentrations and activity ratios in 0-15cm depth samples from a surface transect, Wigtown Martyr's stake, August 1987 (Figure 1.9)

Distance (m)*	Dry/Wet %	^{134}Cs	^{137}Cs	^{238}Pu	$^{239,240}Pu$	^{241}Am	$\frac{^{134}Cs}{^{137}Cs}$	$\frac{^{238}Pu}{^{239,240}Pu}$	$\frac{^{137}Cs}{^{239,240}Pu}$	$\frac{^{137}Cs}{^{241}Am}$	$\frac{^{241}Am}{^{239,240}Pu}$
0	75	2.7±0.3	480±13	12±1	71±4	89±10	0.006±0.0006	0.17±0.01	6.8±0.3	5.4±0.6	1.3±0.2
50	70	BDL	83±4	BDL	BDL	11±1	BDL	BDL	BDL	7.5±0.9	BDL
100	70	BDL	70±3	BDL	BDL	BDL	BDL	BDL	BDL	BDL	BDL
150	68	BDL	26±2	BDL	BDL	BDL	BDL	BDL	BDL	BDL	BDL
200	70	BDL	25±2	BDL	BDL	BDL	BDL	BDL	BDL	BDL	BDL
250	64	BDL	17±2	0.4±0.1	2.4±0.2	BDL	BDL	0.17±0.04	7.1±0.4	BDL	BDL
300	65	BDL	30±3	BDL	BDL	11±1.2	BDL	BDL	BDL	3.5±0.4	BDL
500	69	BDL	30±3	BDL	BDL	7±1.0	BDL	BDL	BDL	4.3±0.7	BDL

TABLE 3.19b: Radionuclide concentrations and activity ratios in 15-30cm depth samples from a surface transect. Wigtown Martyr's stake, August 1987 (Figure 1.9)

BDL = Below Detection Limit
* = Distance inland from mean high water mark (m)
Units = Bq kg^{-1}

Distance m	Dry/Wet %	Particle size <75μm %	LOI %
0	74	54.5	4.5
50	67	27.5	7.1
100	63	18.4	8.9
150	61	29.4	10.2
200	64	11.2	9.7
250	59	39.3	11.6
300	65	11.6	13.1
500	61	7.7	11.5

TABLE 3.20: Dry/Wet ratio, % loss on ignition and fraction of silt of size <75μm (%) data for the Wigtown Martyr's stake 0-15cm depth samples

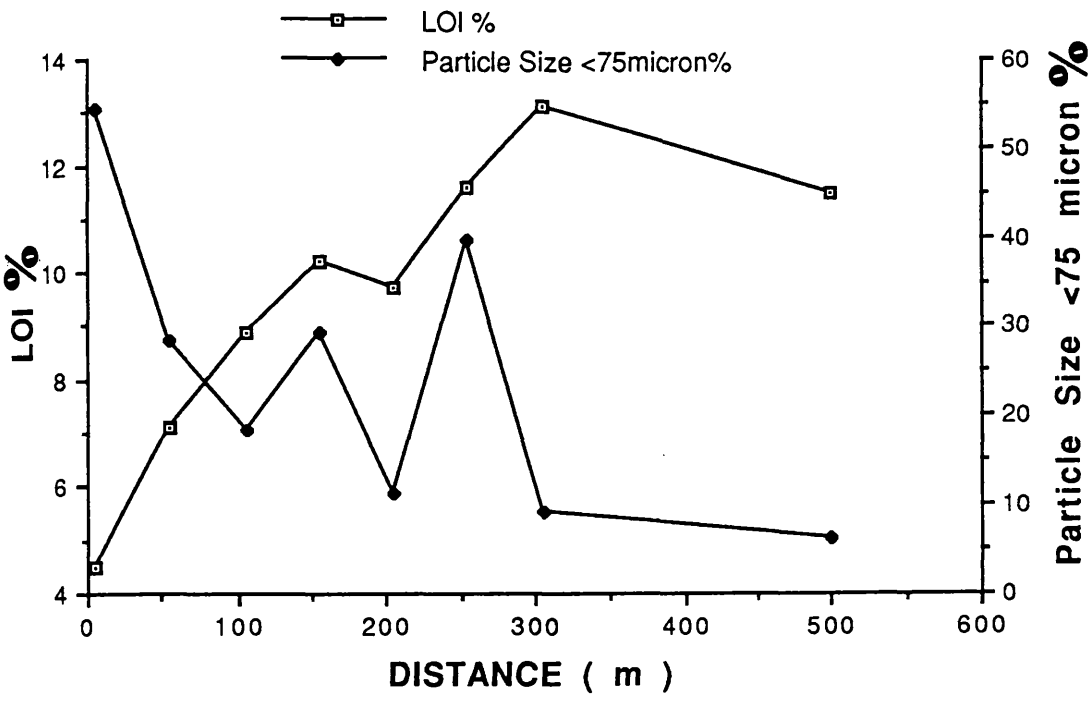

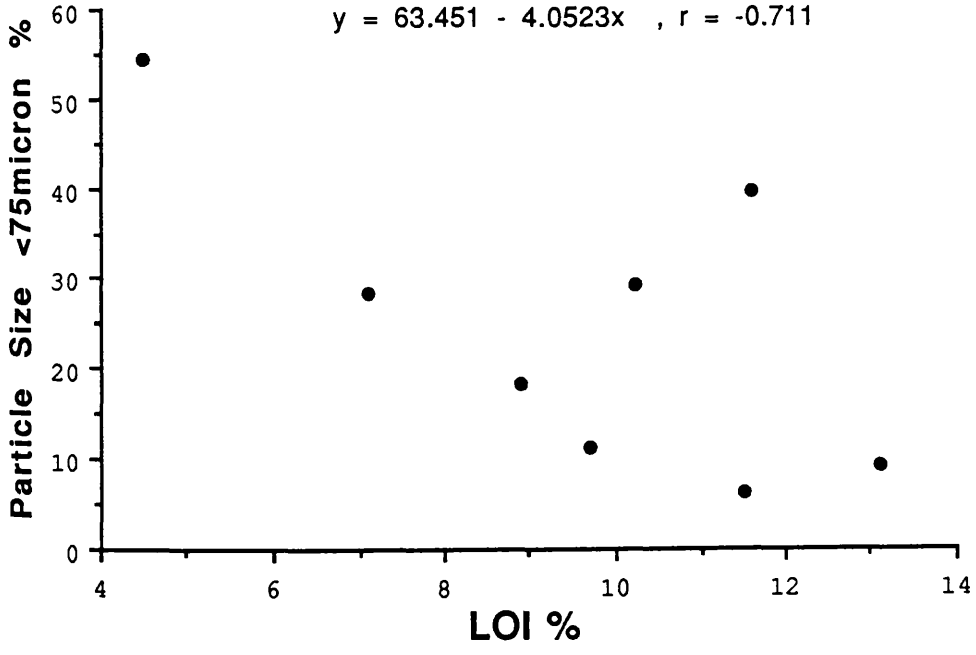

Figure 3.16 Plot of total organic content and percentage of sample of size <75μm for 0-15cm depth samples from the Wigtown Martyr's stake transect

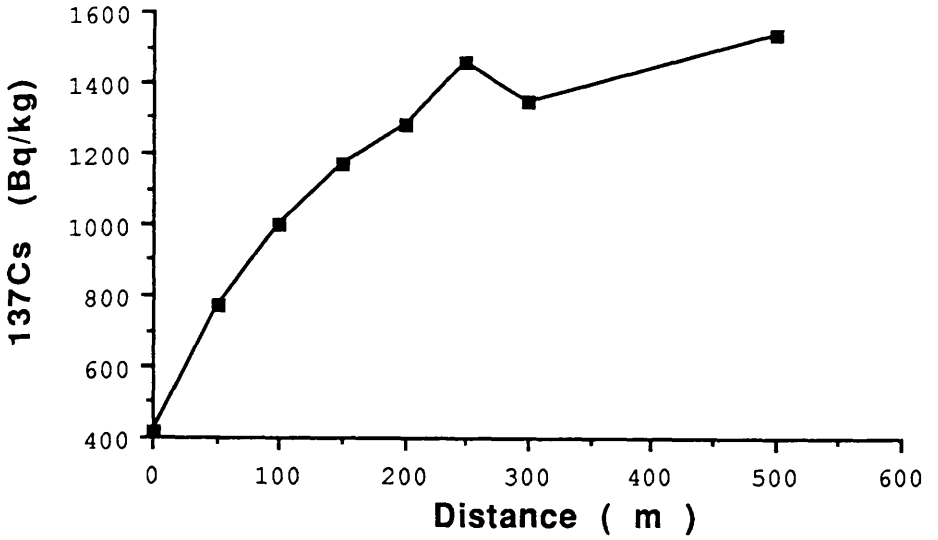

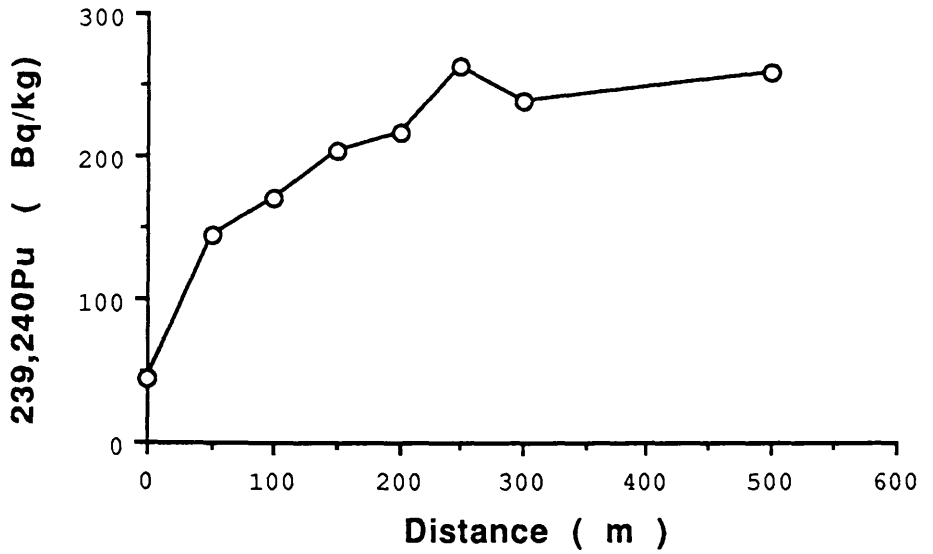

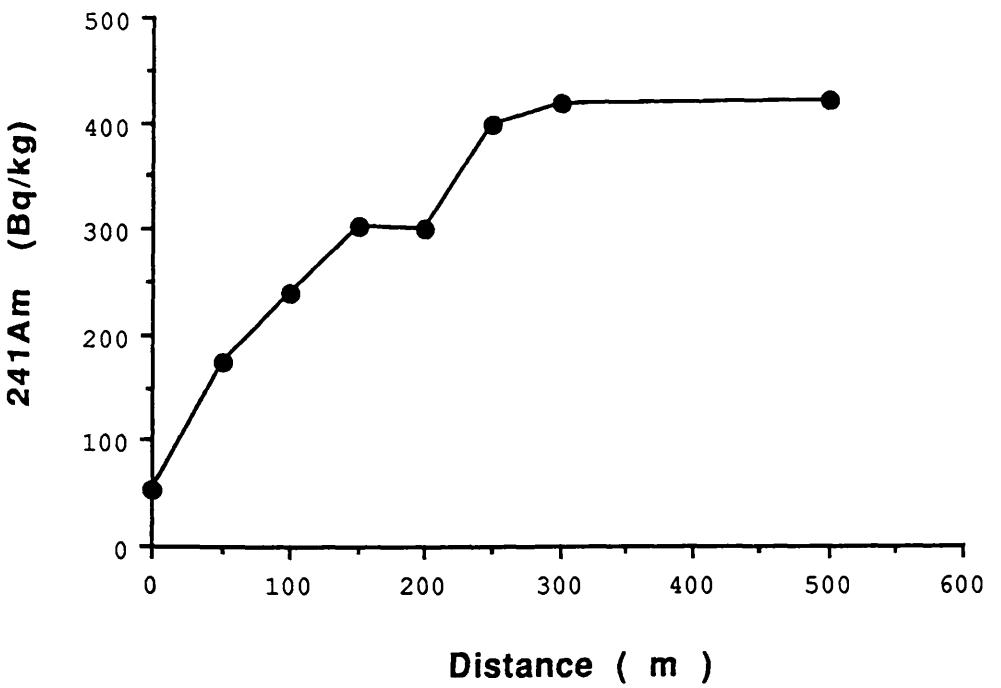

Figure 3.17 Plot of radionuclide concentrations for 0-15cm depth samples from the Wigtown Martyr's stake transect

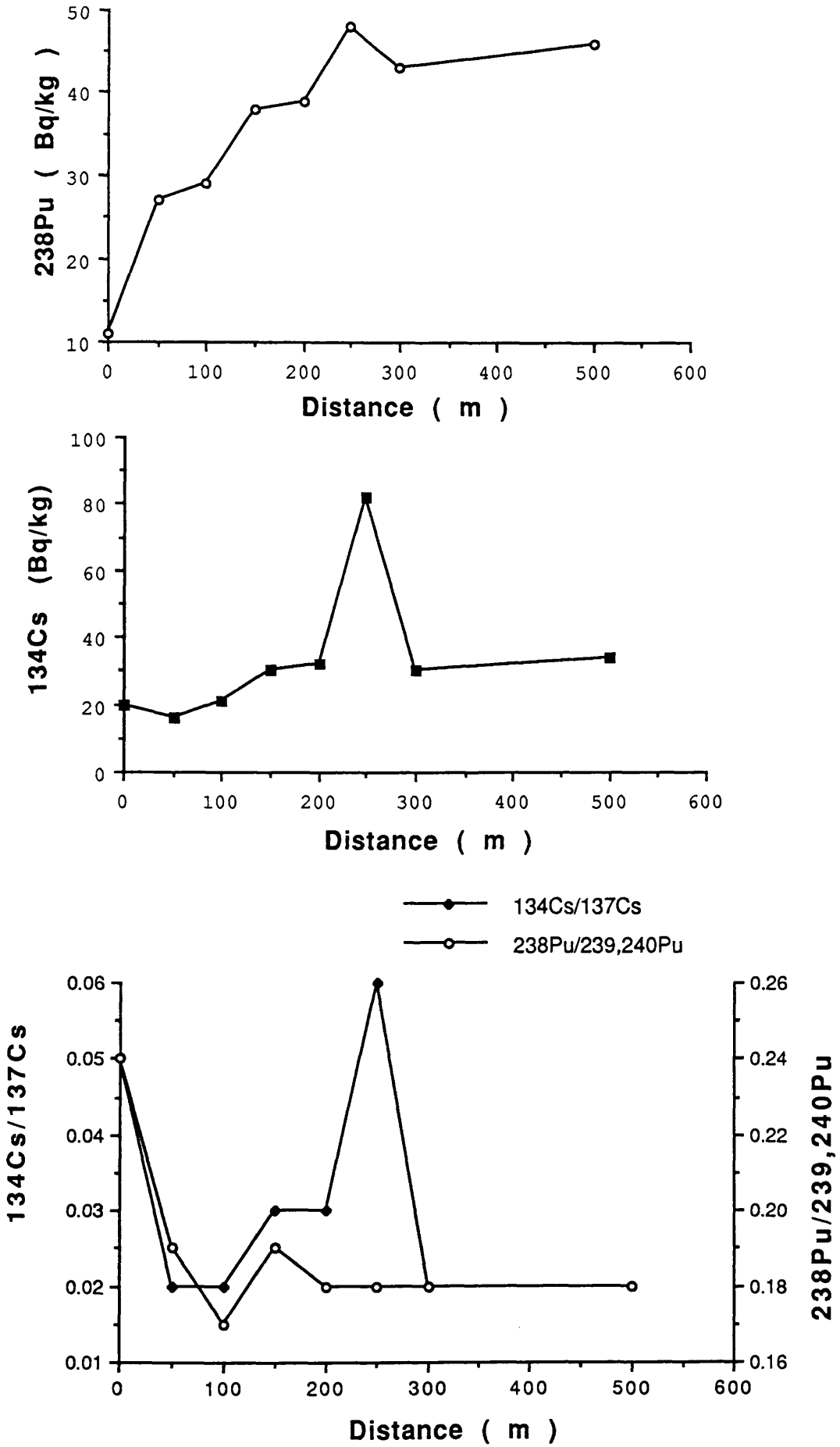

Figure 3.18 Plot of radionuclide concentrations and isotope activity ratios for 0-15cm depth samples from the Wigtown Martyr's stake transect

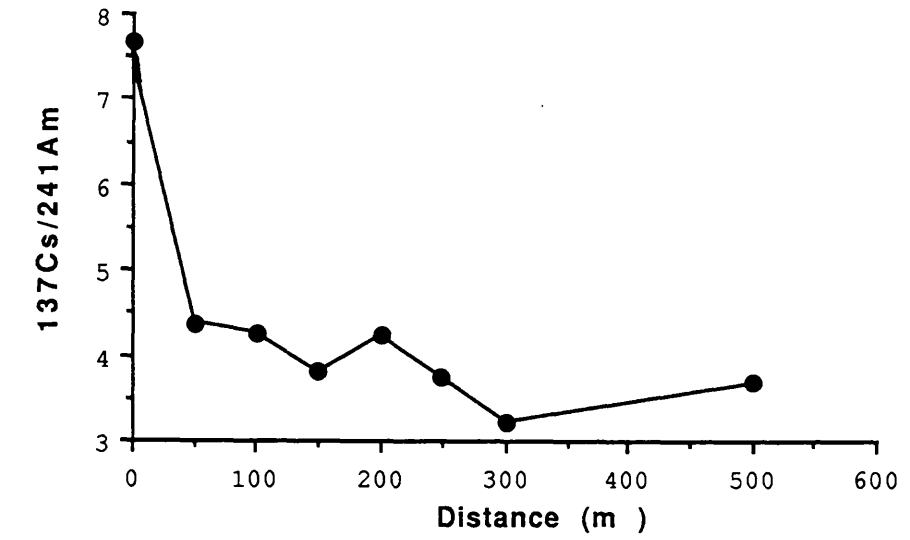

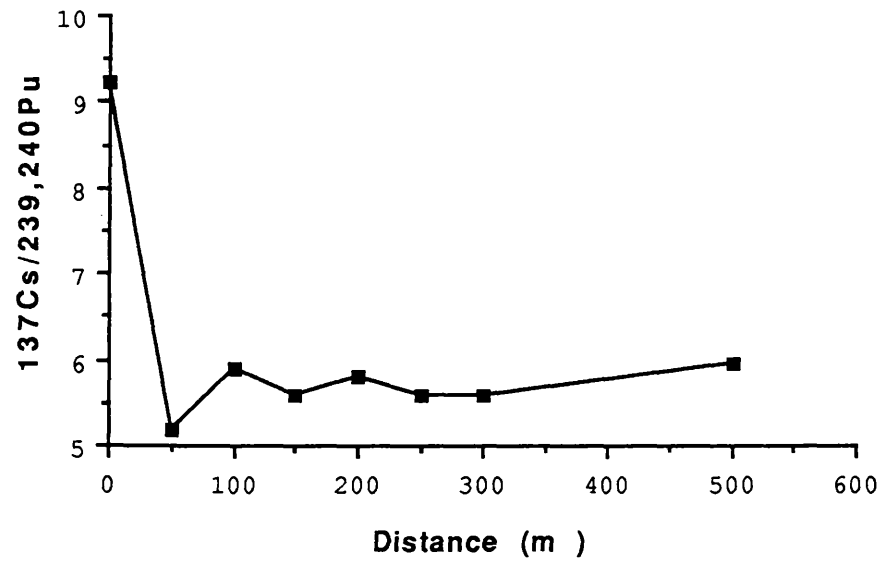

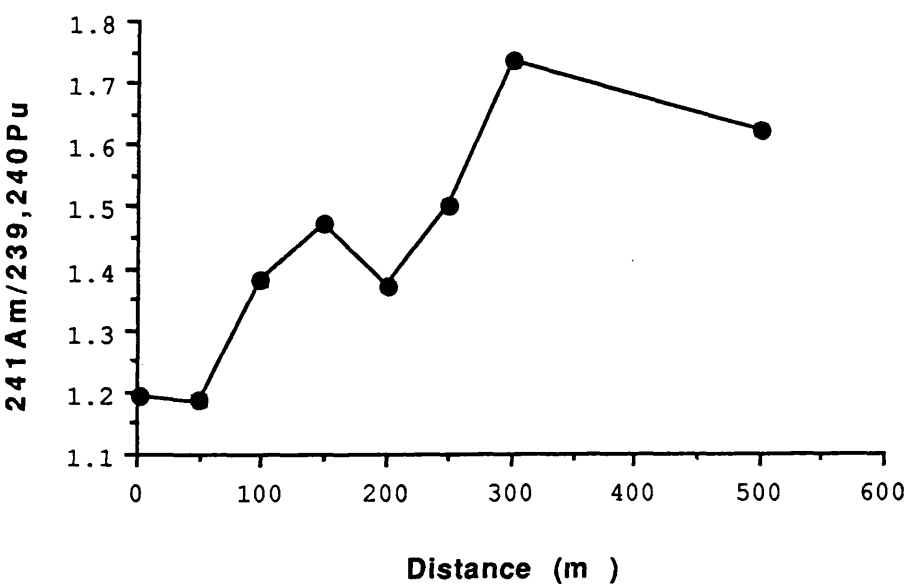

Figure 3.19 Plot of radionuclide activity ratios for 0-15cm depth samples from the Wigtown Martyr's stake transect

Distance (m)*	^{134}Cs	^{137}Cs	^{241}Am	^{238}Pu	$^{239,240}Pu$
(a) 0-15cm depth					
0	4.0×10^3	8.2×10^4	1.1×10^4	2.1×10^3	8.9×10^3
50	3.0×10^3	1.4×10^5	3.2×10^4	5.1×10^3	2.7×10^4
100	4.2×10^3	2.0×10^5	4.7×10^4	5.7×10^3	3.4×10^4
150	4.9×10^3	1.9×10^5	5.0×10^3	6.3×10^3	3.4×10^4
200	6.4×10^3	2.5×10^5	5.9×10^4	7.7×10^3	4.3×10^4
250	1.1×10^4	1.9×10^5	5.1×10^4	6.2×10^3	3.4×10^4
300	4.3×10^3	1.9×10^5	5.9×10^4	6.2×10^3	3.4×10^4
500	4.8×10^3	2.2×10^5	6.0×10^4	6.5×10^3	3.7×10^4
(b) 15-30cm depth					
0	4.7×10^2	8.3×10^4	1.5×10^4	2.1×10^3	1.2×10^4
50	BDL	1.6×10^4	2.3×10^3	BDL	BDL
100	BDL	1.4×10^4	BDL	BDL	BDL
150	2.8×10^2	4.8×10^3	BDL	BDL	BDL
200	5.5×10^2	4.9×10^3	1.3×10^3	BDL	BDL
250	2.9×10^2	2.8×10^3	BDL	6.2×10^1	3.9×10^2
300	3.2×10^2	5.4×10^3	1.6×10^3	BDL	BDL
500	1.9×10^2	2.4×10^3	5.3×10^2	BDL	BDL
(c) 0-30cm depth					
0	4.5×10^3	1.7×10^5	2.6×10^4	4.2×10^3	2.1×10^4
50	3.0×10^3	1.6×10^5	3.5×10^4	5.1×10^3	2.7×10^4
100	4.2×10^3	2.1×10^5	4.7×10^4	5.7×10^3	3.4×10^4
150	5.2×10^3	2.0×10^5	5.0×10^4	6.3×10^3	3.4×10^4
200	6.9×10^3	2.6×10^5	6.1×10^4	7.7×10^3	4.3×10^4
250	1.1×10^4	1.9×10^5	5.1×10^4	6.2×10^3	3.4×10^4
300	4.6×10^3	2.0×10^5	6.1×10^4	6.2×10^3	3.4×10^4
500	4.9×10^3	2.2×10^5	6.0×10^4	6.5×10^3	3.7×10^4

TABLE 3.21: Radionuclide inventories (Bq m^{-2}) for samples from the Wigtown merse site (a) 0-15cm, (b) 15-30cm and (c) 0-30cm depth (Figure 1.9)

* = Distance inland from mean high water level

Units = Bqm^{-2}

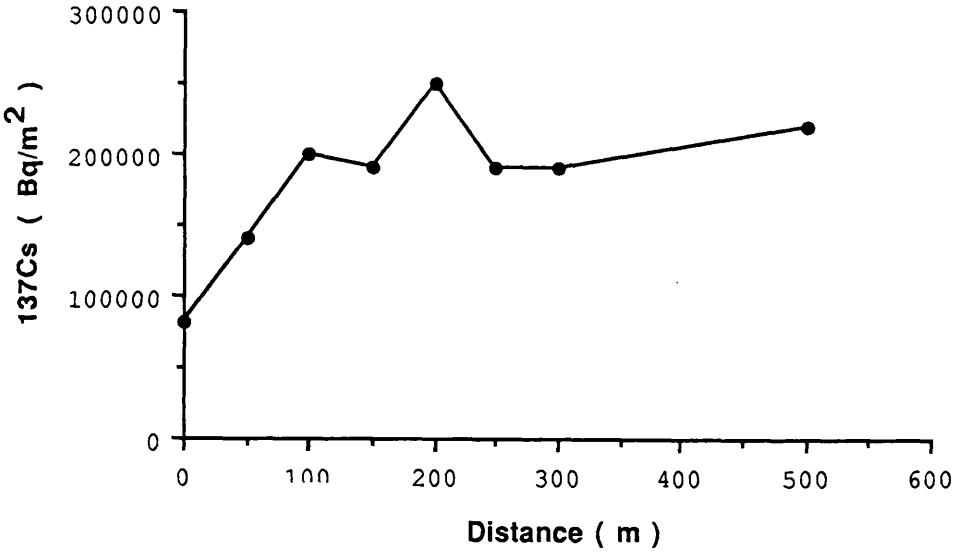

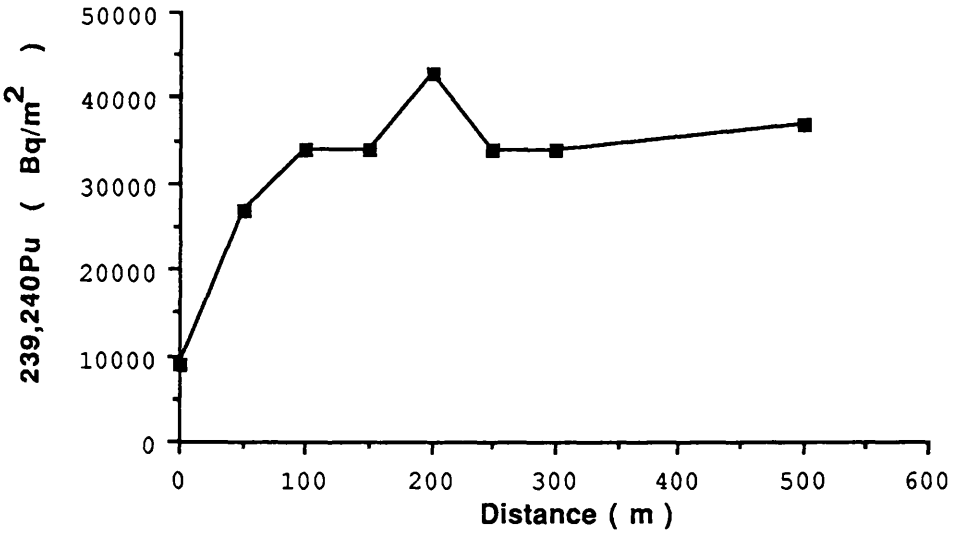

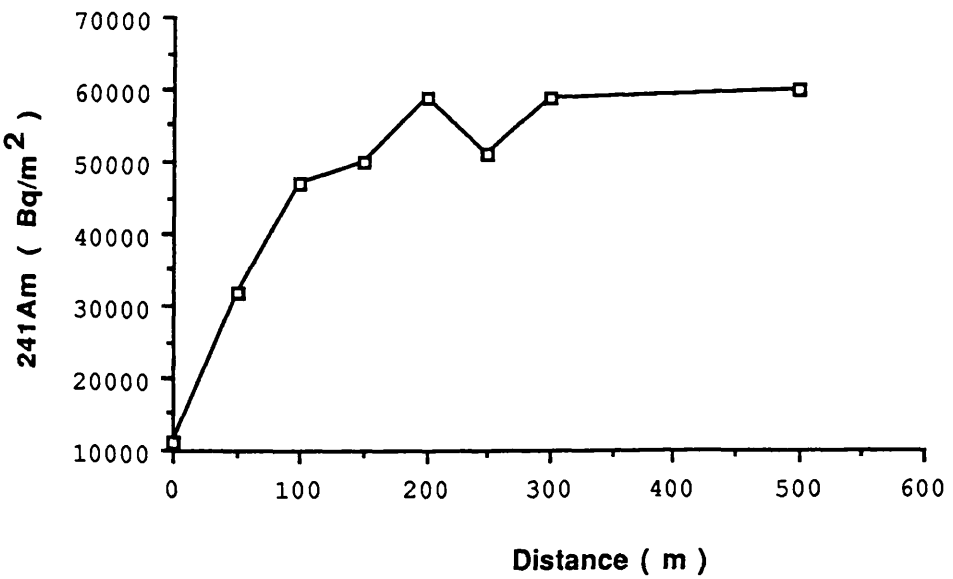

Figure 3.20 Radionuclide inventories (0-15cm) for the Wigtown Martyr's stake transect

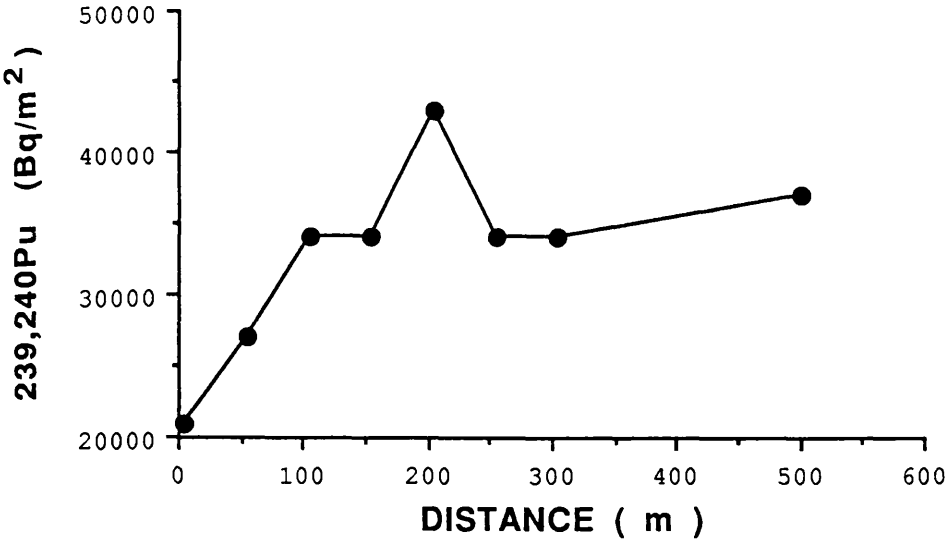

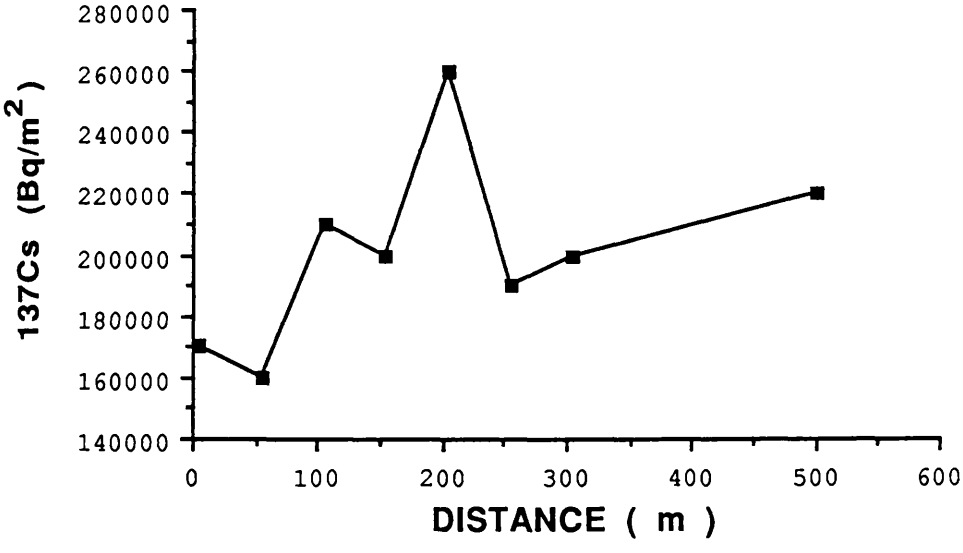

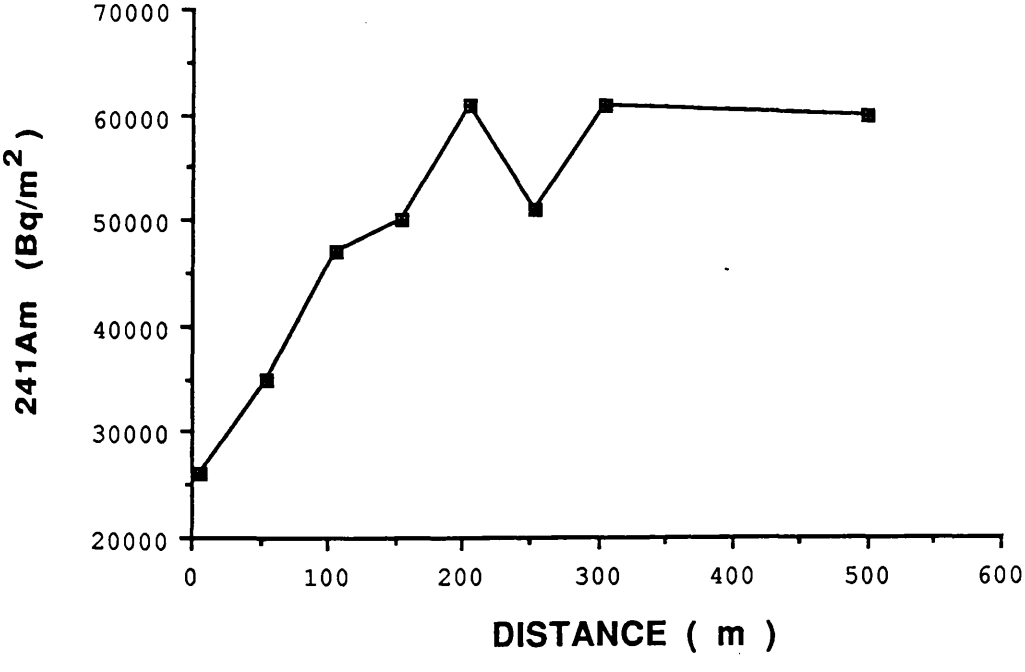

Figure 3.21 Radionuclide inventories (0-30cm) for the Wigtown Martyr's stake transect

Depth	Dry/Wet	LOI							$\frac{^{134}Cs}{^{137}Cs}$	$\frac{^{238}Pu}{^{239,240}Pu}$	$\frac{^{137}Cs}{^{239,240}Pu}$	$\frac{^{137}Cs}{^{241}Am}$	$\frac{^{241}Am}{^{239,240}Pu}$
cm	%	%	^{134}Cs	^{137}Cs	^{238}Pu	$^{239,240}Pu$	^{241}Am	^{210}Pb					
zero	75	6.4	135±9.4	473±7	5.9±1.2	27±3	30±8	106±8	0.29±0.02	0.22±0.05	17.5±2.0	15.8±4.2	1.1±0.3
0-5	77	5.7	29±2.3	291±11	6.0±1.5	24±3	30±7	76±5	0.10±0.009	0.25±0.7	12.1±1.6	9.7±2.3	1.3±0.3
5-10	78	4.5	9±0.7	244±10	5.2±0.8	23±2	24±7	73±5	0.04±0.004	0.22±0.04	10.5±1.0	10.2±2.9	1.0±0.3
10-15	76	4.5	4±0.3	316±10	5.0±1.0	23±4	25±4	72±4	0.01±0.008	0.22±0.06	13.7±2.4	12.6±2.1	1.1±0.3
15-20	76	5.6	6±0.7	399±12	5.8±1.2	28±3	25±6	56±3	0.02±0.002	0.21±0.05	12.3±1.3	13.6±3.3	0.9±0.2
20-25	76	5.4	3±0.2	344±12	6.4±1.7	29±3	29±6	54±5	0.008±0.0006	0.22±0.05	11.9±0.9	11.9±2.5	1.0±0.3
25-30	76	5.0	BDL	411±14	6.3±1.6	32±3	41±7	53±4	BDL	0.20±0.02	12.8±1.3	10.0±1.7	1.2±0.2
30-35	76	4.5	BDL	593±20	8.1±0.2	43±4	76±12	85±6	BDL	0.19±0.02	13.8±1.4	7.8±1.3	1.7±0.3
35-40	74	5.5	BDL	544±17	13.1±1.3	74±5	163±18	58±2	BDL	0.18±0.02	7.3±0.5	3.3±0.4	2.2±0.3
40-45	71	6.7	BDL	238±9	7.0±0.8	41±3	30±6	46±4	BDL	0.17±0.02	5.8±0.5	7.9±1.6	0.7±0.1
45-50	73	5.8	BDL	76±4	2.9±0.3	16±2	BDL	46±3	BDL	0.17±0.03	4.8±0.7	BDL	BDL
50-55	75	4.3	BDL	32±3	BDL	BDL	BDL	66±3	BDL	BDL	BDL	BDL	BDL
55-60	74	5.4	BDL	16±2	BDL	BDL	BDL	69±5	BDL	BDL	BDL	BDL	BDL
60-65	75	3.6	BDL	5±0.2	BDL	BDL	BDL	51±2	BDL	BDL	BDL	BDL	BDL
65-70	75	5.7	BDL	BDL	BDL	BDL	BDL	52±2	BDL	BDL	BDL	BDL	BDL
70-75	76	4.7	BDL	BDL	BDL	BDL	BDL	43±4	BDL	BDL	BDL	BDL	BDL
75-80	74	4.7	BDL	BDL	BDL	BDL	BDL	BDL	BDL	BDL	BDL	BDL	BDL

TABLE 3.22: Radionuclide concentrations and activity ratios for samples from section WMS871 Wigtown Martyr's Stake, August 1987 (Figure 1.9)

BDL = Below Detection Limit
Units = Bq kg^{-1}

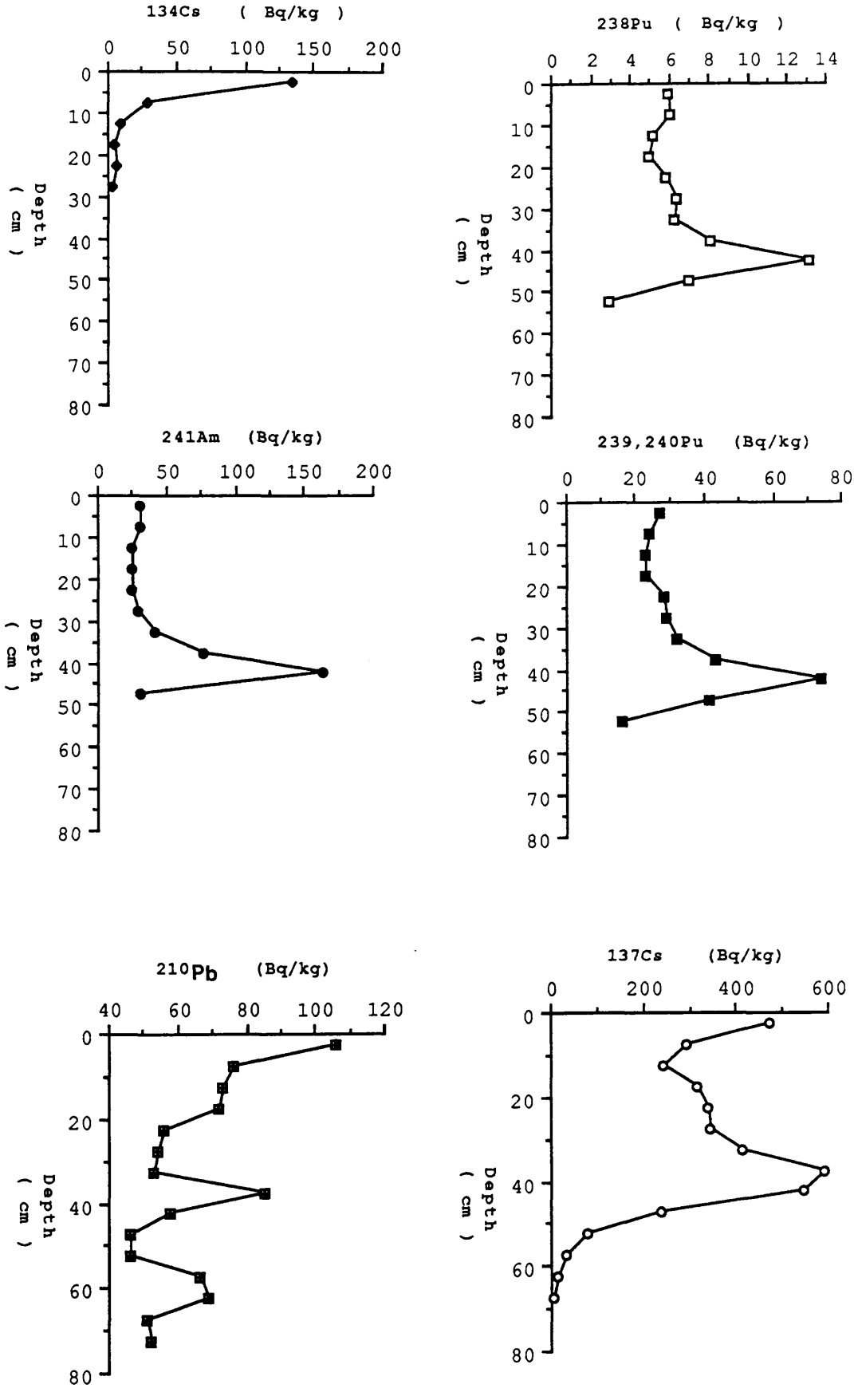

Figure 3.22 Radionuclide concentration profiles for section WMS871, Wigtown Martyr's stake

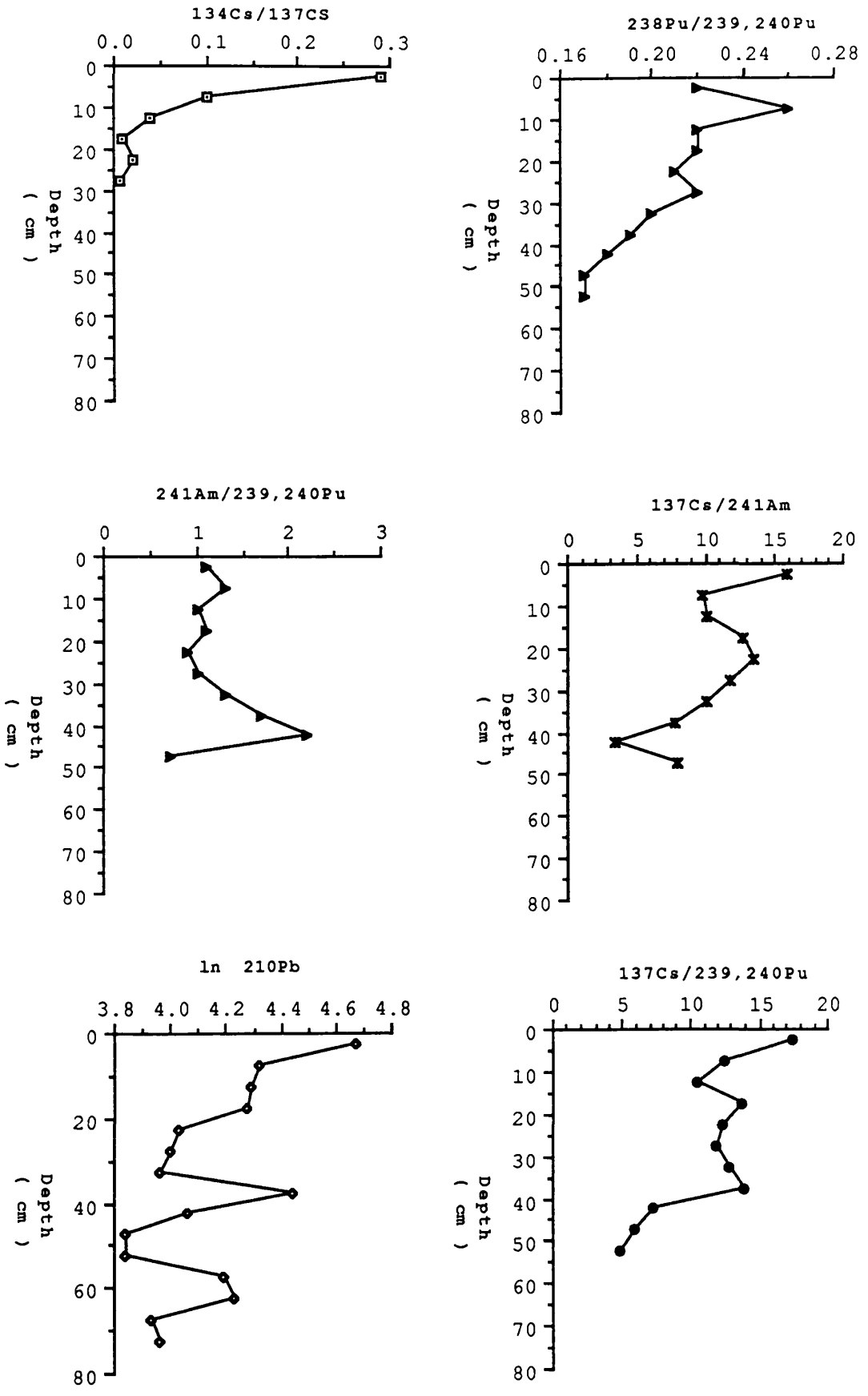

Figure 3.23 Radionuclide activity ratio profiles for section WMS871, Wigtown Martyr's stake

Distance cm	^{134}Cs	^{137}Cs	^{241}Am	$\frac{^{134}Cs}{^{137}Cs}$	$\frac{^{137}Cs}{^{241}Am}$
0-1	94±7	307±12	22±7	0.31±0.03	14.0±4.5
1-2	91±7	296±11	27±5	0.31±0.03	11.0±2.1
2-3	90±7	292±12	33±8	0.31±0.03	8.8±2.2
3-4	7±2	283±11	28±7	0.03±0.009	10.1±2.6
4-5	8±2	287±11	22±7	0.03±0.008	13.0±4.2
5-6	BDL	281±11	21±7	BDL	13.4±4.5
6-7	13±2	300±11	26±8	0.04±0.006	11.5±3.6
7-8	12±2	295±10	28±7	0.04±0.006	10.5±2.6
8-9	BDL	302±11	18±7	BDL	16.8±6.6
9-10	BDL	296±10	25±7	BDL	11.8±3.3
20-21	BDL	271±10	6±1	BDL	45.2±7.7
30-31	BDL	270±10	11±2	BDL	24.5±4.5

TABLE 3.23 : Radionuclide concentrations and ratios in samples from a section cut into an exposed vertical face of merse deposit at depth of 5cm, Wigtown Martyr's Stake, August 1987 (Figure 1.7)

BDL = Below Detection Limit
Units = Bq kg^{-1}

Distance cm	^{134}Cs	^{137}Cs	^{241}Am
0-1	BDL	20±4	BDL
1-2	BDL	9±1	BDL
2-3	BD	BDL	BDL

TABLE 3.24 : Radionuclide concentrations and ratios in a section cut into an exposed vertical face of merse deposit at a depth of 75cm, Wigtown Martyr's Stake, August 1987 (Figure 1.7)

BDL = Below Detection Limit
Units = Bq kg^{-1}

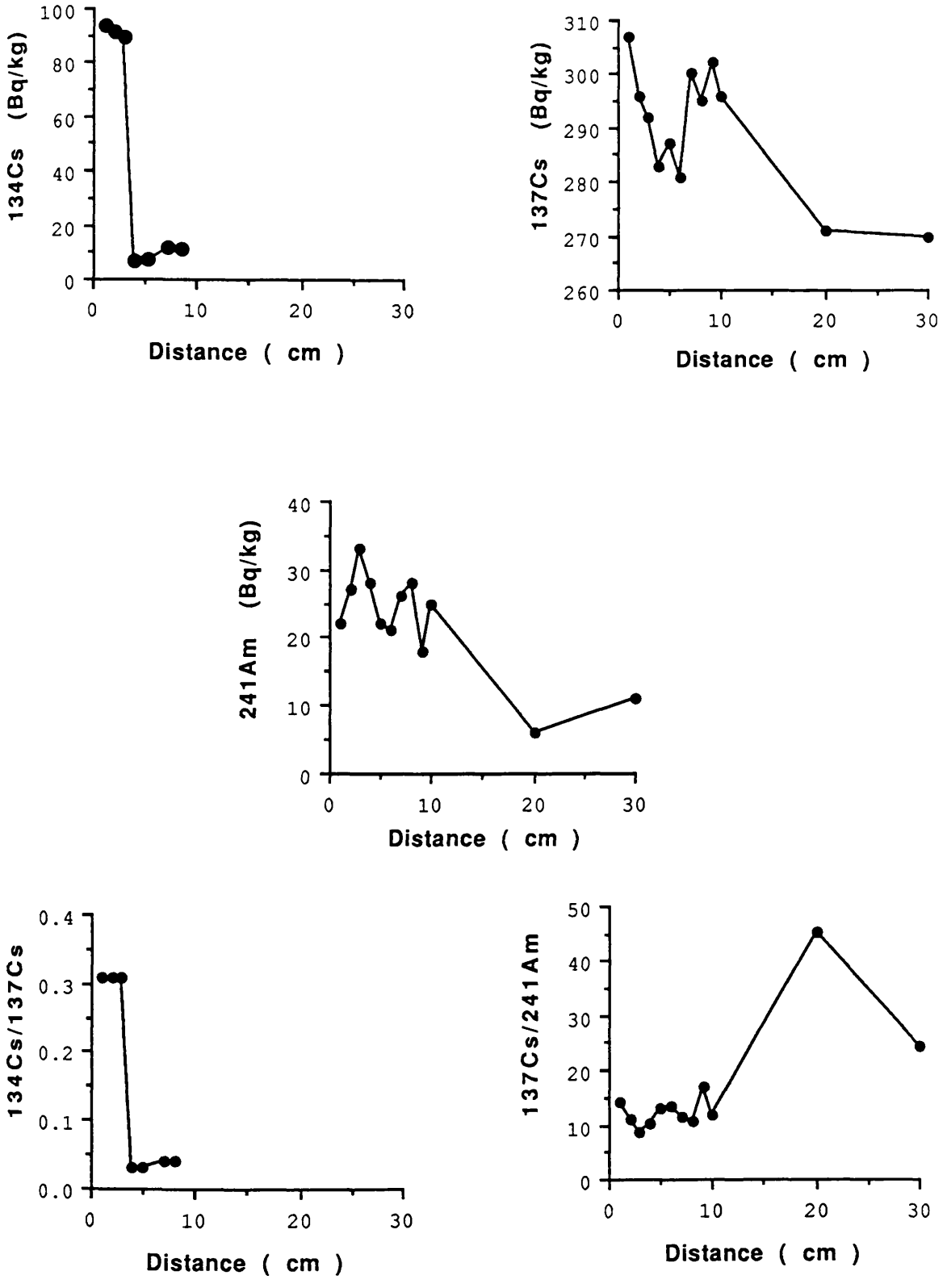

Figure 3.24 Radionuclide concentrations and activity ratios for samples from the horizontal section at 5cm depth in the Wigtown Martyr's stake merse

SAMPLE	Na %	K %	Sc	Cr	Fe %	Co	As	Br	Rb	Sb	Ba
(a) Netherclifton											
SECTION NCS861											
0-5cm	1.2±0.05	1.7±0.2	5.8±0.2	65±2	1.7±0.06	6.8±0.3	4.3±1.3	14±1.0	63±5	0.8±0.1	246±23
20-25cm	1.1±0.05	1.5±0.2	5.3±0.2	57±2	1.7±0.06	6.1±0.3	3.8±1.2	11±0.8	59±5	0.8±0.1	240±20
45-50cm	1.1±0.05	1.2±0.2	4.9±0.2	49±2	1.5±0.05	6.1±0.3	3.6±1.1	9±0.7	50±5	0.8±0.1	249±22
SECTION NCS862											
0-5cm	1.1±0.04	1.3±0.1	5.8±0.2	66±2	1.7±0.06	6.6±0.3	8.0±0.8	25±1.8	75±5	0.8±0.1	366±26
45-50cm	1.0±0.04	1.3±0.1	6.9±0.2	69±3	1.9±0.07	7.6±0.3	9.2±0.9	26±1.9	84±5	0.7±0.1	363±26
95-100cm	1.1±0.04	1.4±0.1	11.2±0.4	76±3	2.1±0.7	7.8±0.3	11.0±1.4	21±1.6	73±3	0.8±0.1	413±22
SECTION NCS863											
0-5cm	1.0±0.05	1.3±0.1	6.7±0.2	66±3	2.0±0.07	7.8±0.3	6.1±1.9	68±4.1	62±5	0.8±0.1	204±22
10-15cm	1.1±0.05	1.7±0.2	6.4±0.2	84±3	1.9±0.06	5.8±0.2	3.4±1.0	8±0.7	60±4	0.7±0.1	227±19
25-30cm	1.0±0.04	1.4±0.1	5.8±0.2	69±3	1.7±0.06	6.4±0.3	3.1±0.9	6±0.6	58±4	0.8±0.1	229±20
SECTION NCS864											
0-5cm	0.9±0.04	1.5±0.1	7.2±0.2	63±2	1.9±0.07	6.1±0.3	7.7±2.3	159±9.3	61±4	1.0±0.2	168±16
10-15cm	1.2±0.05	1.6±0.1	8.0±0.3	77±3	2.4±0.08	5.6±0.2	6.4±2.0	81±4.8	72±5	1.0±0.2	219±21
30-35cm	1.2±0.05	1.8±0.1	7.7±0.3	82±3	2.3±0.08	13.0±0.5	4.9±1.5	28±1.7	67±5	0.7±0.1	210±21
(b) Wigtown Martyr's Stake											
SECTION WMS871											
0-5cm	2.6±0.1	3.5±0.3	7.2±0.2	101±4	2.4±0.08	12.6±0.5	41.4±3	102±7.1	181±5	1.0±0.2	395±28
60-65cm	1.1±0.04	1.3±0.1	7.7±0.3	93±3	2.1±0.07	8.2±0.3	9.1±0.9	34±2.4	83±5	1.0±0.2	356±22
110-115cm	1.0±0.04	1.5±0.1	8.5±0.3	88±3	2.3±0.08	8.4±0.3	BDL	45±3.1	88±6	1.2±0.2	356±28

TABLE 3.25: Neutron activation analysis results for merse silt samples (a) Netherclifton (b) Wigtown Martyr's stake. Sampling locations are indicated in Figures 1.8 and 1.9. All results are in ppm unless otherwise indicated. Errors are based upon 1σ counting statistics plus apriori and systematic errors as discussed in the text.

SAMPLE	Cs	La	Ce	Eu	Sm	Tb	Yb	Lu	Hf	Ta	Th	U
(a) Netherclifton												
SECTION NCS861												
0-5cm	2.5±0.1	20.6±0.9	36±1.0	0.9±0.05	3.9±0.1	0.3±0.01	1.9±0.2	0.3±0.003	7.2±0.3	0.7±0.06	5.8±0.2	1.9±0.6
20-25cm	2.5±0.1	18.9±0.8	32±1.0	0.7±0.1	3.7±0.1	0.4±0.1	0.2±0.009	0.2±0.003	5.7±0.2	0.7±0.06	5.3±0.2	1.7±0.5
45-50cm	2.5±0.1	16.9±0.7	29±1.0	0.7±0.05	3.3±0.1	0.4±0.01	1.0±0.1	0.4±0.004	5.3±0.2	0.7±0.06	4.7±0.2	1.5±0.4
SECTION NCS862												
0-5cm	2.7±0.1	17.0±0.8	37±1.3	0.8±0.05	2.9±0.1	0.6±0.08	1.7±0.09	0.22±0.009	6.0±0.3	0.7±0.06	6.2±0.2	1.3±0.2
45-50cm	3.1±0.2	18.0±0.8	41±1.5	0.9±0.05	3.2±0.1	0.8±0.08	2.0±0.09	0.23±0.009	5.7±0.2	0.7±0.06	6.8±0.2	1.7±0.3
95-100cm	3.1±0.1	20.4±1.1	42±1.5	0.9±0.04	3.6±0.1	0.5±0.04	1.8±0.09	0.4±0.01	5.6±0.2	20.0±1.0	6.0±0.2	1.9±0.4
SECTION NCS863												
0-5cm	3.7±0.2	22.8±0.9	37±1.4	0.9±0.06	4.4±0.2	0.5±0.01	1.7±0.3	0.2±0.01	5.8±0.3	0.8±0.07	5.8±0.2	2.2±0.7
10-15cm	2.5±1.0	25.6±1.0	43±1.5	0.9±0.07	4.9±0.2	0.4±0.05	0.5±0.02	0.2±0.01	11.0±0.02	1.3±0.09	7.4±0.3	2.1±0.4
25-30cm	2.6±0.2	21.5±1.3	37±1.3	0.9±0.05	4.3±0.2	0.5±0.08	12.4±0.3	0.2±0.01	9.1±0.4	0.9±0.07	6.2±0.2	1.7±0.4
SECTION NCS864												
0-5cm	3.9±0.2	21.6±0.9	35±1.3	0.8±0.06	4.0±0.1	0.2±0.04	1.6±0.1	0.4±0.02	5.1±0.2	0.9±0.08	5.7±0.2	2.3±0.7
10-15cm	4.1±0.2	26.0±1.0	43±1.5	1.0±0.06	4.8±0.2	0.6±0.08	1.6±0.2	0.2±0.01	7.4±0.3	0.9±0.08	7.2±0.3	2.1±0.6
30-35cm	3.4±0.2	25.3±1.0	44±1.6	1.0±0.06	5.0±0.2	0.9±0.1	2.1±0.3	0.1±0.007	8.4±0.4	0.9±0.07	7.1±0.2	2.5±0.6
(b) Wigtown Martyr's Stake												
SECTION WMSS871												
0-5cm	2.9±0.2	62±3.0	59±2	1.0±0.06	5.0±0.2	0.9±0.1	2.6±0.1	0.3±0.01	12.2±0.5	0.9±0.07	9.3±0.3	2.3±0.3
60-65cm	3.1±0.2	22±1.0	48±2	1.0±0.06	3.8±0.1	1.0±0.1	2.3±0.1	0.3±0.01	8.9±0.4	0.9±0.07	7.8±0.3	1.9±0.4
110-115cm	3.4±0.2	22±1.0	50±2	1.0±0.06	4.0±0.1	0.5±0.09	2.2±0.1	0.4±0.02	7.1±0.3	0.9±0.09	8.2±0.3	2.2±0.2

TABLE 3.25 continued

4. DISCUSSION

4.1 ARDMORE BAY

Ardmore Bay, on the north bank of the Clyde Estuary (Figure 1.6), is a site of considerable biological interest, being a nature reserve and bird sanctuary, and is the focus of numerous marine biological research programmes. Little was known, however, about the geochemistry of the sediments of the bay or their accumulation and mixing characteristics before a previous study of these topics by Ben Shaban (1985) which has been extended into the present work.

In the previous work at Ardmore Bay (Ben Shaban, 1985), radiocaesium distributions in four sediment profiles from locations within the bay, as shown in Figure 1.6, were used to identify sediment accumulation and mixing characteristics. Similarly, the distributions of rare earth and other stable elements in the above four profiles were determined using instrumental neutron activation analysis, in the investigation of the geochemical characteristics of the sediments and of diagenetic processes taking place within them.

The main conclusions of this work can be summarized as follows. It was observed that the shapes of the concentration profiles obtained for radiocaesium and the stable elements analysed are dominantly controlled by the relative distributions of the two main sediment types found in the bay, namely a sand layer of varying thickness overlying clay. Mixing processes were found to dominate over accumulation in determining the shape of the radiocaesium profiles, which failed to provide any evidence of accumulation.

The sand layer was found to be very well mixed with uniform ^{137}Cs distribution as a function of depth, while the clay

exhibited a low level of mixing with a very low degree of penetration of radiocaesium.

The radiocaesium concentrations in the sediment were very low, with ^{134}Cs being below the limit of detection so that it was not possible to unambiguously identify the source of the radiocaesium, with both Sellafield waste and atmospheric fallout from nuclear weapons testing being possible. However, comparison with other reported values for radiocaesium in Clyde Sea Area sediments (Swan et al, 1982) indicates that the Sellafield contribution must be small relative to fallout.

The clay component of the sediment was identified on the basis of its chemical composition as probably being derived from a single source and the relative concentrations of trace elements were found to be constant throughout the bay despite variations in the proportion of clay to sand in the sediment. Diagenetic processes were found to have a negligible influence in determining element distributions in the sediment.

In order to confirm the nature of the mixing/accumulation processes by methods complementary to the above radiocaesium study, ^{210}Pb dating was applied in the present study to the previously analysed cores. ^{210}Pb concentrations were found to be low in the authigenic component of the sediment while ^{226}Ra was below the detection limit using gamma spectroscopy. The analysed ^{210}Pb concentrations were therefore taken as unsupported ^{210}Pb (Table 3.1). Also, one more sediment profile was collected from the bay approximately one year after the Chernobyl nuclear reactor accident in order to utilize the Chernobyl fallout radiocaesium as a tracer in the study of the sedimentary processes in the bay.

The unsupported ^{210}Po profiles, shown in Figure 3.1 as ln (excess ^{210}Pb) versus depth, generally reflect the nature of

the chemical composition of the sediment in the cores. For instance, the profile for core ABC841 which consisted of sand shows a very small variation, at low concentration, of unsupported ^{210}Pb over the depth range 0 to 25cm suggesting intense mixing, and consistent with the similar conclusion derived on the basis of the radiocaesium results. However, below 24-26cm, the unsupported ^{210}Pb activity falls off relatively rapidly, giving a good linear fit for ln (excess ^{210}Pb) versus depth in this section ($r = 0.92$). This indicates either the effects of accumulation in conjunction with decay below the mixed zone or else a progressively decreasing level of mixing in this depth zone. Core ABC842, which consisted of a sand layer of depth 8cm overlying clay, shows an excess ^{210}Pb distribution with low concentrations in the top 8cm but higher concentrations in the underlying clay material. Core ABC843 consisted of a mixture of sand and clay, and the unsupported ^{210}Pb distribution reflects the nature of the sediment, with concentrations varying as a function of the clay content in the core. The ^{210}Pb data therefore confirm the general features of the previously postulated mixing pattern for the bay and reveal that accumulation is occurring at a low rate relative to mixing.

The excess ^{210}Pb data are clearly not suitable for application of the constant initial concentration method (see section 1.3.5) of dating, with the possible exception of the lowest section of core ABC841. However, application of a constant rate of supply model (as discussed in section 1.3.5.) does allow some conclusions to be drawn from the ^{210}Pb data. Thus, the total inventories of unsupported ^{210}Pb in cores ABC841, ABC842 and ABC843 were 1.1×10^3, 3.5×10^3 and 3.8×10^3 Bq m^{-2} respectively. These inventories were calculated as follows:

$$I = \Sigma_o^x \frac{C.W.}{A} \times 10^4$$

where:

I = inventory (Bq m^{-2})

C = concentration (Bq kg^{-1})

W = weight (kg)

A = Area of core (cm^2)

X = Depth (cm)

If steady state conditions are assumed, then the number of ^{210}Pb atoms that decay under unit area of the sediment in a given time must be balanced by the number of atoms added to the same area in the same time. The ^{210}Pb flux for cores ABC841, ABC842 and ABC843 can therefore be calculated as 3.5 x 10^{10}, 1.1 x 10^{11}, 1.2 x 10^{11} atoms m^{-2} y^{-1} respectively.

It is apparent that the unsupported ^{210}Pb specific activity of any new material deposited must be at least equal to the average ^{210}Pb concentration in the mixed sediment. Thus if the initial excess ^{210}Pb content of deposited material is taken as being equal to the average value, then division of the flux by the average concentration generates a sedimentation rate which is in fact the maximum possible value for this parameter. Thus maximum sedimentation rates of 1.4, 1.2 and 1.5g cm^{-2} y^{-1} can be derived for cores ABC841, ABC842 and ABC843 respectively (the value for core ABC842 having a large uncertainty due to the difficulty in selecting a value for the average concentration in this core). Since compaction is relatively insignificant in these cores, these limits on sedimentation rates can be translated into values of 1.4, 1.2 and 1.5cm y^{-1} respectively for the maximum rate of accumulation. Even with the differences in the nature of sediments at the three locations, the unsupported ^{210}Pb profile results therefore

show that the ^{210}Pb fluxes and the maximum sedimentation rates are very similar at the different locations.

The lower section of core ABC841 is amenable to application of a modified constant initial concentration calculation (see section 1.3.5) and gives a sedimentation rate of 0.9cm y^{-1} on this basis, which is consistent with the above limit of less than 1.4cm y^{-1} for this core.

These data can be used to estimate the maximum rate of replacement of sediment in the mixed layer of the bay. Thus the total weight of sediment in a typical mixed layer of depth 25cm is:

$$\frac{\text{Depth . Average Weight of 1cm depth increment}}{\text{Area}} = \frac{25\text{cm} \cdot 23.5\text{g cm}^{-1}}{15.2\text{cm}^2} = 38.6\text{g cm}^{-2}$$

$$\therefore \%\text{ replacement per year} = \frac{\text{maximum sedimentation rate}}{38.6\text{g cm}^{-2}} \times 100\%$$

$$= \frac{1.5}{38.6} \times 100\% = 3.9\%$$

This confirms the conclusion of Ben-Shaban (1985) that there is very little transfer of sediment from the estuary to the bay.

Additional support for the ^{137}Cs and ^{210}Pb derived mixing pattern, was obtained from the Chernobyl radiocaesium distribution in core ABC871 collected in July 1987, the results of which are presented in Table 3.2 and are shown graphically in Figure 3.2.

This core consisted of 6cm of sand overlying clay and in the sand, Chernobyl radiocaesium was detected at a relatively uniform level confirming that the sand layer is almost

totally mixed within 1.25 year. In contrast, in the clay section of the core only the top sample was influenced by the Chernobyl radiocaesium. This penetration of less than 2cm in about 1.25 year in the clay confirms a low rate of diffusion of radiocaesium into the clay and also a low level of bioturbation occurring within this material.

The plot of the residual ^{137}Cs profile obtained by subtraction of the Chernobyl component on the basis of ^{134}Cs content, shows a low concentration in the sand layer with a higher value at the top of clay layer and an exponential decrease below this. A very good linear correlation between ln (^{137}Cs concentration) and depth was obtained below the mixed section (correlation coefficient of 0.958). This exponential decrease of ^{137}Cs within the clay section reflects the low degree of physical and biological mixing and low rate of ^{137}Cs diffusion into the clay material.

An effective diffusion coefficient can be calculated for ^{137}Cs in the clay by using the solution of Fick's diffusion equation (2.1) for a situation in which the ^{137}Cs is assumed to be added to a uniform plane surface (the top of the clay layer) at a given time and then undergoes diffusion into the clay. The solution to the diffusion equation under these conditions is given by:

$$C = \frac{M}{(\pi Dt)^{1/2}} e^{-x^2/4Dt}$$ (Crank, 1956)

where:

C = concentration of diffusing substance

M = amount of diffusing substance

D = diffusion coefficient

t = time in sec

x = depth cm

For a fixed value of t and D, the term $(M/(\pi Dt)^{1/2}$ is constant and can be replaced by k_1.

Similarly (-1/4Dt) can be replaced by k_2.

Thus, $C = k_1 e^{-k_2x^2}$ and

$\ln C = k_1 - k_2x^2$

If we redefine a new variable $Z = x^2$ then

$\ln C = k_1 - k_2Z$

ie. a simple linear equation which is readily solved by regression analysis.

Two possible values for t could be used namely 24 years, relative to the weapons testing fallout maximum or 12 years, relative to the Sellafield discharge maximum. These give respective D values for radiocaesium of 1.3×10^{-12} and 2.7×10^{-12} m^2 sec^{-1}.

The values for the effective diffusion coefficient of ^{137}Cs in clay obtained in this way are consistent with values reported by other workers for both field observation and laboratory experiments. For instance, on the basis of laboratory studies, Christiansen and Torstenfelt (1988) reported a value of $3.3 \times 10^{-11} m^2$ sec^{-1} for the caesium diffusion coefficient in clay. Moreover, Aston and Stanners (1979) reported a value of $10^{-12} m^2$ s^{-1} for the radiocaesium diffusion coefficient on the basis of results for intertidal silts in Cumbria and Higgo et al (1988) reported a range of

values for the diffusion coefficient of ^{137}Cs of 4.1×10^{-12} to $8.8 \times 10^{-13} m^2 sec^{-1}$ in deep sea sediment studies.

Finally, the inventory of ^{137}Cs originating from Chernobyl fallout in Ardmore Bay sediments can be derived from the ^{134}Cs data and knowledge of the initial $^{134}Cs/^{137}Cs$ activity ratio of 0.55 for the Chernobyl fallout. This gives a value of $1.2 \times 10^3 Bq\ m^{-2}$ for the ^{137}Cs inventory which is quite small compared with values of 2×10^3 to 6×10^3 reported by Horrill et al (1988), for the Chernobyl ^{137}Cs inventory in soils from this area.

This suggests that a substantial fraction of the Chernobyl radiocaesium initially deposited may have been removed, although this conclusion must be treated with caution in view of the patchy nature of the deposition of Chernobyl fallout.

4.2 TRANSPORT PROCESSES AFFECTING MANMADE RADIONUCLIDES IN INTERTIDAL SEDIMENTS IN SOUTH WEST SCOTLAND

In order to test and extend the hypothesis of MacKenzie et al (1987) that sediment associated transport is the dominant mechanism involved in the transfer of Sellafield waste radionuclides to the Solway Firth intertidal area (as described in detail in section 1.3.6), two related studies were undertaken, namely (a) analysis of manmade radionuclide concentrations in an additional suite of samples and (b) chemical characterisation of some of the original samples studied by MacKenzie et al. All of the additional samples studied were collected from region A, (Figure 2.1) east of Burrow Head as defined by MacKenzie et al (Figure 1.13). The results are contained in Tables 3.3 and 3.4, and the highest radionuclide activities were found, as expected, in the fine silts from locations such as Wigtown Martyr's Stake, Carty Port and Innerwell Fishery, while lower activities were obtained for sand samples collected from the

Rockcliffe and Preston Merse intertidal areas.

It was necessary to consider the contribution of Chernobyl fallout radiocaesium to these results since the sampling took place after the Chernobyl accident. The Chernobyl fallout radiocaesium contribution was calculated on the basis of the known Chernobyl $^{134}Cs/^{137}Cs$ activity ratio of 0.55 to 0.60 at the time of deposition in conjunction with the observed $^{134}Cs/^{137}Cs$ ratios of about 0.01 to 0.04 for Solway Firth intertidal sediments prior to the Chernobyl accident (eg. see Table 3.11). On this basis, only the Innerwell Fishery silt shows a definite Chernobyl contamination at a level of about 50Bq kg^{-1} of ^{137}Cs. For the other samples the values for the $^{134}Cs/^{137}Cs$ activity ratio and the similarity of the post Chernobyl ^{137}Cs concentrations with those for previous years for Solway intertidal sediments suggests that most of the deposited Chernobyl radiocaesium had been removed from the sediment, possibly by leaching into seawater.

The low values for Chernobyl radiocaesium in the intertidal sediment samples can be contrasted with concentrations reported by Baxter et al (1989) of up to 30,000 Bq m^{-2} for Chernobyl ^{137}Cs in soils from the Solway coastal area, again indicating a low degree of retention of the deposited radiocaesium in the intertidal sediments. This is consistent with the above observation for Chernobyl radiocaesium behaviour in Ardmore Bay and with the generally soluble behaviour of radiocaesium in seawater.

The observed $^{137}Cs/^{239,240}Pu$ and $^{137}Cs/^{241}Am$ activity ratios of less than 10 and the $^{241}Am/^{239,240}Pu$ ratios of greater than 1 obtained for all of the new intertidal samples from region A are in good agreement with corresponding values for this region reported by MacKenzie et al (1987) and are consistent with the particle associated model for transport of Sellafield radionuclides from further south in the Irish

Sea.

The $^{137}Cs/^{241}Am$ and $^{137}Cs/^{239,240}Pu$ ratios obtained are much higher than those expected from the Sellafield discharge ratios in conjunction with the K_D values of these nuclides (of the order of 10^2 for ^{137}Cs, 10^5 for $^{239,240}Pu$ and 10^6 for ^{241}Am as discussed in section 1.3.6). The results compare well with those reported by other workers for Irish Sea intertidal sediments and a summary of relevant data is shown in Table 4.1 The $^{241}Am/^{239,240}Pu$ activity ratios obtained in this study and in the others summarized are slightly greater than unity in most cases, which is incompatible with recent Sellafield discharges with $^{241}Am/^{239,240}Pu$ activity ratios in the range 0.2 to 0.6 (Table 1.6) in conjunction with the appropriate K_D values. However, these $^{241}Am/^{239,240}Pu$ ratios are similar to the total integrated ^{241}Am to total integrated $^{239,240}Pu$ ratio for the Sellafield discharge (Table 1.6) suggesting that highly efficient mixing of past discharges has occurred before deposition of radionuclides in these sediments. Similarly, the $^{238}Pu/^{239,240}Pu$ ratio values of 0.18 to 0.26 observed both in the present work and in the others summarised in Table 4.1, are incompatible with recent Sellafield discharge ratio values of 0.31 (Table 1.6) and again indicate that efficient mixing of recent and old discharges affects the nuclides deposited in the Solway area.

A significant feature of the work by MacKenzie et al (1987) was the observation of linear correlations between the activities of each of ^{137}Cs, $^{239,240}Pu$ and ^{241}Am, despite the differences in K_D appropriate to these nuclides. In the present study, linear correlation coefficients of 0.60, 0.80, 0.90 were obtained for the ^{137}Cs - $^{239,240}Pu$, ^{137}Cs - ^{241}Am and $^{239,240}Pu$ - ^{241}Am relationships respectively.

The observed constancy of the radionuclide activity ratios over a distance of about 100km along the length of the north

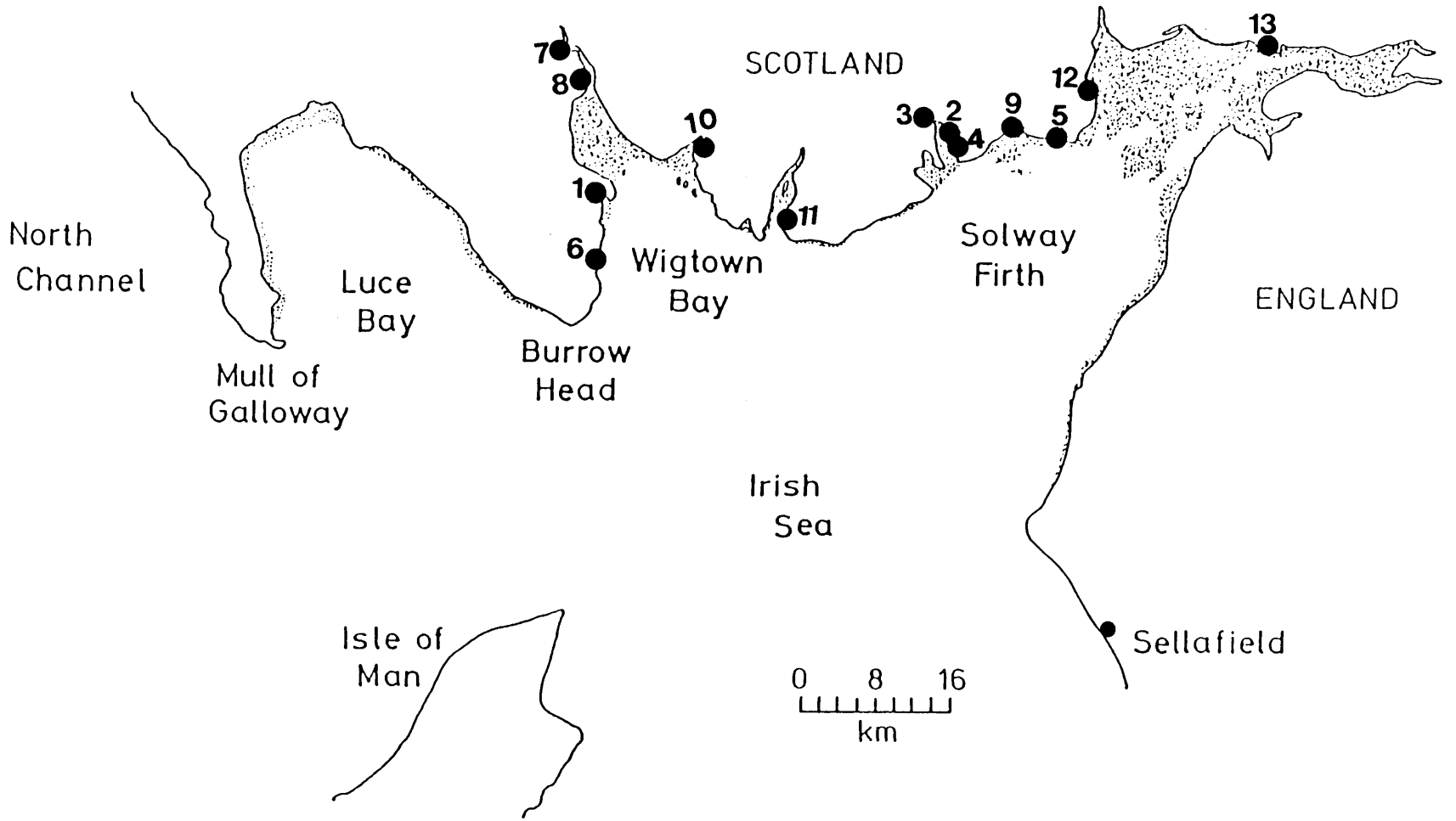

Figure 4.1 Map showing sampling sites referenced in Table 4.1.

Sample Location	^{134}Cs	^{137}Cs	^{241}Am	^{238}Pu	$^{239,240}Pu$	$\frac{^{134}Cs}{^{137}Cs}$	$\frac{^{137}Cs}{^{241}Am}$	$\frac{^{137}Cs}{^{239,240}Pu}$	$\frac{^{241}Am}{^{239,240}Pu}$	$\frac{^{238}Pu}{^{239,240}Pu}$
Garlieston (sand) (1)	2.7	110	24	-	-	0.025	4.6	-	-	-
Garlieston (silt) (1)	13	510	150	25	110	0.025	3.4	4.6	1.3	0.21
Kippford (silt) (2)	28	1200	430	76	360	0.023	2.8	3.3	1.2	0.21
Kippford merse (silt) (2)	33	1500	460	80	380	0.022	3.3	3.9	1.2	0.21
Kippford merse (marsh) (2)	34	1800	600	170	780	0.019	3.0	2.3	0.8	0.22
Kippford jetty (silt) (2)	22	940	330	65	290	0.023	2.8	3.2	1.1	0.22
Palmackie (silt) (3)	35	1500	480	87	390	0.023	3.1	3.8	1.2	0.22
Rockcliffe (sand) (4)	BDL	266	BDL	7.9	31	BDL	BDL	8.6	BDL	0.25
Preston (sand) (5)	BDL	150	BDL	4.9	21	BDL	BDL	7.1	BDL	0.20
Wigtown (silt) (6)	7.3	371	154	28.7	119	0.02	2.4	3.1	1.3	0.24
Carty port (silt) (7)	18.0	606	219	24.4	98	0.03	2.8	6.2	2.2	0.24
Innerwell fishery (silt) (8)	40.1	596	323	85.5	372	0.07	1.8	1.6	0.9	0.16
Netherclifton [1] (silt) (9)	2.4	615	137	16	86	0.004	4.5	7.2	1.6	0.19
Netherclifton [2] (silt) (9)	9.7	804	280	41	206	0.01	3.1	3.9	1.3	0.20
Skyreburn Bay (sand) (10)	6.4	328	33	4	17	0.02	9.9	19.3	1.9	0.24
Garlieston (sand) (1)	-	320	60	-	39	-	5.3	8.2	1.5	0.21
Wigtown (silt) (6)	-	1030	194	-	132	-	5.3	7.8	1.5	0.24
Skyreburn Bay (sand) (10)	-	412	91	-	53	-	4.5	7.8	1.2	0.21
Kippford (2)	-	1170	186	-	124	-	6.3	9.4	1.5	0.22
St Mary's Isle (11)	-	768	137	-	105	-	5.6	7.3	1.3	0.25
Carsethorn (12)	-	431	37	-	31	-	11.6	13.9	1.2	0.23
Annan (13)	-	328	15	-	5.4	-	21.9	60.7	2.8	0.29

TABLE 4.1: Summary of radionuclide concentration and activity ratios reported for Solway intertidal sediments (MAFF, 1985 and MacKenzie et al, 1987) locations shown in (Figure 4.1)

Units = Bq kg^{-1}
- = Not available

Solway coast is totally inconsistent with solution transport and continuous uptake by the sediment which, as discussed in detail in section 1.3.5, would for example, give an exponential decrease in the $^{241}Am/^{137}Cs$ ratio with increasing distances from the discharge point. The magnitude of the exponential variation can be estimated by assuming that at least 90% of the americium is removed from solution within 10km of the discharge point whereas, less than 10% of the caesium is removed from solution within about 100km of the discharge point. Thus, using equation 1.5. (p. 104)

$$C_D = C_o\, e^{-\beta_3 D}$$

$$\therefore \text{For } ^{241}Am,\ 0.1 = 1.0e^{-\beta_3 . 10}$$

$$\text{gives } (\beta_3)\ Am = 0.23km^{-1}$$

$$\text{For } ^{137}Cs\ 0.9 = 1.0e^{-\beta_3 . 100}$$

$$\text{gives } (\beta_3)\ Cs = 1.05 \times 10^{-3}km^{-1}$$

$$\therefore \text{For } \frac{(^{241}Am)_D}{(^{137}Cs)_D} = \frac{(^{241}Am)_o\, e^{-(\beta_3)_{Am} D}}{(^{137}Cs)_o\, e^{-(\beta_3)_{Cs} D}}$$

$$\frac{(^{241}Am)_D}{(^{137}Cs)_D} = \frac{(^{241}Am)_o}{(^{137}Cs)_o}\, e^{-(0.23-0.00105)D}$$

$$\frac{(^{241}Am)_D}{(^{137}Cs)_D} = \frac{(^{241}Am)_o}{(^{137}Cs)_o}\, e^{-0.229D}$$

Thus since $D_{\frac{1}{2}} = \frac{\ln 2}{(\beta_3)}$ the half distance for the $^{241}Am/^{137}Cs$

ratio is $D_{1/2} = \frac{0.693}{0.229} = 3km$

Assuming a uniform rate of removal from solution (in proportion to their respective K_D values) of both americium and caesium as a function of distance means that surface sediment concentrations (and ratios) would simply be proportional to the water concentrations (and ratios). Thus the $^{241}Am/^{137}Cs$ ratio in surface sediment would half every 3km if this model was applicable. Over a distance of 50km this would therefore result in a reduction in the $^{241}Am/^{137}Cs$ ratio by a factor of 10^5, a decrease which is clearly not observed in the north east Irish Sea. Thus, the above results and discussion provide strong support for the concept that particle associated movement of radionuclides is the main transport mechanism moving Sellafield waste to the intertidal sediments of the Solway Firth at present.

Furthermore, the probability that the highly contaminated mud patch off Sellafield is the source of the contaminated silt is strongly supported by the results of Baxter et al (1989) for Irish Sea surface sediments taken in a transect running away from the mud patch towards the Solway Coast (at distances of 14, 20, 29, 49, 63km from Sellafield). This work revealed that the radionuclide concentrations in Irish Sea surface sediments are independent of the distance from Sellafield but are dependent upon the size fraction characteristics of the sediment and that the radionuclide activity ratios are reasonably constant across this transect, supporting the argument that solution transport with continuous removal to the sediment is not the mechanism operating.

The above pattern of radionuclide transport implies the movement of fine silt from a very well mixed source area in the Irish Sea with an efficient transfer to region A and a

less efficient, but still significant, transfer to region B. On this basis, it would be reasonable to expect the intertidal silts in region A, and perhaps also those in region B, to show a relatively uniform chemical composition. In contrast, if the intertidal silts along the Solway Coast were derived dominantly from eroded material from the landward area to the north, they might readily be expected to show variations in chemical composition corresponding to variations in the local geology and surface soil type.

The instrumental neutron activation analysis results shown in Table 3.4 provide a characterization of the chemical composition of the sediment samples which can be used in attempts to differentiate the sources of sediments in different regions. In selecting elements to use in attempting to characterize the sediments, it was decided to concentrate mainly upon those species which are relatively refractory and are not involved to a major extent in diagenetic processes occurring in surface sediments. Thus, less emphasis was placed upon Na, K, Fe, Mn, Ca, Rb and Br in these considerations since, being geochemically relatively reactive, their distribution could be dominated by post depositional processes in the sediment. The remaining elements were considered to be much less reactive and therefore to have a higher probability of reflecting the original source of the sediments. As discussed in section 1.3.6 the rare earth elements are particularly useful in this context on account of their generally low geochemical reactivity and characteristic concentration patterns in individual rocks and minerals. The following discussion of the neutron activation analysis data is therefore dominantly focussed upon the rare earth elements.

The Masuda-Coryell plots for the intertidal sediment samples from regions A, are shown in Figure 4.2, using Mason's (1966) figures for shale as the normalizing reference material.

Considering first of all the samples from region A, it is immediately obvious that all of the samples show similar rare earth element distribution patterns, in particular for the light rare earth elements such as La, Ce, Sm and Eu. The plots of the rare earths in region A are characterized by Ce and Eu maxima and La and Sm minima. Also the silts of this region are in general more enriched in rare earth elements than the samples from regions B and C. These results are therefore consistent with the hypothesis that the silts in region A are derived from a common source.

The Criffel pluton represents a possible source rock for the silts in region A so for comparison, the rare earth element data for a representative sample from Stephens et al (1985) are plotted in Figure 4.3. (It should be noted that in this case, these data have been normalized to shale for comparison with the sediment data whereas the discussion in the original text by Stephens et al used chondrite normalization). From the plot it is apparent that the Criffel data show a greater enrichment of light rare earth elements relative to heavy rare earth elements than is observed for the silts in region A, (Figure 4.2) and that the positive Eu anomaly in the silt results is less pronounced in the Criffel data. Thus, considerable modification of the rare earth element relative concentrations during weathering would have to have occurred if the Criffel pluton is the source rock for the silts in region A.

Considering the results for region B, Figure 4.4, the Drumore and Port Logan samples show similar concentrations and Masuda-Coryell patterns to each other for the rare earths. However, the Port William sample shows concentration and Masuda-Coryell patterns which are very similar to those of the region A samples, despite major differences in the geology of the landward coastal area to

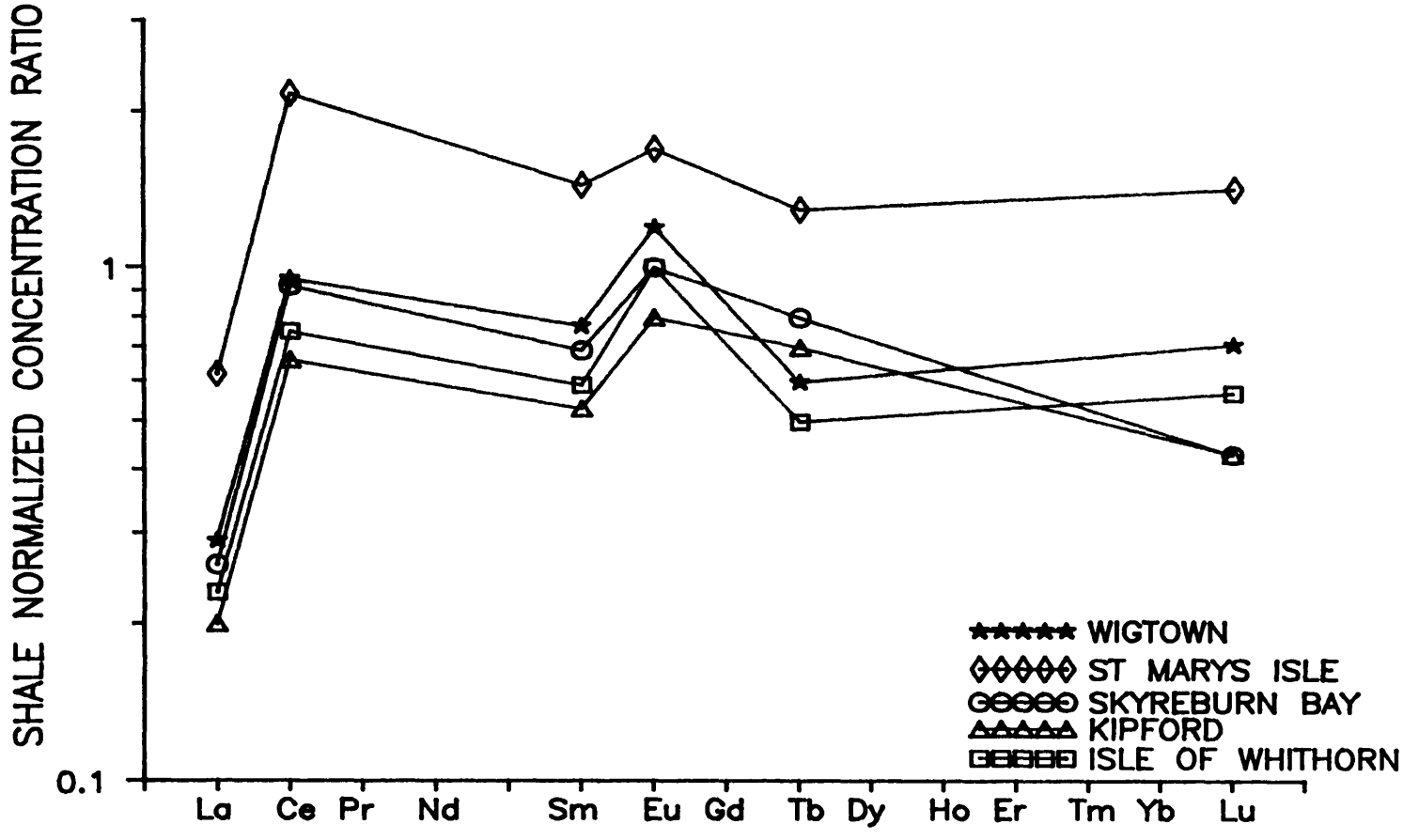

Figure 4.2 Masuda-Coryell plot for intertidal sediment samples from Region A (Figure 1.13)

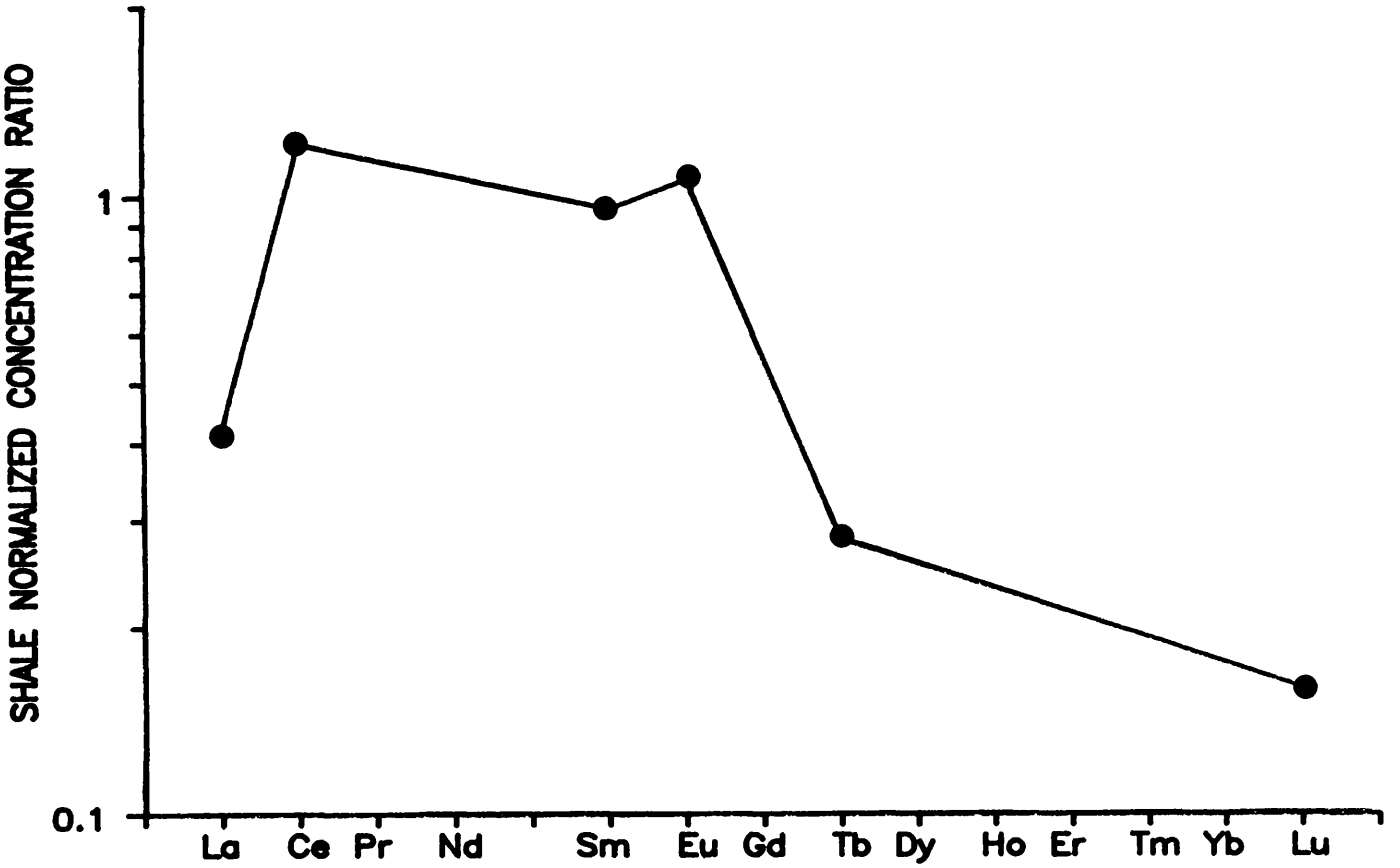

Figure 4.3 Masuda Coryell plot for a representative sample from Stephens et al (1985)

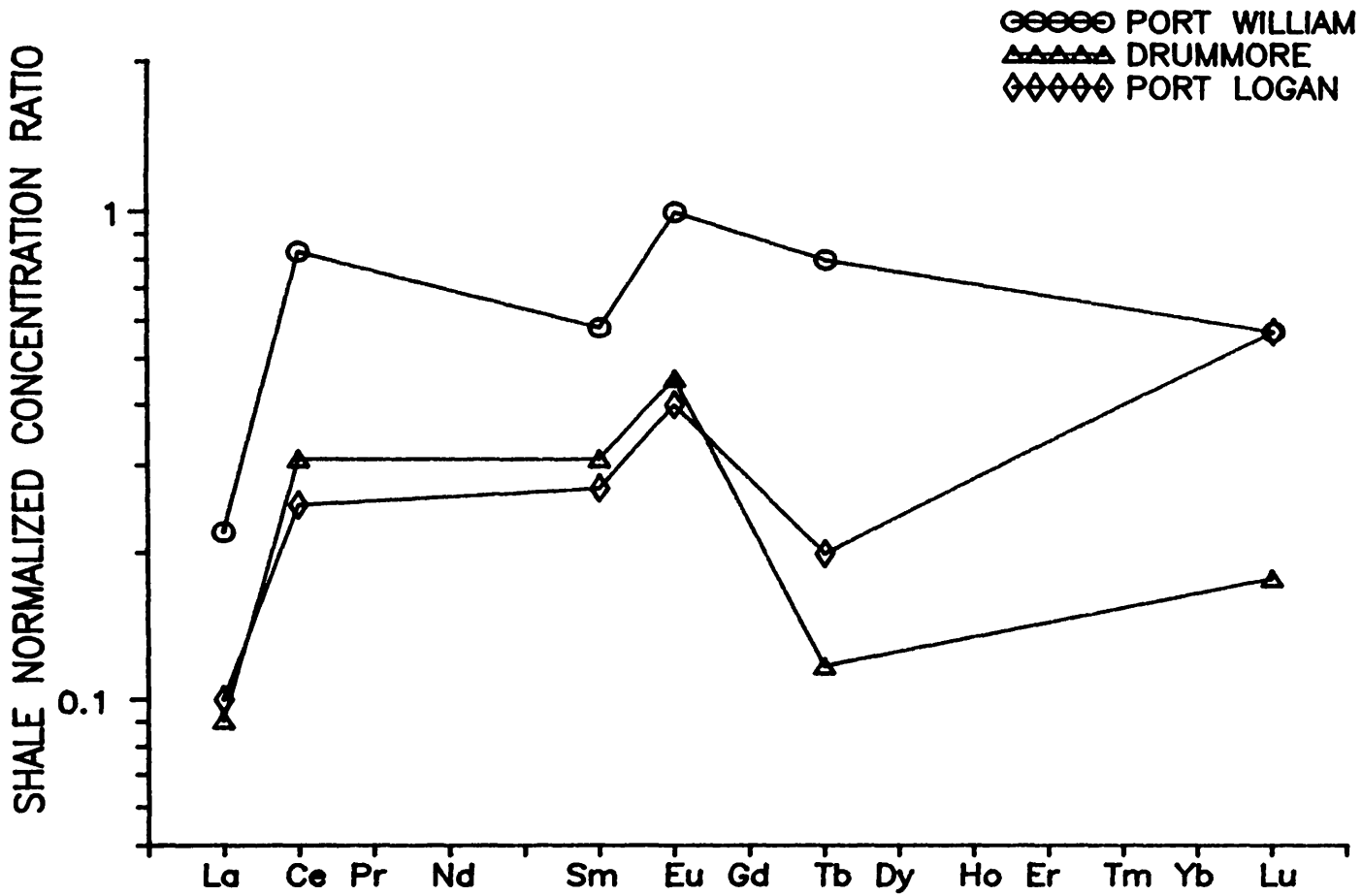

Figure 4.4 Masuda-Coryell plot for intertidal sediment samples from Region B (Figure 1.13)

the north of these sampling sites.

Some similarity is apparent between the Masuda-Coryell plots for the Drumore and Port Logan samples and those of region A but much less convincingly than for Port William.

Finally, the normalized results for samples from region C, (Figure 4.5) show similarities to each other, with pronounced Eu maxima for the two sites from the Mull of Kintyre (RH5 and Ardnacross Bay) and the Kildonan sample from Arran. In contrast, the Ardmore Bay and Girvan samples show distributions which are markedly different from each other and from the other samples in region C and those for samples from regions A and B. Generally, the rare earth distribution patterns for region C are all dissimilar to those for regions A and B.

An alternative method for interpretation of geochemical data of this type is to observe the relative distribution of different samples in simple plots of one element concentration against another or in plots of element concentration ratios against each other, which can provide an indication of the geochemical association of different samples (eg. Halliday et al, 1983). As examples of this approach, plots of La versus Ce, La versus Sm, K versus Fe; Na versus K, Ba/Rb versus Th/U and Sm/Eu versus Ce/Lu are shown in Figures 4.6, 4.7 and 4.8.

In the plots of La versus Ce and La versus Sm it can be observed that four of the samples from region A are tightly grouped together while the St Mary's Isle sample is isolated at a higher concentration position. The samples from regions B and C are grouped together at a lower concentration position, with the notable exception of the Port William silt sample from region B. This pattern is consistent with that observed in the Masuda-Coryell plots. Another striking feature of these plots is the very good

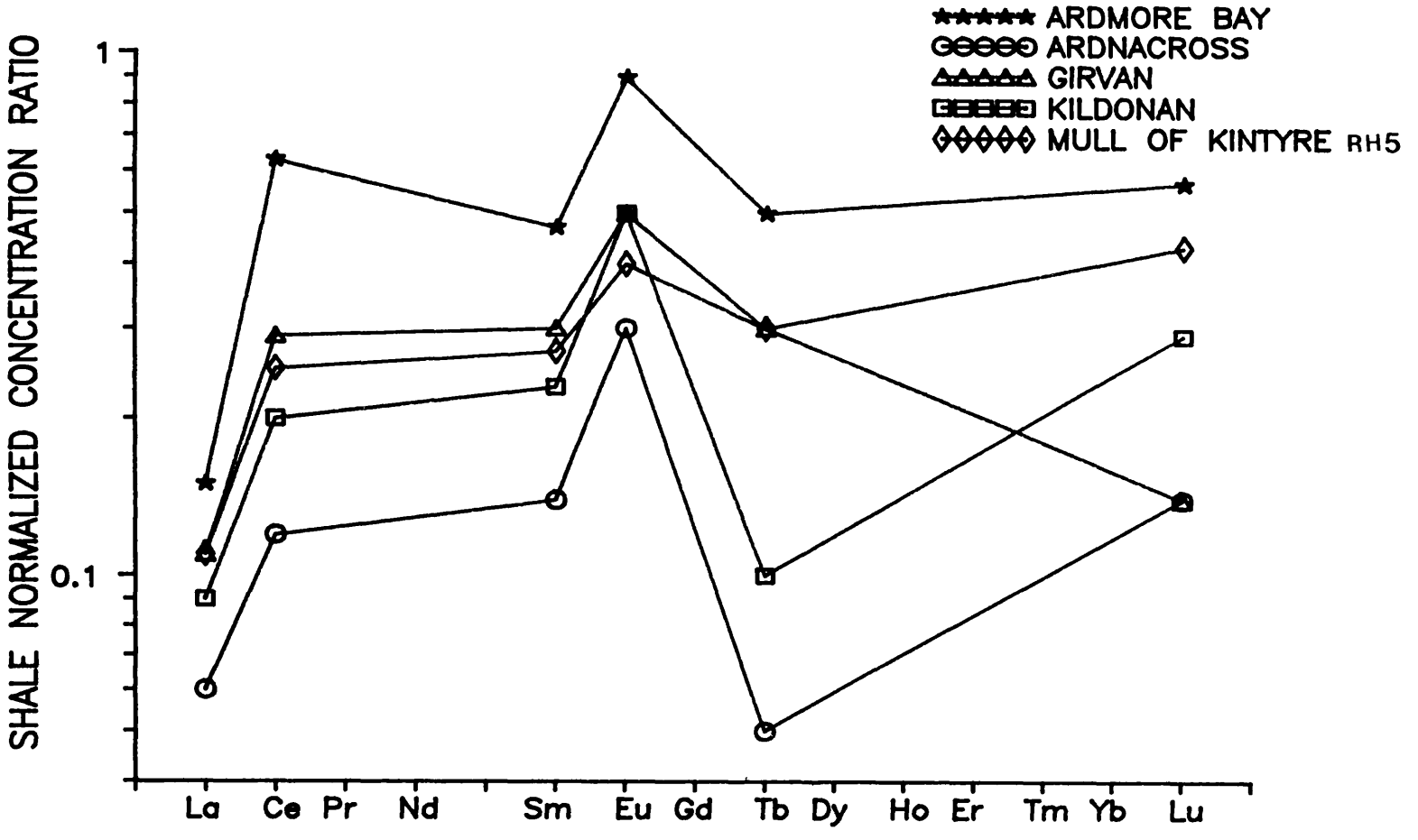

Figure 4.5 Masuda-Coryell plot for intertidal sediment samples from Region C (Figure 1.13)

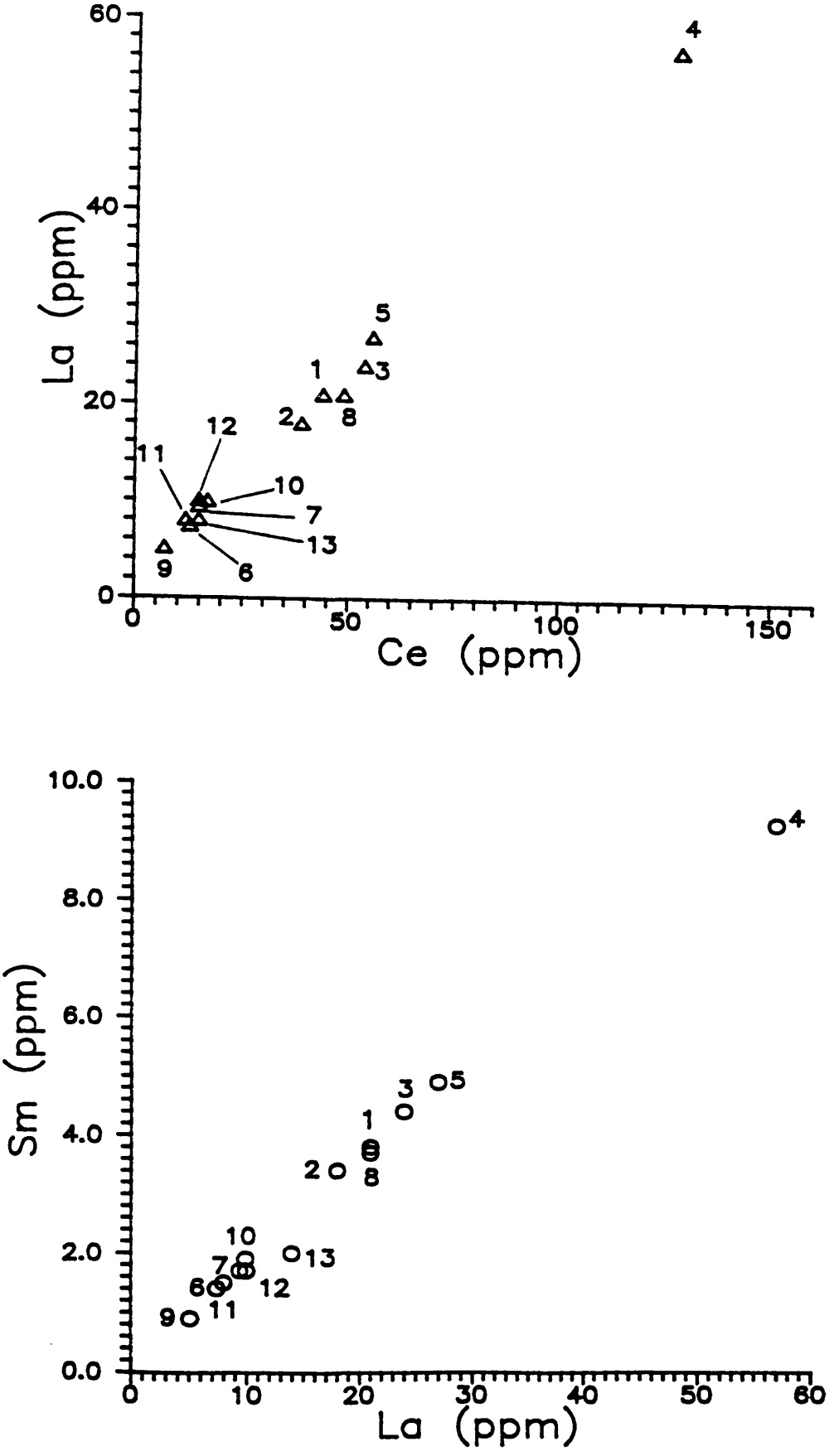

Figure 4.6 Element concentration versus element concentration plots for intertidal sediment samples from Regions A, B and C. Samples code relate to Figure 1.13 and Table 3.4.

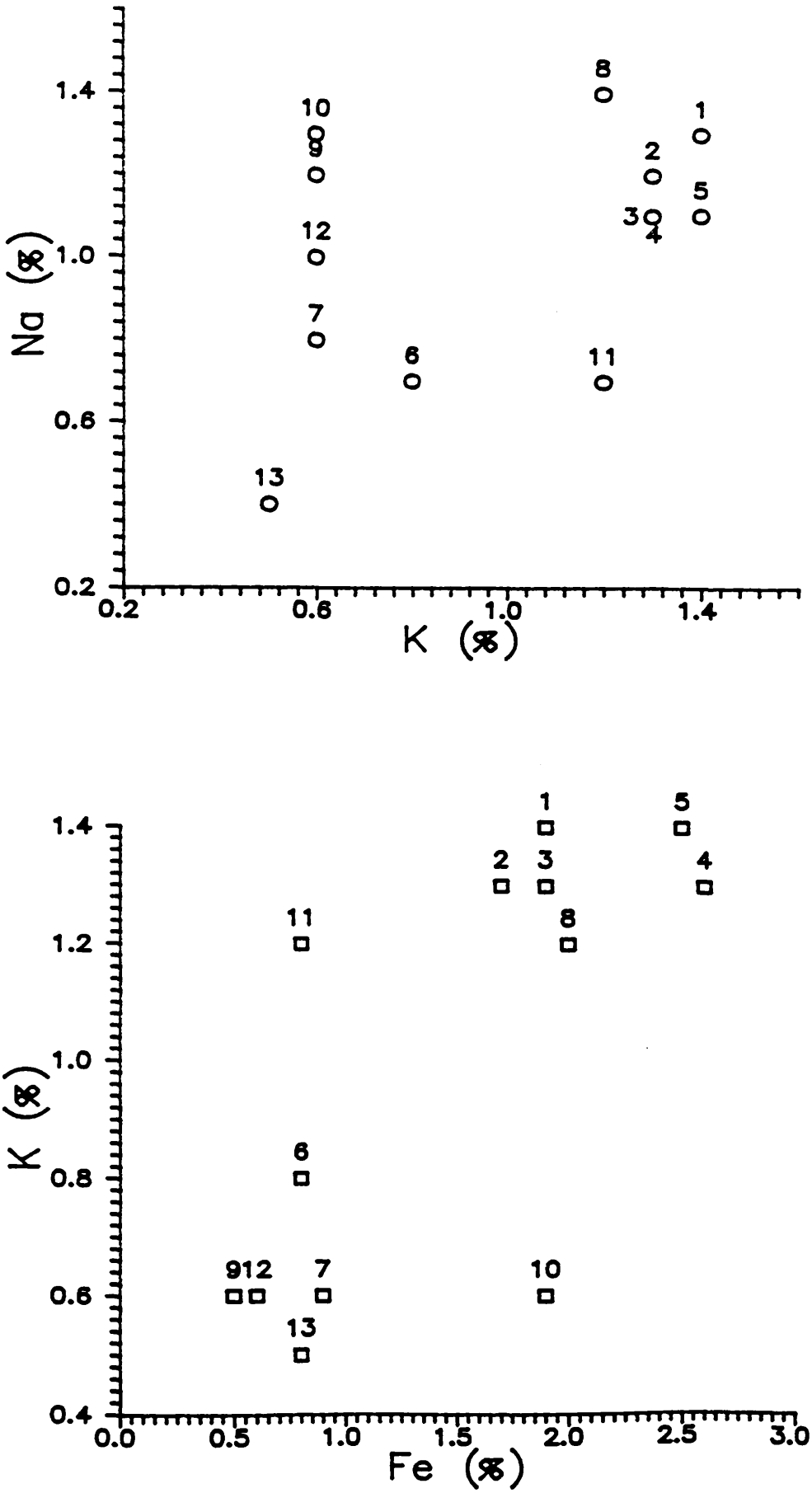

Figure 4.7 Element concentration versus element concentration plots for intertidal sediment samples from Regions A, B and C. Sample codes relate to Figure 1.13 and Table 3.4.

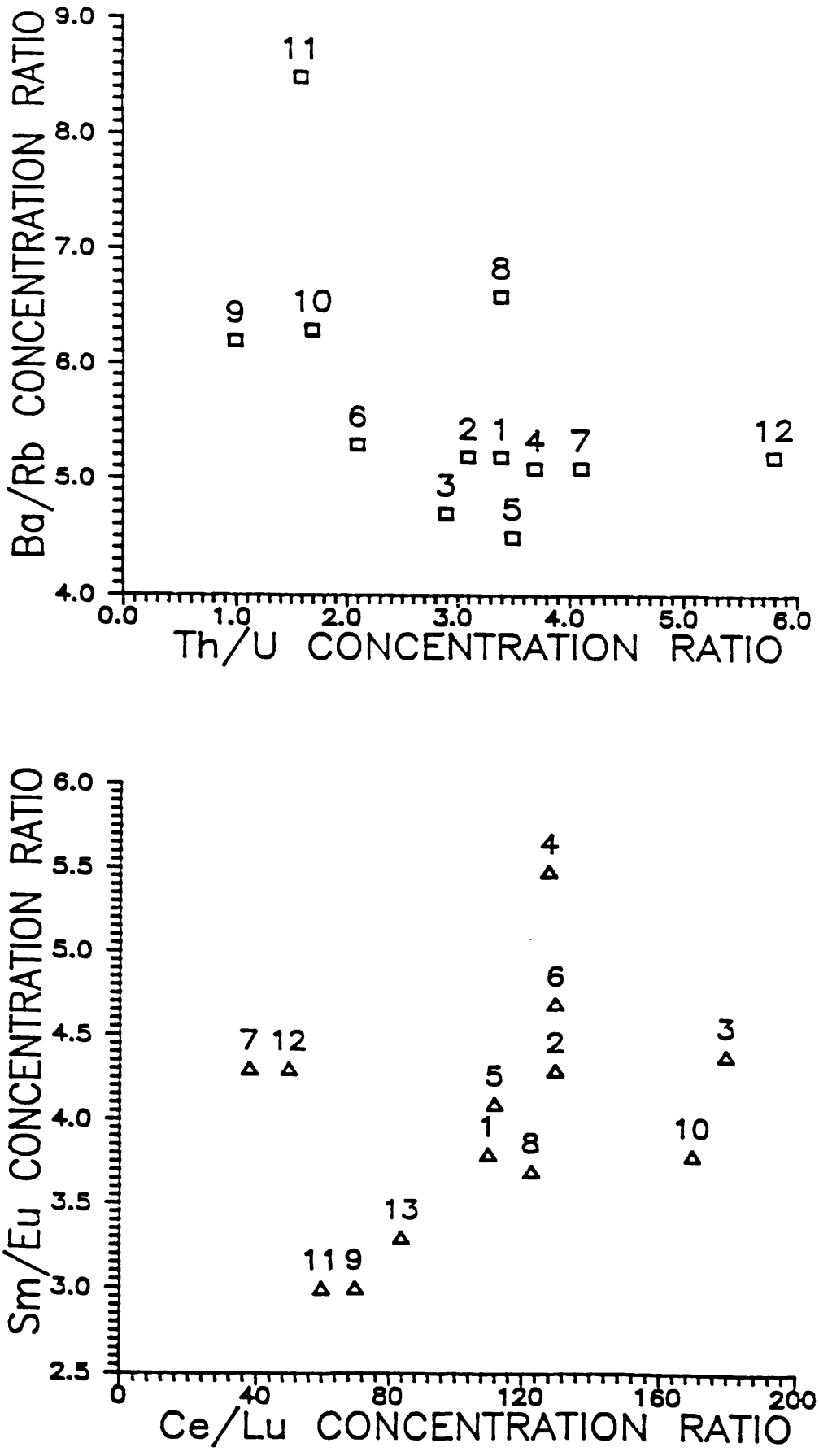

Figure 4.8 Element concentration ratio versus element concentration ratio plots for intertidal sediment samples from regions A, B and C. Sample codes relate to Figure 1.13 and Table 3.4.

linear correlation observed between the rare earth element concentrations in the total sample set. This reflects the similar geochemical behaviour of these elements, giving similar ratios in different geological situations.

Similar patterns can be observed for other refractory elements as might be expected but, interestingly, similar conclusions also emerge from plots of concentrations of elements which might be expected to be more geochemically reactive. Thus the samples from region A are once again grouped together in the plots of Na versus K and K versus Fe with the St Mary's Isle sample now being included and once more, the Port William sample being positioned near this group. The other samples from region B and those from region C are distributed over a wider area at lower concentration positions in these diagrams.

The varying chemical properties of Fe, Na and K allow the fractionation of these elements from each other during geochemical reactions and this is reflected in the more random scatter of points in these diagrams relative to the highly linear relationships for La, Ce and Sm.

The plots of concentration ratios against each other allows more information to be included in a single diagram and this clearly has the potential to provide a more sensitive method of distinguishing samples from different sources since a greater number of characteristics is being employed. It can be observed that in the Ba/Rb against Th/U and Sm/Eu against Ce/Lu plots that the region A samples are again grouped together and that the region B samples now all lie much closer to the region A samples than to the group formed by the region C samples. Similar distributions can be observed for other concentration ratio plots.

From the above discussion it can be seen that the chemical analysis results are consistent with, and support, the

postulated particle associated radionuclide transport model, since both suggest that northward transport of silt in the Irish Sea affects region A, and to a lesser extent, region B but provide no evidence of this influence further north (eg. in the Firth of Clyde).

4.3 SKYREBURN BAY

Skyreburn Bay is one of a number of small sandy bays found on the north Solway Coast and the radionuclide content of the intertidal sediments of the bay has been studied over a period of about 10 years (MacKenzie and Scott, 1979; 1982a; b; 1984; MacKenzie et al, 1987; Nebbad, 1988) with previous results for analysis of ^{137}Cs in cores from the study area of the bay being summarised in Table 4.2. These results indicate that temporal variations in the vertical distribution of radiocaesium in the intertidal sediments of Skyreburn Bay are not related in any obviously direct way to the Sellafield liquid effluent discharge pattern and it has been suggested that the sediment radiocaesium profiles are instead related to variations in the composition of the heterogeneous sediment of the bay (MacKenzie and Scott, 1982b).

In the present study three additional intertidal sediment cores from Skyreburn Bay were analysed to extend the above work, in particular by analysis of one of the cores for plutonium isotopes and excess ^{210}Pb (measurements which were not generally performed in the previous work). These three cores, given the codes SBC831, SBC851 and SBC852, exhibited compositions typical of the bay (section 1.2.b) consisting throughout of a heterogeneous mixture of silt, sand, shell fragments and organic matter in the form of small pieces of seaweed. One notable exception to this was the presence of a band of sediment of visually finer composition (mainly silt) between the depths of 9 and 15 cm in core SBC831. Moreover, as shown in Table 3.5 the organic content of this

Depth (cm)	Collection Date										
	17.10.79	18.4.80	25.9.80	22.6.81	8.12.81	1.6.82	10.10.82	1.6.83	13.12.83	27.6.84	20.6.86
0-3	478	788	445	535	350	367	298	345	351	294	109
3-6	657	543	538	938	448	389	366	310	331	318	106
6-9	762	353	1343	848	428	496	738	1084	306	300	111
9-12	950	462	417	350	392	1040	447	1560	341	324	112
12-15	793	832	647	388	927	1053	422	4200	312	1082	127
15-18	742	502	113	175	1135	866	413	423	253	3495	138
18-21			63	240	534	496	398	343	289	1331	142
21-24			42	130	322	128	223	337	280	709	145
24-27			27	57	227	53	116	269	258	460	113
27-30			14	38	278	15	42	143	210	309	120
30-33			12	45	120		9	87	132	164	99
33-36			4	30	60				68	132	92
36-39				1	28				38		119
39-42				1	25						70
42-45											43
45-48											28
48-51											17
51-54											9
54-57											5
57-60											2
60-63											1

TABLE 4.2: ^{137}Cs concentrations (Bq kg^{-1} dry weight) in Skyreburn Bay sediment profiles (MacKenzie pers. comm.)

section of the core was greater than 25% whereas the organic content of other sections was in the range 0.8 to 4.8%. The results for analysis of the three cores are presented in Tables 3.5, 3.6, 3.7, 3.8 and 3.9.

Considering the results for core SBC831, it is initially worth noting that the surface radionuclide activity ratios are consistent with the particle transport mechanism discussed above. The concentration profiles of radiocaesium, plutonium and americium (Figure 3.3) are characterised in each case by a pronounced subsurface maximum at 12 to 15cm depth (corresponding to the depth of the band of high organic content silt) with a very sharp lower slope, but a more gentle gradient above the maximum. The radionuclide activities at the maxima are all an order of magnitude higher than any corresponding results previously reported for Skyreburn Bay and are more akin to values for fine silts in the Irish Sea in the 1980's than to typical results for sandy sediments in this area.

On first sight it might be assumed that the shapes of these radionuclide profiles relate simply to temporal variations in the quantities of radionuclides discharged from Sellafield as a consequence of the deposition of successive layers in an accumulating sediment, each of which is contaminated in proportion to the immediately preceding level of discharge from Sellafield. On this basis, the pronounced subsurface maxima in radionuclide concentrations at 12 to 15 cm depth in the core would correspond to the mid 1970's maximum in the Sellafield discharge. However, the previous work at this site (MacKenzie and Scott, 1979, 1982b) has suggested that transient, but intense, reworking of the sediment takes place and can affect the sediment to as much as half a metre below the surface. These authors further suggested that the structure of radionuclide concentration profiles within the mixed section is determined by heterogeneity of the sediment rather than by

a simple accumulation process. It was therefore necessary to consider in detail both of these opposing possibilities.

In considering the "continuous accumulation" hypothesis, the most basic approach that can be taken in attempting to interpret the radionuclide vertical distributions is simply by direct comparison of the shapes of the sediment concentration profiles with the shapes of the plots of the temporal variations in the quantities of radionuclides discharged from Sellafield. To illustrate this, plots of the radionuclide concentration profiles are shown in Figure 4.9 along with corresponding data for the Sellafield discharge for the appropriate period. In these graphs, the scale for the time axes for the Sellafield discharge data are shown as years before 1983 and the vertical scale is selected to correspond to a sedimentation rate of 1.5 cm y^{-1} (derived by the assumptions that the maximum activities at about 13.5cm depth correspond to the maximum discharges from Sellafield in 1974 and 1975). This allows direct comparison of the Sellafield discharge data with the sediment profiles. From these graphs it is apparent that there is some general similarity between the shapes of the sediment radionuclide concentration profiles and those of the corresponding discharge data plots but detailed comparison reveals several significant differences, namely: (a) the position of the americium maximum in the sediment core is too high relative to the corresponding maximum in the discharge (although this distinction is at the limit of resolution of the sampling frequency used for sectioning the sediment) (b) the radiocaesium and plutonium peaks are too narrow in the sediment profiles relative to those in the discharge data plots and (c) there is no subsidiary maximum in the sediment radiocaesium profile corresponding to the 1971 subsidiary maximum in the Sellafield discharge. A similar conclusion emerges even if decay corrected (on the basis of the assumed sedimentation rate) ^{137}Cs values are used at depth in the sediment profile. Thus some

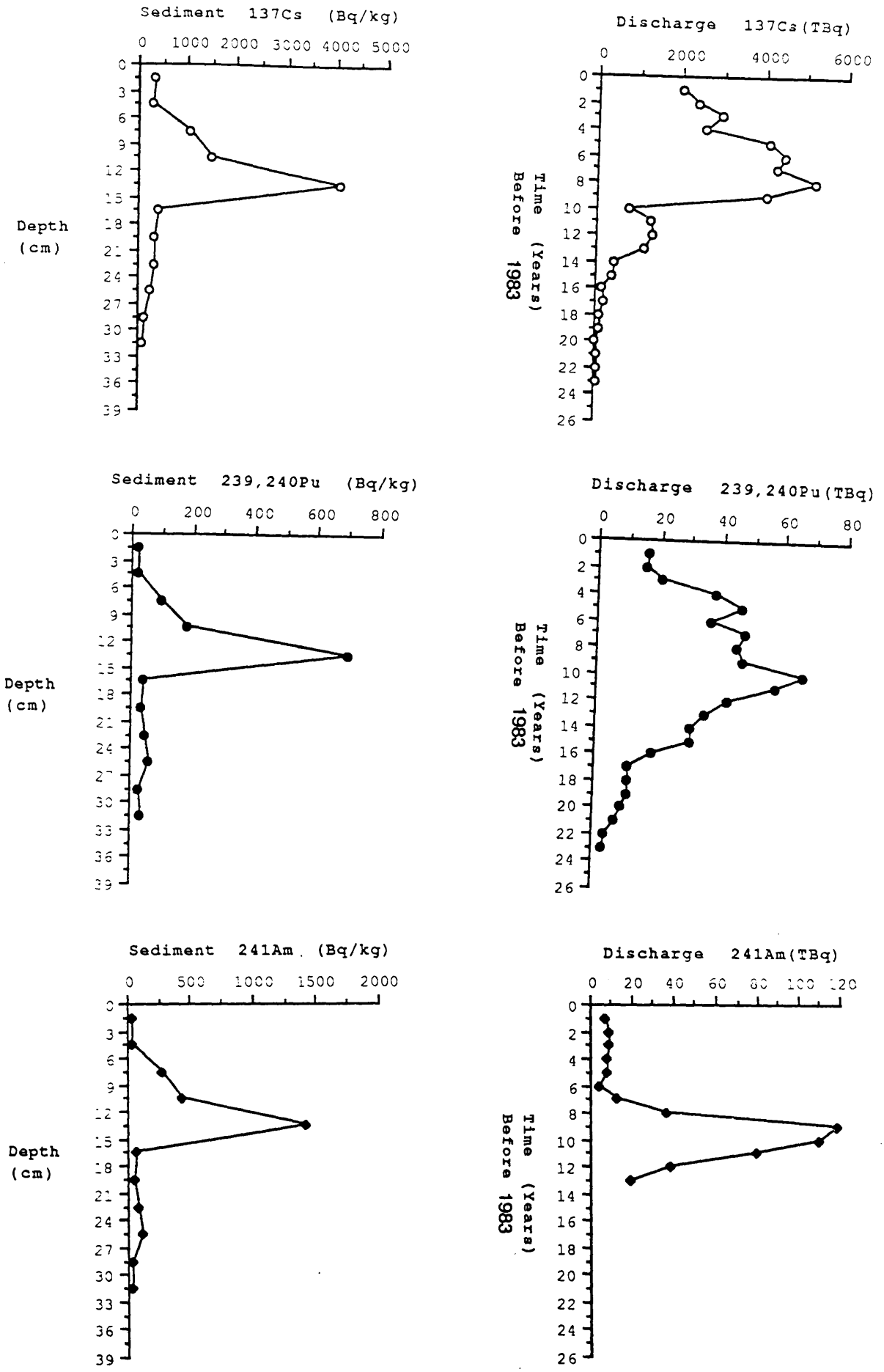

Figure 4.9 Radionuclide concentrations and corresponding Sellafield discharge data normalized to a sedimentation rate of 1.5cm y-1 for core SBC831

inconsistencies are apparent between the shapes of the sediment concentration profiles and the shapes of the plots of the Sellafield discharge data.

Furthermore, if continuous deposition of sediment contaminated in proportion to annual Sellafield discharges was the process operating then the radionuclide activity ratio profiles in the sediment might be expected to show similar shapes to those of plots of the temporal variations of the corresponding ratios in the Sellafield discharge, with the actual values observed for the ratios in the sediment obviously differing from those of the discharge in accordance with some function of the K_D's of the nuclides concerned.

The activity ratio data for core SBC831 are shown along with the corresponding discharge data in Figure 4.10 from which it is clear that the general shapes of the corresponding pairs of graphs do not show a good match for any of the activity ratios. Furthermore, the $^{137}Cs/^{241}Am$, $^{137}Cs/^{239,\ 240}Pu$ and $^{241}Am/^{239,\ 240}Pu$ activity ratios fall within the range 2.4 to 9.9, 2.8 to 19.3 and 0.5 to 2.8 respectively whereas the corresponding ranges of activity ratios in the Sellafield discharge are 7.0 to 1211.6, 1.6 to 153.9 and 0.1 to 2.56 respectively. It is thus apparent that the activity ratio data for the discharge exhibit a much wider variation on a percentage basis than do the sediment values and, while K_D considerations can be invoked in an attempt to explain the observation of different values for radionuclide activity ratios in the sediment from those in the discharge, they do not explain the much smaller percentage variation of activity ratio in the sediment than that of the discharge. Indeed, a steady state system with an accumulating sediment directly influenced by the discharge might well be expected to show a similar percentage variation of activity ratios to the discharge.

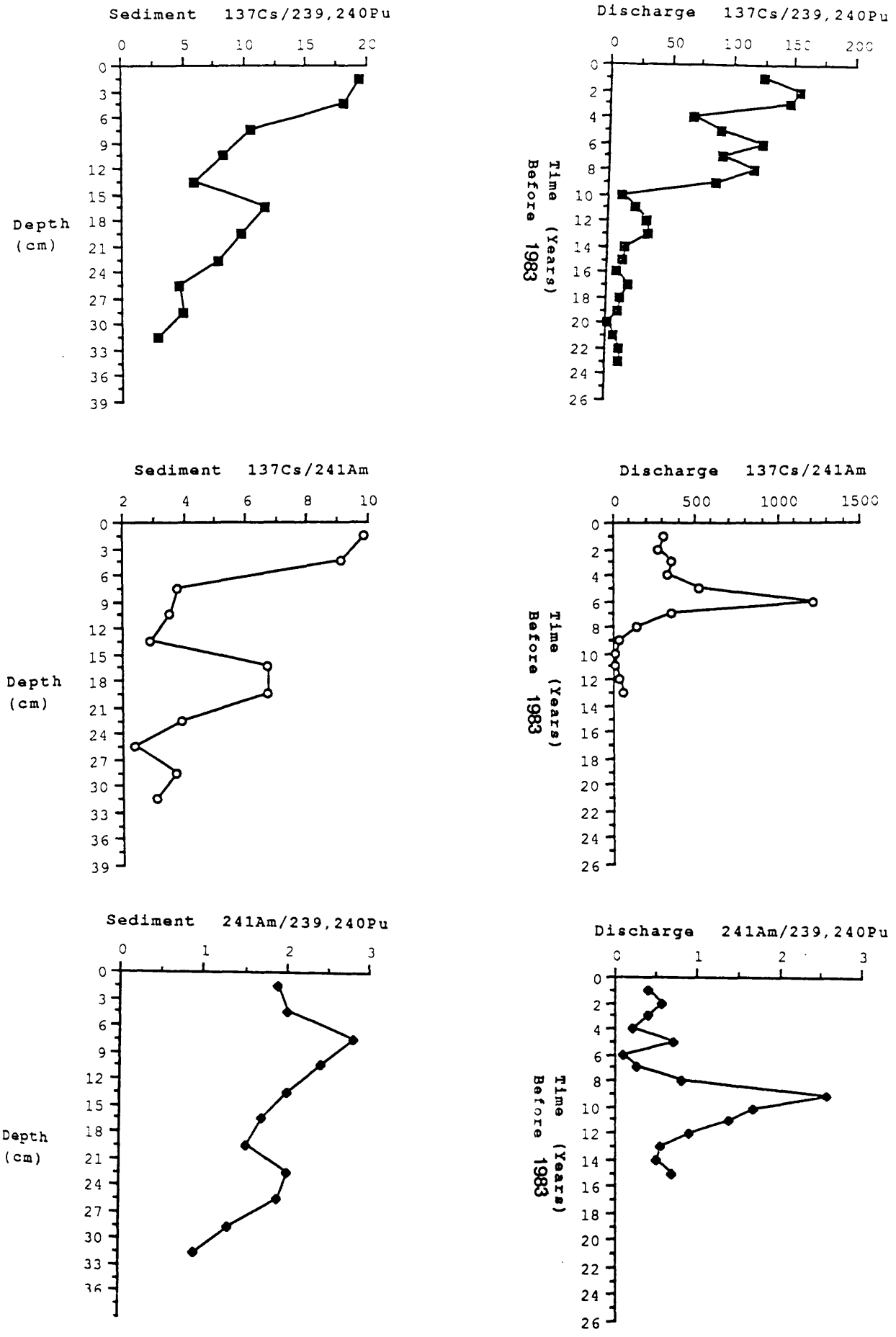

Figure 4.10 Radionuclide activity ratios and corresponding Sellafield discharge data normalized to a sedimentation rate of 1.5 cm y^{-1} for core SBC831.

The relatively small range of activity ratios for the sediment in conjunction with variations in specific activity values of over two order of magnitude in fact results in a strong linear correlation in the activities of radiocaesium, americium and plutonium at different depths in the sediment (eg the linear correlation coefficients for ^{137}Cs versus ^{241}Am, ^{137}Cs versus $^{239,240}Pu$ and ^{241}Am versus $^{239,240}Pu$ are 0.995, 0.987 and 0.997 respectively). This is a highly significant observation since no such strong linear correlation applies to these radionuclides in the data recording annual discharges from Sellafield. The respective correlation coefficients for ^{137}Cs versus ^{241}Am, ^{137}Cs versus $^{239,240}Pu$ and ^{241}Am versus $^{239,240}Pu$ for the Sellafield discharge data are -0.0763, 0.676 and -0.31. Thus only ^{137}Cs and $^{239,240}Pu$ show any evidence of being linearly correlated, and the degree of correlation is much poorer than is observed in the sediment of core SBC831. This clearly indicates that the vertical distribution of radionuclide in the sediment of this core does not bear a simple relationship to the historical record of the Sellafield discharge, indicating that simple accumulation is almost certainly not occurring. Moreover, the observed linear correlation observed for the radionuclides in the sediments must have been caused by some environmental process influencing the radionuclides after discharge.

In addition, if the actual values of the activity ratios observed for the sediment are compared with those of the discharge in the light of probable K_D values, a further inconsistency emerges. For example, the $^{241}Am/^{239,240}Pu$ activity ratio values for the sediment above 30cm depth are all greater than one and the near surface values lie in the range 1.9 to 2.8 whereas the corresponding Sellafield discharge $^{241}Am/^{239,240}Pu$ activity ratio values are all lower than one (in the range 0.10 to 0.57). Thus since it is generally accepted that virtually all of the americium and almost all of the plutonium discharged from Sellafield

remain within the Irish Sea sediment and that americium and plutonium in the Irish Sea have reported K_D's of about 10^6 and 10^5 respectively, it is clear that the observed near surface $^{241}Am/^{239,\ 240}Pu$ activity ratios for the core cannot be directly related to recent Sellafield discharges. The $^{241}Am/^{239,\ 240}Pu$ ratio of 1.9 for the surface sample of core SBC831 means that recently discharged effluent in the sediment is mixed to a large extent with high $^{241}Am/^{239,\ 240}Pu$ discharges of the mid 1970's. Moreover the time integrated value for the $^{241}Am/^{239,\ 240}Pu$ activity ratio for the discharge to 1982 was 1.2 so that the higher value of 1.9 for this ratio in the surface sediment indicates either that mixing is incomplete or else that plutonium is retained at a lower efficiency than americium by these sediments.

The $^{137}Cs/^{239,\ 240}Pu$ activity ratios for core SBC831 lie in the range 2.8 to 19.3 whereas the corresponding Sellafield discharge ratios lie in the range 1.6 to 153.9. Thus the $^{137}Cs/^{239,\ 240}Pu$ activity ratios observed for the sediment are significantly higher than those which might be predicted on the basis of the discharge data and K_D values of the order of 10^3 and 10^5 for radiocaesium and plutonium respectively (Edgington, 1981; IAEA, 1985).

Similarly even if intense mixing of new and old effluent is assumed, the $^{137}Cs/^{239,\ 240}Pu$ activity ratio of 19.3 for the surface sample of this core is too high relative to the time integrated $^{137}Cs/^{239,\ 240}Pu$ activity ratio of 61.4 for the Sellafield discharge up to 1982 in conjunction with K_D considerations.

It could be argued that the higher than expected $^{137}Cs/^{239,\ 240}Pu$ ratios in the Skyreburn Bay Sediments are the result of preferential solution transport of radiocaesium to this area relative to plutonium. For this to be true the surface sediment of the Irish Sea would have to exhibit an increase in $^{137}Cs/^{239,\ 240}Pu$ ratio with increasing distance from

Sellafield (as discussed in section 1.3.7). However, intertidal silts throughout the Irish Sea in 1983 all exhibited similar $^{137}Cs/^{239,\ 240}Pu$ activity ratios in the range of 2.0 to 5.6 (MAFF, 1984) with no significant difference between Cumbrian and Solway values. It is also relevant that more recent work by Baxter et al (1989) demonstrated that surface offshore silts in the Irish Sea also show $^{137}Cs/^{239,\ 240}Pu$ activity ratios in the range 1.1 to 1.8 with no systematic variation with increasing distance from Sellafield.

Similarly there was no obvious geographical trend in the $^{137}Cs/^{239,\ 240}Pu$ ratio results reported for intertidal sands throughout the Irish Sea in 1983 (MAFF, 1984) but the sands exhibited a wider range of $^{137}Cs/^{239,\ 240}Pu$ activity ratios and generally higher values than the silts (eg range of 5.2 to 19.7 reported by MAFF, 1984). Caution must be employed in discussing this difference between sands and silts since different processes may be operating in these different types of sediment and the observed difference may be related to one or a combination of the following possibilities: (a) the K_D value assumed for radiocaesium in the Irish Sea may be too low, (b) the K_D value assumed for plutonium may be too high, or (c) in addition to particulate transport, solution transport of caesium may affect sands to some extent.

The $^{137}Cs/^{241}Am$ activity ratios in the sediment of core SBC831 vary within the range 2.4 to 9.9 whereas the corresponding Sellafield discharge activity ratio data lie in the range 7.0 to 1211.6. Thus the sediment ratio values are significantly higher than would be expected if K_D values of 10^3 and 10^6 respectively are assumed for radiocaesium and americium. This incompatibility also applies even if mixing is assumed to have affected the effluent, since the surface sample of the core has a $^{137}Cs/^{241}Am$ activity ratio of 9.9 which is clearly too high in comparison with the K_D values

and the time integrated $^{137}Cs/^{241}Am$ activity ratio of 54 for the Sellafield discharge to 1982. As discussed above in the context of the $^{137}Cs/^{239,\ 240}Pu$ activity ratio the apparent excess of ^{137}Cs relative to ^{241}Am in the Solway sediments could be taken to suggest preferential solution transport of caesium to this area. Once again, however, intertidal silts throughout the Irish Sea showed relatively constant $^{137}Cs/^{241}Am$ activity ratios in the range 2.2 to 6.0, MAFF (1984). Once again, the more recent work by Baxter et al (1989) which reported a range of $^{137}Cs/^{241}Am$ activity ratios of 1.1 to 1.5 for Irish Sea subtidal silts with no systematic variations with increasing distance from Sellafield can be used to argue against the preferential solution transport of the Sellafield radiocaesium to this area.

However, as with the $^{137}Cs/^{239,\ 240}Pu$ activity ratio, intertidal sands in the Irish Sea showed a wider variation and higher values of $^{137}Cs/^{241}Am$, activity ratio (eg range of 4.6 to 24.0, reported by MAFF, 1984) than silts. Once more, a number of possible causes could be invoked to explain these observations, namely: (a) the assumed K_D value for caesium may be too low, (b) the K_D value assumed for americium may be too high, or (c) solution transport of radiocaesium to sands may be operating to some extent.

It is therefore not possible to derive a single unambiguous conclusion from the above discussion of the $^{137}Cs/^{239,\ 240}Pu$ and $^{137}Cs/^{241}Am$ activity ratios.

Further evidence indicating the nature of sediment supply and mixing processes in Skyreburn Bay can be derived from the $^{134}Cs/^{137}Cs$ and $^{238}Pu/^{239,\ 240}Pu$ activity ratios. The $^{134}Cs/^{137}Cs$ activity ratio in the SBC831 sediment profile is relatively constant from the surface to a depth of 18-21cm, below which ^{134}Cs suddenly drops below the detection limit. This constancy of the $^{134}Cs/^{137}Cs$ activity ratio suggests

either that all of this sediment was deposited at the same time or, perhaps more likely, that the sediment is subject to efficient mixing (on a timescale relative to the 2.05y half-life of ^{134}Cs) to a depth of 18 to 21cm, with a marked decrease in the efficiency of mixing below this depth.

Decay correction of the radiocaesium activity to the values which would have applied at the time of deposition on the basis of the sedimentation rate generated by the continuous accumulation model yields a value of 1.8 for the $^{134}Cs/^{137}Cs$ activity ratio at a depth of 18 to 21 cm whereas the values for the discharge in the corresponding years, 1971 and 1972 (on the basis of the assumed 1.5cm y^{-1} sedimentation rate), were 0.18 and 0.17 respectively and the highest $^{134}Cs/^{137}Cs$ ratio ever observed in the discharge was in fact only 0.25. Thus the $^{134}Cs/^{137}Cs$ ratio data are also incompatible with a simple accumulation model and suggest efficient (relative to the 2.05y half life of ^{134}Cs) mixing of the radiocaesium in the sediment to a depth of about 20cm in this core.

The $^{238}Pu/^{239,\ 240}Pu$ activity ratio values for this core (Figure 3.4) show relatively constant values (0.22 to 0.25) from the surface down to 15cm and slightly lower values (0.19) from 15 to 21cm. Below this there is a sharp discontinuity with values dropping to about 0.07. The $^{238}Pu/^{239,240}Pu$ ratio values of 0.19 to 0.25 which were observed in the upper section of the core (above 21cm) are too low relative to the corresponding Sellafield discharge values (which were in the range 0.27 to 0.34) to be consistent with simple transport and deposition and require a substantial degree of mixing either before deposition at this site or within the core. Below 21cm the $^{238}Pu/^{239,\ 240}Pu$ ratio profile shows much lower values reflecting very early Sellafield discharge $^{238}Pu/^{239,\ 240}Pu$ activity ratios and indicating that the sediment is accumulating and at this depth in the profile is not subject to intense mixing. It is also significant that the high $^{238}Pu/^{239,\ 240}Pu$ activity ratio values are

observed to a depth of 18-21cm which corresponds to the depth of ^{134}Cs penetration into the sediment.

The radiocaesium and plutonium isotope activity ratios for core SBC831, taken in conjunction with the above discussion of radionuclide activity ratios, the existence of the pronounced subsurface radionuclide concentration maxima and the large and irregular changes in the radiocaesium profiles observed for other sediment cores collected from this location at different times (Table 4.2) provides strong support for the system involving transient deposition, reworking and resuspension proposed by MacKenzie and Scott (1982b) for these sediments. Such a regime would be consistent with the high tidal energy of the Solway Firth which can visually be observed to give rise to very high suspended particulate loads in the water and to result in the movement of significant banks (up to 50cm depth) of sand and shell material in this area. This conclusion is also supported by the work of Nebbad (1988) who observed constant excess ^{210}Pb activity to a depth of about 40cm in an intertidal sediment core from Skyreburn Bay indicating mixing to this depth. Below this level, exponential decay of excess ^{210}Pb as a function of depth was observed to occur, giving a calculated sedimentation rate of 0.68 cm y^{-1}.

On the basis of the present study plus previously reported work, it is therefore apparent that the high radionuclide activities observed at 13.5cm depth in core SBC831 are not directly related to the high levels of discharge from Sellafield in 1974 and 1975 and more probably were caused by the influx of a fine silt of high radionuclide content from further south in the Irish Sea. This is supported by the fact that this silt had not been efficiently mixed within the sediment column and it is probable that it had been deposited not long before the time of collection of the core, since such high concentrations of Sellafield waste radionuclides had not previously been observed in Skyreburn

Bay, even in 1982 (Table 4.2).

Finally, considering the excess ^{210}Pb results for core SBC831, the activities were observed to decrease exponentially with depth from the surface and the plot of ln (excess ^{210}Pb) versus depth shows a good linear fit (r = 0.91) as shown in Figure 3.4. The sedimentation rate calculated by application of a constant initial concentration calculation to this profile is 0.29cm y^{-1} which clearly does not agree with any suggestion of the maxima in the sediment radionuclide distribution corresponding to the mid 1970's or to the $^{134}Cs/^{137}Cs$ activity ratios if a decay correction is applied on the basis of this sedimentation rate. In addition this sedimentation rate cannot be equated with the total depth of penetration of Sellafield waste radionuclides in the sediment of 33-36 cm since this depth would correspond to an age of approximately 100 years which is obviously not possible. Once again, therefore, it is apparent that simple accumulation is not occurring in the Skyreburn Bay sediment and it must be concluded that the ^{210}Pb distribution is probably the result of a complex process possibly involving accumulation and downwards mixing of ^{210}Pb in the sediment.

Evidence in support of this is provided by the linear plot of the excess ^{210}Pb versus depth (Figure 3.3) which shows excess ^{210}Pb decreasing exponentially to the same depth to which high values of the $^{238}Pu/^{239,\ 240}Pu$ ratio and detectable ^{134}Cs were observed (ie 18 to 21cm). Below this depth, excess ^{210}Pb values are low, in most cases being near the limit of detection. It is also noticeable that the structure of the ^{210}Pb and $^{238}Pu/^{239,\ 240}Pu$ profiles are similar, again suggesting that the ^{210}Pb profile is a product of mixing. Moreover, the timescale of mixing implied by the ^{134}Cs distribution suggests that this is not a long term, steady state mixing of ^{210}Pb but reflects a single input of sediment with a higher than average ^{210}Pb content shortly

before the date of collection of this core, followed by relatively rapid downwards mixing. This core is therefore anomalous in a number of ways, in that in the section above 15cm depth there is evidence of recent deposition of excess ^{210}Pb, Sellafield waste nuclides and organic matter all at about an order of magnitude higher than normally encountered in Skyreburn Bay. The implications of this is the recent addition, probably in 1982, of some abnormal type of sediment to the bay, possibly as the result of storm action. This material appears to have been deposited in a heterogeneous manner with a number of distinct strata in the depth range 0 to 21cm and there is evidence of subsequent partial mixing of these different layers.

The following general conclusion can therefore be derived from the above discussion of core SBC831.

(a) simple accumulation is not occurring.

(b) the results, in particular for the actinides, are generally consistent with the particle associated transport mechanism of Sellafield waste but there is some evidence that solution transport of radiocaesium may also be of some significance for Solway Firth sands.

(c) rapid mixing (relative to the two year half-life of ^{134}Cs) occurs within the sediment of the bay to a depth of 21cm in core SBC831 (although deeper mixing depths have been reported for other cores from the bay (MacKenzie and Scott, 1982a; b; 1984; Nebbad, 1988).

(d) below 21cm in core SBC831, little or no mixing occurs and the effects of accumulation can be observed.

(e) contaminated silt from further south in the Irish Sea can be transported to and deposited in the bay.

(f) the K_D value appropriate to uptake of caesium in Irish Sea sediments may be greater than the assumed value of 10^3 or the corresponding K_D values of plutonium and americium may be lower than the assumed values, with the former being the more probable.

Only gamma spectroscopy analysis was performed on cores SBC851 and SBC852 so only radiocaesium and americium data are available for these cores.

Unlike core SBC831, the SBC851 radionuclide profiles (Figure 3.5) showed no subsurface maxima and the concentrations of radiocaesium and ^{241}Am were much lower than those of core SBC831. Also the ^{134}Cs and ^{241}Am in core SBC851 showed a lower degree of penetration into the sediment (6 and 9cm for ^{134}Cs and ^{241}Am respectively), while ^{137}Cs was detected down to 40cm. Once again the ^{241}Am and ^{137}Cs profiles do not bear any obvious relationship to the Sellafield discharge historical record.

The clear differences in radionuclide vertical distributions between core SBC831 and core SBC851 is consistent with variations previously reported for this bay by MacKenzie and Scott (1982a; b) and are consistent with the concept discussed above of the sediment of the bay being highly heterogeneous and being subject to transient transport, deposition, resuspension and mixing processes.

The surface sample in core SBC851 shows a $^{137}Cs/^{241}Am$ activity ratio of 4.5 which is clearly consistent with the particle associated transport model and is similar to other intertidal sand sites throughout the Irish Sea (e.g. range of 4.6 to 10.9 reported by Ministry of Agriculture, Fisheries and Food (MAFF, 1986). The radionuclide activity ratio profiles for core SBC851 can be treated similarly to those of core SBC831 and the following conclusions emerge:

1. the radionuclide activity ratio for the surface sample indicates that particle associated transport is the dominant mechanism of supply of Sellafield waste radionuclides.

2. the $^{134}Cs/^{137}Cs$ activity ratios suggest surface mixing (in this case to a depth of only 6cm).

3. the $^{137}Cs/^{241}Am$ activity ratios show a narrower percentage variation than do the corresponding values for the discharge.

4. the ^{137}Cs and ^{241}Am concentrations at different depths in the core once more show a very strong linear correlation ($r = 0.999$) which would not be expected on the basis of variations of the Sellafield discharge with time or the known geochemical behaviour of these species.

5. the $^{137}Cs/^{241}Am$ activity ratio values are again too high relative to the Sellafield discharge values in conjunction with K_D considerations.

Comparison of the results for SBC831 and SBC851 suggests that this particular sampling location may have been subject to erosion between the dates of collection of the two cores (by the strong tidal current of the area or storm action) since no subsurface radionuclide concentration maxima were observed for core SBC851.

Finally, considering the results for core SBC852 only a limited amount of information can be derived from this core since only ^{137}Cs and ^{241}Am data are available. By application of the argument developed above for core SBC831, the following observations can be made for core SBC852.

1. the radionuclide concentration profiles are dissimilar to those of SBC851 but have some similarity with those of SBC831

2. the $^{137}Cs/^{241}Am$ activity ratio at the surface is consistent with the particle associated transport model.

3. caesium and americium concentration values at different depths are again strongly linearly correlated ($r = 0.83$)

4. the shapes of the radionuclide concentration and activity ratio profiles (Figure 4.11) in this core could be taken as being similar to those of the pattern of temporal variations in the Sellafield discharge but the percentage variation of the $^{137}Cs/^{241}Am$ activity ratio is too small relative to that in the discharge.

5. the actual values for the $^{137}Cs/^{241}Am$ activity ratios are once more too high relative to the discharge values and accepted K_D's.

Considering the three sets of results for Skyreburn Bay in the present work, along with the previously reported work for this site, it can be concluded that particle associated transport of radionuclides to the bay is the dominant mechanism of supply of Sellafield waste radionuclides but that solution transport of radiocaesium may be significant to some extent for sands. The sediment of the bay consists of at least a two component system with a lower layer which is subject to very little mixing being overlain by a layer of variable depth and heterogenous composition which is subject to reworking by transient erosion, transport and deposition processes. Upon initial deposition, partial physical sorting can give rise to a heterogeneous vertical structure in the upper layer which is then subject to

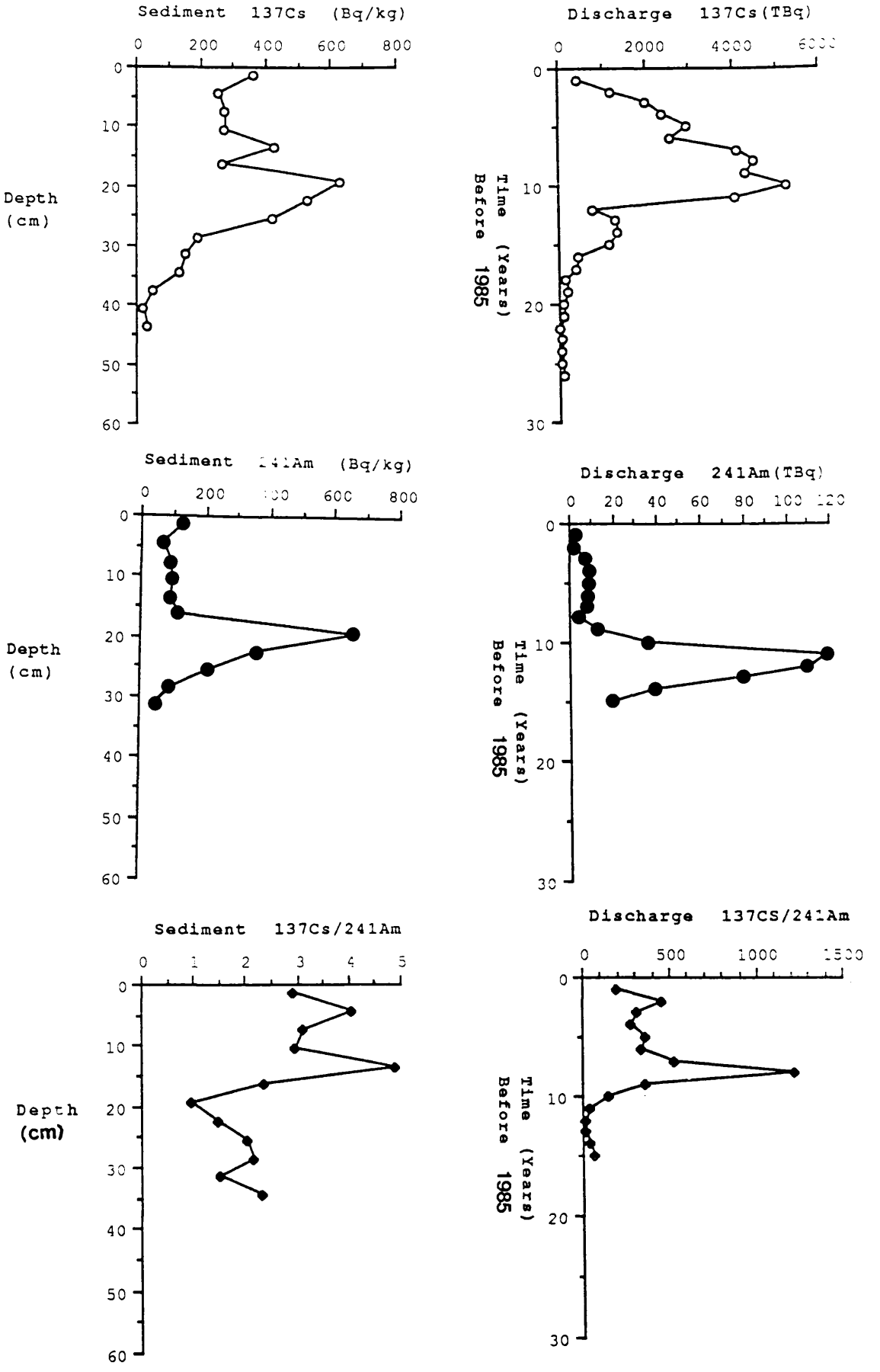

Figure 4.11 Radionuclide profiles and corresponding Sellafield discharge data normalized to a sedimentation rate of 2cm y^{-1} for core SBC852.

mixing. Active transport of sediment to the bay from further south in the Irish Sea is apparent, particularly in the very high activity silt observed in core SBC831.

The sediment supply, mixing and reworking system governing the distribution of Sellafield waste radionuclides in Skyreburn Bay is thus highly complex and if a similar degree of complexity applies at other intertidal sites in the Irish Sea, this could explain the difficulties experienced in previous work attempting to describe such processes (eg Aston and Stanners, 1981; MacKenzie and Scott, 1982b; 1984).

In this part of the study, the applications of manmade radionuclides and ^{210}Pb as tracers failed to provide accumulation rates but did provide useful information about the sedimentary mixing, erosion and transport processes occurring in the bay.

4.4 NETHERCLIFTON MERSE: SUPPLY MECHANISM, INVENTORY AND SURFACE SEDIMENT CONCENTRATIONS OF SELLAFIELD WASTE RADIONUCLIDES

One of the primary objectives of this part of the study was to investigate the mechanism of transport of Sellafield waste radionuclides to the Solway Firth Merse areas and, in order to achieve this, a similar approach to that described above for intertidal sediments (see section 4.2) and based upon the model of MacKenzie et al (1987) was adopted.

Surface sediment samples were analysed from two flood plain sites of the Solway Firth namely, Netherclifton and Wigtown Martyr's Stake (Figures 1.8 and 1.9), both of which are situated in region A (east of Burrow Head) as classified by MacKenzie et al.

Firstly, considering the Netherclifton site, two types of samples were obtained here, namely (a) a set of surface

samples (<1cm depth) collected every 5m along a 55m transect running inland from the Southwick water (see section 2.1.4) and (b) two samples for inventory determination consisting of 10cm x 10cm square sections sampled in two depth increments of 0 to 15cm and 15 to 30cm. The analytical results for these samples are shown in Tables 3.8, and 3.9 respectively, from which it is immediately apparent that the concentrations of radiocaesium, ^{241}Am and plutonium isotopes can be significantly higher in these surface merse sediments than in samples from adjoining intertidal regions, consistent with the generally fine silty composition of the merse sediments.

The isotope and nuclide ratios indicate that Sellafield waste is the dominant source of manmade radionuclides along the complete length of the transect. Moreover, $^{241}Am/^{239,240}Pu$ activity ratios show values greater than unity along the complete transect and from 0 to 25m the $^{137}Cs/^{241}Am$ and $^{137}Cs/^{239,240}Pu$ ratios are less than 10. These values are consistent with the particle associated transport model and are in good agreement with corresponding ratios reported by MacKenzie et al (1987) for intertidal sediment for region A (section 1.3) and also with those obtained for intertidal sediment for this region in the present study (section 4.2).

The samples from 25 to 55m show $^{137}Cs/^{241}Am$ ratios in the range 5.1 to 10.4 consistent with particle associated transport, but have $^{137}Cs/^{239,240}Pu$ ratios in the range 10.9 to 14.1. These $^{137}Cs/^{239,240}Pu$ ratios are slightly higher than expected for particle associated transport ratios but are still much lower than those which would be expected from solution transport of Sellafield waste radionuclides. These results therefore indicate that the particle associated supply mechanism established for intertidal sediments also applies to the merse deposits.

Supporting this suggestion, good linear correlations are observed for the transect results for ^{137}Cs - ^{241}Am, ^{137}Cs - $^{239,240}Pu$ and ^{241}Am - $^{239,240}Pu$ with respective linear correlation coefficients of 0.86, 0.85 and 0.96. The somewhat lower values for the ^{137}Cs - ^{241}Am and ^{137}Cs - $^{239,240}Pu$ correlations were caused by the samples from 30 to 55m which were grouped together above the line defined by the more seaward samples. The higher than expected ^{137}Cs activities for these samples could be the result of a different mechanism of supply of radiocaesium to this section or, perhaps, enhanced fallout influences. The $^{134}Cs/^{137}Cs$ activity ratios however show no indication of an enhanced fallout contribution.

The $^{238}Pu/^{239,240}Pu$ activity ratios ranging from 0.16 to 0.26 indicate the effects of mixing of recent and old discharged plutonium rather than representing recent discharge input for which a value in excess of 0.3 would be appropriate.

The $^{241}Am/^{239,240}Pu$ activity ratios observed in these samples range from 1.3 to 2.1 whereas the Sellafield discharge $^{241}Am/^{239,240}Pu$ ratio data since 1976 have been in the range 0.1 to 0.57. Prior to this, higher values of up to 2.56 were observed (Table 1.6). The $^{241}Am/^{239,240}Pu$ ratios for these sediments agree well with those reported above for intertidal sediment samples from the Solway Firth (Table 4.1) and with most other data reported for intertidal sediment of the Irish Sea over a relatively long time. For example, $^{241}Am/^{239,240}Pu$ ratios with values of 1.1 to 1.5 have been reported by MAFF (1977 to 1985) for intertidal sediment in the Solway area and values of 1.1 to 1.4 were reported by McDonald et al (1989) for river bank soils of the Solway coast. These authors also reported a range of $^{241}Am/^{239,240}Pu$ rates of 1.04 to 1.45 for offshore sediments in the Irish Sea. Finally, MacKenzie et al (1987) reported values of 1.2 to 2.8 for $^{241}Am/^{239,240}Pu$ ratios in intertidal sediments from this area.

Thus, ^{241}Am values are in general found to exceed those of $^{239,240}Pu$ throughout the Irish Sea intertidal and offshore sediments despite the fact that ^{241}Am discharges have been substantially lower than those of $^{239,240}Pu$ for over a decade. This again provides clear evidence of a high degree of mixing of recent and old wastes before deposition of contaminated sediment in the Solway intertidal areas.

On the basis of reported ^{241}Am and $^{239,240}Pu$ discharges (Cambray, 1982), a time integrated $^{241}Am/^{239,240}Pu$ ratio for the discharge (including grow in of ^{241}Am from ^{241}Pu) of 0.92 is obtained. However, ^{241}Am discharge data are not available for the period before 1970 but such discharges certainly took place. Thus, using the approximation proposed by Day and Cross (1981) for estimation of discharges of ^{241}Am prior to 1970, a total time integrated $^{241}Am/^{239,240}Pu$ ratio appropriate to 1986 of 1.22 can be calculated.

Thus, the observed range of $^{241}Am/^{239,240}Pu$ of 1.3 to 2.2 would mean that if 100% of the discharged ^{241}Am is assumed to remain in the Irish Sea then the amount of discharged $^{239,240}Pu$ retained would be in the range of 55% to 94%, with the mean sediment values of 1.6 corresponding to a 76% retention of $^{239,240}Pu$. Similar treatment of the integrated Sellafield $^{137}Cs/^{241}Am$ ratio of 50 relative to the observed sediment values of 3.1 to 10.4 implies that the percentage of ^{137}Cs retained would be in the range 6.2 to 20%, with the mean value of 5.7 corresponding to 11% retention.

These values are in good general agreement with the recognized behaviour of these radionuclides in the marine environment. In attempting to rationalize the detailed features of the surface transect it is necessary to consider the topography of the area, the main features of which are shown schematically in Figure 1.8, and in order to simplify the interpretation, the transect was considered as two distinct sections namely, (a) the intertidal and merse area

below the step and (b) the merse above the step. The most obvious general feature of the radionuclide activities along the transect is the pronounced maximum concentration of each of the nuclides analysed at 20m (Figure 3.7).

The results for determination of the percentage of organic matter and the percentage of the sediment of size fraction <75μm for the transect samples are also plotted in Figure 4.12 from which it is apparent that there is a strong inverse correlation ($r = -0.976$) between these two parameters, with a maximum organic content and minimum silt content at 45m.

In the section from 0m to 15m, all of the samples have a fairly similar composition of 55 to 65% silt and 5 to 12% organics. The samples at 0m and 5m show radionuclide activities similar to those of the intertidal sediment at this site whereas the samples at 10m and 15m show higher concentration of radionuclides than the above samples. The $^{134}Cs/^{137}Cs$ activity ratios systematically decrease on moving from the 0m to the 15m samples. In contrast, the $^{137}Cs/^{241}Am$, $^{137}Cs/^{239,240}Pu$ and $^{241}Am/^{239,240}Pu$ ratios all increase in this direction. This variation of the nuclide ratios suggests that with increasing height of the merse above the mean high water level, different sediment characteristics are observed which could be either time related, in the sense of flooding to different levels at different times, or particle size related if the height variation gives rise to different depths, or energies, of overlying water at any given time.

In the section from 20m to 45m the distributions of ^{137}Cs, $^{239,240}Pu$ and ^{241}Am are directly correlated with the silt content of the sediment, with correlation coefficients of 0.709, 0.948, 0.949 respectively and inversely correlated with the organic content (r values of 0.685, 0.898 and 0.802 for ^{137}Cs, ^{241}Am and $^{239,240}Pu$) which provides further evidence supporting the silt supply mechanism.

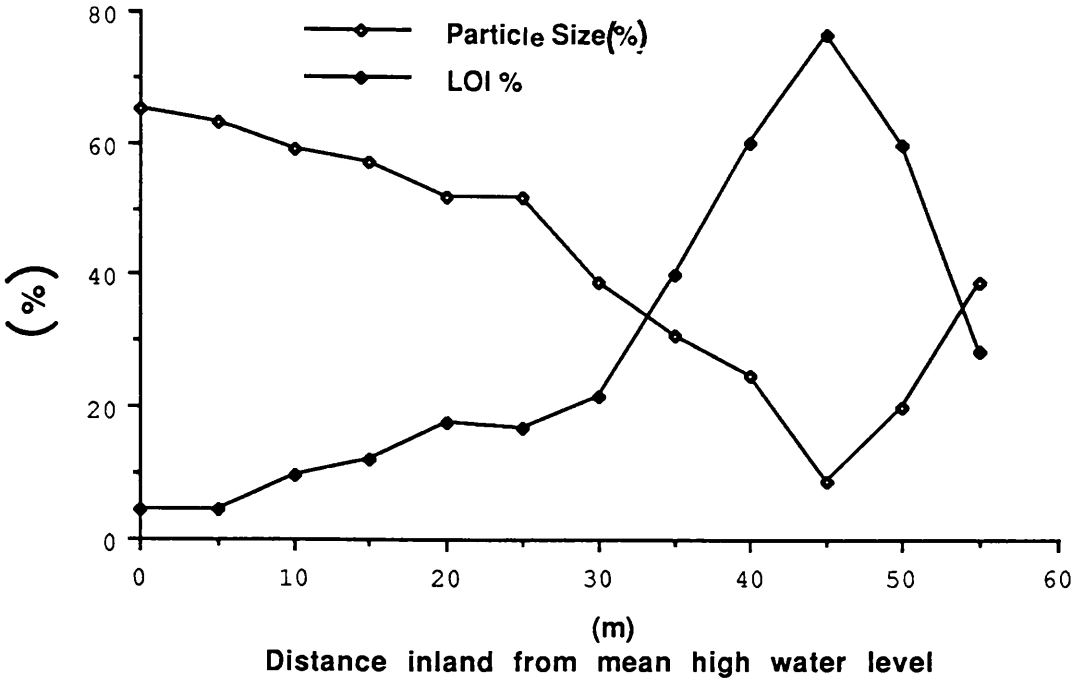

Figure 4.12a Plots of % organic matter and % of sediment in size fraction <75μm for the Netherclifton surface transect samples

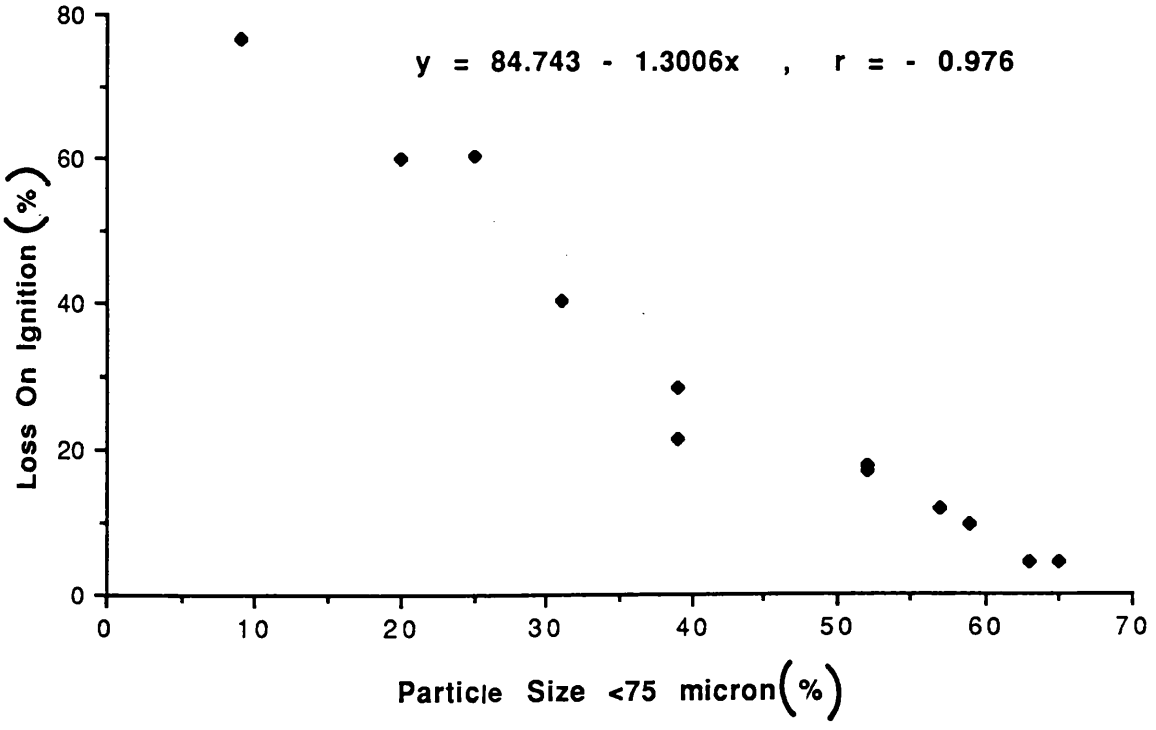

Figure 4.12b Correlation of % organic matter and % of sediment of size fraction <75μm for the Netherclifton surface transect samples

In the remaining three samples from 45m, 50m and 55m, the inorganic content of the sediment increases (Figure 4.12) but the Sellafield radionuclide activities show a continuous decrease. The material giving rise to the inorganic content is therefore not supplied from the Irish Sea but is more likely to be eroded material from the cliff marking the edge of the Criffel granodiorite being transported seaward by the general drainage of the area.

The radionuclide concentrations and isotope and nuclide activity ratios for the total transect generally suggest that the higher section, which is only flooded occasionally, has a surface sediment characteristic of a different 'age' of deposition to the lower section and further suggest either a particle size fractionation or else a variation in these ratios in the material that has been deposited in the Merse area over a timescale of about one year.

The samples obtained from the locations shown in Figure 1.8, in order to estimate the inventories of Sellafield waste radionuclides at this site were collected approximately one year after the Chernobyl accident, so that a correction for this contribution to the radiocaesium inventory had to be considered. The influence of Chernobyl fallout was however concluded to be negligible in these samples since the radiocaesium concentrations and the $^{134}Cs/^{137}Cs$ activity ratios show more or less similar values to characteristic Sellafield waste values obtained from samples from this site before the Chernobyl accident took place. For example, the surface transect average $^{134}Cs/^{137}Cs$ activity ratio before Chernobyl was 0.0093 ± 0.002 at the time of collection in March 1986 and the inventory samples show $^{134}Cs/^{137}Cs$ ratios in the range 0.007 to 0.008 and are thus effectively indistinguishable from the pre-Chernobyl values (even allowing for decay of ^{134}Cs between the two sampling dates).

This suggests that the Chernobyl radiocaesium has been highly efficiently leached out of these sediments, consistent with the above observations for Ardmore Bay and intertidal sediments from the Solway Firth. In contrast, the Sellafield radiocaesium remains bound to the sediments and behaves in the same way as the plutonium and americium associated with it. This argues for different speciations for the Chernobyl and Sellafield radiocaesium. Thus the Chernobyl radiocaesium appears to have been readily available with respect to leaching into seawater despite the high silt content of the sediment. In contrast, the Sellafield radiocaesium appears to be relatively strongly bound to the solid phase and a likely explanation for this could be that the radiocaesium is held inside organic or oxide coatings on the mineral grains preventing its release to solution. This has important implications for application of the K_D concept which would appear to be valid for the Chernobyl radiocaesium but not for the Sellafield radiocaesium since it does not exhibit reversibility with respect to sorption. It is also of interest that MacDonald et al (1989) reported Chernobyl ^{137}Cs inventories for soil samples collected from locations close to this site of about 1.4×10^4 Bq m^{-2}. This suggests that freshwater leaching may be much less efficient in removal of ^{137}Cs than salt water leaching from these soils.

As noted above for Skyreburn Bay (Section 4.3), the surface activity ratios cannot be readily related to the immediately preceding discharge data in conjunction with K_D considerations. Thus, the observed $^{137}Cs/^{241}Am$ and $^{137}Cs/^{239,\ 240}Pu$ activity ratios in the ranges 3.1 to 10.4 and 3.9 to 11.8 respectively are too high when compared with corresponding 1985 discharge ratio values of 203.1 and 125.0 and likely K_D values. As discussed above this casts doubt upon the values used for K_D in this case and lends support to the particle associated transport model.

The Sellafield waste radionuclide inventory results for the merse deposits at this site, shown in Table 3.9, reveal that more than 90% of the total waste radionuclide content is held in the top 15cm depth increment. Good agreement is observed between the radionuclide activities and inventories for the two sampling locations and the average total inventories of ^{137}Cs, ^{241}Am and $^{239,240}Pu$ of 5 x 10^4, 1.7 x 10^4 and 1 x 10^4 Bq m^{-2} respectively obtained for these samples are very similar to corresponding values reported by Baxter et al (1989) for Sellafield waste radionuclides in 0 to 30cm topsoil samples from similar areas on the Solway coast. For instance, these authors reported inventories of 1.8 x 10^5, 4.1 x 10^4 and 4.0 x 10^4Bq m^{-2} for ^{137}Cs, ^{241}Am and $^{239,240}Pu$ respectively for their sampling site closest to this area.

The isotope and nuclide activity ratios also show good agreement between the two sets of Netherclifton inventory samples as shown in Table 3.9. ^{134}Cs was not detectable in the lower 15cm section of either of the samples whereas the upper 15cm sections show $^{134}Cs/^{137}Cs$ activity ratios of 0.007 and 0.01. Similarly, the $^{238}Pu/^{239,240}Pu$ ratio in the sample NCST1 showed values of 0.18 and 0.12 respectively for the upper 15cm and lower 15cm segments, while in NCST2 the $^{238}Pu/^{239,240}Pu$ activity ratio in the upper section was also 0.18 but ^{238}Pu was below detection limit in the lower section. These isotope ratios are more similar to Sellafield integrated $^{134}Cs/^{137}Cs$ and $^{238}Pu/^{239,240}Pu$ activity ratios than to recent values for the discharge, but the lower samples exhibit older values while the upper samples show relatively more recent values. The nuclide ratios $^{137}Cs/^{241}Am$ (4.2 and 5.4), $^{137}Cs/^{239,240}Pu$ (3.6 and 3.9) and $^{241}Am/^{239,240}Pu$ (1.4 and 1.1) for the two upper sections are also similar in both sets of samples and are generally consistent with the particle associated radionuclide transport model. The lower 15cm samples show somewhat higher activity ratios but they are still very far from

those which would be produced by solution transport of the radionuclides. These higher values are therefore probably related to the early years of the Sellafield discharge.

4.5 THE VERTICAL DISTRIBUTION OF SELLAFIELD WASTE RADIONUCLIDES IN FLOOD PLAIN AND INTERTIDAL SEDIMENTS AT THE NETHERCLIFTON SITE

At Netherclifton, vertical profile samples were collected from both the intertidal zone and the merse at various distances from the sea. Considering first of all the intertidal profiles, NCC861 and NCS861, which were collected from two locations in the intertidal area about 6m apart (Figure 1.8), the ^{241}Am and $^{239,240}Pu$ concentration profiles for NCS861 show very similar patterns, with a subsurface peak at 8 to 10cm, below which concentrations decrease rapidly and fall below detection limit at 50cm depth (Figures 3.10 and 3.11). The corresponding ^{137}Cs concentration profile does not have the peak at 8 to 10cm depth but otherwise the general trend of the ^{137}Cs profile is similar to those of ^{241}Am and $^{239,240}Pu$ with a rapid decrease to reach non detectable levels below 50cm.

The nuclide activity ratios $^{137}Cs/^{241}Am$ and $^{137}Cs/^{239,240}Pu$ of less than 10 along with $^{241}Am/^{239,240}Pu$ ratios of greater than unity clearly suggest that the particle associated transport of Sellafield waste radionuclides is the dominant mechanism of supply of manmade radionuclides to these sediments on the basis of the arguments applied above. The $^{238}Pu/^{239,240}Pu$ activity ratio values in the range 0.05 to 0.12 which were observed below 4cm reflect old Sellafield discharge ratios (pre 1970) or possibly the influence of weapons testing fallout during the late 1950's and early 1960's. This indicates either that there has been negligible accumulation since then or else that there has been erosion of this area of sediment at some time. Erosion would be relatively probable at a location such as this, lying on the outer side

of a curve in the river ie. a high velocity and high energy position.

The ^{134}Cs results also suggest a similar conclusion since this nuclide is detected only in the surface 4cm and the $^{137}Cs/^{241}Am$, $^{137}Cs/^{239,240}Pu$ and $^{241}Am/^{239,240}Pu$ activity ratios all show a relatively systematic decrease with depth reflecting the Sellafield discharge pattern during the 1960's and early 1970's.

Reasonable linear correlations were obtained in this core between ^{137}Cs and $^{239,240}Pu$ and between ^{137}Cs and ^{241}Am activities, with correlation coefficients of 0.71 and 0.66 respectively. These correlation coefficients are poorer than those obtained for ^{241}Am and $^{239,240}Pu$ of 0.957 as the result of the sharper decrease in ^{137}Cs concentration with depth relative to those of ^{241}Am and $^{239,240}Pu$.

As discussed above in detail for the Skyreburn Bay sediment radionuclide profiles, this linear correlation would not be expected on the basis of the temporal variation in the Sellafield discharge or the known geochemical behaviour of these nuclides. This observation is therefore significant and could be taken to indicate that the radionuclides present at different depths in this profile have been derived from a single source of contaminated offshore sediment.

The samples from the NCC861 profile were analysed only by direct gamma spectroscopy and only radiocaesium and ^{241}Am data are consequently available. The ^{137}Cs and ^{241}Am profiles (Figure 3.12) show similar distribution patterns to each other with concentrations being relatively constant throughout the profile to a depth of 40cm but with higher concentrations in the lowest two sections. This indicates a discontinuity at about 40cm with old material lying below the fairly homogeneous upper layer. The $^{137}Cs/^{241}Am$ activity

ratios show very little variation (a linear correlation coefficient between ^{137}Cs against ^{241}Am of 0.974 was obtained) and are consistent with the particle associated transport model as discussed in sections 1.3 and 4.2.

^{134}Cs was detectable to a depth of 40cm in NCC861, with the $^{134}Cs/^{137}Cs$ activity ratio being almost constant throughout the 0 to 40cm depth range. This homogeneity of the top 40cm of the core suggests the deposition of a large amount of highly mixed sediment over a very short time.

Thus, if erosion has occurred at this location as suggested above by the results for core NCS861, the section below 40cm in this core profile could be the old erosion surface. If this suggestion is correct, the results imply that very different patterns of accumulation can occur over a very short distance in this system.

Considering next the results for section NCS862 (Table 3.12) which was located in the section of merse between the mean high water mark and the step at 15m at the Netherclifton site (Figure 1.8), the Sellafield waste radionuclide concentration profiles show a reasonable similarity to the Sellafield discharge pattern (Figure 4.13) with subsurface maxima at 50 to 55cm depth for ^{137}Cs and 65 to 70cm depth for ^{241}Am and $^{239,240}Pu$. The specific activities of these nuclides at the maxima are generally higher than those observed for merse surface samples at present. Also, unlike all of the other merse profiles at Netherclifton in which Sellafield waste radionuclides are confined to the top 15cm or so, the Sellafield radionuclides in the NCS862 section occur to more than 1m depth and even the short half life nuclide ^{134}Cs is detected to a depth of 70 to 75cm.

Taking initially the simplest approach to interpretation of the radionuclide activity profiles for NCS862, by relating the subsurface maxima in the sediment profiles to the mid

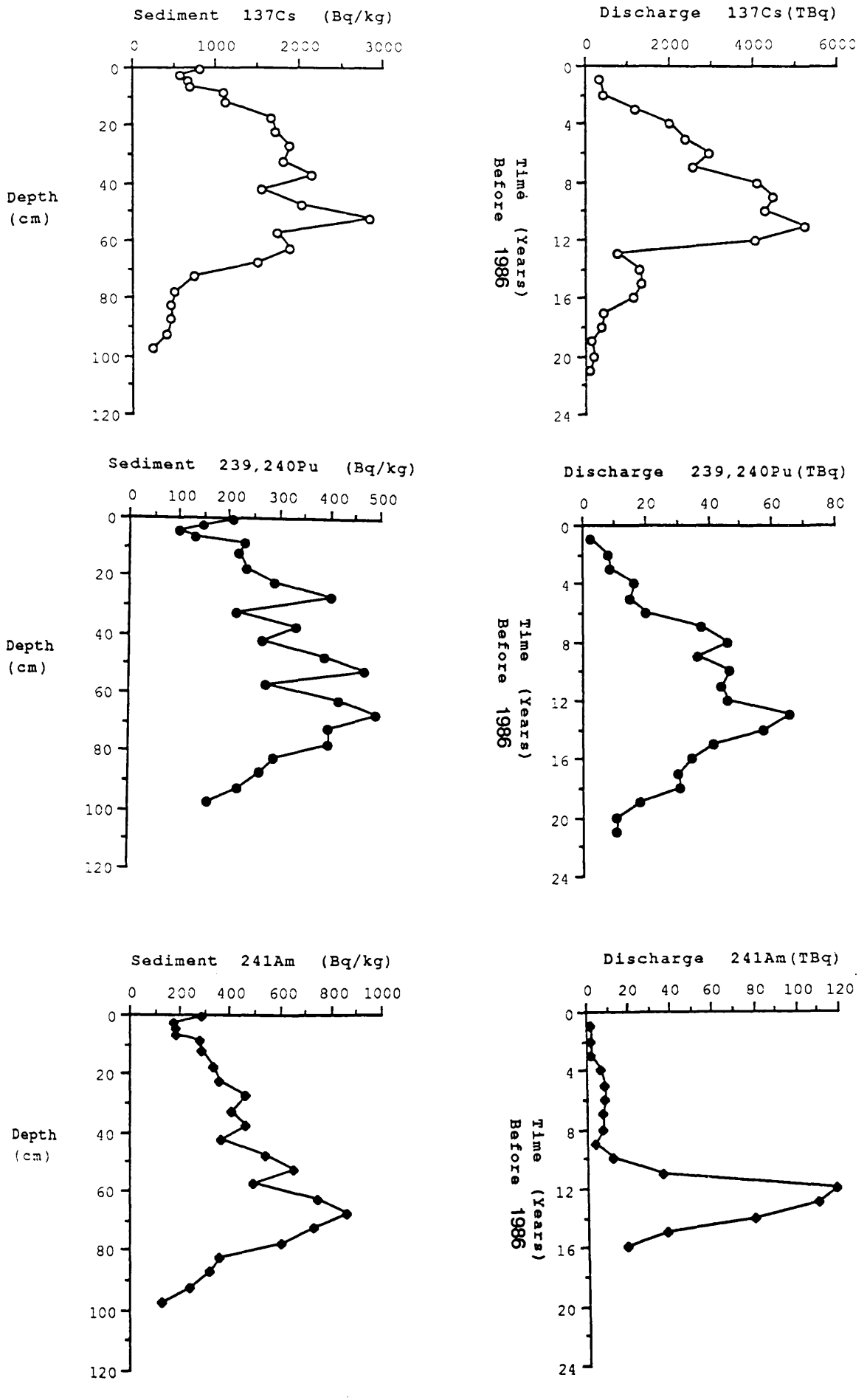

Figure 4.13 Radionuclide concentration profiles and corresponding Sellafield discharge data normalized to a sedimentation rate of 5cm y^{-1} for section NCS862.

1970's peak discharge rates from Sellafield gives accumulation rates of about 5cm y^{-1} from the ^{137}Cs and $^{239,240}Pu$ profiles and 5.4cm y^{-1} from the ^{241}Am profile, the accumulation rate being expressed here in cm y^{-1} (not mg cm^{-2} y^{-1}) since compaction is insignificant in this sediment. The profiles are plotted in Figure 4.13 along with the Sellafield discharge data normalized to a sedimentation rate of 5cm y^{-1} and generally a good match is observed between the Sellafield discharge patterns and the corresponding sediment profiles with appropriate correlation coefficients shown in Table 4.3, from which it can be seen that there is a better correlation between the sediment profile and the discharge data in the lower section of the profile (below the maxima in concentration) than in the upper section.

Thus the general features of the radionuclide distribution in these sediments do reflect the temporal variations in the Sellafield discharge pattern with a better agreement at depth rather than near the surface.

The $^{134}Cs/^{137}Cs$ activity ratios in this profile fall into two groups, with higher values in the range 0.012 to 0.019 in the section from 0 to 10cm depth, while below this, lower and fairly constant values in the range 0.005 to 0.008 are observed to a depth of 60cm and in deeper layers, $^{134}Cs/^{137}Cs$ ratios decrease rapidly to fall below detection limit at 75cm. Figure 4.14 shows a plot of the time corrected $^{134}Cs/^{137}Cs$ ratio and the corresponding Sellafield discharge data with the two sets of data normalized to a sedimentation rate of 5cm y^{-1}. These plots show that the time corrected ^{134}Cs appropriate to the section of the profile below 50cm attains values in excess of those reported for the discharge, suggesting that the implied sedimentation rate may be too high. However, values above 50cm for the decay corrected ratios are lower than those of the discharge, suggestive of mixing with older waste. Thus, while the

Depth (cm)	Discharged ^{137}Cs - Observed ^{137}Cs	Discharged ^{241}Am - Observed ^{241}Am	Discharged $^{239,240}Pu$ - Observed $^{239,240}Pu$
0- 55	0.455	0.649	0.560
55-100	0.627	0.816	0.912
0-100	0.640	0.520	0.723

Table 4.3: Radionuclide concentration correlation coefficient for samples from section NCS862, Netherclifton, (a) 0-55cm, (b) 55-100cm and (c) 0-100cm

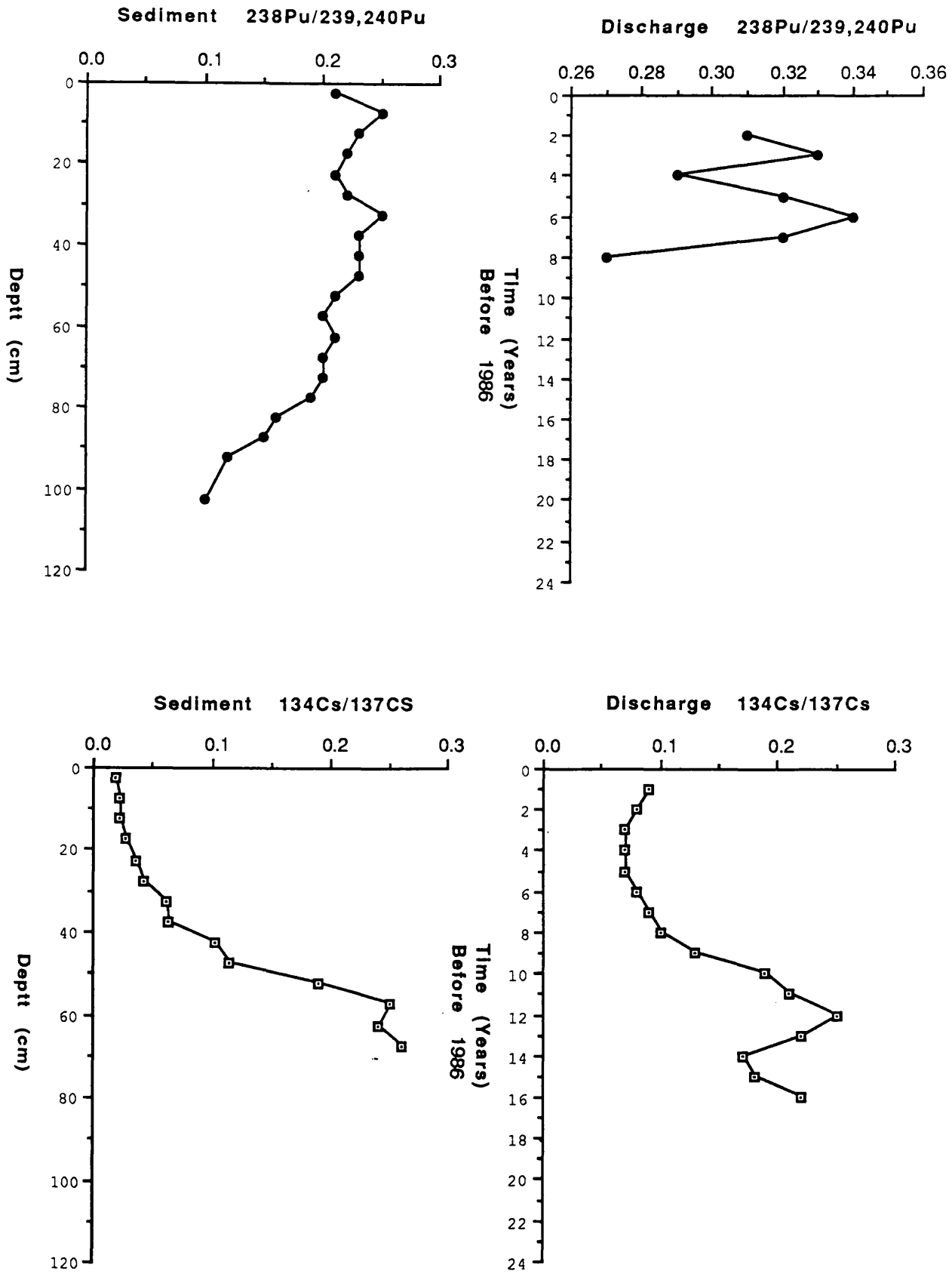

Figure 4.14 Decay corrected radionuclide activity ratio profiles and corresponding Sellafield discharge data normalized to a sedimentation rate of 5cm y^{-1} for section NCS862.

general trend of the decay corrected $^{134}Cs/^{137}Cs$ ratio plot is similar to that of the discharge, the two sets of data are not consistent with simple accumulation at a rate of 5cm y^{-1}.

The $^{238}Pu/^{239,240}Pu$ ratios for this core fall into three depth groups as follows. From 0 to 50cm the $^{238}Pu/^{239,240}Pu$ ratio is relatively constant in the range 0.20 to 0.23 whereas from 50 to 80cm slightly lower values of 0.17 and 0.19 are observed. From 80 to 100cm the ratio exhibits very low values in the range 0.09 to 0.14. The variations in time corrected $^{238}Pu/^{239,240}Pu$ activity ratios in the sediment show reasonable similarity to the trends of the discharge as shown in Figure 4.14, but since $^{238}Pu/^{239,240}Pu$ ratios were not reported for the discharge prior to 1978, insufficient information is available to draw any definite conclusion from this comparison.

It should, however, be mentioned that the time corrected ratios for the sediment above 65cm are significantly lower than those for the corresponding Sellafield waste, clearly demonstrating mixing with older discharges. It is also significant that at depths greater than 65cm the lower values for this ratio correspond to the values reported by Hetherington (1975) for surface intertidal sediments in Cumbria during the period up to the early 1970's. Thus the $^{238}Pu/^{239,240}Pu$ ratio data do provide support for rapid accumulation of this sediment but also reveal a high degree of mixing before deposition.

Plots of the sediment nuclide activity ratios $^{137}Cs/^{241}Am$, $^{137}Cs/^{239,240}Pu$ and $^{241}Am/^{239,240}Pu$ are shown in Figure 4.15 along with the corresponding discharge ratios, again using the 5cm y^{-1} accumulation rate to provide the time scale for the discharge data.

The $^{137}Cs/^{239,240}Pu$ ratios pattern in the sediment and the

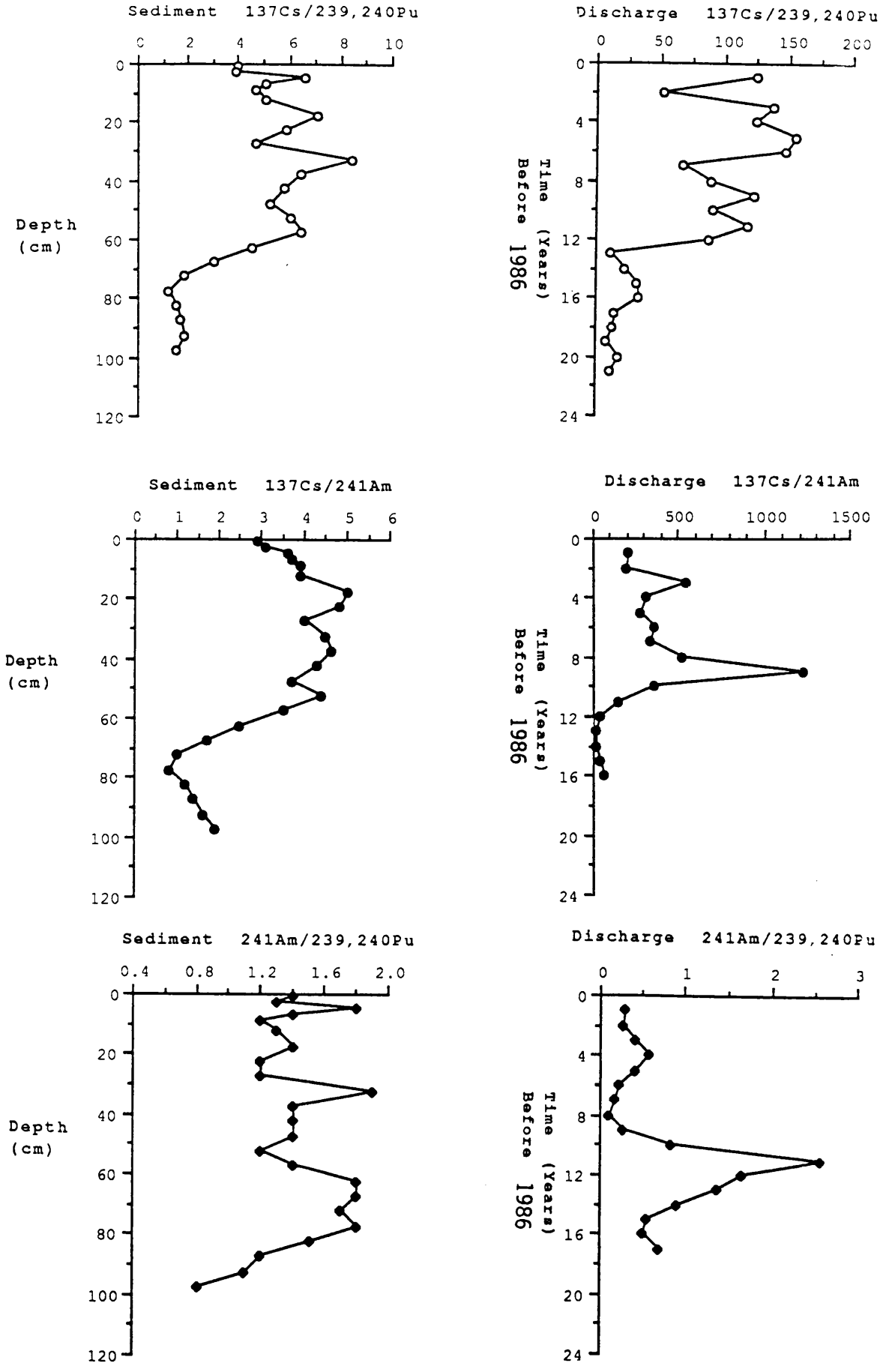

Figure 4.15 Decay corrected radionuclide activity ratio profiles and corresponding Sellafield discharge data normalized to a sedimentation rate of 5cm y^{-1} for section NCS862.

discharge do show a reasonable agreement on this basis but the $^{137}Cs/^{241}Am$ and $^{241}Am/^{239,240}Pu$ ratios patterns do not. However, the $^{137}Cs/^{241}Am$ and $^{137}Cs/^{239,240}Pu$ activity ratios for the sediment both show similar patterns to those of the time integrated ratios for the Sellafield discharge (Table 1.6).

Linear correlations between ^{137}Cs - ^{241}Am, ^{137}Cs - $^{239,240}Pu$ and ^{241}Am - $^{239,240}Pu$ over the length of the core produce respective correlation coefficient of 0.870, 0.850 and 0.927. Once again this linear correlation would not be expected on the basis of the temporal variation in the Sellafield discharge or the known geochemical behaviour of these nuclides. This observation is therefore significant and could be used as evidence for a single source of sediment to this area (as discussed in section 4.3). This provides strong evidence that the particle associated supply mechanism, demonstrated to be operating at present has probably been effective throughout the time of accumulation of this profile. However, the correlations between ^{137}Cs -^{241}Am and ^{137}Cs - $^{239,240}Pu$ below the activity maxima show lower values of 0.510 and 0.559 whereas above the maxima, values of 0.962 and 0.910 are obtained. The ^{241}Am - $^{239,240}Pu$ correlations above and below the maxima are 0.934 and 0.972 respectively.

These differences in the correlation coefficients in conjunction with those described above for comparison of the radionuclide activity profiles with the disharge pattern may indicate that, while particle associated transport dominates at present, solution transport, particularly of radiocaesium may have been of relatively more significance before the establishment of high levels of contamination in the Irish Sea sediments.

The ^{210}Pb profile for this core shows a good fit to an exponential decrease of activity with depth (ln activity against depth gives a linear correlation coefficient of 0.81) confirming that accumulation is occurring at this

location and giving a sedimentation rate of 4.3cm y^{-1} on the basis of a constant initial concentration calculation. This sedimentation rate is in good agreement with those derived from the manmade radionuclides profiles on the basis of relating the subsurface maxima to those of the discharge in the mid 1970's. Therefore, the ^{210}Pb results confirm the conclusion derived from the manmade radionuclide results that continuous accumulation is occurring at this particular location of the merse and also suggest that post depositional physical and biological mixing are not significant.

Thus there is excellent agreement between the natural and manmade radionuclide estimate of the sedimentation rate for this site, leaving little doubt that abnormally rapid accumulation is occurring at this location relative to other parts of the merse. This is consistent with the above suggestion of erosion of the intertidal profiles at this location and suggests that the step feature is the result of an erosion event, probably occurring in the early 1960's, which affected this part of the merse.

The final analyses of manmade radionuclides to be considered for the Netherclifton site are for sections NCS863 and NCS864 the locations of which, as shown in Figure 1.8, were at 15 and 29m inland from the mean high water mark respectively. NCS863 was sampled in 2cm intervals from the surface to 10cm and in 5cm intervals from 10 to 30cm and was analysed only for radiocaesium isotopes and ^{241}Am (Table 3.13). ^{137}Cs was found to a depth of 10cm while ^{241}Am was restricted to the top 6cm and for both nuclides, the profiles showed subsurface maxima at 2 to 4cm depth. If this profile shape is related to the peak Sellafield discharge during the 1970's a sedimentation rate of about 0.3cm y^{-1} is implied. Moreover, if the total depth of penetration of 10cm is taken to correspond to the early 1950's, a sedimentation rate of about 0.3cm y^{-1} is again

suggested. Also if an average of about 10 years is taken for the 2 to 4cm section, a decay corrected $^{134}Cs/^{137}Cs$ value of 0.18 is obtained, reasonably consistent with the discharge value. However, time correction of the 4 to 6cm $^{134}Cs/^{137}Cs$ activity ratio on this basis would give a value of about 3, too high for the Sellafield discharge and indicating some degree of mixing or diffusion of radiocaesium in this profile.

The 0 to 2cm $^{137}Cs/^{241}Am$ activity ratio of 5.3 is consistent with the particle associated radionuclide transport model (section 4.2).

NCS864 was sampled in 5cm increments down to 40cm and the samples were analysed for ^{238}Pu and $^{239,240}Pu$ in addition to direct gamma spectroscopy analysis for radiocaesium and ^{241}Am, the results being shown in Table 3.14. As with the results for NCS863, the Sellafield waste radionuclides in this core were confined mainly to the top 10cm and the observed concentrations were lower than those of NCS863, consistent with the pattern described above for the surface transect at this site. The total depth of penetration of Sellafield radionuclides of 10 to 15cm suggests a sedimentation rate of about 0.4cm y^{-1} at this location.

The uniform $^{238}Pu/^{239,240}Pu$ activity ratio of 0.15 for both the surface and the 5 to 10cm depth samples, however, suggests either that sudden deposition of this sediment occurred at some time during the late 1960's and earlier 1970's with no significant accumulation since then or else that mixing is occurring, with the latter being the more likely.

The nuclide activity ratios $^{137}Cs/^{241}Am$, $^{137}Cs/^{239,240}Pu$ and $^{241}Am/^{239,240}Pu$ once again show values in good agreement with the particle associated radionuclide transport model.

It is also apparent that the activity ratio data for the

discharge exhibit a much wider variation on a percentage basis than do the sediment values and while K_D considerations can be invoked in an attempt to explain the observation of different values for radionuclide activity ratios in the sediment from those in the discharge, they do not explain the much smaller percentage variation of activity ratio in the sediment than that of the discharge, as discussed in detail in section 4.3.

4.6 NATURAL DECAY SERIES RADIONUCLUDE STUDIES AT THE NETHERCLIFTON SITE

The final part of the study at the Netherclifton site was concerned with investigation of the distribution, and possible migration, of uranium within the merse sediments. The Netherclifton merse presents a particularly interesting situation in this context since there is a system of uranium mineralization veins (as indicated in Figure 1.8) at the edge of the Criffel granodiorite forming the boundary of the merse at this location (Miller and Taylor, 1966). This site is of considerable importance as the focus of a natural analogue study of processes of relevance to radioactive waste disposal (Hooker et al, 1986; 1987; Scott et al, 1990). This work has established that the mineralization veins in the cliff act as an effective source of uranium for groundwaters draining towards the merse but that most of the uranium mobilized in this way is subsequently taken up by anoxic organic deposits at the base of the cliff. The retention of uranium by these anoxic deposits is, however, incomplete and a small amount of uranium is consequently transported in solution into the merse sediments. Thus, it has been established that the small stream draining into the merse from the organic bog has ^{238}U concentrations in the range 0.03 to 0.19Bq l^{-1}. There is also evidence of an artesian input of groundwater at the base of the sediment with a ^{238}U activity of 0.26Bq l^{-1}.

In the present work, some of the samples collected for analysis of manmade radionuclides were also analysed for uranium and thorium isotopes and a sample of Irish Sea offshore surface silt (provided by P McDonald, SURRC) was similarly analysed for comparison with the merse samples.

The samples from the surface transect (running inland for 55m from the Southwick water as shown in Figure 1.8), exhibited major variations in ^{238}U activity which could be, in part, related to the topography of the merse (Table 3.15). Thus the lowest ^{238}U activity of 18Bq kg^{-1} was observed for the 0m sample which was collected from the intertidal zone. The 5, 10 and 15m samples from the area below the step showed slightly higher and fairly constant activities in the range 23.3 to 27.8Bq kg^{-1}. Above the step the ^{238}U concentration was found to increase exponentially from the 20m to the 45m sampling point, reaching a maximum activity level of about 1.1×10^{3}Bq kg^{-1} at 45m. Further inland, activities were lower at about 2.2×10^{2}Bq kg^{-1}. The highest uranium concentration was obtained for the sample closest to the stream draining from the organic bog, suggesting a direct influence of this source. The systematic decrease of ^{238}U concentration from 45m towards the sea suggests that the uranium being transported in solution in the surface drainage of the merse is subject to continuous removal to the sediment. The $^{234}U/^{238}U$ activity ratio for the transect samples varied from 0.89 to 1.06 but there was no obvious pattern in the variation. In contrast, the $^{230}Th/^{234}U$ activity ratio showed values significantly greater than unity in the samples from 0m to 25m and values well below one in the samples from 30 to 55m, the lowest value of 0.02 being observed at 45m, which was also the position of highest uranium concentration (Figure 3.15). The very low values for the $^{230}Th/^{234}U$ activity ratio in the landward section of the transect clearly demonstrate the deposition of uranium from groundwater and are consistent with the established geochemistry of uranium and thorium,

in that the uranium is undergoing transport and deposition in this system in the virtual absence of its daughter ^{230}Th. Moreover, the trend in $^{230}Th/^{234}U$ activity ratio is consistent with the above suggestion of continuous deposition of uranium as the surface drainage waters move towards the sea.

It has been established above by the use of the Sellafield waste radionuclides that the silts presently being deposited in the merse area are being transported from further south in the Irish Sea. In agreement with this, the results for the uranium and thorium isotope activities and ratios for the 0 to 15m samples were observed to be very similar to those of the Irish Sea surface sediment (Table 3.16).

The results of the Irish Sea sample were therefore taken to characterize the uranium/thorium properties of the silts being deposited in the merse and were regarded as a background level against which to observe any excess uranium (or thorium) deposition. The excess uranium activity was calculated by normalization of the results to the ^{232}Th and assumption that the activity ratio values observed for the Irish Sea sediment apply to any newly deposited silt in the merse. The results calculated in this way are shown in Table 4.4. If the 45m sample is excluded (on the assumption that it is anomalous due to the influence of the stream), the remaining results show an exponential decrease in excess ^{238}U on moving towards the Sea, with, as shown in Figure 4.16, the plot of ln (excess ^{238}U) versus distance having a linear correlation coefficient of 0.945. This indicates that removal of uranium from solution in surface groundwaters in the merse is a concentration dependent process and the exponential decrease in excess uranium concentration with distance is characterised by a removal, or retardation, coefficient of $0.0695m^{-1}$, corresponding to a halving distance for the uranium concentration of 10m. The data in Table 4.4 reveal that throughout the length of the transect, a significant fraction of the uranium in the samples is in excess of that normally present in the Irish

Distance Inland from Mean High Water Mark (m)	Excess ^{238}U	Excess ^{238}U / Total ^{238}U x 100%	Excess ^{230}Th	^{230}Th / ^{234}U for Excess
0	-2.6	-	-2.7	-
5	6.3	26	-2.5	-
10	11.3	41	-1.7	-
15	-0.3	-	-5.3	-
20	11.2	33	0.8	0.09
25	12.5	42	3.9	0.31
30	30.5	67	0.9	0.03
35	23.7	67	0.7	0.03
40	40.3	81	10.3	0.25
45	1071	99	7.8	0.007
50	208	95	28.7	0.14
55	199	91	91.3	0.45

TABLE 4.4: Excess ^{238}U concentrations relative to Irish Sea silt for the Netherclifton surface transect samples

Units = Bq kg^{-1}

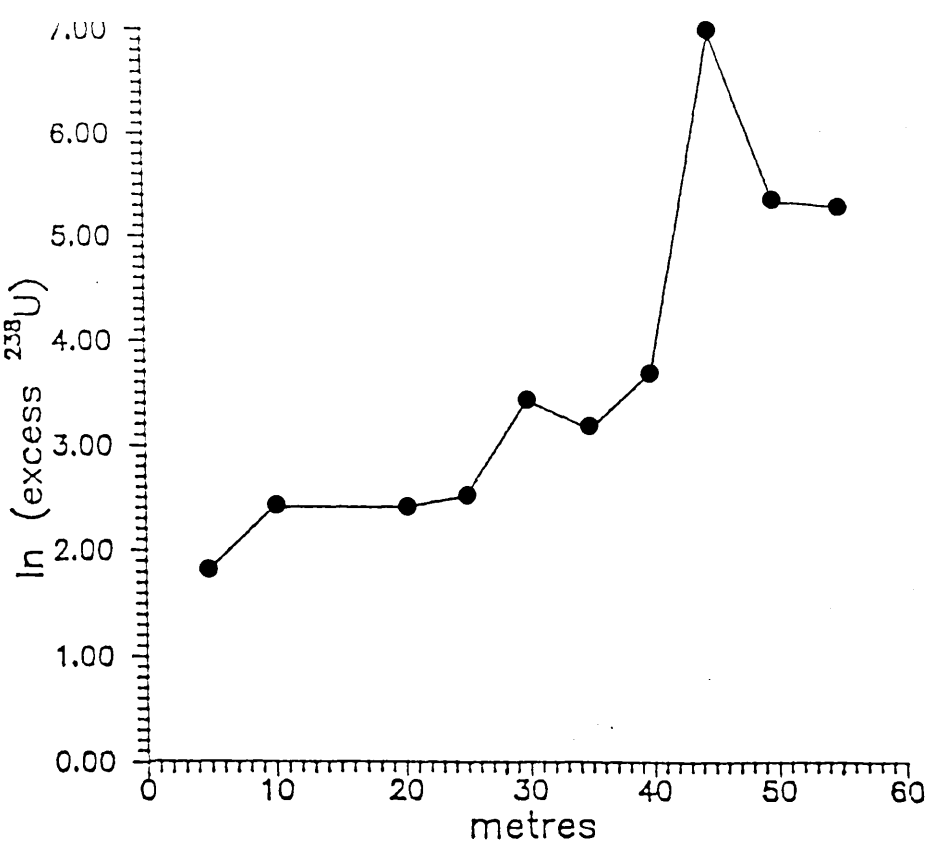

DISTANCE INLAND FROM MEAN HIGH WATER LEVEL (m)

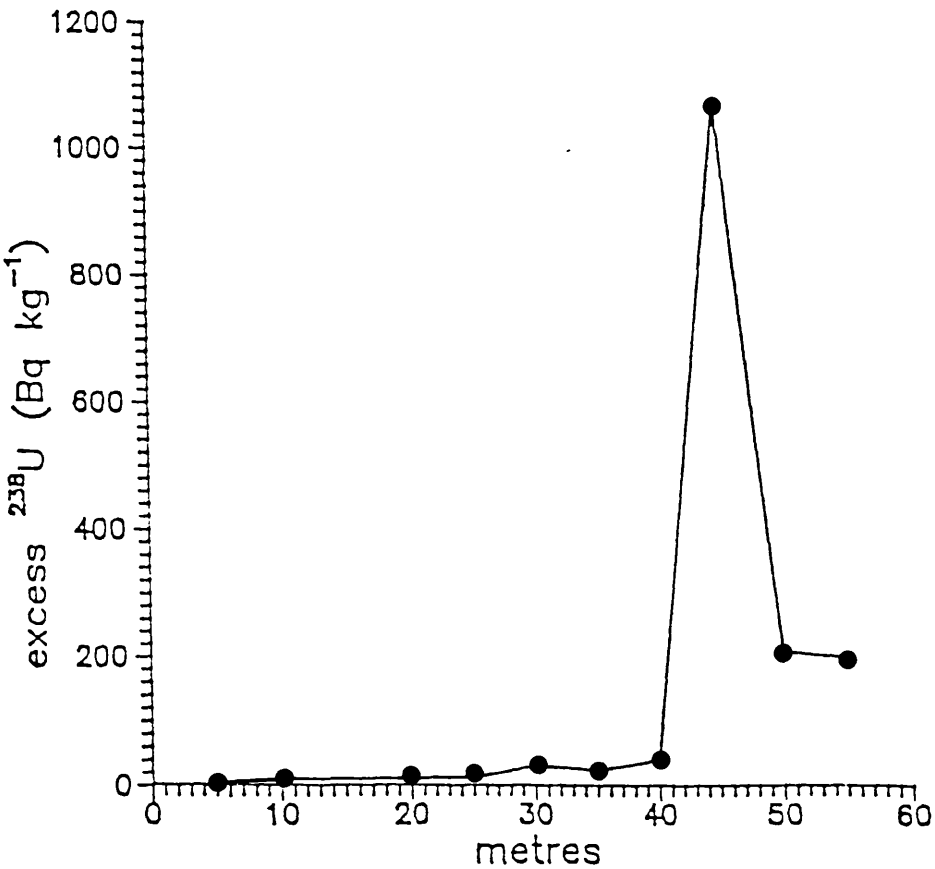

DISTANCE INLAND FROM MEAN HIGH WATER LEVEL (m)

Figure **4.16 :** Excess ^{238}U concentration and ln (excess ^{238}U) plots for samples from the Netherclifton surface transect

Sea silt. Moreover, the data suggest that in most of the samples, all of the ^{230}Th can be accounted for by the Irish Sea contribution. The samples from 40, 50 and 55m, however, contain ^{230}Th well in excess of the values appropriate to the Irish Sea silt, which suggests that incorporation of detrital material has occurred from a source other than the Irish Sea and probably indicates seaward movement of fragments of rock and mineral from the cliff area.

The results presented in Table 3.16 for the samples from the sections dug in the intertidal and merse areas (Figure 1.8) can be treated in the same way as the surface transect results and Table 4.5 shows the excess ^{238}U and ^{230}Th components for these samples. The intertidal samples show uranium values similar to the Irish Sea silt but have lower ^{230}Th concentrations and lower $^{230}Th/^{232}Th$ ratios. This may arise as the result of additional terrigenous detrital material (U and Th poor) transported by the Southwick water to these sediments diluting the marine excess of ^{230}Th. The section NCS862 samples are all very similar to the Irish Sea silt with no indication of uranium deposition. This is consistent with the fact that, as discussed above, ^{210}Pb dating plus Sellafield waste radionuclide profiles indicate that this area, in an eroded section of the merse, is accumulating at a rate of about 5cm y^{-1}. The section NCS863 samples show evidence of slight uranium deposition at the surface but not at depth and it is notable that the 50 and 100cm samples are much less enriched in ^{230}Th than present day Irish Sea silt. This could indicate either that the $^{230}Th/^{234}U$ ratio in the silt deposited from the Irish Sea has varied with time or alternatively that the material at more than 50cm depth in this section is from a different source from that at the surface. In the samples from section NCS864, there is clear evidence of uranium deposition at the surface and also at 55cm but not at the intermediate depth (25cm) sample. This deposition pattern is consistent with that predicted by the BGS hydrological model for the site

Sample	Excess ^{238}U	$\frac{\text{Excess } ^{238}U}{\text{Total } ^{238}U} \times 100$	Excess ^{230}Th	$\frac{^{230}Th}{^{234}U}$ for Excess
Intertidal Section NCS861				
Surface	0.3	1.9	-11.0	-
25cm	1.3	10.4	-3.0	-
50cm	0.4	3.4	-8.0	-
Merse Section NCS862 (7.5m)				
Surface	-2.4	-	-2.0	-
50cm	1.2	7.1	-0.2	-
100cm	-0.4	-	-3.0	-
Merse Section NCS863 (15m)				
Surface	5.3	26	0.8	0.20
50cm	2.5	13	-	-
100cm	-1.9	-	-14.2	-
Merse Section NCS864 (30m)				
Surface	14.7	14	1.5	0.10
25cm	-0.3	-	-13.9	-
55cm	30.6	65	-14.9	-

TABLE 4.5: Excess ^{238}U concentration relative to Irish Sea silt for the Netherclifton section samples

Units = Bq kg^{-1}

(Hooker et al, 1986; 1987; Scott et al, 1989) which suggests that uranium deposition should occur at the surface and at depth in the sediment where groundwater flow occurs. Once again, the deeper samples from this section are less enriched in ^{230}Th than present day Irish Sea surface sediment. In all of the samples from the merse section, there is no evidence of any excess ^{230}Th deposition.

The final set of results relating to the merse sediment at Netherclifton is for the sequential leaching study summarised in Table 3.17. The data relating to the intertidal sediment samples from section NCS861 are much as would be expected, with a small amount of uranium in the exchangeable, organic and oxide fractions, but with about 80% in the detrital phase. The section NCS862 samples show about 84% of the uranium in the surface sample to be in the detrital phase whereas in the 100cm section only 42.7% of the uranium is in the detrital phase and about 47.3% in the organic phase. This active involvement of organics in the retardation of uranium is consistent with the observations of Basham et al (1989) of the distribution of uranium in samples from this site using fission track techniques. The samples from section NCS864 show 81.6% of the uranium in the surface sample and 20.2% in the 55cm sample to be associated with the oxide component.

In summary, therefore, the results for the merse samples indicate that uranium dispersion for distances of up to about 50m from the cliff takes place both in the surface sediments and at depths where groundwater flow occurs. Retardation of uranium in the surface silts occurs by a process of continuous removal, appears to depend only upon the uranium concentration in solution and the removal process is characterized by a halving distance of about 10m. The evidence of the leaching experiment suggests that the retardation process may involve uptake by iron and manganese oxides as well as by organic species.

As discussed above, the section NCS862, was demonstrated to consist of silt being deposited relatively rapidly at this location following transport from further south in the Irish Sea and this material was selected for investigation of the possible occurrence of hot particles in the merse sediment since it appears to provide a continuous record of deposition over the last 30 years. Samples from various depths were investigated, as described in section 2.5 and the results did show that "hot particles " (ie. particles of enhanced alpha activity relative to the general background) were present at all depths in this profile. Figure 4.17 shows some typical examples of these "hot particles" from which it is apparent that particle diameter is around 100 to 200μm. This is in fact similar to the diameters of the hot particles found in the Cumbrian coastal environment (Hamilton, 1981; Hamilton and Clifton, 1987). Baxter et al (1989) have also reported the presence of hot particles in samples from the Solway intertidal area between Kippford and Wigtown Bay with particle diameters ranging from 200μm to 500μm. The intensity of the discrete (as opposed to hot particle) alpha tracks was assessed by inspection of 20 random fields of view for each sample using a magnification of X200 and the results are presented in Table 3.18. These results do show somewhat higher values for the alpha track density in the sections of the core with higher plutonium and americium concentrations, but the correlation between the track density and plutonium and americium concentrations is poor (r values of 0.43 and 0.39 respectively). A similar approach was adopted in an attempt to evaluate the distribution of hot particles but the number of hot particles observed per sample in this way was typically of the order of 10, thus making it impossible to derive meaningful conclusions from the observation. It was not possible, therefore, to draw any firm conclusions from the alpha particle track studies and the "hot particles" could be Sellafield derived or could simply be natural uranium bearing minerals (eg. zircons) but the results

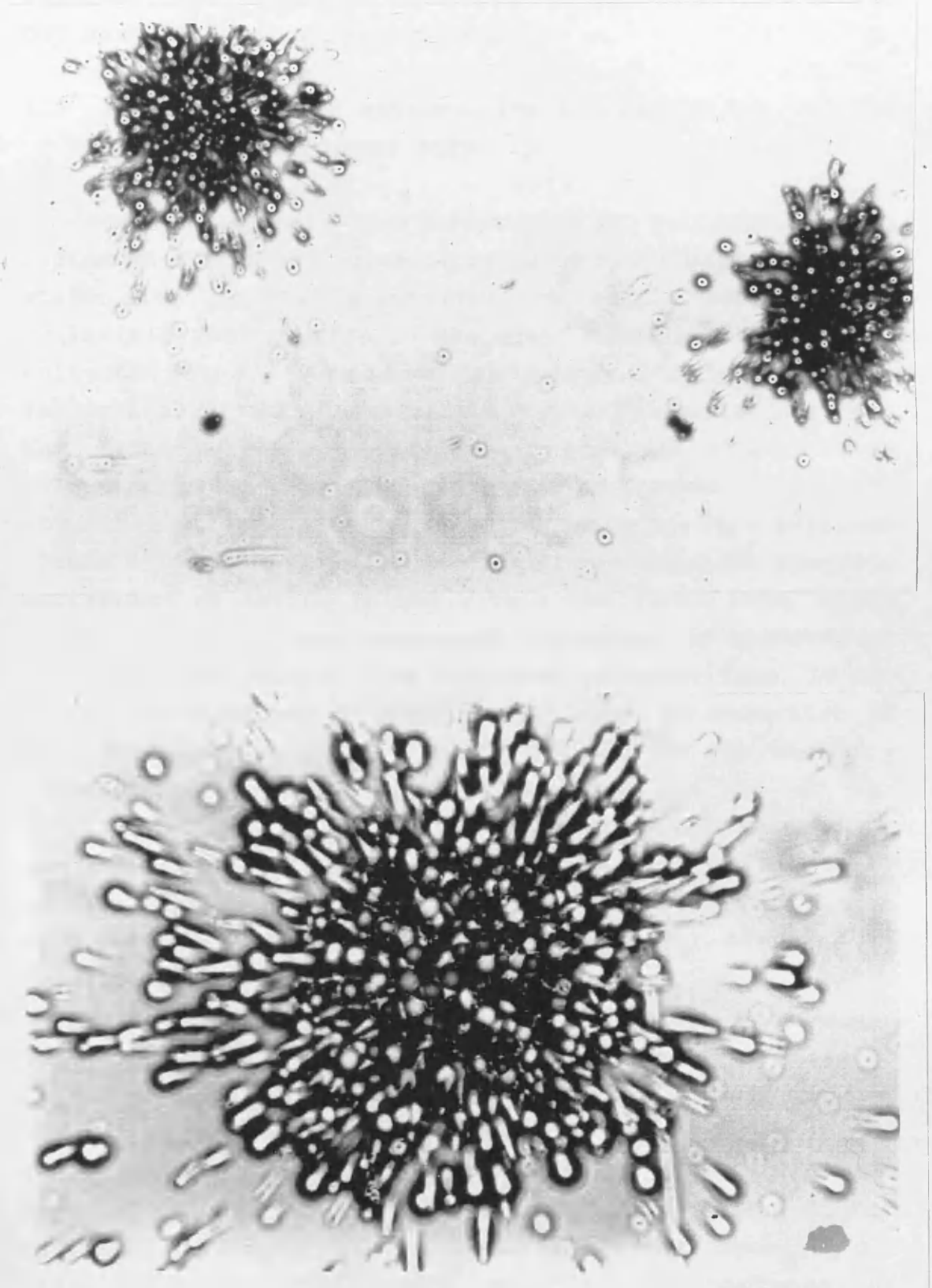

Figure 4.17: Examples of alpha particle track distributions produced by silt from section NCS862 showing typical hot particle plus background alpha particle track distribution

suggest that further work using automated image analysis equipment and attempted isolation or concentration of the hot particles would be worthwhile.

4.7 SELLAFIELD WASTE RADIONUCLIDE STUDIES AT THE WIGTOWN MARTYR'S STAKE MERSE SITE

In order to estimate the inventories of Sellafield waste radionuclides in the merse deposits at the Wigtown Martyr's stake site and to investigate the supply mechanism of Sellafield radionuclide to the area, surface samples were collected along a transect of length 500m and from a vertical profile as described in detail in chapter 2 above. The surface transect samples of area 10 x 10cm were collected in two depth intervals of 0 to 15cm and 15 to 30cm at each location. The results for the 0 to 15cm sections (Table 3.19) show a rapid increase of radionuclide specific activities on moving inland within the first 100m, after which a further, less pronounced, increase was observed on moving further inland. The radionuclide activities, in the 15 to 30cm sections were below the limit of detection in most cases as shown in Table 3.19 and ^{137}Cs was the only manmade radionuclide that was detected in all of the samples. The ^{137}Cs activity distribution for the deeper samples shows a different pattern from that of the upper section samples, with a sharp decrease from 480Bq kg^{-1} at 5m to 83Bq kg^{-1} at 55m and then a more gradual decrease to lower values on moving further inland.

The observed depth distribution of the radionuclides provides a possible indication of the reason for the increasing radionuclide specific activities on moving inland (when intuitively the reverse situation might have been expected). Thus the 5m (15 to 30cm) sample shows higher radionuclide activities that those of the corresponding 0 - 15cm sample indicating a relatively high rate of sedimentation at this location and suggesting that older,

higher activity sediment is buried at depth, with recent, lower activity material at the surface. The 55 and 100m samples also have an indication of significant ^{137}Cs activities in the 15 - 30cm samples whereas the remaining 15 - 30cm samples all have lower values.

It was necessary to consider the Chernobyl contribution to the radiocaesium activity to the upper 15cm samples and the $^{134}Cs/^{137}Cs$ activity ratios in these samples show a range of values from 0.02 to 0.05, which can in fact be attributed entirely to the Sellafield discharge.

This failure to detect Chernobyl radiocaesium could, in part, be due to dilution of any Chernobyl contribution within these comparatively large samples, but in view of the high values for Chernobyl fallout deposition in this area reported by McDonald et al (1990) it is more likely to have been caused by the Chernobyl radiocaesium being leached out of the sediment by seawater, as observed above for other intertidal areas in this study.

The $^{238}Pu/^{239,240}Pu$ activity ratios in the 0 to 15cm samples ranged from 0.17 to 0.19 except for the 5m sample which had a value of 0.24 reflecting a more recent $^{238}Pu/^{239,240}Pu$ ratio than those of the other samples, thus supporting the above suggestion of a higher accumulation rate at this location than further inland. The 5m and 255m samples were the only locations for which the 15 to 30cm sections provided measurable plutonium concentration with values for the $^{239,240}Pu$ activity of 71Bq kg^{-1} and 2.4Bq kg^{-1} respectively. These two samples both showed $^{238}Pu/^{239,240}Pu$ activity ratios of 0.17 which again suggests late 1960's or early 1970's Sellafield discharge values.

The nuclide ratios $^{137}Cs/^{241}Am$ and $^{137}Cs/^{239,240}Pu$ show values of less than 10 in all of the samples in conjunction with $^{241}Am/^{239,240}Pu$ activity ratios of greater than one. These

activity ratio values once more indicate that particle associated radionuclide transport is the dominant mechanism supplying Sellafield waste radionuclides to this area. Confirmation of this is provided by the very good linear correlations between ^{137}Cs - ^{241}Am, ^{137}Cs - $^{239,240}Pu$ and ^{241}Am - $^{239,240}Pu$ for the transect samples, with correlation coefficients of 0.979, 0.989 and 0.977 respectively.

The $^{241}Am/^{239,240}Pu$ ratios observed for these samples, in the range 1.2 to 1.7, mean that, on the basis of the argument developed above for the Netherclifton site, if 100% of the ^{241}Am discharged from Sellafield is assumed to be retained in the Irish Sea sediment then the plutonium retention would be in range 72% to 100% (average 85%). Similar treatment of the integrated Sellafield $^{137}Cs/^{241}Am$ activity ratio of 50 compared to the above sediment ratios of 3.2 to 7.7 provides values in the range 6.4 to 15% for the ^{137}Cs retained in the sediments of the Irish Sea (average 8.7%). These observations agree well with the conclusions derived above for the Netherclifton site.

The transect samples were also analysed for size fraction distribution and total organic content (Table 3.20 and Figure 3.16) in an attempt to identify any potential relationship between these parameters and the radionuclide activity distribution. The plots of the radionuclide activities (Figure 3.17) along with those of percentage of the sediment of size fraction <75μm and percentage organic content reveal a negative relationship between the nuclide activities and the <75μm particle content. The percentage of organic matter does, however, show a generally similar pattern to those of the radionuclides, in particular that of ^{241}Am. The organic percentage correlation with each of ^{137}Cs, ^{241}Am and $^{239,240}Pu$ gives good linear fits, with correlation coefficients of 0.942, 0.983 and 0.950 respectively. In view of the marine particulate origin of the radionuclides, a direct association with the organic

matter is, however, unlikely and it is more probable that both parameters are showing a related response to some other variable such as the increasing height of the merse above the mean high water level which controls the frequency and depth of flooding with seawater and will thus affect both the organic content and radionuclide concentration of the sediment. The observed correlation of radionuclide activity and organic content is, however, of considerable interest and is worthy of further investigation.

The total inventories of ^{137}Cs, ^{241}Am and $^{239,240}Pu$ in these sediments were of the order of 10^5, 10^4 and 10^4Bq m^{-2} respectively as shown in Table 3.21 and Figures 3.20 and 3.21, and the radionuclide inventories show a much smaller increase on moving inland than the corresponding trend in the specific activities discussed above. The specific activity values of ^{137}Cs for example vary from 415 to 1542Bq kg^{-1} whereas the corresponding values of the total ^{137}Cs inventory vary in the range 1.6×10^5 to 2.6×10^5. Moreover, the incomplete collection of the radionuclides (which were present to depths of greater than 30cm) at the 5 and 55m locations means that the inventories for these two sites will be significantly underestimated, while over the remaining length of the transect the inventories are relatively constant. This observation is consistent with the above suggestion that the observed variation in specific activities on moving inland is a consequence of varying depth distribution of the radionuclides in the sediment rather than a variation of supply to different parts of the transect.

The total inventories of ^{137}Cs, ^{241}Am and $^{239,240}Pu$ obtained for the Wigtown Martyr's stake samples show average values of 2.0×10^5. 4.6×10^4 and 3.3×10^4Bq m^{-2} respectively, which are higher than those for the Netherclifton site where average total inventories of 5×10^4, 1.7×10^4 and 1×10^4 respectively for ^{137}Cs, ^{241}Am and $^{239,240}Pu$ were observed. In

both cases, however, the inventories reflect a significant input of Sellafield radionuclide waste to the flood plain areas of the North Solway coast.

On the basis of the above radionuclide inventories (assuming average ^{137}Cs, $^{239,240}Pu$ and ^{241}Am inventories of 10^5, 10^4 and $10^4 Bq\ m^{-2}$ respectively) and a total assumed area for the Solway merse deposits of $70km^2$ it can be estimated that approximately 7, 1 and 1TBq of ^{137}Cs, ^{241}Am and $^{239,240}Pu$ respectively have been deposited in these areas as the result of the discharge of waste radionuclides from Sellafield during the last 30 years. These can be compared with the total inventories of 2.0 and 0.1TBq for ^{137}Cs and $^{239,240}Pu$ respectively estimated to have been deposited in Cumbria by onshore transfer as discussed in section 1.3.7.

The sediment section WMS871 was collected from a location at the edge of the merse at Wigtown (Figure 1.9) which forms a sharp step of height 1.5m, the top of which marks the normal maximum high water level. This gives a distinct boundary between the merse and the extensive intertidal mudflats of Wigtown Bay. The radionuclide vertical distributions in the sediment, shown in Table 3.22, indicate a penetration of Sellafield waste radionuclides to a depth of 60 to 65cm with a ^{137}Cs activity maximum at 35 to 40cm and ^{241}Am and $^{239,240}Pu$ activity maxima at 40 to 45cm.

The plots of the ^{137}Cs, ^{241}Am and $^{239,240}Pu$ profiles and corresponding Sellafield discharge data are shown in Figure 4.18 and these plots show some similarity between the sediment radionuclide profiles and the discharge trends particularly in the case of ^{241}Am. The sediment profiles, however, show a less rapid decrease towards the surface than the discharge data do, with this effect being more pronounced for ^{137}Cs and $^{239,240}Pu$ than for ^{241}Am. The implied accumulation rate of $3.0cm\ y^{-1}$ at this location provides strong support for the above suggestion that the surface

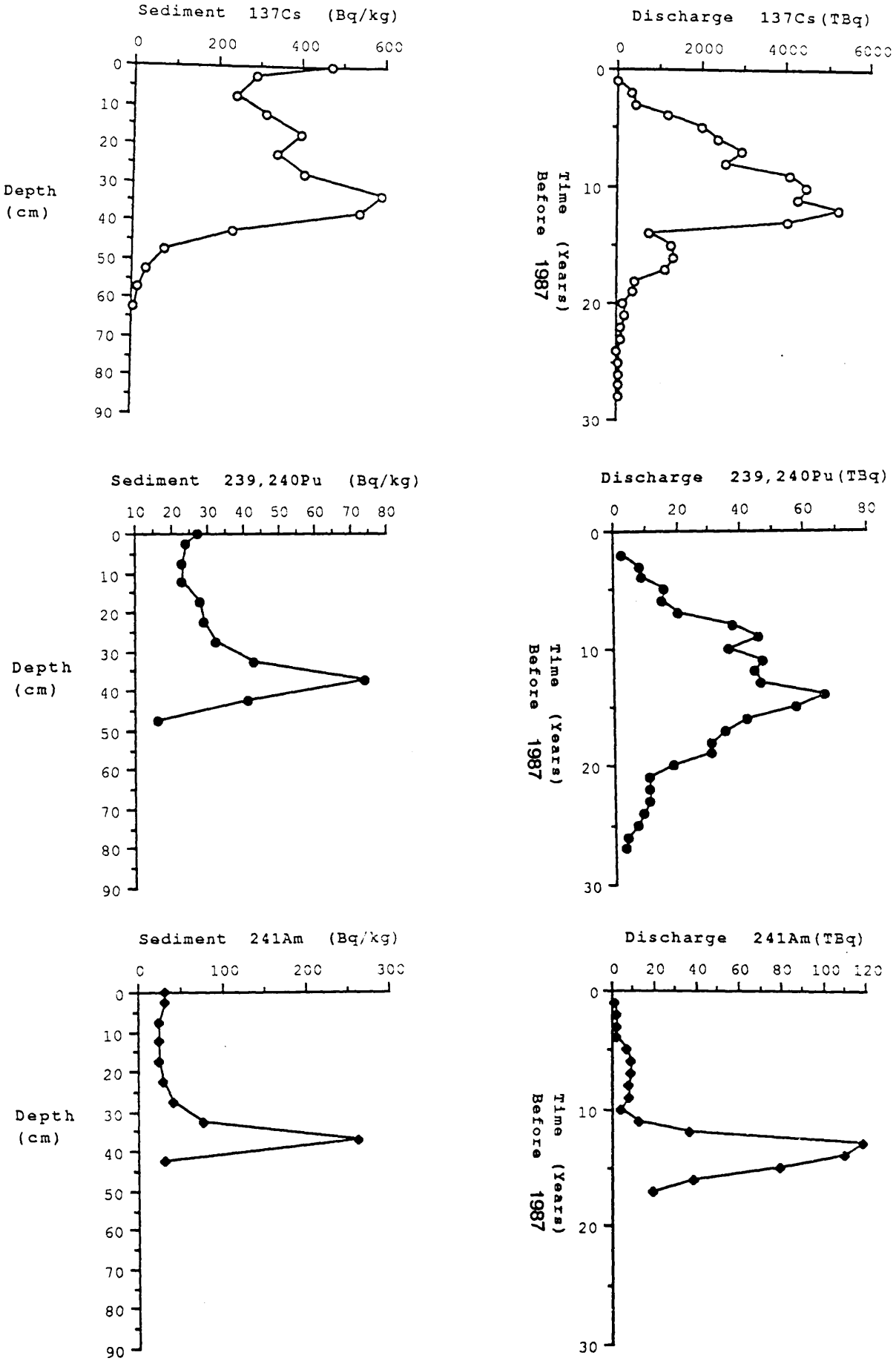

Figure 4.18 Radionuclide concentration profiles and corresponding Sellafield discharge data normalized to a sedimentation rate of 3.0 cm y^{-1} for section WMS871.

transect specific activity variations are largely influenced by variations in the vertical distribution of the radionuclides, with a higher rate of accumulation near the edge of the merse.

The decay corrected radionuclide activity ratios $^{134}Cs/^{137}Cs$ and $^{238}Pu/^{239,240}Pu$ based upon a 3.0cm y^{-1} sedimentation rate are shown along with the corresponding discharge data in Figure 4.19. The $^{134}Cs/^{137}Cs$ values for the uppermost two samples of the profile showed a significant Chernobyl influence while sections below this had typical Sellafield values for this ratio. The time corrected $^{134}Cs/^{137}Cs$ values for lower sections of the profile did show an increasing trend with depth matching the trend in the Sellafield discharge data but the decay corrected sediment values were too high relative to those of the discharge. This reveals that simple accumulation is not occurring and implies the existence of some degree of mixing. The limited amount of data available for $^{238}Pu/^{239,240}Pu$ activity ratios in the discharge means that little can be concluded from the comparison of the sediment and discharge data except for the significant fact that the sediment values for samples above the maxima are systematically lower than the corresponding discharge values, once more clearly demonstrating a high degree of mixing of the plutonium waste discharges over a timescale of at least two decades.

The time corrected radionuclide activity ratios $^{137}Cs/^{241}Am$, $^{137}Cs/^{239,240}Pu$ and $^{241}Am/^{239,240}Pu$ in the sediment profile are plotted along with the corresponding discharge ratio data in Figure 4.20. The shapes of the $^{241}Am/^{239,240}Pu$ plots show some degree of similarity between the discharge and sediment data but with the sediment values for samples from above the concentration maximum being too high relative to those of the discharge.

Some similarity is also apparent in the patterns of the

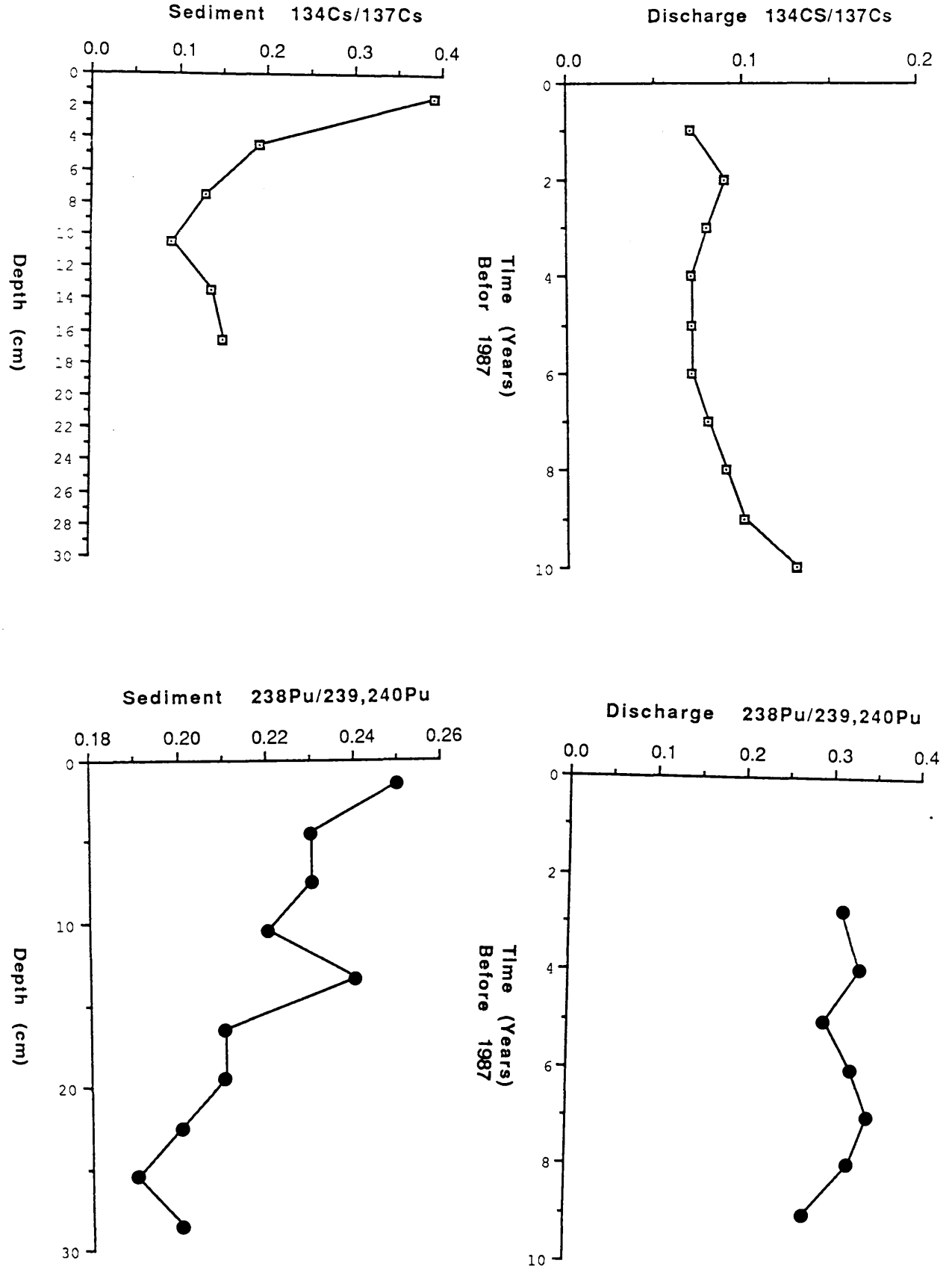

Figure 4.19 Decay corrected isotopic activity ratios and corresponding Sellafield discharge data normalized to a sedimentation rate of 3.0 cm y-1 for section WMS871.

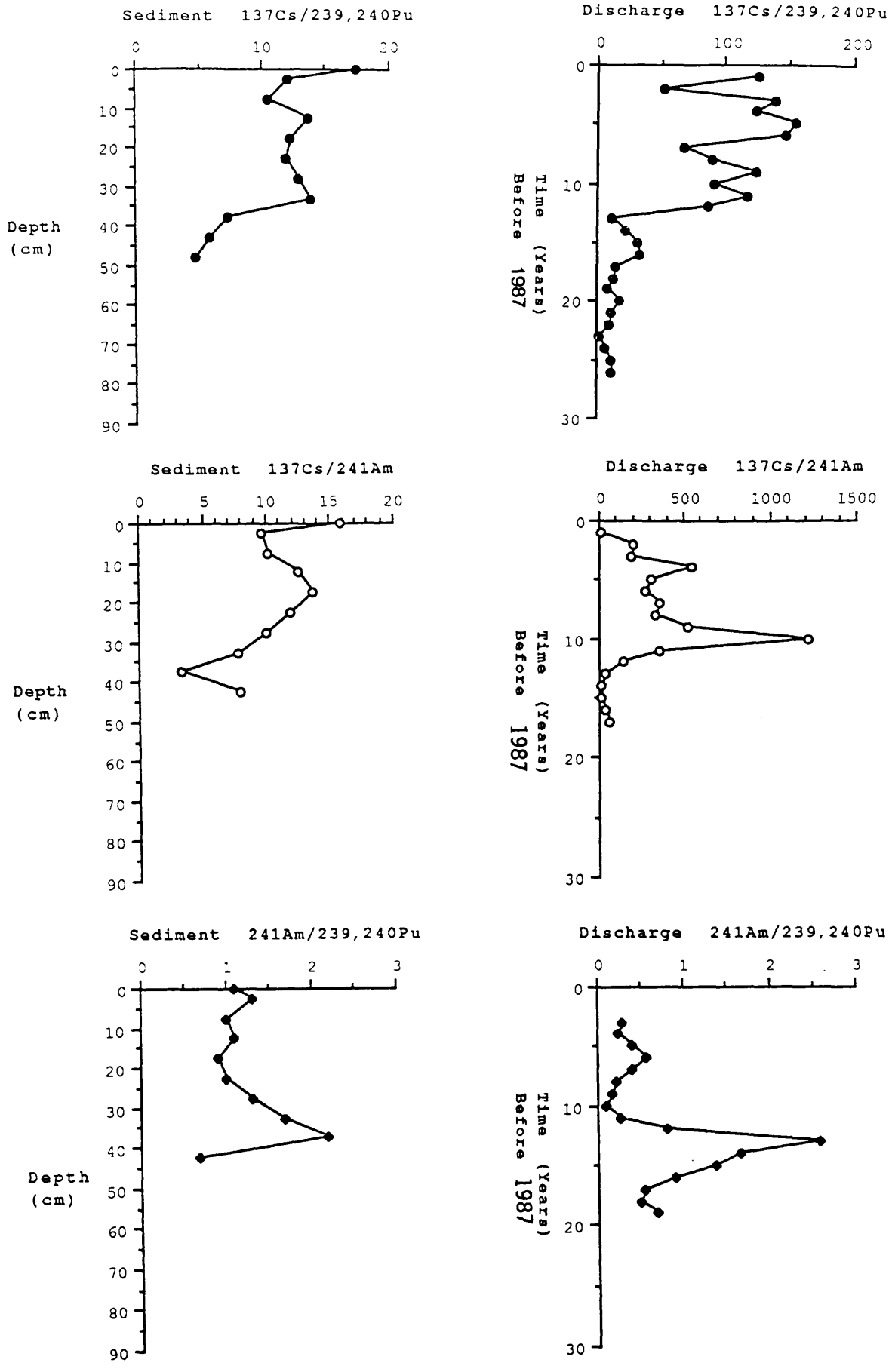

Figure 4.20 Radionuclide activity ratio profiles and corresponding Sellafield discharge data normalized to a sedimentation rate of 3.0 cm y^{-1} for section WMS871.

$^{137}Cs/^{239,240}Pu$ activity ratio data plots, but the near surface trend is markedly different although this may, in part, be due to the Chernobyl influence on the sediment profile. Finally, it can be observed that the sharp variations in the discharge $^{137}Cs/^{241}Am$ ratio do not appear in the sediment profile.

Despite the fact that small variations in the activity ratios of the sediment samples do occur, the large variation in the sediment specific activity which occur lead to strong linear correlations between the concentrations of Cs, Pu and Am. Very good linear correlations were obtained for the plots of ^{137}Cs against ^{241}Am, ^{137}Cs against $^{239,240}Pu$ and ^{241}Am against $^{239,240}Pu$, with respective correlation coefficients of 0.980, 0.989 and 0.976. These correlations are not consistent with the Sellafield discharge trends and strongly suggest that all of the sediment has a common origin before deposition.

As discussed previously for Skyreburn Bay, this linearity is significant since the temporal variation in the Sellafield discharge do not show any linear relationship between ^{137}Cs and ^{241}Am or $^{239,240}Pu$ and ^{241}Am and a much lower degree of linear correlation between ^{137}Cs and $^{239,240}Pu$ than is observed for the sediment. Moreover such linear correlations would not be expected on the basis of the very different geochemical properties of these species.

The general conclusion can therefore be derived from the above discussion that the distribution patterns of the radionuclide activities and activity ratios in the sediment do not bear a simple relationship to the Sellafield discharge pattern over the appropriate time, indicating that simple accumulation is not occurring but that a combination of accumulation and mixing is probable.

The ^{210}Pb profile for section WMS871 shows a generally exponential decrease of activity with depth perturbed by the

presence of higher activity material at 30 to 40cm and 50 to 60cm. Application of a constant initial concentration calculation to this profile provides a sedimentation rate of 1.9cm y^{-1} if all of the data are used whereas if the two higher activity sections are excluded, a sedimentation rate of 2.5cm y^{-1} is obtained, which is in reasonable agreement with those achieved from the manmade radionuclides of about 3.0cm y^{-1}.

Two horizontal sections were cut into the exposed vertical face of the edge of the merse deposit at depths of 5 and 75cm below the merse surface as shown in Figure 1.9. Samples were collected in 1cm increments starting from the face and were analysed to investigate the extent of any penetration of radionuclides into the sediment from Irish Sea water in contact with the exposed face. As shown in Table 3.23 and Figure 3.24, the section WMSH871 from 5cm below the surface showed readily detectable levels of manmade radionuclides throughout the entire length sampled with a small degree of variation of ^{137}Cs and ^{241}Am activities over the first 10cm of the section but with lower values at 20 to 21cm and 30 to 31cm, particularly for ^{241}Am. ^{134}Cs showed a higher activity in the outermost three samples reflecting a significant Chernobyl fallout influence whereas in the 4cm to 8cm sections the ^{134}Cs activity was typical of Sellafield values, with a maximum $^{134}Cs/^{137}Cs$ activity ratio of 0.04. In the innermost four samples of the section WMSH871 ^{134}Cs was found to be below detection limit.

Interpretation of the results for this section is complicated since the section was collected horizontally from a location where the topography of the merse shows an increase in height on moving away from the edge. Moreover, as shown above, this section of the merse is subject to relatively rapid accumulation so that the observed distribution of radionuclides is probably a reflection of variable accumulation (and possibly mixing) in a vertical

rather than a horizontal sense. It is of note that the first three samples (like the uppermost samples of section WMSH871) were clearly affected by Chernobyl fallout but with increasing distance into the section there was no evidence of the presence of Chernobyl fallout. The reason for observation of Chernobyl radiocaesium in some of the section samples but not in the inventory samples is not clear although, as mentioned above, this may simply represent a sampling effect with the Chernobyl radiocaesium being diluted to non detectable levels by mixing in the relatively large samples used for the inventory measurements. If the Chernobyl contribution to the three outermost samples is subtracted from the total radiocaesium concentration, the residual radiocaesium activity shows an increase with depth in the section which could be related to the reduction in the Sellafield discharge of radiocaesium in recent years suggesting a younger 'age' for the outermost samples. The fact that ^{134}Cs falls below the detection limit and the $^{137}Cs/^{241}Am$ activity ratio increases markedly in the deeper sections could also be taken to support this suggestion.

The ^{241}Am activity in this profile shows similar values to the ^{241}Am activity in the 0 to 5cm sample from section WMSH871 which was collected from the same location.

In the 75cm section (Table 3.24), radionuclide activities were below the detection limit throughout, with the exception of low levels of ^{137}Cs in the 0 to 1 and 1 to 2cm sections. This is in good agreement with the results from section WMS871, which showed no detectable activity below 60 to 65cm depth. Thus on the assumption of no erosion of this part of the section, these results indicate a very low degree of uptake of Sellafield waste radionuclides on the exposed face of the merse silt and negligible movement of such nuclides horizontally into the sediment.

4.8 STABLE ELEMENT GEOCHEMICAL STUDIES IN NETHERCLIFTON AND WIGTOWN MARTYR'S STAKE MERSE SECTION SAMPLES

The concentrations of stable elements, in particular the rare earths, were investigated by instrumental neutron activation analysis in samples from the top, middle and bottom sections of the vertical profiles at the Netherclifton and Wigtown Martyr's stake merse sites and the results are shown in Table 3.25. The Masuda-Coryell diagrams derived from the data are shown in Figure 4.21, 4.22, 4.23, 4.24 and 4.25.

The plots for all three samples from section NCS861 show similar patterns to each other and to those obtained for surface intertidal sediments from this area (section 4.2), with the only exception being that the Sm values are somewhat higher for the NCS861 samples. This similarity of the plots for the three depths suggests a common origin for the sediment material throughout the profile. These data are therefore generally consistent with the instrumental neutron activation analysis data for the surface intertidal samples from the Solway coast and the higher Sm values in the Netherclifton samples may represent the influence of some terrigenous material being transported to this location by the Southwick water.

The section NCS862 plots are very similar to each other and are also very similar to those of the surface intertidal samples. This similarity between the top, middle and bottom samples of the profile and the surface intertidal sediments is consistent with the previous argument (section 4.5) for rapid sediment accumulation at this location with the sediment being derived from the same source in the Irish Sea as is affecting the true intertidal areas.

Considering section NCS863, the Masuda-Coryell plots show very similar patterns to those of section NCS861, with the

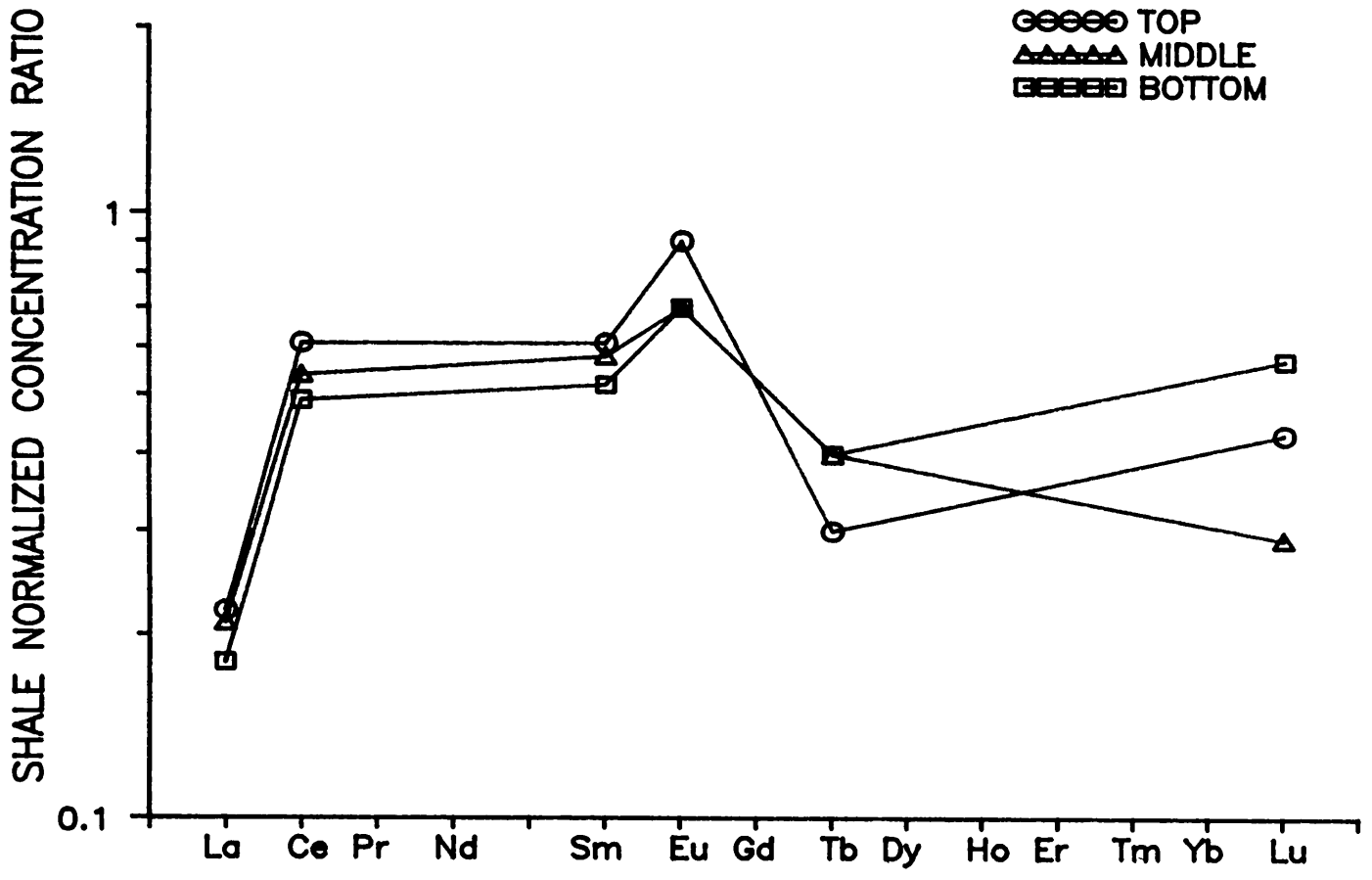

Figure 4.21 Masuda-Coryell plots for Section NCS861, Netherclifton Site (Figure 1.8)

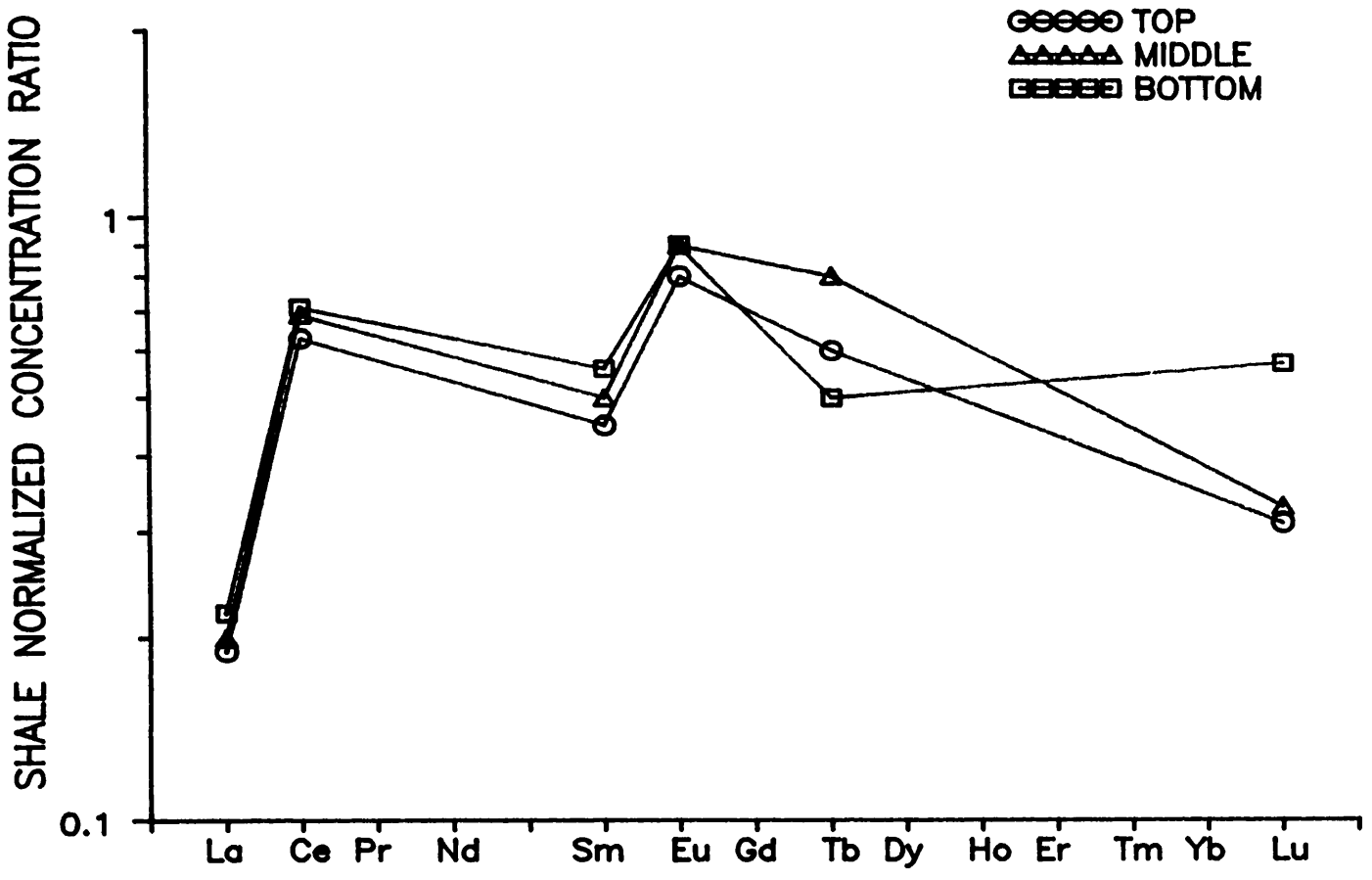

Figure 4.22 Masuda-Coryell plots for Section NCS862, Netherclifton Site (Figure 1.8)

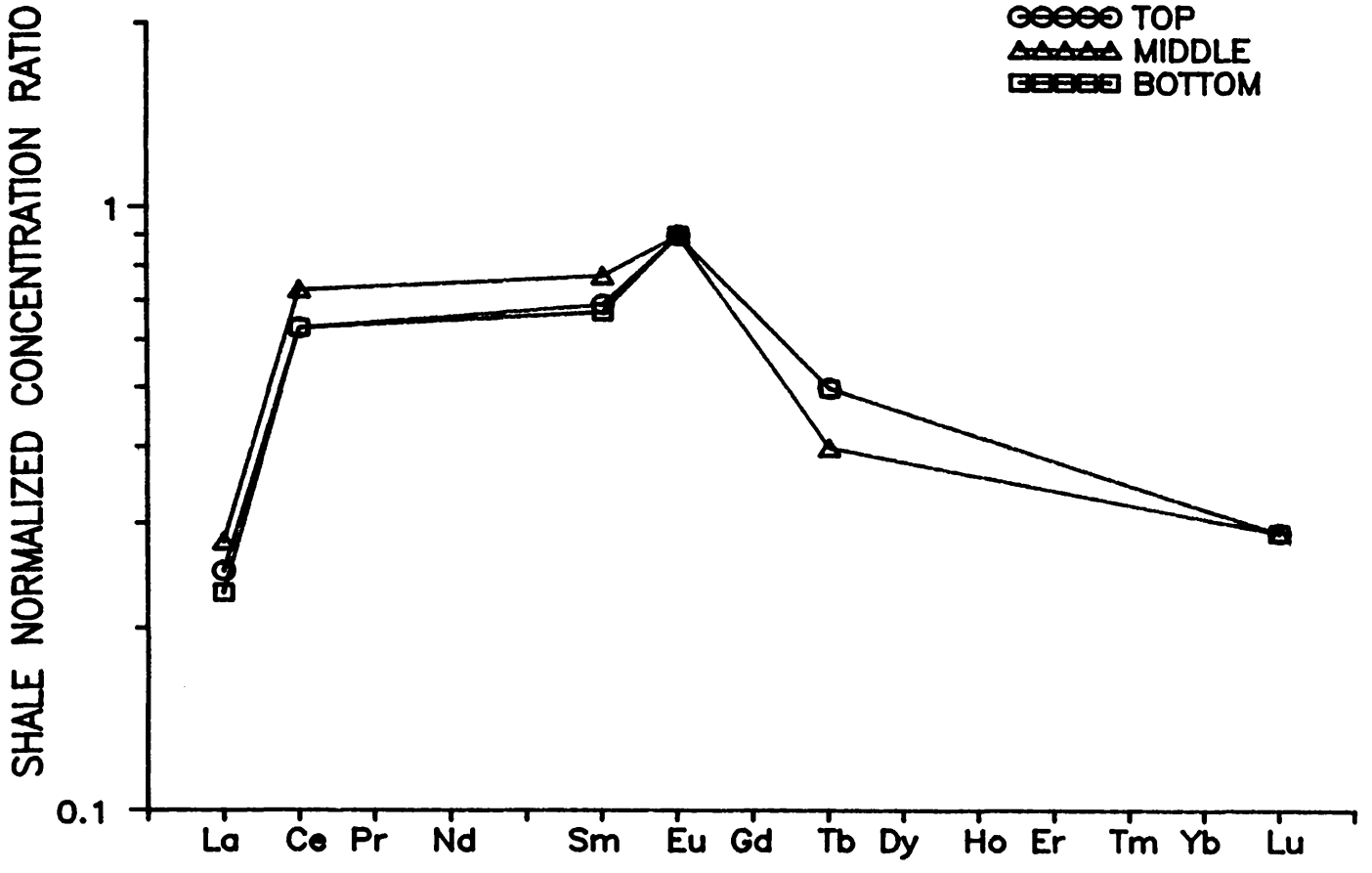

Figure 4.23 Masuda-Coryell plots for Section NCS863, Netherclifton Site (Figure 1.8)

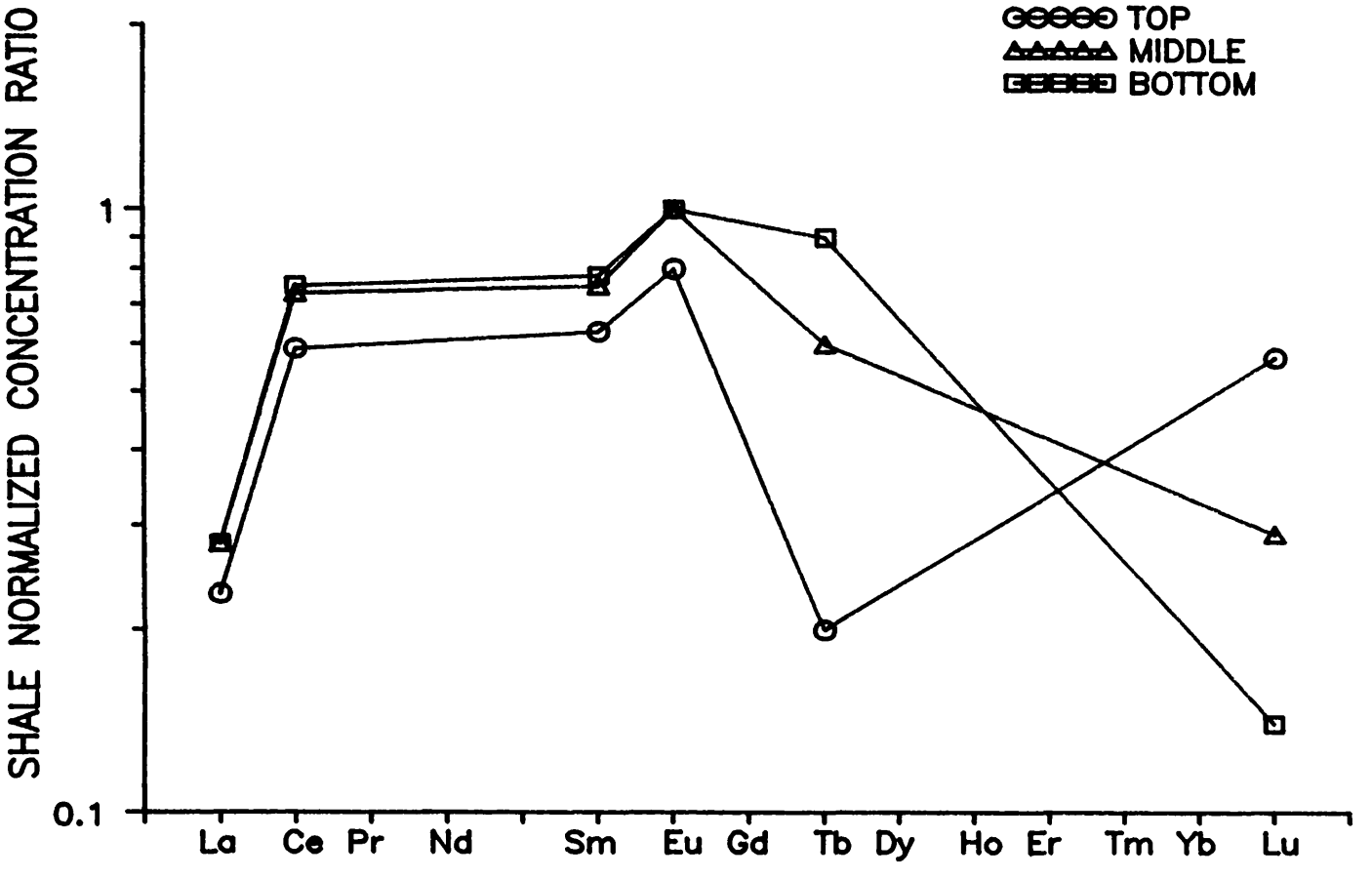

Figure 4.24 Masuda-Coryell plots for Section NCS864, Netherclifton Site (Figure 1.8)

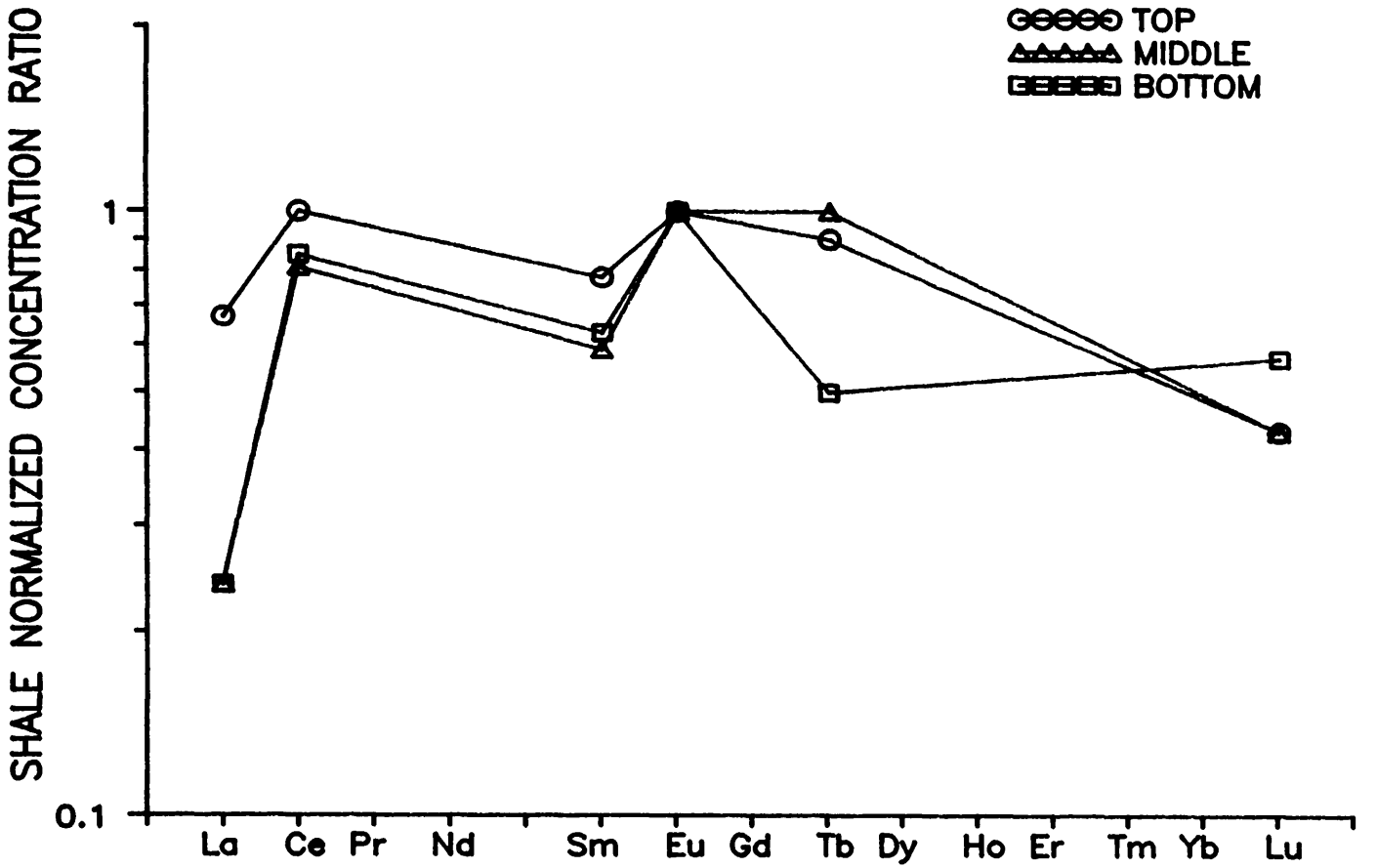

Figure 4.25 Masuda-Coryell plots for Section WMS871, Wigtown Martyr's Stake (Figure 1.9)

exception of the abnormally high Lu value for the sample from the middle of the profile.

Section NCS864, from the location furthest inland at Netherclifton shows similar La-Eu patterns to those in the other Netherclifton profiles and to the surface intertidal sediment. However, the heavy rare earths, Tb and Lu, show a much greater scatter for the NCS864 samples which may indicate the deposition of minerals from a source other than Irish Sea silt, (possibly eroded material from the Criffel granodiorite being transported seaward by the general drainage of the area).

The data for the Wigtown section WMSS871 show similar light rare earth element distributions (La-Eu) to those for samples from Netherclifton and the surface intertidal sediments but show differences in Tb and Lu values. The Wigtown results are generally similar to the Port William intertidal sediment results.

The general conclusion can therefore be drawn from this set of results that all of the samples from the Merse area show generally similar rare earth element plots, consistent with the dominant source of sediment being Irish Sea silts, but that variations do occur in heavy rare earth element concentrations in some samples which are possibly subject to input of some terrigenous material.

Most of the other elements analysed showed little significant variation either within individual profiles or between sampling locations. One notable exception to this is Br which showed a systematic increase in surface sediment concentration on moving inland at Netherclifton from 14ppm in the intertidal sediment to 159ppm in section NCS864. Moreover in sections NCS863 and NCS864 at Netherclifton and in section WMSS871 at Wigtown Martyr's stake, Br concentrations were observed to decrease with increasing

depth. This may simply represent a variation of Br concentration in response to variations in the organic content of the sediments or could represent some chemical process actively causing enrichment of Br in the upper layers. A slight decrease in Br content with increasing depth is also observed in the intertidal section at Netherclifton but it is notable that there is a relatively constant Br concentration in the three samples from section NCS862. This is consistent with the concept of rapid accumulation of this profile and suggests that a timescale significantly in excess of 30 years is required to generate the decreasing Br profiles observed at the other merse sections. As concentrations show a very similar pattern of behaviour to Br suggesting that both elements may be subject to some common control in these sediments. Both Br and As have active biological properties and the latter is a redox sensitive element so a number of possibilities exist for processes which could produce these distributions. These results suggest that further study of the distribution of these elements in the merse deposits would be useful.

4.9 CONCLUSIONS

On the basis of the preceding discussion, the major conclusions presented below can be drawn from this study.

The Sellafield waste radionuclide concentrations and activity ratios observed in this work for Solway Firth intertidal sediments are in good agreement with those previously reported for this area by MacKenzie et al (1987) and provide strong support for the model of transport of Sellafield waste radionuclides to this area proposed by these authors. Further evidence in support of this mechanism was provided by (a) the instrumental neutron activation analysis data and (b) the temporal variations in the Skyreburn Bay intertidal sediment radionuclide profiles. The general conclusion can therefore be drawn that the

movement of contaminated silt particles from a single, relatively well mixed, source area in the Irish Sea is the main mechanism of transport of Sellafield waste radionuclides to the Solway Firth intertidal sediments.

On the basis of a similar interpretation of the analytical data for the Solway merse samples, it has been established that particle associated transport of radionuclides is also the dominant mechanism of supply of Sellafield waste radionuclides to these areas of the Solway flood plain. The neutron activation analysis results and the uranium and thorium data for the Netherclifton site provide support for this hypothesis. Moreover, the results for section NCS862 reveal that the particle associated transport mechanism has been dominant for at least two decades.

The total inventories of ^{137}Cs, ^{241}Am and $^{239,240}Pu$ in the merse sediments as a result of the Sellafield discharge were respectively of the order of 10^5, 10^4 and $10^4 Bq\ m^{-2}$ and the inventories for the total Solway merse area were estimated to be 7, 1 and 1TBq. These represent 0.02%, 0.15% and 0.12% respectively of the time integrated discharge from Sellafield to 1987 and can be compared with onshore transfer of 2TBq and 0.1TBq of ^{137}Cs and $^{239,240}Pu$ from the surf zone in Cumbria.

A further observation of interest was that, on the basis of this work, and other reported data (MAFF, 1977-1986; McDonald et al, 1990) showing a high degree of uniformity of radionuclide activity ratios throughout the north eastern section of the Irish Sea, there is no evidence of significant desorption of caesium from the sediment. Moreover, once deposited in intertidal sediments, ^{137}Cs, ^{241}Am and $^{239,240}Pu$ appear to behave similarly, with no evidence of fractionation between these radionuclides. This applies not only in intertidal sediments (which can be regarded as marine sediments) but also in merse sediments which have

significantly lower Eh and pH values than seawater. Thus the Sellafield waste radionuclides appear to be relatively tightly associated with the silt particles and it is apparent that the K_D values observed from radionuclide uptake observations do not apply to desorption in this case. This suggests that the radionuclides are not accessible for desorption and could indicate that they are physically contained within coatings, of perhaps iron and manganese oxides or organic materials, covering the silt particles. The results also suggest a difference in speciation of Sellafield and Chernobyl derived radiocaesium, with the former behaving similarly to americium and plutonium but the latter being highly available for removal by leaching.

The uranium and thorium results for the Netherclifton merse silt reveal significant uranium migration over a distance of up to 55m towards the sea from the source area near the mineralisation vein. There is evidence of continuous removal of uranium from solution by uptake on iron/manganese oxides and organic materials and the removal process was found to be characterized by a halving distance for the uranium concentration of about 10m. There was no evidence of any significant movement of ^{230}Th along with the uranium.

The study demonstrated that both natural and manmade radionuclides can be used successfully as tracers of processes occurring in the intertidal area. Thus, while ^{210}Pb was not as useful for establishing sedimentation rates in this high energy environment as in lower energy regions (eg. offshore sediments, lakes or peats), a constant initial concentration calculation could be applied in a number of situations with, for example, accumulation rates of 1.5, 3.0 and 5.0cm y^{-1} being observed for the Skyreburn Bay, Wigtown and Netherclifton sites respectively. A constant rate of supply approach was applicable in other circumstances and provided an upper limit for the accumulation rate at Ardmore Bay of 0.9cm y^{-1}.

Finally, ^{210}Pb proved highly suitable for establishing mixing patterns such as those derived for the sediment profiles from Ardmore Bay and for section NCS861 at the Netherclifton site, which were in good agreement with the patterns obtained on the basis of the Sellafield waste radionuclide distributions.

The uranium and thorium results, in particular the $^{230}Th/^{234}U$ activity ratio, showed characteristic values for Irish Sea sediment which were similar to those found in the surface intertidal and merse samples at Netherclifton which had not been subject to deposition of uranium derived from the vein. This provides further evidence that the sediment of this area is being supplied from the Irish Sea, supporting the supply mechanism derived from the results for manmade radionuclides. Finally, the $^{230}Th/^{234}U$ activity ratio could also provide a potential for dating of these sediments if suitably long sediment cores could be obtained.

The Sellafield waste radionuclides were demonstrated to be extremely useful tracers for sediment mixing and movement both in the Irish Sea in general (as illustrated in the discussion of radionuclide transport) and in local areas such as Skyreburn Bay and Ardmore Bay. It was established that both of these bays are well mixed sandy environments and that highly efficient exchange of sediment with offshore sediment occurs at Skyreburn Bay but not at Ardmore Bay, where very little transport of sediment from the Clyde Estuary was observed.

The Sellafield waste radionuclides were particularly useful in establishing the details of vertical mixing of sediments at specific locations and the radionuclide activities, isotope ratios, vertical profiles and total depth of penetration into the sediment were all found to be of value in this context. In the case of some of the merse locations

the Sellafield radionuclide profiles provided accumulation rates by relating subsurface maxima in the radionuclide activities to the peak Sellafield discharges of the mid 1970's, and the results were compatible with ^{210}Pb chronologies.

Finally, it can be noted that while most of the samples studied in this work were dominated by Sellafield radionuclides, the same general approach to the use of tracers in studying intertidal sediments could be applied in other areas not affected by Sellafield, but where weapons testing fallout, Chernobyl fallout or some local source of manmade radionuclides is present (eg. The Mediterranean Sea).

REFERENCES

Aarkrog, A., 1988. The radiological impact of the Chernobyl debris compared with that from nuclear weapons fallout. J. Environ. Radioactivity, 6, 151-162.

Adams, F. and Dams, R., 1970. Applied gamma-ray spectrometry. Pergamon Press, Oxford.

Ahrland, S., Bagnall, K. W., Brown, D., Dell, R. M., Eberle, S. H., Keller, C., Lee, J. A., Liljenzin, J. O., Mardon, P. G., Marples, J. A. C., Milner, G. W. C., Philips, G., Potter, P. E. and Rydberg, J., 1975. The Chemistry of the actinides. Chapter 45 of Comprehensive Inorganic Chemistry, Pergamon Press, Oxford, New York, Toronto, Sydney, Paris, Braunschweig.

Allard, B. and Rydberg, J., 1983. Behaviour of plutonium in natural waters. American Chemical Society Symp. Series, 216, 275-295.

Aller, R. C. and Cochran, J. K., 1976. $^{234}Th/^{238}U$ disequilibrium in nearshore sediment; particle reworking and diagenetic time scale. Earth Planet. Sci. Lett., 29, 37-50.

Aller, R. C., 1977. The influence of macrobenthos on chemical diagenesis of marine sediments. PhD Thesis, Yale University.

Aller, R. C., 1980. Diagenetic processes near the sediment - water interface of Long Island Sound, I. Decomposition and nutrient element geochemistry (S, N, P). In: Estuarine Physics and Chemistry: Studies in Long Island Sound. Advances in Geophysics, 22, (Ed. Saltzerman, B.), Academic Press.

Aller, R. C., Benninger, L. K. and Cochran, J. K., 1980. Tracking particle associated processes in nearshore environments by use of $^{234}Th/^{238}U$ disequilibrium. Earth Planet. Sci. Lett., 47, 161-173.

Aller, R. C. and DeMaster, D. J., 1984. Estimates of particle flux and reworking at the Deep-Sea Floor using $^{234}Th/^{238}U$ disequilibrium. Earth Planet. Sci. Lett., 67, 308-318.

Anderson, R. F., 1982. Concentration, vertical flux and remineralization of particulate uranium in seawater. Geochim. Cosmochim. Acta, 46, 1293-1299.

Anderson, R. F., Bacon, M. P. and Brewer, P. G., 1983a. Removal of ^{230}Th and ^{231}Pa from the open oceans. Earth Planet. Sci. Lett., 62, 7-23.

Anderson, R. F., Bacon, M. P. and Brewer, P. G., 1983b. Removal of ^{230}Th and ^{231}Pa at ocean margins. Earth Planet. Sci. Lett., 66, 73-90.

Assinder, D. J., Kelley, M. J. and Aston, S. R., 1985. Tidal variations in dissolved and particulate phase radionuclide activities in the Esk Estuary, England, and their distribution coefficients and particulate activity fractions. J. Environ. Radioactivity, 2, 1-22.

Aston, S. R. and Duursma, E. K., 1973. Concentration effects of ^{137}Cs, ^{65}Zn, ^{60}Co, ^{106}Ru sorption by marine sediments with geochemical implications. Neth. J. Sea. Res., 6, 225-240, RITS. No. 31.

Aston, S. R. and Stanners, D. A., 1979. The determination of estuarine sedimentation rates by $^{134}Cs/^{137}Cs$ and other artificial radionuclide profiles. Estuarine Coastal Mar. Sci., 9, 529-541.

Aston, S. R. and Stanners, D. A., 1981. Plutonium transport to and deposition and immobility in Irish Sea intertidal sediments. Nature, 289, 581-582.

Aston, S. R., Assinder, D. J., Stanners, D. A. and Rae, J., 1981. Plutonium occurrence and phase distribution in sediments of the Wyre Estuary, Northwest England. Mar. Poll. Bull., 12, 9, 308-

Aston, S. R. and Stanners, D. A., 1982. The transport to and deposition of americium in intertidal sediments of the Ravenglass Estuary and its relationship to plutonium. Environ. Pollut. (Series B) 3, 1-9.

Basham, I. R. and Hyslop, E. K. (1989). Uranium location studies at the Needle's Eye natural analogue site - a preliminary account. BGS Technical Report WG/89/6R. British Geological Survey, Edinburgh.

Baxter, M. S. and McKinley, I. G., 1978. Radioactive species in sea water. Proc. Roy. Soc. Edinburgh, 768, 17-35.

Baxter, M. S., McKinley, I. G., MacKenzie, A. B. and Jack, W., 1979. Windscale radiocaesium in the Clyde Sea Area. Mar. Pollut. Bull., 10, 116-120.

Baxter, M. S., Cook, G. T. and McDonald, P. (1989). An Assessment of Artificial Radionuclide Transfer from Sellafield to South West Scotland. DOE Report No DOE/RW/89/127, 99pp.

Bayer, A., 1983. The radiological impact on the Rhine-Meuse regions from the normal operations of nuclear facilities. In: Ecological Aspects of Radionuclides Release. (Eds. Coughtrey, P. J., Bell, J. N. B. and Roberts, T. M.). British Ecology Society, Special Publ. No 3, Blackwell, Oxford, 229-250.

Bennett, B. G., 1978. Environmental aspects of americium. Environmental Measurements Laboratory report. EML-348, New York, USA.

Benninger, L. K., Lewis, D. M. and Turekian, K. K., 1975. The use of natural ^{210}Pb as a heavy metal tracer in the river-estuarine system. In Marine Chemistry in the Coastal Environment. ACS Symposium Series;18, 202-210. (Ed. Gould, R. F.) ACS, Washington DC, USA.

Benninger, L. K., 1978. ^{210}Pb balance in Long Island Sound. Geochim. Cosmochim. Acta, 42, 1165-1174.

Benninger, L. K., Aller, C., Cochran. J. K. and Turekian, K. K., 1979. Effect of biological sediment mixing on the ^{210}Pb chronology and trace metal distribution in a Long Island Sound sediment core. Earth Planet. Sci. Lett., 43, 241-259.

Ben-Shaban, Y. A., 1985. A radiochemical study of intertidal sediments. MSc Thesis, Glasgow University.

Berner, R. A., 1980. Early diagenesis: A theoretical approach. Princeton University Press, Princeton, UK.

Bhat, S. G., Krishnaswami, S., Rama, L. D. and Moore, W. S., 1969. $^{234}Th/^{238}U$ ratios in the ocean. Earth Planet. Sci. Lett., 5, 483-491.

BNFL 1981. Annual report on radioactive discharges and monitoring of the environment. British Nuclear Fuels Limited. Health and Safety Directorate, 1982. Risley.

BNFL, 1982. Annual report on radioactive discharges and monitoring of the environment. British Nuclear Fuelds Limited. Health and Safety Directorate 1983. Risley.

BNFL, 1984. Annual report on radioactive discharges and monitoring of the environment. Health and Safety Directorate, 1985. Risley.

BNFL, 1985. Annual report on radioactive discharges and monitoring of the environment. British Nuclear Fuels Limited. Health and Safety Directorate, 1986. Risley.

BNFL, 1986. Annual report on radioactive discharges and monitoring of the environment. British Nuclear Fuels Limited. Health and Safety Directorate, 1987. Risley.

BNFL, 1987. Annual report on radioactive discharges and monitoring of the environment. British Nuclear Fuels Limited. Health and Safety Directorate, 1988. Risley.

BNFL, 1988. Annual report on radioactive discharges and monitoring of the environment. British Nuclear Fuels Limited. Health and Safety Directorate, 1989. Risley.

Bohn, H. L., McNeal, B. L. and O'Connor, G. A., 1979. Soil Chemistry. John Wiley & Sons, New York, Chichester, Brisbane, Toronto.

Bondietti, E. A. and Brantley, J. N., 1988. Size distributions and growth of natural and Chernobyl derived submicron aerosols in Tennessee. J. Environ. Radioactivity, 6, 99-120.

Borole, D. V., Krishnaswami, S. and Somayajulu, B. L. K., 1977. Investigations on dissolved uranium silicon and particulate tracer elements in estuaries. Estuarine Coastal Mar. Sci., 5, 743-754.

Bowen, V. T. and Roether, W., 1973. Vertical distributions of ^{90}Sr, ^{137}Cs and tritium near 45° north in the Atlantic. General summary of progress, 1972-1973, Woods Hole Oceanogrpahic Institution, Mass. (US), 35pp.

Bowen, V. T., 1977. Oceanic distributions of radionuclides from nuclear weapons testing on methods for seabed disposal of nuclear wastes. Trans. Am. Nucl. Soc. , 26, 297p, New York, USA.

Bowen, V. T., Noshkin, V. E., Livingston, H. D. and Volchok, H. L., 1980. Fallout radionuclides in the Pacific Ocean: Vertical and horizontal distribution, largely from Geosecs stations. Earth Planet. Sci. Lett., 49, 411-434.

Brewer, P. G. and Spencer, D. W., 1975. Minor element modules in coastal water. Am. Chem. Soc. Symp. Series 18, 80-96.

Brewer, P. G., Nozaki, Y., Spencer, D. W. and Fleer, A. P., 1980. A sediment trap experiment in the deep sub-tropical Atlantic: Isotopic and element fluxes. J. Mar. Res., 38, 703-728.

Broecker, W. S., Bonebackker, E. R. and Rocco, G. G. 1966. The vertical distribution of caesium-137 and strontium-90 in the oceans, II. J. Geophys. Res., 71, 1999-2003.

Broecker, W. S., Kaufman, A. and Trier, R. M., 1973. The residence time of thorium in surface sea water and its implications regarding the rate of reactive pollutants. Earth Planet. Sci. Lett., 20, 35-44.

Broecker, W. S., 1974. Chemical Oceanography. Harcourte Brace Jovanovich Inc. New York, Chicago, San Francisco, Atlanta.

Browne, E. and Firestone, R. B. (1986). Table of radioactive isotopes. 7th Edition. John Wiley and Sons, New York.

Bruland, K. W., Koide, M. and Goldberg, E. D., 1974. The comparative marine geochemistries of lead-210 and radium-226. J. Geophys. Res., 79, 3083-3086.

Burton, J. D., 1975. Radioactive nuclides in the marine environment. In: Chemical Oceanography, Vol. 3, 2nd Edition, 91-191. Eds. Riley, J. P. and Skirrow, G. Academic Press, London, New York, San Francisco.

Butler, F. E., 1965. Determination of uranium and the americium - curium in urine by liquid ion exchange. Anal. Chem., 37, 340-342.

Byrne, A. R., 1988. Radioactivity in Fungi in Solvenia following the Chernobyl accident. J. Environ. Radioactivity, 6, 177-183.

Calvert, S. E., 1976. The mineralogy and geochemistry of near-shore sediments. In: Chemical Oceanography, 6, 2nd section,

187-271. Academic Press, London, New York, San Francisco.

Calvert, S. E. and Price, N. B., 1976. Composition of manganese nodules and manganese carbonates from Loch Fyne, Scotland. Contrib. Mineral. Petrol., 29, 215-233.

Cambray, R. S., Fisher, E. M. R., Parker, A. and Peirson, D. H., 1973. Radioactive fallout in air and rain. Results to the middle of 1973. Atomic Energy Research Establishment, Harwell. AERE-R7540.

Cambray, R. S. and Eakins, J. D., 1980. Studies of environmental radioactivity in Cumbria. Part 1: Concentrations of plutonium and caesium-137 in environmental samples from west Cumbria and a possible maritime effect. UKAEA report AERE-R-9807, HMSO.

Cambray, R. S., 1982. Annual discharges of certain long-lived radionuclides to the sea and to the atmosphere from the Sellafield works, Cumbria 1975-1981. UKAEA report AERE-M-3269, HMSO.

Cambray, R. S. and Eakins, J. D., 1982. Pu, ^{241}Am and ^{137}Cs in soil in West Cumbria and a maritime effect. Nature, 300, 46-48.

Cambray, R. S., Playford, K. and Lewis, G. N. J., 1982. Radioactive fallout in air and rain: results to the end of 1981. UKAEA Harwell Report AERE-R-10485, HMSO.

Cambray, R. S., Lewis, G. N. J. and Playford, K., 1984. Radioactive fallout in air and rain. Results to end of 1983. Atomic Energy Research Establishment, Harwell, AERE-R11475.

Cambray, R. S., Cawse, P. A., Garland, J. A., Gibson, J. A. B., Johnson, P., Lewis, G. N. J., Newton, D., Salmon, L. and Wade, B. O., 1987. Observations on radioactivity from the Chernobyl accident. Nucl. Energy, 26, 77-101.

CANMET, 1983. Radium-226 in certified uranium reference ores DL-1a, BL-4a, DH-1a and BL-5. CANMET Report 39-9E, Canadian Centre for Mineral and Energy Technology, Ottawa.

Carpenter, R. and Beasley, T. M., 1981. Plutonium and americium in anoxic marine sediments: evidence against remobilisation. Geochim. Cosmochim. Acta, 45, 1917-1930.

Carpenter, R., Peterson, M. L., Bennett, J. T. and Somayajulu, B. L. K., 1984. Mixing and cycling of uranium, thorium and ^{210}Pb in Paget Sound Sediments. Geochim. Cosmochim. Acta, 48, 1949-1963.

Cawse, P. A., 1980. Studies of environmental radioactivity in Cumbria: part 4. Caesium-137 and plutonium in soils of Cumbria and the Isle of Man. UKAEA, Harwell R-9851.

Cawse, P. A., 1983. The accummulation of ^{137}Cs and $^{239,240}Pu$ in soils of Great Britain and transfer to vegetation. In: Ecological aspects of radionuclide release. (Eds. Coughtrey, P. J., Bell, J. N. B. and Roberts, T. M.). Blackwell Scientific Publications.

Cawse, P. A. and Horrill, A. D., 1986. A survey of ^{137}Cs and plutonium in British soils in 1977. AERE Harwell Report R10155, HMSO.

Chapman, V. J., 1960. Salt marshes and salt deserts of the world. Leonard Hill Ltd. Interscience Publ. Inc., New York, 392pp.

Cheng, H. and Hamoguchi, H., 1968. The adsorption of radioisotopes on marine sediment. In: Role of exchangeable cations of the adsorption of caesium and exchange equilibria. Health Phys., 14(4), 353-363.

Chesne, A., 1983. Chemical problems associated with reprocessing. In: Actinides in perspective. Proc. of the

Actinides 1981 Conf. (Ed. Edelstein, N. M.). Pergamon Press, 541-552.

Christiansen, B. and Tors enfelt, B. 1988. Diffusion of Nickel, Strontium, Iodine, Caesium and Americium in loosely compacted Bentonite at high pH. Radiochimica Acta 4/45, 219-293.

Chu, N. Y., 1971. Plutonium determination in soil by leaching and ion exchange separation. Anal. Chem., 43, 449-452.

Clark, M. J. and Smith, F. B., 1988. Wet and dry deposition of Chernobyl releases. Nature, 332, 245-249.

Cleveland, J. M., 1979. Critical review of plutonium equilibria of environmental concern. In: Chemical Modelling in Aqueous Systems, (Ed. Jenne, E. A.). Am. Chem. Soc., 321-338.

Cleveland, J. M., 1970a. The Chemistry of plutonium. Gordon and Breach, New York.

Cleveland, J. M., 1970b. Aqueous coordination complexes of plutonium. Coord. Chem. Rev., 5, 101-137.

Clifton, R. J. and Hamilton, E. I., 1979. Lead-210 chronology in relation to levels of elements in dated sediment core profiles. Estuarine Coastal Mar. Sci., 8, 259-269.

Clifton, R. J. and Hamilton, E. I., 1982. The application of radioisotopes in the study of estuarine sedimentary processes. Estuarine Coastal Shelf Sci., 14, 433-446.

Cochran, J. K. and Aller, R. C., 1979. Particle reworking in sediments from the New York Bight Apex: Evidence from Th-234/U-238 disequilibrium. Estuarine Coastal Mar. Sci., 9, 739-747.

Cochran, J. K., 1982. The atomic chemistry of the U- and Th-series nuclides. In: Uranium Series Disequilibrium: Applications to Environmental Problems. (Eds. Ivanovich, M. I.

and Harmon, R. S.), 384-430, Clarendon Press, Oxford, England.

Cochran, J. K., Carey, A. E., Sholkovitz, E. R. and Surprenant, L. D., 1986. The geochemistry of uranium and thorium in coastal marine sediments and sediment pore waters. Geochim. Cosmochim. Acta, 50, 663-680.

Coleman, G. H., 1965. The Radiochemistry of Plutonium. US National Research Council, NAS-NS 3058, 184pp.

Collar, R. H. P., 1974. The River Clyde Estuary. Current knowledge of water and sediment movement. In: The Clyde Estuary and Firth, 10-13. Natural Environmental Research Council Publications Series C, No. 11.

Cook, G. T., Baxter, M. S., Duncan, H. J. and Malcolmson, R., 1984a. Geochemical associations of plutonium and γ-emitting radionuclides in Caithness soil and marine particulates. J. Environ. Radioactivity, 1, 119-131.

Cook, G. T., Baxter, M. S., Duncan, H. J., Toole, J. and Malcolmson, R., 1984b. Geochemical association of plutonium in the Caithness environment. Nucl. Instr. Methods Phys. Res., 223, 517-522.

Cowart, J. B. and Osmond, J. K., 1974. ^{234}U and ^{238}U in the carrizo sandstone aquifer of south Texas. Isotope techniques in groundwater hydrology, II, 131-149, IAEA, Vienna.

Craig, H., Krishnaswami, S. and Somayajulu, B. L. K., 1973. ^{210}Pb - ^{226}Ra : Radioactive disequilibrium in The Deep Sea. Earth Planet. Sci. Lett., 17, 295-305.

Craig, G. Y., 1983. Geology of Scotland. 2nd Edition, Scottish Academic Press, Edinburgh.

Crank, J., 1956. The mathematics of diffusion. Clarendon Press, Oxford.

Dahlman, R. C., Grten, C. T. and Hakonson, T. E., 1980. Comparative distribution of plutinium in contaminated ecosystems at Oak Ridge, Tennessee and Los Alams, New Mexico. In: Transuranic elements in the environment. (Ed. Hanson, W. C.), US Department of Energy, Technical Information Centre, DOE-TIC-22800, 371-380.

Day, J. P. and Cross, J. E., 1981. ^{241}Am from the decay of ^{241}Pu in the Irish Sea. Nature, 292, 43-45.

De Baar, H. J. W., Bacon, M. P. and Brewer, P. G. 1985. Rare earth elements in the Pacific and Atlantic Oceans. Geochimica et Comsochimica Acta, 49, 1943-1959.

De Baar, H. J. W., Brewer, P. G. and Bacon, M. P. 1985. Anomalies in rare earth distributions in seawater: Gd and Tb. Geochimica et Cosmochimica Acta, 49, 1961-1969.

De Soete, D., Gijbels, R. and Hoste, J., 1972. Neutron activation analysis. John Wiley & Sons, London, New York, Sydney and Toronto.

Devell, L., Tovedal, H. and Bergstrom. U. L., 1986. Initial observations of fallout from the reactor accident at Chernobyl. Nature, 321, 192-193.

Duursma, E. K. and Bosch, C., 1970. Theoretical, experimental and field studies concerning diffusion of radioisotopes in sediment and suspended particles of the sea. Part B: Methods and experiments. Netherlands J. Sea. Res., 4, 395-469. RITS No. 26.

Duursma, E. K. and Eisma, D., 1973. Theoretical experimental and field studies concerning reactions of radioisotopes with sediments and suspended particles of the sea. Part C: Applications to field studies. Netherlands J. Sea Res., 6, 256-324.

Dryak, P. and Kokta, L., 1984. Alpha spectrometric sources: their standardisation and practical aspects. Nucl. Instr. Methods Phys. Res., 223, 268-269.

Durani, S. A. and Bull, R. K., 1987. Solid state nuclear track detection. International Series in Natural Philosophy, Volume 111, Pergamon Press, Oxford.

Dyer, K. R., 1986. Review of oceanogrphic processes influencing radioactive waste disposal in the Irish Sea. IOS Report No 232, 59pp.

Eakins, J. D., Lally, A. E., Burton, P. J., Kilworth, D. R. and Pratley, F. A., 1982. Studies of environmental radioactivity in Cumbria. Part 5: The magnitude and mechanism of enrichment of Sea spray with actinides in west Cumbria. UK Atomic Energy Authority, Harwell, AERE-R10127, 47pp.

Edgington, D. N. and Robbins, J. N., 1975. The behaviour of plutonium and other long lived radionuclides in Lake Michigan. II patterns of deposition in the sediments. In: Impacts of Nuclear Releases into the Aquatic Environment. IAEA, Vienna, 245-260.

Edgington, D. N., Wahlgren, M. A. and Marshall, J. S. 1976. The Behaviour of plutonium in Aquatic Ecosystems. A summary of studies on the Great Lakes. In: Environmental Toxicity of Aquatic Radionuclides Models and Mechanisms. (Eds. Miller, M. W. and Stannard, J. N.). Ann. Arbor., 45-79.

Edgington, D. N., 1981. A review of the persistence of long-lived radionuclides in the marine environment - sediment/water interactions. Proc. Symp. Vienna (1980). IAEA-SM-248/148, 67-91.

Elderfield, H. and Greaves, M. J., 1982. The rare earth elements in sea water. Nature, 296, 214-219.

Essington, E. H., Fowler, E. B., Gilbert, R. O. and Eberhardt, L. L., 1976. Plutonium americium and uranium concentrations in Nevada test site soil profiles. In: Transuranium Nuclides in the Environment. IAEA-SM-199/76, 157-172, Vienna.

Facer, G., 1980. Quantities of transuranic elements in the environment from operations relating to nuclear weapons. In: Transuranic elements in the environment. (Ed. Hanson, W. C.). DOE Publication Series. 86-91, TID-22800 Washington DC.

Fews, A. P. and Henshaw, D. L., 1984. High resolution alpha-particle spectroscopy using CR39 plastic track detector. Nucl. Instr. Methods Phys. Res., 23, 609-616.

Fleet, A. J. 1984. Aqueous and sedimentary geochemistry of the rare earth elements. In: Developments in Geochemistry 2. Rare Earth Element Geochemistry. Ed: Henderson, P., Elsevier, Oxford.

Fleischer, R. L., Price, P. B. and Walker, P. M., 1975. Nuclear tracks in solids. The Univ. of California Press, Berkeley, Los Angeles and London.

Fleischer, R. L. and Raabe, O. G., 1978. Recoiling alpha emitting nuclei. mechanism for uranium disequilibrium. Geochim. Cosmochim. Acta, 42, 973-978.

Fleischer, R. L., 1980. Isotopic disequilibrium of uranium: alpha-recoil damage and preferential solution effects. Science, 207, 979-981.

Fleischer, R. L., 1982. Alpha-recoil damage and solution effects in minerals: Uranium isotopic disequilibrium and radon release. Geochim. Cosmochim. Acta, 46, 2191-2201.

Fowler, S. W., Buat-Menard, P., Yokoyama, Y., Ballestra, S., Holm, E. and Nguyen, H. V., 1987. Rapid removal of Chernobyl fallout from Mediterranean surface waters by biological activity. Nature, 329, 56-58.

Fraizier, A., Masson, M. and Guarg, J. C., 1977. Recherches preliminaires sur le role des aerosols dans la transfert de certains radioelements du miliéu marin au milieu terrestre. J. Rech. Atmos., 11, 49-60.

Friedlander, G., Kennedy, J. W., Macias, E. S. and Miller, J. M., 1981. Nuclear and Radiochemistry. 3rd Edition, John Wiley & Sons, New York.

Ganapathy, S., Pillai, K. C. and Ganguly, A. K., 1968. Absorption of trace elements by near shore sea-bed sediments. BARC-376, 113pp. (Bhabha Atomic Research Centre, Bombay, India).

Gascoyne, M. and Schwarcz, H. P., 1982. Carbonate and sulphate precipitates. In: Uranium Series Disequilibrium Applications to Environmental Problems. (Eds. Ivanovich, M. I. and Harmon, R. S.). Clarendon Press, Oxford.

Goldberg, E. D. and Koide, M., 1963. Rates of sediment accumulation in the Indian Ocean. In: Earth Science and Meteoritics. (Eds. Geiss, J. and Goldberg, E. D.), 90, Amsterdam, Holland.

Goldberg, E. D. and Bruland, K., 1974. The sea. (Ed. Goldberg, E. D.), 451-489. Wiley-Interscience, New York.

Goldberg, E. D., Gamble, E., Griffin, J. J. and Koide, H., 1977. Pollution history of Narragansett Bay as recorded in its sediment. Estuarine Coastal Mar. Sci., 5, 549-561.

Goreau, T. J., 1977. Quantitative effects of sediment mixing on stratigraphy and biogeochemistry. Nature, 265, 525-526.

Greenwood, N. N. and Earnshaw, A. 1984. Chemistry of the Elements. Pergamon Press, 1564pp.

Grenthe, I. and Noren, B., 1960. Stability of nitrate and chloride complexes of plutonium (IV). Acta Chem. Scand., 14, 2216-2229.

Grindler, J. E., 1962. The Radiochemistry of Uranium. NAS-NS3050. US Atomic Energy Commission.

Hallberg, L., Brise, H., Anderson, S. and Jelc, C., 1960. Determination of Fe^{55} and Fe^{59} in blood. Int. J. Appl. Radiat. Isotopes, 9, 100-108.

Halliday, A. N., Fallick, A. E., Dickin, A. P., MacKenzie, A. B., Stephens, W. E. and Hildreth, W., 1983. The isotopic and chemical evolution of Mount St Helens. Earth Planet. Sci. Lett., 63, 241-256.

Hamilton, E. I., 1980. Concentration and distribution of uranium in Mytilus Edulis and associated materials. Mar. Ecol. Prog. Ser., 2, 61-73.

Hamilton, E. I., 1981. α-particle radioactivity of hot particles from the Esk Estuary. Nature, 290, 690-693.

Hamilton, E. I. and Clifton, R. J., 1981. CR-39, a new α-particle sensitive polymeric detector applied to investigations of environmental radioactivity. Int. J. Appl. Radiat. Isotopes, 32, 313-324.

Hamilton, E. I. and Clifton, R. J., 1987. The origin composition and distribution of "hot particles" derived from the nuclear industry and dispersed in the environment. DOE Report No DOE/RW/88001.

Hansen, R. O., 1965. Isotopic distribution of uranium and thorium in soils weathered from granite and alluvium. Thesis,

Berkeley, Calif. Univ. of California, 1965, 135p.

Hansen, R. O. and Stout, P. R., 1968. Isotope distributions of uranium and thorium in soils. Soil Sci., 105, 45-50.

Hardy, E. P., Krey, P. W. and Volchok, H. L., 1973. Global inventory and distribution of fallout plutonium. Nature, 241, 444-445.

Hardy, E. P. 1974. Worldwide Distribution of Plutonium. In: Plutonium and other transuranic elements. Sources, Environmental Distribution and Biomedical Effects. Ed: Wacholz, B. W. US Atomic Energy Commission, Washington. WASH-1359, 115-130.

Harmon, R. S., and Rosholt, J. N., 1982. Igneous rocks. In: Uranium Disequilibrium Applications to Environmental Problems. (Eds. Ivanovich, M. I. and Harmon, R. S.). Clarendon Press, Oxford.

Harris, I., 1987. NAA - neutron activation analysis programme. Scottish Universities Research and Reactor Centre (SURRC).

Harvey, B. G., 1969. Introduction to nuclear physics and chemistry. 2nd edition, Prentice-Hall, INC, London, England.

Henderson, P., 1982. Inorganic geochemistry. Pergamon Press, Oxford.

Henderson, P., 1984. Rare Earth Element Geochemistry. Developments in Geochemistry 2. Elsevier, Oxford, England.

Hetherington, J. A. and Jefferies, D. F., 1974. The distribution of some fission product radionuclides in sea and estuarine sediments. Netherlands J. Sea Res., 8(4), 319-338.

Hetherington, J. A., 1975. Radioisotopes in the aquatic environment: Models and mechanisms. (Proc. Symp. Rochester,

1975). Ann Arbor Sciences Publishers Inc., Michigan.

Hetherington, J. A., Jefferies, D. F. and Lovett, M. B., 1975. Some investigations into the behaviour of plutonium in the marine environment. In: Impacts of Nuclear Releases into the Aquatic Environment. IAEA Vienna. IAEA-SM-198, 193-212.

Hetherington, J. A., 1976. The behaviour of plutonium nuclides in the Irish Sea. In: Environmental Toxicity of Aquatic Radionuclides: Models and Mechanisms. (Eds. Miller, M. W. and Stannard, J. N.). Ann Arbor Science Publishers Inc., Michigan, 81-106.

Hetherington, J. A., Jefferies, D. F., Mitchell, N. T., Pentreath, R. J. and Woodhead, D. S., 1976. Environmental and public health consequences of the controlled disposal of transuranic elements to the marine environment. In Proc. IAEA Symp., Transuranium nuclides in the environment. San Francisco 1975, 139-154. International Atomic Energy Agency, Vienna, Austria.

Hetherington, J. A., 1978. The uptake of plutonium nuclides by marine sediments. Mar. Sci. Comm., 4, 239-274.

Higgo, J. J. W., Cole, T. G. and Rees, L. V. C., 1988. Diffusion of Radionuclides through Deep-Sea Sediments. Radiochimica Acta 44/45, 231-238.

Holm, E. and Fukai, R., 1977. Method for multi-element alpha spectrometry of actinides and its application to environmental radioactivity studies. Talenta, 24, 659-664.

Holm, E. and Persson, R. B. R., 1977. Pu-241 and Am-241 in the environment. Proc. 4th Intern. Cong. of IRPA. April 1977 Paris, Vol 3, 845-848. RITS No 62.

Holm, E., Ballestra, S. and Fukai, R., 1979. A method for ion-exchange separation of low-level americium in environmental

materials. Talenta, 26, 791-794.

Hooker, P. J., MacKenzie, A. B., Scott, R. D., Ivanovich, M. I., Ball, T. K., Basham, I. R., Bloodworth, A. J. and Roberts, P. D., 1986. Natural analogues of radionuclide migration reconnaissance study of sites (May 1985 - March 1986). BGS Report FLPU 86-6. British Geological Survey, Keyworth.

Hooker, P. J., Chapman, A. B., MacKenzie, A. B., Scott, R. D. and Ivanovich, M. I., 1987. Natural analogues of radionuclide migration in sediments in Britain. (Eds. Côme, B. and Chapman, N. A.). Radioactive Waste Management Series (Natural analogues in radioactive waste disposal. Graham and Trotman Publishers, London, 104-115.

Horrill, A. D., Lowe, V. P. W., Howson, G., 1988. Chernobyl Fallout in Great Britain. (UK) DOE-RW-88.101. 88pp.

Humphries, S. E., 1984. The mobility of the rare earth elements in the crust. In: Developments in Geochemistry 2. Rare earth element Geochemistry. (Ed: Henderson, P., Elsevier, Oxford.

Hussain, N. and Krishnaswami, S., 1980. ^{238}U series radioactive disequilibrium in groundwater: Applications to the origin of excess ^{234}U and fate of reactive pollutants. Geochim. Cosmochim. Acta, 44, 1287-1291.

Hyde, E. K., 1960. The radiochemistry of thorium. US National Academy of Science. (Nuclear Science Series) US Atomic Energy Commission.

IAEA, 1978. Natural fission reactors. Proceedings of a technical committee meeting, Paris 19-21 December 1977. ST1/PUB/475. IAEA, Vienna.

IAEA, 1982. Transuranic Cycling Behaviour in the Marine Environment. IAEA, Vienna.

IAEA, 1985. Sediment K_DS and concentration factors for radionuclides in the marine environment. IAEA, Vienna.

Ivanovich, M. I., 1982. Uranium Series Disequilibria Application in Geochronology. In; Uranium Series Disequilibrium: Application to Environmental Problems. (Eds. Ivanovich, M. A. and Harmon, R. S.). Clarendon Press, Oxford, England.

Ivanovich, M. I. and Harmon, R. S., 1982. Uranium series disequilibrium. Applications to environmental problems. Clarendon Press, Oxford.

Jakubick, A. T., 1976. Migration of plutonium in natural soils. In: Transuranium nuclides in the environment. IAEA-SM-199-3.

James, D. B., 1967. Anion-exchange processing of plutonium. Nucl. Sci. Abst., 21(6), 8191.

James, A. C., Strather, J. W., Greenhalgh, J. R., Hodgson, J. C. and Rodwell, P., 1978. The distribution of ^{241}Am between components of sediments from the Ravenglass Estuary. National Radiological Protection Board, Research and Development Board Ann. Rep., 136-140, Harwell.

Janne, E. A. and Wahlberg, J. S., 1968. Role of Certain Stream Sediment Components in Radio-ion Sorption. US Geological Survey, Professional Paper, 433-F, 16pp.

Jefferies, D. F., Preston, A. and Steele, A. K., 1973, Distribution of ^{137}Cs in British coastal waters. Mar. Pollut. Bull., 4, 118-122.

Jefferies, D. F., Steele, A. K. and Preston, A., 1982. Further studies on the distribution of ^{137}Cs in British coastal waters - Irish Sea. Deep sea research, 29, 713-738.

Jones, D. G., Miller, J. M. and Roberts, P. D., 1984. The distribution of ^{137}Cs in surface intertidal sediments from the

Solway Firth. Mar. Pollut. Bull., 15, 187-194.

Joseph, A. B., Gustafson, P. F., Russell, I. R., Schuert, E. A., Volchok, H. L. and Tamplin, A., 1971. Radioactivity in the marine environment, 6-41. National Academy of Sciences, Washington DC.

Joshi, L. V. and Ganguhly, A. K., 1976. Anomalous behaviour of uranium isotopes in coastal marine environment of the West Coast of India. Geochim. Cosmochim. Acta, 50, 593-607.

Katz, J. J., Seaborg, G. T. and Morss, L. R., 1986. The chemistry of the actinide elements. 2nd edition, Vol 1, 2. London, New York (Chapman and Hall).

Kaufman, A., Li, Y. H. and Turekian, K. K., 1981. The removal rates of ^{234}Th and ^{228}Th from waters of the New York Bight. Earth Planet. Sci. Lett., 54, 385-392.

Kershaw, P. J., Swift, D. J., Pentreath, P. J. and Lovett, M. B., 1983. Plutonium redistribution by biological activity in Irish Sea sediments. Nature, 306, 774-775.

Kershaw, P. J., Brealey, J. H., Woodhead, D. S. and Lovett, M. B.., 1986. Alpha-emitting, hot particles in Irish Sea sediments. Sci. Total Environ., 53, 77-87.

Kershaw, P. and Young, A., 1988. Scavenging of ^{234}Th in the Eastern Irish Sea, J. Environ. Radioactivity, 6, 1-23.

Kershaw, P. J., Gurbutt, P. A., Young, A. K. and Allington, D. J., 1988a. Scavenging and bioturbation in the irish sea from measurements of $^{234}Th/^{238}U$ and $^{210}Pb/^{226}Ra$ disequilibria. Radionuclides: A tool for oceanography (Guary, J. C., Guengueniat, P. A. and Pentreath, R. J.). Elsevier, 131-142.

Kershaw, P. J., Swift, D. J. and Denoon, D. C., 1988b. Evidence of Recent Sedimentation in the Eastern Irish Sea. Marine Geology, 85, 1-14.

Khopar, S. M. and De, A. K., 1960. Rapid extraction and spectrophotometric determinations of uranium with 2-thenoyl trifluoroacetone. Analyst, 85, 376-379.

Kigoshi, K., 1971. Alpha recoil Th-234 dissolution into water and U-234/U-238 disequilibrium in nature. Science, 173, 47-48.

Kirby, R., Parker, W. R., Pentreath, R. J. and Lovett, M. B., 1983. Sedimentation Studies Relevent to Low-level Radioactive Effluent Dispersed Into The Irish Sea. Part III. An evaluation possible mechanisms for the incorporation of radionuclides into marine sediments. IOS Rep. No. 178, 66pp.

Knauss, K. G., Ku, T. L. and Moore, W. S., 1978. Radium and thorium isotopes in the surface waters of the east Pacific and coastal south California. Earth Planet. Sci. Lett., 39, 235-249.

Ko, R. and Weiller, M. R., 1962. Spectrographic determination of thorium in uranium ore. Anal. Chem., 34, 85-87.

Koide, M., Bruland, K. W., Goldberg, E. D., 1973. Th-228/Th-232 and Pb-210 geochronologics in marine and lake sediments. Geochim. Cosmochim. Acta, 37, 1171-1187.

Koide, M., Griffin, J. J. and Goldberg, E. D., 1975. Records of plutonium fallout in marine and terrestrial samples. J. Geophys. Res., 80, 4153-4162.

Korkisch, J., Anal, P. and Hecht, F., 1960. Ion exchange in solvent mixtures. I. On the distribution of uranium between alcoholic mineral acid solutions, and the strongly basic anion exchanger Dowex-I. J. Inorg. Nucl. Chem., 14, 247-250.

Korkisch, J., 1966. Ion exchange in mixed and non-aqueous media. Progress in nuclear energy, series IX. Analytical Chemistry, 6. Pergamon Press.

Korkisch, J., 1969. Modern methods for the separation of rarer metal ions. Pergamon Press, Oxford, London, Edinburgh, New York, Toronto, Sydney, Paris, Braunschweig.

Krauskopf, K. B., 1979. Introduction to geochemistry. McGraw-Hill International Book Company, London, Paris, Tokyo.

Krishnaswami, S., Lal, D., Martin, J. M. and Meybeck, M., 1971. Geochronology of lake sediments. Earth Planet. Sci. Lett., 11, 407-414.

Krishnaswami, S., Somayajulu, B. L. K. and Chung, Y., 1975. $^{210}Pb/^{226}Ra$ disequilibrium in the Santa Barbara Basin. Earth Planet. Sci. Lett., 27, 388-392.

Ku, T. L., 1965. An evaluation of the $^{234}U/^{238}U$ method as a tool for dating palagic sediment. J. Geophys. Res., 70, 3457-3474.

Ku, T. L., 1966. Uranium series disequilibrium in deep sea sediments. PhD thesis, Columbia University, New York, 157pp.

Ku, T. L. and Glasby, G. P., 1972. Radiometric evidence for the rapid growth rate of shallow-water, continental margin manganese nodules. Geochim. Cosmochim. Acta, 36, 699-703.

Ku, T. L., Knauss, K. G. and Mathieu, G. G., 1974. Uranium in open oceans: concentration and isotopic composition. Deep-Sea Res. 24, 1005-1017.

Ku, T. L., 1976. The uranium series methods of age determination. Ann. Rev. Earth Planet. Sci., 4, 347-379.

Lally, A. E. and Eakins, J. D., 1978. Some recent advances in environmental analysis at AERE, Harwell. In: Symposium on the

Determination of Radionuclides in Environmental and Biological Materials. CEGB Sudbury House, 9-10 October, 1978.

Lally, A. E., 1982. Chemical Procedures. In: Uranium series disequilibrium: Application to environmental problems. (Eds. Ivanovich, M. I. and Harmon, R. S.). Clarendon Press, Oxford.

Lally, A. E. and Glover, K. M., 1984. Source preparation in alpha spectrometry. Nuclear Instr. Methods Physics Res., 223, 259-265.

Lalou, C. and Brichet, E., 1980. Anomalously high uranium contents in the sediment under Galapagos hydrothermal mounds. Nature, 284, 251-253.

Lammers, W. T., 1968. The distribution of ^{60}Co, ^{106}Ru and ^{137}Cs among suspended and dissolved particles in White Oak Lake. Oak Ridge Gaseous Diffusion Plant Tenn. 20pp.

Laul, J. C.,1982. Chemical migration by contact metamorphism between granite and SiH/Carbonate system. Proc. Int. Long-lived Radionuclides from the Nuclear Fuel Cycle. IAEA-SM-257, 603-612.

Lederer, C. M. and Shirley, V. S. (Eds.), 1978. Table of isotopes. 7th edition, John Wiley & Son, New York.

Lewis, D. M., 1976. The geochemistry of manganese, iron, uranium, ^{210}Pb and major ions in the Susquehanna River. PhD thesis, Yale University, Connecticut.

Lewis, D. M., 1977. The use of ^{210}Pb as a heavy metal tracer in the Susquenhanna River system. Geochim. Cosmochim. Acta, 41, 1557-1564.

Li, Y. H. and Chan, L. H., 1979. Desorption of Ba and Ra-226 from river-borne sediments in the Hudson estuary. Earth Planet. Sci. Lett., 43, 343-350.

Little, C. A., 1980. Plutinium in a grassland ecosystem. In: Transuranic elements in the environment. (Ed. Hanson, W. C.), US Department of the Energy, Technical Information Centre. DOE/TIC, 22800, 420-440.

Livens, F. R., 1985. Geochemistry of plutonium and other Artifical Radionuclides in Cumbrian Soils. PhD Thesis, Glasgow Univ.

Livens, F. R. and Baxter, M. S., 1988. Particle size and radionuclide levels in some West Cumbrian soils. Sci. Total Environ., 70, 1-17.

Livingston, H. D. and Bowen, U. T., 1975. Americium in the marine environment relationship to plutonium. Chapter 6, Environmental Toxicity of Aquatic Radionuclides.

Livingston, H. D. and Bowen, V. T., 1976. Americium in the marine environment: relationships to plutonium. In: Radioisotopes in the aquatic environment: models and mechanisms. (Eds. Miller, M. W. and Stannard, J. N.) Ann Arbor, 107-130.

Livingston, D. H. and Bowen, V. T., 1977. Windscale effluent in the waters and sediments of the Minch. Nature, 269, 5-86.

Livingston, H. D. and Bowen, V. T., 1978. Pu and ^{137}Cs in coastal sediments. Earth Planet. Sci. Lett., 43, 29-45.

Livingston, H. D. and Bowen, V. T., 1979. Pu and ^{137}Cs in coastal sediments. Earth Planet. Sci. Lett., 43, 29-45.

Livingston, H. D., Bowen, V. T. and Kupferman, S. L., 1982. Radionuclides from Windscale discharges. J. Non-equilibrium tracer experiment in high latitude oceanography. J. Mar. Res.,

40, 253-272.

Lomenick, T. F. and Tamura, T., 1965. Naturally occurring fixation of ^{137}Cs on sediments of Lacustrine Origin. Soil Sci. Am. Proc., 29, 383-387.

Lovett, M. B. and Nelson, D. M., 1978. The determination of the oxidation states of plutonium in sea water and associated particulate matter. Proc. CEGB Conf. Determiantion of radionuclides in environmental and biological materials. CEGB, Sudbury House, 10-11 Oct. 1978.

Lovett, M. B. and Nelson, D. M., 1981. Determination of some oxidation states of plutonium in sea water and associated particulate matter. In: Techniques for identifying transuranic speciation in aquatic environments. 27 - 35, IAEA, Vienna.

MacKenzie, A. B. and Scott, R. D., 1979. Separation of bismuth-210 and polonium-210 from aqueous solutions by spontaneous adsorption on copper foils. Analyst., 104, 1151-1158.

MacKenzie, A.. B., Baxter, M. S., McKinley, I. G., Swan, D. S. and Jack, W., 1979. The determination of ^{134}Cs, ^{137}Cs, ^{210}Pb, ^{225}Ra and ^{228}Ra concentrations in nearshore marine sediments and seawater. J. Radioanalyt. Chem., 48, 29-47.

MacKenzie, A. B., 1981. A proposed approach to the study of radionuclide geochemistry in intertidal sediments. In: IAEA/CEC Conf. Techniques for identifying transuranic speciation in aquatic environment. STI/PUB/613, 257-262, IAEA, Vienna.

MacKenzie, A. B., Scott, R. D., 1982a. Artifical radionuclides in the coastal zone of Southern Scotland. In: Transuranic cycling behaviour in the marine environment. IAEA TECDOC-265, 111-119, IAEA, Vienna.

MacKenzie, A. B. and Scott, R. D., 1982b. Radiocaesium and plutonium in intertidal sediments from southern Scotland. Nature, 299, 613-616.

MacKenzie, A. B. and Scott, R. D., 1984. Some aspects of coastal marine disposal of low-level liquid radioactive waste. Nucl. Eng., 25, 110-127.

MacKenzie, A. B., Scott, R. D. and Williams, T. M., 1987. Mechanisms for northwards dispersal of Sellafield waste. Nature, 329, 42-45.

MacKenzie, A. B. and Scott, R. D., 1989. Personal Communication.

MAFF, 1973. Radioactivity in surface and coastal waters of the British Isles, 1971. Ministry of Agriculture, Fisheries and Food, Fisheries Radiological Laboratory Technical Report FRL 9, Lowestoft, UK.

MAFF, 1975. Radioactivity in surface and coastal waters of the British Isles, 1972-73. Ministry of Agriculture, Fisheries and Food, Fisheries Radiological Laboratory Technical Report FRL 10, Lowestoft, UK.

MAFF, 1976. Radioactivity in surface and coastal waters of the British Isles, 1974. Ministry of Agriculture, Fisheries and Food, Directorate of Fisheries Research, Fisheries Radiological Laboratory Technical Report FRL 11, Lowestoft, UK.

MAFF, 1977. Radioactivity in surface and coastal waters of the British Isles, 1975. Ministry of Agriculture, Fisheries and Food, Directorate of Fisheries Research, Fisheries Radiological Laboratory Technical Report FRL 12, Lowestoft, UK.

MAFF, 1977. Radioactivity in surface and coastal waters of the British Isles, 1976. Part 1: The Irish Sea and its Environs. Ministry of Agriculture, Fisheries and Food, Directorate of Fisheries Research, Fisheries Radiological Laboratory Technical

Report FRL 13, Lowestoft, UK.

MAFF, 1978. Radioactivity in surface and coastal waters of the British Isles, 1976. Part 2: Areas other than the Irish Sea and its Environs. Ministry of Agriculture, Fisheries and Food, Directorate of Fisheries Research, Fisheries Radiological Laboratory Technical Report FRL 14, Lowestoft, UK.

MAFF, 1979. Radioactivity in surface and coastal waters of the British Isles, 1977. Ministry of Agriculture, Fisheries and Food, Directorate of Fisheries Research, Aquatic Environment Monitoring Report No 3, Lowestoft, UK.

MAFF, 1980. Radioactivity in surface and coastal waters of the British Isles, 1978. Ministry of Agriculture, Fisheries and Food, Directorate of Fisheries Research, Aquatic Environment Monitoring Report No 4, Lowestoft, UK.

MAFF, 1981. Radioactivity in surface and coastal waters of the British Isles, 1979. Ministry of Agriculture, Fisheries and Food, Directorate of Fisheries Research, Aquatic Environment Monitoring Report No 6, Lowestoft, UK.

MAFF, 1982. Radioactivity in surface and coastal waters of the British Isles, 1980. Ministry of Agriculture, Fisheries and Food, Directorate of Fisheries Research, Aquatic Environment Monitoring Report No 8, Lowestoft, UK.

MAFF, 1983. Radioactivity in surface and coastal waters of the British Isles, 1981. Ministry of Agriculture, Fisheries and Food, Directorate of Fisheries Research, Aquatic Environment Monitoring Report No 9, Lowestoft, UK.

MAFF, 1984. Radioactivity in surface and coastal waters of the British Isles, 1981. Ministry of Agriculture, Fisheries and Food, Directorate of Fisheries Research, Aquatic Environment Monitoring Report No 11, Lowestoft, UK.

MAFF, 1985. Radioactivity in surface and coastal waters of the British Isles, 1983. Ministry of Agriculture, Fisheries and Food, Directorate of Fisheries Research, Aquatic Environment Monitoring Report No 12, Lowestoft, UK.

MAFF, 1985. Radioactivity in surface and coastal waters of the British Isles, 1984. Ministry of Agriculture, Fisheries and Food, Directorate of Fisheries Research, Aquatic Environment Monitoring Report No 13, Lowestoft, UK.

MAFF, 1986. Radioactivity in surface and coastal waters of the British Isles, 1985. Ministry of Agriculture, Fisheries and Food, Directorate of Fisheries Research, Aquatic Environment Monitoring Report No 14, Lowestoft, UK.

MAFF, 1987. Radioactivity in surface and coastal waters of the British Isles, 1986. Ministry of Agriculture, Fisheries and Food, Directorate of Fisheries Research, Aquatic Environment Monitoring Report No 18, Lowestoft, UK.

MAFF, 1988. Radioactivity in surface and coastal waters of the British Isles, 1987. Ministry of Agriculture, Fisheries and Food, Directorate of Fisheries Research, Aquatic Environment Monitoring Report No 19, Lowestoft, UK.

Manheim, F. T., 1976. Interstitial waters of marine sediments. In: Chemical Oceanography. 2nd Edition, 6, 114-186. J. P Riley and Skirrow, Academic Press, London, New York, San Francisco.

Marcus, Y., 1966. Anion exchange of metal complexes-XV. Anion exchange and amino extraction of lanthamides and trivalent actinides for chloride solutions. J. Inorg. Nucl. Chem., 28, 209-219.

Marshall, T. R., 1962a. The physiographic development of Caerlaverock merse. Trans. Dumfries and Galloway Nat. Hist. and Antiq. Soc., 39, 102.

Marshall, T. R., 1962b. The morphology of the upper Solway marshes. Scot. Geog. Mag., 78, 81.

Martin, J. M., Mijampukar, V., Salvadori, F., 1978. Uranium and thorium isotopes behaviour in estuarine systems. In: Biogeochemistry of estuarine sediments, proc. Unesco/SCOR Workshop, Melreuse (Belgium), Unesco press, 111-126.

Mason, B., 1966. Principles of geochemistry. 3rd Edition. John Wiley & Sons Inc., New York, London.

Mason, B. and Moore, C. B., 1982. Principles of geochemistry. 9th Edition. John Wiley & Sons Inc., New York.

Matsumoto, E., 1975. ^{234}Th-^{238}U radioactive disequilibrium in the surface layer of the ocean. Geochim. Cosmochim. Act, 39, 205-212.

Mc Donald, P., Cook, G. T., Baxter, M. S. and Thomson, J. C. 1990 . Radionuclide transfer from Sellafield to south west Scotland. J. Environ. Radioactivity. (In press)

McDowell, W. J., Fassas, D. T. and Billings, M. R., 1974. Plutonium and uranium determination in environmental samples. Combined Solvent Extraction - Liquid Scintilllation Method. Talanta, 21, 1231-1245.

McKay, H. A. C., 1971. Principles of Radiochemistry. Butterworth & Co (Publishers) Ltd, London.

McKay, W. A. and Baxter, M. S., 1985. The partitioning of Sellafield derived radiocaesium in Scottish coastal sediments.. J. Environ. Radioactivity, 2, 93-114.

McKinley, I. G. and Baxter, M. S., 1980. A radiotracer study of water renewal and sedimentation in a Scottish fjord. NATO Conf. Ser., 4, 539-544.

McKinley, I. G., Baxter, M. S., Ellett, D. J. and Jack, W., 1981a. Tracer applications of radiocaesium in the sea of the Hebrides. Estuarine Coastal Shelf Sci., 13, 69-80.

McKinley, I. G., Baxter, M. S. and Jack, W., 1981b. A simple model of radiocaesium transport from Windscale to the Clyde Sea Area. Estuarine Coastal Shelf Sci., 13, 59-67.

McLaren, R. B. and Crawford, D. V., 1973. Studies on soil copper 1. The fractionation of copper in soils. J. Soil Sci., 24, 172-181.

Means, J. L., Crerar, D. A. and Borcsik, M. P., 1978. Adsorption of cobalt and selected actinides by manganese and iron oxides in soils and sediments. Geochim. Cosmochim. Acta., 42, 1763-1773.

Miller, J. M. and Taylor, K., 1966. Uranium mineralisation near Dalbeattie, Kirkcudbrightshire. Bull. Geol. Surv. Great Britain, 25, 1-18.

Miller, J. M., Thomas, B. W., Roberts, P. D. and Creamer, S. C., 1982. Measurement of marine radionuclide distribution using a towed sea-bed spectrometer. Mar. Pollut. Bull., 13, 315-319.

Minczewski, J., Chwastowska, J., Dybczynski, R., 1982. Separation and preconcentration methods in inorganic trace analysis. John Wiley & Sons Inc., New York.

Mitchell, N. T. and Steele, A. K., 1988. The marine impact of ^{134}Cs and ^{137}Cs from the Chernobyl reactor accident. J. Environ. Radioactivity, 6, 163-175.

Moore, F. L., 1958. Liquid-liquid extraction of uranium and plutonium from hydrochloric acid solution with tri (iso-octyl) amino. Anal. Chem., 30, 908-911.

Moore, W. S., 1967. Amazon and Mississippi River concentrations of uranium, thorium and radium isotopes. Earth Planet. Sci.

Lett., 2, 231-234.

Moore, W. S., 1969. Oceanic concentrations of ^{228}Ra. Earth Planet. Sci. Lett., 6, 437-446.

Moskvin, A. I., Essen, L. N. and Bukhtiyarova, T. N. (1967a). The formation of thorium (III) and uranium (III) complexes in phosphate solutions. Russian J. Inorg. Chem., 12, 1794.

Moskvin, A. I., Shelyakina, A. and Perminov, P. S. (1967b). Solubility product of uranyl phosphate and the composition and dissociation constants of uranyl phosphato-complexes. Russian J. Inorg. Chem., 12, 1756.

Muller, R. N., 1978. Chemical characterisation of local and stratospheric plutonium in Ohio soils. Soil Sci., 125, 131-136.

Murray, S. M., 1975. Accumulation rates of sediments and metals off southern California as determined by ^{210}Pb method. PhD Thesis, University Southern California, Los Angeles, 146pp.

Murray, C. N., Kautsky, H., Hoppenheit, M. and Domian, M., 1978. Actinide activites in water entering the northern North Sea. Nature, 276, 225-230.

Murray, C. N., Kautsky, H. and Eicke, H. E., 1979. Transfer of actinides from the English Channel into the southern North Sea. Nature, 278, 617-620.

NEA, 1981. The environmental and biological behaviour of plutonium and some other transuranic elements. OECD Nuclear Energy Agency, Paris.

Nebbad, N., 1988. Natural ^{210}Po and manmade ^{137}Cs as tracers of sediment accumulation and mixing in intertidal and marine sediments. Application to the South and West Coast of Scotland. MSc Thesis, Haut Commissariat a la Recherche, Algeria.

Nesbitt, H. W., 1979. Mobility and fractionation of rare earth elements during weathering of a granodiorite. Nature, 279, 206-210.

Newton, G. W. A., Gilmore, G. R. and Hemingway, J. D., 1972. Radiochemistry. A review of the literature published between July 1969 and August 1971, Volume 1. The Chemical Society, Burlington House, London.

Noshkin, V. E. and Bowen, V. T., 1973. Concentrations and distributions of long-lived fallout radionuclides in open ocean sediments. In: Radioactive Contamination of the marine environment. IAEA Symp. (SM 158/45), 671-686.

Nozaki, Y., Turekian, K. K. and Von Damm, K., 1980. ^{210}Pb in Geoscecs water profiles from the north Pacific. Earth Planet. Sci. Lett., 49, 393-400.

NRPB, 1987. Interim guidance on the implications of recent revision of risk estimates and ICRP 1987 Como Statement. Report GS-9 National Radiological Protection Board, Chilton, Didcot, Oxon OX11 0RA, November 1987.

Nyhan, J. W., Miera, F. R. and Peters, R. J., 1976. Distribution of soil plutonium in soil particle size fraction of liquid effluent receiving a reus at Los Alamos. J. Env. Qual., 5, 431-437.

Oldfield, F., Appleby, P. G. and Butterbee, R. W., 1978. Alternative ^{210}Pb dating: results from the New Guinea Highlands and Lough Erne, Nature, 271, 339-342.

Osmond, J. K. and Cowart, J. B., 1976. The theory and uses of natural uranium isotopic variations in hydrology. Atomic Energy Rev., 144, 621-679.

Pattenden, N. J., Cambray, R. S., Playford, K., Eakins, J. D. and Fisher, E. M. R., 1980. Studies of environmental

radioactivity in Cumbria. Part 3: measurements of radionuclides in airborne and deposited material. UKAEA Harwell Report No AERE-R9857, HMSO.

Paunescu, N., 1986. Determination of uranium and thorium concentration in natural waters. J. Radioanalyt. Nucl. Chem. Lett., 104, 4, 209-216.

Peirson, D. H., Cambray, R. S., Cawse, P. A., Eakins, J. D. and Pattenden, N. J., 1982. Environmental radioactivity in Cumbria. Nature, 300, 27-31.

Pentreath, R. J., 1980. Nuclear Power Man and the Environment. Taylor and Francis Ltd, London.

Pentreath, R. J., 1981. The use of isotopic ratios in determining the relative biological availabilities of transuranium elements. Proceedings of a technical committee meeting on: Techniques for identifying transuranic speciation in aquatic environments. STI/PUB/613, 141, 149. IAEA, Vienna.

Pentreath, R. J., Lovett, M. B., Jefferies, D. F., Woodhead, D. S., Talbot, J. W., Mitchell, N. T., 1984. Impact on public radiation exposure of transuranium nuclides discharged in liquid wastes from fluel element reprocessing at Sellafield, UK. (Radioactive waste management). IAEA CN-43, Vienna 1983.

Pentreath, R. J., Harvey, B. R., Lovett, M. B. and Ibbett, R. D., 1985. Chemical separation of long-lived radionuclides discharged into the marine environment. In: Proc. Seminar on Speciation of Fission and Activation Products in the Environment. Oxford, 16-19 April 1985.

Perkins, D. W., Phillips, D. R. and Sullivan, R. A. L., 1970. Airborne dust collections over the North Atlantic. J. Geophys. Res., 75, 1782-1793.

Perkins, E. J., 1968. The marine fauna and flora of the Solway Firth area. Trans. Dumfries and Galloway Nat. Hist. and Antiq. Soc., 45, 15.

Perkins, R. W. and Thomas, C. W., 1980. Worldwide fallout. In: Transuranic Elements in the Environment (Ed. Hanson, W. C.). US Department of Energy, Technical Information Centre, DOE/TIC 22800, 53-82.

Petit, J. C., Langevin, Y. and Dran, J. C., 1985. $^{234}U/^{238}U$ disequilibrium in nature: theoretical reassessment of the various proposed models. Bull. Mineral., 108, 745-753.

Pillai, K. C., Dey, N. N., Mathew, E. and Kothari, B. U., 1975. Behaviour of discharged radionuclides from fuel reprocessing operations in the aquatic environment of the Bombay harbour bay. In: Radiological Impact of Releases from Nuclear Facilities into Aquatic Environments. (Proc. IAEA Symp. Helsinki.)

Poet, S. E., Moore, H. E. and Martell, E. A., 1972. Lead-210, Bi-210 and Po-210 in the atmosphere: Accurate ratio measurement and application to aerosol residence time determination. J. Geophys. Res., 77, 6515.

Price, W. J., 1964. Nuclear Radiation Detection. McGraw-Hill Book Co., New York.

Price, N. B., 1976. Chemical diagenesis in sediments. In: Chemical Oceanography, Vol 6, 2nd Edition. (Eds. Riley, J. P. and Chester, R.). Academic Press, London, New York, San Francisco.

Rama, Koide, M. and Goldberg, E. D., 1961. ^{210}Pb in natural waters. Science, 134, 98-99.

Reynolds, S. A. and Scott, T. G., 1975. Determination of plutonium in environmental samples. Part I: Development of Methods. Radiochem. Radioanal. Lett., 23, 269-274.

Rhodes, D. W., 1957. The effect of pH on the uptake of radioactive isotopes from solution by a soil. Proc. Soil. Sci. Soc. Am., 21, 389-392.

Riley, J. P. and Skirrow, G. (Eds.), 1975. Chemical oceanography, Vol 3, 2nd Edition, Academic Press, London, New York.

Riley, J. P. and Chester, R. (Eds.), 1976. Chemical oceanography, Vol 6, 2nd Edition, Academic Press, London, New York.

Robbins, J. A. and Edgington, D. N., 1975. Determination of recent sedimentation rates in Lake Michigan using ^{210}Pb and ^{137}Cs. Geochim. Cosmochim. Acta, 39, 285-304.

Robbins, J. A., Edgington, D. N. and Kemp, A. L. W., 1978. Comparative ^{210}Pb, ^{137}Cs and pollen geochronologies of sediments from Lakes Ontario and Erie. Quaternary Res., 10, 87-92.

Rocco, G. G. and Broecker, W. S., 1963. The vertical distribution of ^{137}Cs and ^{90}Sr in the oceans. J. Geophys. Res., 68, 4501-4512.

Rosholt, J. N., Shields, W. R. and Garner, E. L., 1963. Isotopic fractionation of uranium in sandstone. Science, 139, 224-226.

Rosholt, J. N., Doe, B. R. and Yatsumoto, M., 1966. Evaluation of isotopic composition of uranium and thorium in soil profiles. Bull. Geol. Soc. Amer., 77, 987-1004.

Rosholt, J. N., 1980. Uranium trend dating of quaternary sediments. US Geological Survey Open File Report, 80-1087pp.

Rosholt, J. N., 1982. Mobilization and weathering. In: Uranium disequilibrium series applications to the environmental problems. (Eds. Ivanovich, M. I. and Harmon, R. S.). Clardon Press,

Oxford.

Rudran, K., 1969. A comparative study of electrodeposition of actinides from aqueous ammonium sulphate and isopropyl alcohol. AERC Report No R-5987.

Ryan, J. L., 1960. Species involved in the anion exchange absorption of quadrivalent actinide nitrates. J. Phys. Chem., 64, 1375-1385.

Sackett, W. M., Potratz, H. A. and Goldberg, E. D., 1958. Ionium-uranium, ratios in marine deposited calcium carbonates and related materials. Washington Univ. PhD., thesis, St Louis, Mo.

Saito, N., 1984. Selected data on ion exchange separations in radioanalytical chemistry. Pure Appl. Chem., 56, 523-539.

Santschi, P. H., Li, Y. H. and Bell, J., 1979. Natural radionuclides in the water of Narragensett Bay. Earth Planet. Sci. Lett., 45, 201-213.

Santschi, P. H., Li, Y. H., Adler, D. M., Amdurer, M., Bell, J. and Nyffeler, V. P., 1983. The relative mobility of natural (Th, Pb and Po) and fallout (Pu, Am, Cs) radionuclides in the coastal marine environment: results from model ocosystem MERL and Narragansett Bay. Geochim. Cosmochim. Acta., 47, 201-210.

Schmidt-Collerus, J. J. (1967). Research in uranium geochemistry. (Investigations of the relationship between organic matter and uranium deposits - I). Denver Research Inst. (USAEC Contract No AT(05-1)-933.

Scott, M. R., 1982. The chemistry of U- and Th-series. Nuclides in rivers. In: Uranium Series Disequilibrium: Application to Environmental Problem. (Eds. Ivanovich, M. I. and Harmon, R.). 181-201, Claredon Press, Oxford.

Scott, R. D., MacKenzie, A. B., Ben-Shaban, Y. A., Hooker, P. J. and Houston, C. M., 1990. Uranium transport and retardation at the Needle's Eye Natural Analogue Site, south west Scotland. Radiochimica Acta, (in press).

Seelman-Eggebert, W., Pfennig, G., Münzel, H. and Klewe-Nebenius, H., 1981. Karlsruher nuklidkarte. Chart of the Nuclides, Institut für Radiochemie, Drukhaus Haberbeck.

Seymour, A. H., 1971. Radioactivity in the marine environment. National Academy of Science, Washington DC, USA.

Sholkovitz, E. R., 1979. Chemical and physical processes controlling the chemical composition of suspended material in the River Tay Estuary. Estuarine Coastal Mar. Sci., 8, 523-545.

Sholkovitz, E. R., 1983. The geochemistry of plutonium in fresh and marine water environments. Earth Sci. Rev., 19, 95-161.

Sholkovitz, E. R. and Mann, R. D., 1984. The pore water chemistry of $^{239,240}Pu$ and ^{137}Cs in sediments of Buzzards Bay, Massachusetts. Geochim. Cosmochim. Acta., 48, 1107-1114.

Sillen, L. G., 1966. Tellus, 18, 198.

Singh, N. P., Linsalata, P. G., Entry, R. and Wrenn, M. E., 1979. Determination of plutonium in sediments by solvent extraction and alpha spectrometry. Anal. Chim. Acta., 111, 265-274.

Singh, N. P., Zimmerman, C. J., Lewis, L. L. and Wrenn, M. E., 1984. Quantitative determination of environmental levels of uranium, thorium and plutonium in bone by solvent extraction and alpha spectroscopy. N. I. M. Phys. Rev. 223, 558-562, Amsterdam.

Smith, J. N., Schafer, C. T., Loring, D. H., 1980. Depositional processes in an anoxic, high sedimentation regime in the Saguenay Fjord. In: Fjord Oceanography. (Eds. Freeland, H. J., Farmer, D. M., Levings, C. D.). Plenum Publ. Corp., New York.

Smith, J. N., Bondreau, B. P. and Noshkin, V., 1986. Plutonium and ^{210}Pb distributions in the east Atlantic sediments. Subsurface anomalies caused by non-local mixing. Earth Planet. Sci. Lett., 81, 15-28.

Smith, T. J., Parker, W. R. and Kirby, R., 1980. Sedimentation studies relevant to low-level radioactive effluent dispersal in the Irish Sea. Part 1. Radionuclides in marine sediments. IOS Report No 110, 87pp.

Spencer, D. W., Brewer, P. G., Fleer, A. P., Honjo, S., Krishnaswami, S. and Nozaki, Y., 1978. Chemical fluxes from sediment trap experiment in the deep Sargasso Sea. J. Mari. Res., 36, 493-523.

Stanners, D. A. and Aston, S. R., 1981. An improved method of determining sedimentation rates by the use of artificial radionuclides. Estuarine Coastal and Shelf. Sci., 13 101-106.

Stanners, D. A. and Aston, S. R., 1982. ^{134}Cs:^{137}Cs and ^{106}Ru:^{137}Cs ratios in intertidal sediments from the Cumbria and Lancashire Coasts, England. Estuarine Coastal and Shelf. Sci., 13, 409-417.

Steers, J. A., 1973. The coastline of Scotland. Cambridge University Press.

Stephens, W. E., Whitley, J. E., Thirlwall, M. F. and Halliday, A. N., 1985. The Criffell zoned pluton: correlated behaviour of rare earth element abundances with isotopic systems. Contrib. Mineral Petrol. 89, 226-238.

Strelow, F. W. E., Rethemeyer, R. and Bothma, C. J. C., 1965. Ion exchange selectivity scales for cations in nitric acid and sulfuric acid media with a sulfonated polystyrene resin. Anal. Chem. 37, 106-111.

Strelow, F. W. E., Victor, A. H., van Zyl, C. R. and Eloff, C., 1971. Distribution coefficients and cation exchange behaviour of elements in hydrochloric acid - acetone. Anal. Chem., 43, 870-876.

Swan, D. S., Baxter, M. S., McKinley, I. G. and Jack, W., 1982. Radiocaesium and ^{210}Pb in Clyde Sea Loch sediments. Estuarine Coastal Shelf. Sci., 15, 515-536.

Szalay, A., 1964. Cation exchange properties of humic acid and their importance in the geochemical enrichment of UO^{2+}_2 and other cations. Geochim. Cosmochim. Acta, 28, 1605.

Talvitie, N. A., 1971. Radiochemical determination of plutonium in environmental and biological samples by ion exchange. Anal. Chem., 43, 1827-1830.

Tamura, T. and Jacobs, D. G., 1960. Structural implications in caesium sorption. Health Phys., 2, 391-396.

Tamura, T., 1964. Selective sorption reactions of caesium with soil minerals. Nuclear Safety, 5, 262-268.

Tamura, T., 1975. Characterization of plutonium in surface soils from area 13 of the Nevada Test Site. J. Environ. Quality, 4, 350.

Taylor, P. J., 1982. The impact of nuclear waste disposals to the marine environment. Political Ecology Research Group, Oxford. Report RR-8.

Thompson, J., Turekian, K. K. and McCafferty, R. J., 1975. The accumulation of metals in and release from sediments of Long Island Sound. In: Estuarine Research: Recent Advances. (Cronin, L. L. Ed.). 11, 28-43. Academic Press Inc., New York.

Thurber, D. L., 1962. Anomalous $^{234}U/^{238}U$ in nature. J. Geophys. Res., 67, 4518-4520.

Thurber, D. L., 1963. Anomalous $^{234}U/^{238}U$ ratios and an investigation of the potential of ^{234}U for Pleistocene chronology. PhD thesis, Columbia University, New York.

Topping, P. G. and MacKenzie, A. B., 1988. A test of the use of neutron activation analysis for clay source characterisation. Archaeometry, 30, 1, 92-101.

Turekian, K. K. and Chau, L. H., 1971. The marine geochemistry of the uranium isotopes, ^{230}Th and ^{231}Pa. In: Activation Analysis in Geochemistry and Cosmochemistry. (Eds. Brunfelt, A. O. and Steinnes, E.). 311-320. Universites for Laget, Oslo.

Turekian, K. K., Nozaki, Y. and Benninger, L. K., 1977. Geochemistry of atmospheric radon and radon products. Ann. Rev. Earth Planet. Sci., 5, 227-255.

Veeh, H. H., 1967. Deposition of uranium from the ocean. Earth Planet. Sci. Lett., 3, 145-150.

Veselsky, J. C., 1976. The determination of plutonium in environmental samples by extraction with tridoclcylamine. Int. J. Appl. Rad. Isotopes, 27, 499-506.

Volchok, H. L. and Planque, G. (Eds.), 1982. US Department of Energy Environmental Measurements Laboratory Procedures Manual, New York.

Williams, S. J., Kirby, R., Smith, T. J. and Parker, W. R., 1981. Sedimentation studies relevant to low level radioactivity effluent dispersal in the Irish Sea. Part II: Seabed morphology, sediments and shallow sub-bottom stratigraphy of the eastern Irish Sea. IOS Report No 120, 50pp.

Williams, T. M., 1985. A quantitative method of analysis for 241-americium in environmental matrices. MSc Thesis, Strathclyde University.

Williams, T. M., MacKenzie, A. B., Scott, R. D., Price, N. B. and Ridgway, I. M. (1988). Radionuclide distribution in the surface sediments of Loch Etive. In: Radionuclides: A Tool for Oceanography (Guary, J. C., Guegueniat, P. and Pentreath, R. J. Eds). Proceedings of an Int. Symp. Cherbourg, France, 1-5 June 1987. 341-350.

Wilson, T. S. R., 1974. Caesium-137 as a water movement tracer in the St Georges Channel. Nature, 248, 125-127.

Wong, K. M., 1971. Radiochemical determination of plutonium in seawater, sediments and marine organisms. Anal. Chim. Acta., 56, 355-364.

Yamada, M. and Tsunogai, S., 1983. Post depositional enrichment of uranium in sediment from the Bering Sea. Marine Geology, 54, 263-276.

Yamamoto, M., Yamamori, S., Komura, K. and Sakanoue, M., 1980. Behaviour of plutonium and americium in soils. J. Radiat. Res., 21, 204-212.

Yarwood, J., 1973. Atomic and nuclear physics. University Tutorial Press Ltd., London.